Wireless Interference Networks with Limited Feedback

vorgelegt von
Diplom-Mathematiker (FH)
Jan Schreck
aus Berlin

von der Fakultät IV - Elektrotechnik und Informatik
der Technischen Universität Berlin
zur Erlangung des akademischen Grades

Doktor der Ingenieurwissenschaften
- Dr.-Ing. -

genehmigte Dissertation

Promotionsausschuss:

Vorsitzender: Prof. Dr.-Ing. Hans-Joachim Grallert
Gutachter: Prof. Dr. Giuseppe Caire
Gutachter: Prof. Dr. David Gesbert
Gutachter: Prof. Dr. Sławomir Stańczak
Gutachter: Dr.-Ing. habil. Gerhard Wunder

Tag der wissenschaftlichen Aussprache: 27. März 2015

Berlin 2015

To my family.

Abstract

We consider the problem of acquiring accurate channel state information at the transmitters of a wireless network. We develop different feedback and transmit strategies for different network architectures and analyze their performance. First, we consider a single cell of cellular system and assume that the beamforming vectors are given by a fixed transmit codebook. We develop and analyze a new feedback and transmit strategy which combines flexibility and robustness needed for efficient and reliable communication. We prove that it has better scaling properties compared to classical results on the limited feedback problem in the broadcast channel and that this benefit improves with an increasing number of transmit antennas. We show how feedback codebooks can be designed for different propagation environments. Link level and system level simulations sustain the analytic results showing performance gains of up to 50% or 70% compared to zeroforcing when using multiple antennas at the base station and multiple antennas or a single antenna at the terminals, respectively.

We characterize the degrees of freedom (i.e. the multiplexing gain) of multi-cellular systems under different assumptions on the channel model and for different system setups. We propose different algorithms that possibly achieve the optimal degrees of freedom. The first algorithm aims on aligning the interference at each receiver in a subspace of the available receive space. Our second algorithm aims on directly maximizing the signal-to-interference-plus-noise ratio (SINR) of all receivers. By allowing symbol extensions over time or frequency and including a user selection we are able to achieve the alignment of interference for many system setups and exploit multi-user diversity. For coordinated transmit strategies we find the scaling of the performance loss with the feedback load. A distributed interference alignment algorithm is introduced. The algorithm makes efficient use of quantized channel state information and significantly reduces the feedback overhead.

We develop a framework that we call compressive rate estimation. To this end, we assume that the composite channel gain matrix (i.e. the matrix of all channel gains between all network nodes) is compressible which means it can be approximated by a sparse or low rank representation. We develop a sensing protocol that exploits the superposition principle of the wireless channel and enables the receiving nodes to obtain non-adaptive random measurements of columns of the composite channel matrix. The random measurements

are fed back to a central controller who decodes the composite channel gain matrix (or parts of it) and estimates individual user rates. We analyze the rate loss for a linear and a non-linear decoder and find the scaling laws according to the number of non-adaptive measurements.

Zusammenfassung

Wir betrachten das Problem der Akquirierung von Kanalzustandsinformationen an den Sendern von drahtlosen Netzwerken und entwickeln Feedbackverfahren und Sendestrategien für verschiedene Netzwerk Architekturen. Die entwickelten Verfahren werden analysiert und die Skalierung der Performance des Gesamtsystems anhand bestimmter Systemparameter bestimmt. Zuerst betrachten wir eine einzelne Zelle eines zellularen Systems und nehmen an, dass die Beamformingvektoren durch ein festes Codebuch vorgegeben sind. Wir entwickeln und analysieren ein neues Feedbackverfahren, dass Flexibilität und Robustheit vereint und dadurch effiziente und zuverlässige Kommunikation mit den Empfängern ermöglicht. Eine Analyse des Verfahrens zeigt, dass die Skalierung des Ratenverlustes durch quantisierte Kanalzustandsinformation besser ist als bei vergleichbaren Verfahren. Für das Feedbackverfahren wird ein spezieller Algorithmus entwickelt der es ermöglicht Codebücher für verschiedene Kanalmodelle zu generieren und zu optimieren. Die analytischen Ergebnisse werden durch Simulationen validiert und bestätigen einen Gewinn gegenüber vergleichbaren Verfahren.

Anschließend betrachten wir zellulare Systeme mit mehreren Zellen. Wir charakterisieren die Freiheitsgrade (degrees of freedom) unter verschiedenen Annahmen über das Kanalmodell. Des weiteren entwickeln wir verschiedene Algorithmen, die die optimalen Freiheitsgrade erreichen können. Anschließend wird ein Feedbackverfahren entwickelt, dass den Feedbackaufwand für die entwickelten Algorithmen signifikant reduziert. Wir analysieren eine breite Klasse von zellularen Systemen die beliebige koordinierte Sendestrategien verwenden. Für diese Klasse von Systemen leiten wir die Skalierung des Ratenverlustes relativ zum Feedbackaufwand her. Abschließend zeigen wir, wie die analytischen Ergebnisse auf das entwickelte Feedbackverfahren angewendet werden können.

Im letzten Kapitel entwickeln wir ein Framework, dass das Potenzial von Compressed Sensing nutzt um den Messaufwand und Feedbackaufwand in zellularen Systemen mit vielen Teilnehmern signifikant zu reduzieren. Das Framework ermöglicht es die Datenraten der Nutzer innerhalb gegebener Fehlerschranken zu schätzen. Grundlage ist neben Compressed Sensing ein neues Messverfahren, dass die Überlagerung von Signalen im Kanal nutzt, um zufällige nicht adaptive Messungen der Kanalkoeffizienten am Empfänger zu ermöglichen. Diese Messungen werden zu einer zentralen Steuereinheit übertragen und

dort dekodiert. Wir analysieren die Genauigkeit der Rekonstruktion für einen linearen und einen nicht-linearen Dekodierer und leiten die Skalierung mit der Anzahl der Messungen her. Abschließend zeigen wir, wie der entwickelte Ansatz in zellularen Systemen angewendet werden kann.

Acknowledgements

I like to thank Prof. Giuseppe Caire for giving me the opportunity to work with his group at the Technical University of Berlin. I am grateful to Prof. Sławomir Stańczak for taking his time to guide and support me throughout my time at the Technical University of Berlin. My gratitude extends to Dr. Gerhard Wunder for his guidance and continuous support. I would also like to express my gratitude to Prof. David Gesbert who served in my thesis committee. I like to thank Dr. Peter Jung for sharing and discussing ideas and problems. Moreover, I would like to thank all colleagues at the Heinrich Hertz Institute and the Technical University of Berlin for stimulating discussions and creating an optimal working environment.

Contents

List of Figures

List of Tables

1 Introduction

The information age is a historical period which is characterized by the significance of information as a primary product and commodity [Cas96]. Of central importance in the shift from the industrial age to the information age are global information flows and electronic data processing. To date the fastest expanding communication technology are wireless networks. Over the last decades cellular networks have been a subject of intense theoretical and practical research. The requirements on the data rates and coverage of cellular networks have been dramatically increased, due to the huge commercial success of smart phones, tablets and other mobile devices. It is expected that global mobile data traffic will increase 11-fold over the course of the next five years [Cis14]. While former networks had to support only voice and data services, future so-called fifth generation networks are expected to support novel services which require a dramatic delay decrease and guaranteed maximum latencies. Researchers are currently trying to meet delay constraints around 1 ms referring to the next big thing; the Tactile Internet. Moreover, the introduction of the Internet of Things will lead to a massive increase of mobile devices. Most of those mobile devices are sensor nodes that are conveying information to distributed cloud services. With the current centralized approach, this would lead to a massive consumption of energy and spectral resources. To cope with all those challenges, researchers around the globe are currently rethinking wireless networks and inventing new network architectures, network protocols and signal processing schemes.

Due to the scattering of electromagnetic waves in the environment, different components of the transmitted signal arrive at the intended receiver through different angles, time delays, and frequency shifts. Due to the superposition of different multi-path components at a receiver, the wireless channels fluctuate in space, time and frequency. This fading effects substantially limit the reliability of a communication channel. However, at the same time it is well known that channel variations in time frequency and space increase the diversity of a communication system [PW98]. But, to efficiently exploit the variations of the channel, a substantial amount of maintenance signaling is required. Maintenance signaling includes pilot signals for channel estimation and feedback messages containing information about the channel states. To increase the spectral efficiency of wireless networks, the signaling schemes are getting more and more involved which usually comes at

the cost of increased sensitivity. Therefore, also the amount of feedback and maintenance signaling increases and, if not carefully designed, this overhead may eats up most of the performance gains.

The wireless channel is a shared medium. Due to the large and growing number of wireless devices competing for access to the wireless channel, interference is another major challenge [GHH+10]. To minimize the performance loss caused by interference, the signaling strategies must be carefully designed. In [FKV06] coherent and coordinated transmission of multiple base stations to users has been considered to be a promising candidate to achieve enormous gains in spectral efficiency. However, today it is still difficult to realize these gains under practical constraints [IDM+11]. One major drawback is that data sharing between base stations is needed, which requires a huge capacity and low latency of the back haul network. Another possibility to enhance the spectral efficiency of future cellular systems is coordinated scheduling, which requires no data sharing. The only information that needs to be exchanged between base stations is a certain amount of scheduling information. In the landmark paper [CJ08] interference alignment was used to show that the capacity of the interference channel in fading environment is much higher than previously assumed. Under certain assumptions the downlink or uplink of a cellular system can be modeled as multiple mutually interfering broadcast or multiple access channels. Interference alignment for cellular systems was considered in [ST08].

Another possibility to mitigate the interference problem is to deploy additional sites (base stations) to the existing network infrastructure. This approach is based on a simple observation: if the distance between transmitting and receiving nodes is decreased, less transmit power is required and this leads to a decrease of the overall interference in the network. At the same time, with less distance and less interference, the serving nodes can be much simpler and therefore consume less power, are cheaper, smaller and so on. Adding more and more base stations is usually infeasible due to the cost for the physical deployment and maintenance of base stations. Therefore, in order to provide significantly more wireless bandwidth at lower costs, novel types of network architectures and protocols are envisioned and implemented, including stationary relay stations or mini base stations positioned within macro-cell areas. The relay stations are deployed to form (in a decentralized manner) a high capacity wireless backbone that provides multi-hop wireless connectivity between the central base station and mobile users. In such scenarios, channel state information at the central base station plays a crucial role in the ability of the network to optimally utilize the wireless resources. However, channel state information is not for free and therefore training and feedback protocols have to be carefully designed.

In summary, modern and future cellular systems need to make efficient use of channel adaptive signaling schemes. Efficient strategies to acquire channel state information at

the transmitting nodes are of utmost importance. This thesis is devoted to the problem of channel state information quantization and feedback. An outline and the main results are summarized in the next section.

1.1 Outline and Main Results

This thesis deals with the so-called limited feedback problem[1] in wireless networks. If channel state information is available at the transmitter, channel adaptive transmission can be performed which is known to significantly increase the spectral efficiency of wireless networks. In nowadays cellular systems, channel state information can be acquired at the receiving nodes through training and channel estimation and must than be fed back to the transmitting nodes. But, the feedback channel is usually rate-constrained. Therefore, channel state information needs to be compressed and quantized before it can be fed back to the transmitting nodes. We develop different feedback protocols for different network architectures and analyze their performance. We start by considering a single cell and assume that the beamforming vectors are given by a fixed transmit codebook. Next, we consider a multi-cellular system and characterize the degrees of freedom (i.e. multiplexing gain) for certain system setups under different channel models. If the number of serving nodes (e.g. base stations, relays, mini base stations, device to device links) and their number of antennas increases, standard pilot based channel measurement schemes result in the pollution of the available spectrum with pilot signals. Therefore, acquiring channel state information at the receiving nodes can be a challenging task on its own. To this end we explore the potential of compressed sensing and simpler related methods which enable the reduction of the training and feedback overhead in dense wireless networks. Throughout this thesis we use tools from matrix analysis, information theory, covering theory and compressed sensing. The main topics and results are outlined in more details below.

In **Chapter 2** we investigate the downlink performance of the multi-user MIMO channel under a limited feedback constrained. We present and analyze a new robust feedback and transmit strategy for multi-user MIMO downlink communication systems, termed Rate Approximation. Rate approximation combines flexibility and robustness needed for efficient and reliable communications with the user terminals. Loosely speaking, using the proposed rate approximation strategy, the terminal selects a channel quantization vector from a feedback codebook considering any possible scheduling decision that can be taken by the base station. As we show, this enables the base station *to approximate the achievable user rates*, rather than the *user channels*, subject to a small uniform a

[1] Carefully defined later on.

priori error. We analyze the a priori rate error at the base station (before any scheduling decision) for each individual terminal evoked by our rate approximation strategy. We prove that the rate error can have better scaling properties compared to classical baseline results on the limited feedback problem in the broadcast channel. It is shown that the rate approximation strategy achieves the optimal multi-user multiplexing gain. Moreover, we show how feedback codebooks can be designed for different propagation environments. Link level and system level simulations sustain the analytic results, showing performance gains of up to 50% or 70% compared to zeroforcing when using multiple antennas at the base station and multiple antennas or a single antenna at the terminals, respectively.

The work presented in Chapter 2 has been published in [1], [2], [3], [4], [5] , [6] and [7]. Based on the work the following patents have been filled [8], [9] and [10] .

In **Chapter 3** we investigate the degrees of freedom of cellular systems for certain scenarios and system setups. First, we assume a fading environment and allow a asymptotically large number of symbol extensions. Here, we find the degrees of freedom for certain system setups. Next, we find sufficient conditions for the feasibility of interference alignment if the number of symbol extensions is limited. Finally, we assume that transmission needs to be performed over constant channels (i.e. no symbol extensions); here we find a sufficient condition for the feasibility of interference alignment. Based on the insight achieved by the analysis, we propose different algorithms, which possibly achieve the optimal degrees of freedom. The first algorithm aims on aligning the interference at each receiver in a subspace of the available receive space. Our second algorithm aims on directly maximizing the signal-to-interference-plus-noise ratio (SINR) of all receivers. By allowing symbol extensions over time or frequency and including a user selection, we are able to achieve the cancellation of interference for any system setup (if perfect channel state information is available) and exploit multi-user diversity. Finally, our findings are underlined by extensive simulations. First, we consider a Wyner-like channel model to validate the analytic results. Then, we use a LTE related channel model to evaluate the performance of the proposed algorithms in practical scenarios. *The work presented in Chapter 3 has been published in [11], [12], [13] and [14]*

In **Chapter 4** we analyze the performance of multi-cellular systems under a limited feedback constrained. We make a step forward towards a more realistic assessment of the limited feedback problem by introducing a new metric for the performance evaluation. The new metric captures the throughput degradation due to beamforming and link adaption based on partial channel state information. We obtain the relevant scaling laws of the throughput degradation (lower and upper bounds) and show that they differ from existing

ones. A distributed interference alignment algorithm is introduced which makes efficient use of quantized channel state information and significantly reduces the feedback overhead. The algorithm includes a user selection which, under certain assumptions ensures the feasibility of interference alignment. Finally, we underline our findings with simulations.

The work presented in Chapter 4 has been published in [15], [16] and [17].

In **Chapter 5** we develop a framework that we call compressive rate estimation. To this end, we assume that the composite channel gain matrix (i.e. the matrix of all channel gains between all network nodes) is compressible which means it can be approximated by a sparse or low rank representation. We develop a sensing protocol that exploits the superposition principle of the wireless channel and enables the receiving nodes to obtain non-adaptive random measurements of columns of the composite channel matrix. The random measurements are fed back to a central controller who decodes the composite channel gain matrix (or parts of it) and estimates individual user rates. We analyze the rate loss for a linear and a non-linear decoder and find the scaling laws according to the number of non-adaptive measurements.

The work presented in Chapter 5 has been published in [18] and [19],

Further results which are not part of this thesis:

- In [20] a remote channel estimation scheme for multi-user MIMO OFDM systems that is based on compressed sensing was proposed. The feedback scheme significantly reduces the feedback load and the complexity at the receiver site. Extensive simulations showed significant advantages of the proposed scheme over conventional feedback schemes.

- In [21] a feedback and rate control protocol for two-hop wireless networks is proposed. The protocol is based on estimates of a function of the channel gains, the Perron root, which can be efficiently computed in the wireless channel by exploiting the superposition property. It is shown that the proposed protocol significantly reduces the training and feedback overhead. Numerical experiments demonstrate that the protocol enables efficient rate allocation in two-hop wireless networks.

1.2 Mathematical Preliminaries

Unless stated otherwise, the following notation and conventions are used throughout the thesis. The logarithm to the base 2 is given by $\log(x)$ and the natural logarithm is given by $\ln(x)$. Bold letters denote vectors and bold capital letters matrices. The conjugate

transpose of a matrix $\boldsymbol{X}$ is denoted as $\boldsymbol{X}^H$ and $\boldsymbol{X}^T$ is the transpose of matrix $\boldsymbol{X}$. The element in the ith row and jth column of a matrix $\boldsymbol{X}$ is given by $x_{i,j}$, similarly, the ith element of a vector $\boldsymbol{x}$ is given by x_i. The operator $\boldsymbol{x} = \mathrm{vec}(\boldsymbol{X})$ stacks the columns of matrix $\boldsymbol{X}$ in a large column vector $\boldsymbol{x}$. Element wise non–negativity is denoted by $\boldsymbol{X} \geq 0$. The set of all natural numbers $1, 2, \ldots$ is denoted as $\mathbb{N}$, the set of all real numbers is denoted as $\mathbb{R}$ and the set of all complex numbers is denoted as $\mathbb{C}$. The $n \times n$ identity matrix is defined as $\boldsymbol{I}_n$ and the ith column is given by $\boldsymbol{e}_i$. The vector of all zeros is denoted as $\mathbf{0}$. The support of a vector $\boldsymbol{x}$ is the number of non-zero elements and denoted as $\mathrm{supp}(\boldsymbol{x})$. The null space or kernel of a matrix $\boldsymbol{X} \in \mathbb{C}^{M \times N}$ is denoted as $\ker(\boldsymbol{X}) = \{\boldsymbol{v} \in \mathbb{C}^N : \boldsymbol{X}\boldsymbol{v} = \mathbf{0}\}$.

Sets are denoted in calligraphic letters. We use the concept of index sets to denote entities of the system (e.g. base stations, users, data streams). An index set is defined as a set whose elements index elements of another set. For example we will collect the indices of the users denoted as $u_1, u_2, \ldots$ in the index set $\mathcal{U} = \{1, 2, \ldots\}$. We will also use ordered lists to collect different elements; lists are denoted as $V = (a, b, c, \ldots)$.

The expected value of a random variable X is denoted as $\mathbb{E}[X]$. The probability of some event A is denoted as $\Pr(A)$. We frequently consider circularly-symmetric complex Gaussian random variables $X = Y + iZ \sim \mathcal{CN}(0, \sigma^2)$, with $i = \sqrt{-1}$ and $Y, Z \sim \mathcal{N}(0, \sigma^2/2)$ Gaussian distributed with zero mean and variance $\sigma^2/2$. Usually we say that $X \sim \mathcal{CN}(0, \sigma^2)$ is complex Gaussian distributed without stating "circularly-symmetric" explicitly.

We will typically consider normed vector spaces. In the case of a discrete and finite domain N we will look at vectors in $\mathbb{C}^N$. For $\boldsymbol{x}, \boldsymbol{y} \in \mathbb{C}^N$ we consider the standard inner product

$$\langle \boldsymbol{x}, \boldsymbol{y} \rangle = \boldsymbol{x}^H \boldsymbol{y} = \sum_{i=1}^{N} \bar{x}_i y_i.$$

which yields the ℓ_2 norm

$$\|\boldsymbol{x}\|_2 = \sqrt{\langle \boldsymbol{x}, \boldsymbol{x} \rangle}.$$

The unit sphere in $\mathbb{C}^N$ with the norm $\|\cdot\|_2$ is defined as

$$\mathbb{S}^{N-1} = \{\boldsymbol{x} \in \mathbb{C}^N : \|\boldsymbol{x}\|_2 = 1\},$$

and will be denoted as the unit sphere without referring explicitly to the used norm. We will frequently use the Cauchy-Schwarz inequality, which states that for any two vectors $\boldsymbol{x}, \boldsymbol{y} \in \mathbb{C}^N$,

$$|\langle \boldsymbol{x}, \boldsymbol{y} \rangle| \leq \|\boldsymbol{x}\|_2 \|\boldsymbol{y}|_2.$$

A proof of the Cauchy-Schwarz inequality can be found in [HJ85]. Also useful will be the

Parseval's identity which asserts that for every $\boldsymbol{x} \in \mathbb{C}^N$ and any orthonormal basis $\mathcal{B}$ of $\mathbb{C}^N$

$$\sum_{\boldsymbol{e} \in B} |\langle \boldsymbol{x}, \boldsymbol{e} \rangle|^2 = \|\boldsymbol{x}\|_2^2.$$

If a sequence of vectors $\mathcal{C} \subset \mathbb{C}^N$ satisfies

$$\sum_{\boldsymbol{w} \in \mathcal{C}} |\langle \boldsymbol{x}, \boldsymbol{w} \rangle|^2 = A\|\boldsymbol{x}\|_2^2, \tag{1.1}$$

for every $\boldsymbol{x} \in \mathbb{C}^N$ and with a fixed constant $A \geq 1$, we say that $\mathcal{C}$ is tight frame of $\mathbb{C}^N$. We will also use other ℓ_p norms, which are defined for $1 \leq p < \infty$ as

$$\|\boldsymbol{x}\|_p = \left(\sum_{i=1}^{N} |x_i|^p \right)^{1/p}$$

and for $p = \infty$ as

$$\|\boldsymbol{x}\|_\infty = \max_{i=1,\dots,N} |x_i|.$$

For matrices $\boldsymbol{X} \in \mathbb{C}^{M \times N}$ we will consider the Schatten-p norm which is given by

$$\|\boldsymbol{X}\|_{s_p} = \left(\sum_{i=1}^{\min(M,N)} \sigma_i^p(\boldsymbol{X}) \right)^{1/p}$$

where $\{\sigma_i(\boldsymbol{X})\}_i$ are the singular values of the matrix $\boldsymbol{X}$ in decreasing order. Moreover the special case of the Frobenius norm will be denoted as

$$\|\boldsymbol{X}\|_F = \sqrt{\sum_{i=1}^{M} \sum_{j=1}^{N} |x_{i,j}|^2} = \|\boldsymbol{X}\|_{s_2}.$$

1.3 Modeling of Cellular Systems and Basic Assumptions

Here we describe our approach to model cellular systems which is used throughout this thesis. We introduce the channel model, discuss transmit and receive strategies and define performance measures. In the subsequent chapters the model will be refined to fit the individual needs of each chapter.

1.3.1 Channel Model

We describe the downlink model of a cellular system (i.e. data is transmitted from the base stations to the users); the uplink model will be introduced in place when required.

Consider the downlink of a cellular system with T base stations (cells) and U users. The indices of all users are collected in the index set $\mathcal{U} = \{1, 2, \ldots, U\}$ and the indices of users connected to base station b are collected in the index set $\mathcal{U}_b \subseteq \mathcal{U}$. It is assumed that each user is connected to at least one base station, i.e., $\mathcal{U} = \bigcup_{i=1}^{T} \mathcal{U}_i$. For simplicity we assume that all base stations are equipped with n_t antennas and all users are equipped with n_r antennas. We assume a discrete-time flat-fading channel model. The channel model is based on several simplifications but for most parts of the present work the model is of sufficient detail; if required extensions are introduced in place. The discrete-time representation represents the symbol rate of the system. Moreover we assume that the system is perfectly synchronous in time and frequency. The signal received by user m in time slot t is

$$\boldsymbol{y}_m[t] = \sum_{l=1}^{T} \boldsymbol{H}_{m,l}[t]\boldsymbol{x}_l[t] + \boldsymbol{n}_m[t] \in \mathbb{C}^{n_r},$$

where $\boldsymbol{n}_m[t] \sim \mathcal{CN}(0, \boldsymbol{I}_{n_r})$ is complex Gaussian noise with zero mean and unit variance, $\boldsymbol{x}_l[t]$ is the signal transmitted by base station l, and $\boldsymbol{H}_{m,l}[t]$ is the linear channel transfer function from base station l to user m. We adopt a block fading channel model. That is, we assume that the channels stay constant for a time frame of T_s time slots and change independently in the next frame of T_s time slots. We assume that the channel coefficients from time frame to frame are given by an ergodic process. If not stated explicitly we assume that the absolute values of the channel coefficients are bounded between a non-zero minimum and a finite maximum, this is to avoid degenerated channel conditions. Most of the results in this thesis do not assume a specific distribution of the channel fading process; if we assume a specific random model it is defined in place. For a given time slot t all channels that can be observed by user m are collected in the list

$$H_m[t] := (\boldsymbol{H}_{m,l}[t])_{l=1,\ldots,T}\,.$$

Throughout this thesis we assume that the channels $H_m[t]$ can be perfectly tracked by each user $m \in \mathcal{U}$. Finally, all channel realizations for a given time slot t are collected in the list

$$H[t] := (H_m[t])_{m\in\mathcal{U}}\,.$$

For simplicity we will drop the time slot reference in the following. For example for an

arbitrary but fixed time slot the signal received by user m is

$$\boldsymbol{y}_m = \sum_{l=1}^{T} \boldsymbol{H}_{m,l}\boldsymbol{x}_l + \boldsymbol{n}_m \in \mathbb{C}^{n_r}.$$

1.3.2 Transmit Protocol

A set of distributed algorithms that are performed to respond to variations of the network state is called a protocol. Here we describe the downlink transmit protocol which is invoked periodically for each frame of T_s time slots.

1) Channel measurement Throughout this thesis we assume that all receivers m can perfectly track the channels H_m. However we stress that in a practical system typically pilot signals need to be transmitted by the base stations from each antenna separately. For each of the Tn_t transmit antennas in the system the pilot signals must be transmitted on a different time slot, i.e. pilot signals must be transmitted on orthogonal resources. In Chapter 5 we will show how the requirement of orthogonal pilot signals can be relaxed.

2) Feedback The measured channels are quantized and fed back to the base stations or, depending on the system architecture, a central controller. We will develop and discuss different feedback schemes throughout this work. The general approach and challenges are described in Subsection 1.4 below.

3) Scheduling Scheduling is performed based on the channel state information available at the base stations or a central controller. Throughout this thesis we assume that scheduling includes a user selection and the determination of transmit parameters like precoding vectors, number of scheduled data streams and transmit powers. We will apply different scheduling strategies. The general approach is specified in Subsection 1.3.3.

4) Measurement of effective channels Orthogonal precoded pilots (i.e. dedicated pilots) are transmitted by all base stations $b = 1, \ldots, T$ and used by the users m to measure the effective channels $\boldsymbol{H}_{m,b}\boldsymbol{\pi}(i)$, where $\boldsymbol{\pi}(i)$ is a precoding vector (defined later on) used to precode data stream i. Similar to the first channel measurement phase we assume that all receivers can perfectly track the effective channels.

5) Data transmission The rest of the transmission frame is used to transmit data to the selected users. Data transmission is performed simultaneously by all base stations

to all selected receivers. Interference is treated as noise. Different transmit and receive strategies are discussed in Section 1.3.3.

Remark 1.1. Throughout this thesis we assume that the number of time slots τ required for training and feedback of the channel states is much smaller than the length of a time frame $\tau \ll T_s$. This assumption enables us to focus our effort on the limited feedback problem and the performance loss due to precoding and scheduling based on quantized channel state information.

1.3.3 Transmit and Receive Strategies

We restrict the class of transmit and receive strategies to linear beamforming strategies, i.e., we assume linear transmit precoding and linear receive filtering (defined below). We stress that linear beamforming strategies are in general not performance optimal but known to perform reasonably well in many systems. For example, [DS05] showed for the Gaussian broadcast channel with more users than transmit antennas that linear beamforming with user selection performs close to the optimal dirty paper coding limit [CS03]. Non-linear dirty paper coding based techniques are known to achieve the performance of the Gaussian broadcast channel, but in general implementations of dirty paper coding based techniques are to complex for practical systems. On the other hand, linear beamforming strategies are known to yield a good trade off between implementation complexity and achievable performance.

If the base stations and the users have multiple antennas, beamforming strategies enable the transmission of multiple data streams on the same spectral resources (i.e. in the same frequency band and in the same time slot). For point-to-point MIMO systems spatial multiplexing was shown in [PK94, Fos96] to yield a substantial increase of the system performance. On the other hand, in point-to-point MIMO systems multiple antennas can be used to increase the reliability of communication by increasing the receive and transmit diversity [Ala98, TSC98]. The concepts of transmit/receive diversity and multiplexing can also be extended to systems with multiple users. In systems with multiple users multiple antennas can also be used to reduce interference and in this way increase the overall performance of the system. All these goals are mutually conflicting and therefore a smart balancing is required in order to maximize the system sum-rate or any other performance metric. In fact, [ZT03] showed for the point-to-point MIMO channel that there is a fundamental trade off between multiplexing and diversity.

Scheduling

Assume that each user is associated with at least one data stream and that all data streams have a full buffer of infinite length. In a fully loaded system adaptive adjustment of the number of active data streams is crucial to maximize the performance. Thus, for each transmission frame a scheduling decision must be taken. A scheduling decision is defined as follows.

Definition 1.2. *A scheduling decision is given by a pair $(S, \boldsymbol{\pi})$, which consists of i) the list of all scheduled data streams*

$$S := (\mathcal{S}_1, \mathcal{S}_2, \ldots, \mathcal{S}_T),$$

with $\mathcal{S}_b$ the index set of data streams scheduled for transmission by base station b, and ii) a precoding vector for each scheduled data stream $i \in \mathcal{S} := \mathcal{S}_1 \cup \mathcal{S}_2 \cup \ldots \cup \mathcal{S}_T$, given by the mapping

$$\boldsymbol{\pi} : \mathcal{S} \to \mathbb{S}^{n_t - 1}. \tag{1.2}$$

We stress the difference between the list of scheduled data streams S and the index set of scheduled data streams $\mathcal{S}$. The first will be convenient later on since it preserves the cardinality of the sets $\mathcal{S}_b$, and the latter mainly acts as domain of the mapping $\boldsymbol{\pi}$. We will not state the domain of $\boldsymbol{\pi}$ explicitly if it is clear from the context. Further we define the index set of all scheduled data streams assigned to user $m \in \mathcal{S}$ as,

$$\mathcal{R}_m = \{i \in \mathcal{S} : \text{data stream } s_i \text{ is assigned to user } m\}.$$

Linear Beamforming

The transmitted signal must fulfill an average transmit power constraint $\mathbb{E}\left[\|\boldsymbol{x}_b\|_2^2\right] \leq P$. If not stated otherwise, we assume that the base station distributes its available power equally among all scheduled data streams. The signal transmitted by base station b is given by the superposition

$$\boldsymbol{x}_b = \sum_{i \in \mathcal{S}_b} \sqrt{\frac{P}{|\mathcal{S}_b|}} \boldsymbol{\pi}(i) s_i.$$

Each data stream is given by a sequence of i.i.d. complex Gaussian random variables with zero mean and unit variance. After passing through the channel the signal received by user $m \in \mathcal{U}$ can now be written as

$$\boldsymbol{y}_m = \sum_{b=1}^{T} \sum_{i \in \mathcal{S}_b} \sqrt{\frac{P}{|\mathcal{S}_b|}} \boldsymbol{H}_{m,b} \boldsymbol{\pi}(i) s_i + \boldsymbol{n}_m.$$

To decode data symbol s_i from the received signal $\boldsymbol{y}_m$ user m applies a linear receive filter, which is given by the mapping

$$\boldsymbol{\rho} : \mathcal{S} \rightarrow \mathbb{S}^{n_r-1}.$$

The receive filter $\boldsymbol{\rho}(i)$ for data stream i transmitted from base station b to receiver m usually depends on the effective channel $\boldsymbol{H}_{m,b}\boldsymbol{\pi}(i)$. If the receiver is able to estimate the effective channel $\boldsymbol{H}_{m,l}\boldsymbol{\pi}(j)$ for some base station l and data stream $j \in \mathcal{S}_l$, the receive filter may also consider interference from other data streams. However, we stress that throughout this thesis we consider only linear receive filter techniques and no non-linear techniques like successive interference cancellation or other multi-user detection schemes. For now we just assume that each user independently optimizes its receive filter. Specific receive strategies are introduced in place when required.

1.3.4 Achievable Rates

The capacity C of a channel is defined as the maximum achievable rate at which reliable communication is possible. In [Sha48] Shannon showed for the Gaussian discrete time channel with average power constraint that for any rate $R < C$ and error probability bound $P_e > 0$ there exists a channel code that achieves P_e. Conversely, a code with a rate $R > C$ cannot achieve an arbitrary small error probability. Consider the discrete-time channel

$$y = x + n,$$

with complex input symbols $x \in \mathbb{C}$, $n \sim \mathcal{CN}(0, N_0)$ i.i.d. complex Gaussian noise, and assume an average power constraint P and unit bandwidth, then the channel capacity is maximized if the input is complex Gaussian distributed with zero mean and variance P and equal to [Sha49]

$$C = \log(1 + \mathrm{SNR}), bit/s,$$

where $\mathrm{SNR} = P/(N_0)$ is the SNR per receive dimension. If we consider a discrete-time fast-fading channel, the received signal per channel use is

$$y = hx + n$$

where h is an ergodic process, the ergodic capacity [Eri70] without channel state information at the transmitter is given by

$$C = \mathbb{E}\left[\log(1 + |h|^2\mathrm{SNR})\right], bit/s.$$

For a fast-fading ($T_s = 1$) point-to-point MIMO channel

$$\boldsymbol{y} = \boldsymbol{H}\boldsymbol{x} + \boldsymbol{n},$$

with $\boldsymbol{n} \sim \mathcal{CN}(0, \boldsymbol{I}_{n_r})$ and the elements of $\boldsymbol{H}$ distributed as $h_{i,j} \sim \mathcal{CN}(0, \sigma^2)$ and $\boldsymbol{x} \sim \mathcal{CN}(0, P/n_t \boldsymbol{I}_{n_t})$, the ergodic channel capacity with channel state information at the receiver was shown by [Tel99, FG98] to be

$$C = \mathbb{E}\left[\log\det(\boldsymbol{I}_{n_r} + (P/n_t)\boldsymbol{H}\boldsymbol{H}^H)\right].$$

The fast-fading point-to-point "Rayleigh" channel is one of a few examples the channel capacity is known for. However, for most of the channels we are going to consider the capacity is generally unknown, and, even if it is known, the capacity achieving coding schemes are usually very complex and by no means applicable under practical constraints. In fact, we will mainly consider cellular systems which can be modeled as multiple interfering broadcast channels (downlink), interfering multiple access channels (uplink) or interference channel (single user per base station). To the best of our knowledge, for none of these channels the capacity region is known so far.

Therefore, we resort to linear beamforming schemes with Gaussian inputs and adopt an achievable rate as performance measure. If the input symbols are i.i.d. complex Gaussian distributed, $s_i \sim \mathcal{CN}(0, 1)$, and the channels H, the precoders $\boldsymbol{\pi}$, and the receive filters $\boldsymbol{\rho}$ are fixed, the achievable rate can be given as a function of the SINR. The SINR is defined as the ratio of the desired signal power to the sum of the interference plus noise power. For fixed receive filters $\boldsymbol{\rho}$ the SINR of data stream $i \in \mathcal{S}_b$ transmitted by base station b and decoded by receiver m can be given as a function of the linear precoding vectors $\boldsymbol{\pi}$, scheduled data streams $S = \{\mathcal{S}_1, \ldots, \mathcal{S}_T\}$ and a channel realization H,

$$\mathrm{SINR}_i(P, \boldsymbol{\pi}, S, H_m) = \frac{\frac{P}{|\mathcal{S}_b|}|\langle \boldsymbol{\rho}(i), \boldsymbol{H}_{m,b}\boldsymbol{\pi}(i)\rangle|^2}{1 + \sum_{l=1}^{T}\sum_{\substack{j\in\mathcal{S}_l \\ j\neq i}} \frac{P}{|\mathcal{S}_l|}|\langle \boldsymbol{\rho}(i), \boldsymbol{H}_{m,l}\boldsymbol{\pi}(j)\rangle|^2}. \tag{1.3}$$

Now, if receiver m has perfect knowledge of the effective channels $\langle \boldsymbol{\rho}(i), \boldsymbol{H}_{m,l}\boldsymbol{\pi}(j)\rangle$, for all $j \in \mathcal{S}_l$ and $l = 1, \ldots, T$, then, for fixed channels the achievable rate of stream $i \in \mathcal{S}_b$ transmitted by base station b and decoded by receiver m is

$$r_i(P, \boldsymbol{\pi}, S, H_m) = \log\left(1 + \mathrm{SINR}_i(P, \boldsymbol{\pi}, S, H_m)\right). \tag{1.4}$$

To see this, without loss of generality assume a single data stream per user and let data stream m be associated with user m. Define the effective channel $\alpha_{m,b} = \langle \boldsymbol{\rho}(m), \boldsymbol{H}_{m,b}\boldsymbol{\pi}(m)\rangle$,

such that the filtered received signal of user $i \in \mathcal{S}_b$ can be written as

$$\hat{s}_i = \langle \boldsymbol{\rho}(i), \boldsymbol{y}_i \rangle = \sqrt{\frac{P}{|\mathcal{S}_b|}} \alpha_{i,b} s_i + \sum_{l=1}^{T} \sum_{m \in \mathcal{S}_l \setminus \{i\}} \sqrt{\frac{P}{|\mathcal{S}_l|}} \alpha_{m,l} s_m + \langle \boldsymbol{\rho}(i), \boldsymbol{n}_m \rangle \tag{1.5}$$

Since the sum is taken over complex Gaussian random variables with zero mean and variance $\frac{P}{|\mathcal{S}_l|}|\alpha_{m,l}|^2$, the channel (1.5) is a Gaussian channel with noise variance

$$\sum_{l=1}^{T} \sum_{m \in \mathcal{S}_l \setminus \{i\}} \frac{P}{|\mathcal{S}_b|} |\alpha_{m,l}|^2 + 1$$

and therefore has the achievable rate (1.4). However, to achieve this rate a large number of symbols must be transmitted. We stress that throughout this thesis we use the achievable rate as *utility function* to measure the performance of the considered systems. We will further use the achievable sum-rate of the system

$$R(P, \boldsymbol{\pi}, S, H) := \sum_{b=1}^{T} \sum_{m \in \mathcal{U}_b} \sum_{i \in \mathcal{R}_m} r_i(P, \boldsymbol{\pi}, S, H_m) \tag{1.6}$$

as utility function. To evaluate the average achievable sum-rate, we assume a specific signaling strategy that adapts $\boldsymbol{\pi}$ and S to the instantaneous channel realization. For example, if we assume perfect channel state information at a central controller, the sum-rate optimal signaling strategy is the solution to the optimization problem

$$\max_{\boldsymbol{\pi}: \mathcal{S} \to \mathbb{S}^{n_t - 1}} \max_{S = \{\mathcal{S}_1, \ldots, \mathcal{S}_T\}} R(P, \boldsymbol{\pi}, S, H), \tag{1.7}$$

with the domain of $\boldsymbol{\pi}$ given by $\mathcal{S} = \mathcal{S}_1 \cup \ldots \cup \mathcal{S}_T$, as defined above. Define the sum-rate optimal scheduling decision with perfect channel state information as $(S_H, \boldsymbol{\pi}_H)$. Assuming that the random process underlying the channel statistics is ergodic, the average achievable sum-rate with perfect channel state information is

$$\bar{R}_H(P) = \mathbb{E}\left[R(P, \boldsymbol{\pi}_H, S_H, H)\right], \tag{1.8}$$

where the expectation is taken over the channel realizations H. We stress that solving (1.7) without further constraints is in general not feasible. Therefore, if we need to solve (1.7) explicitly we will resort to sub-optimal solutions. For instance, in Chapter 2 we assume that the beamforming vectors are given by a fixed codebook, and in Chapter 3 we consider interference alignment. Moreover, in the theoretical setting of Chapter 2 and 4

will assume that (1.7) has been perfectly solved.

1.4 Limited Feedback Problem

In multi-user and multi-cellular MIMO systems channel adaptive signaling can yield large performance gains. To perform channel adaptive signaling channel state information at the base station is required. For instance, to exploit multi-user diversity in a multi-user MIMO channel, channel state information at the base station is essential. In fact, [CS03] showed for the multi-user MIMO channel, if the base station has no channel state information and all channels have the same statistics, then point-to-point communication is optimal. A comprehensive survey on the limited feedback problem in wireless communication systems can be found [LHN+08]. A review of related literature will be presented in the introduction of each chapter.

As describe above (Subsection 1.3.2) we assume no significant delay in the process of channel measurement, quantization and feedback. In other words, for an arbitrary channel realization H the base stations (or the central controller) have instantaneous knowledge of the quantized channel state information,

$$V_m := \left(\tilde{\boldsymbol{H}}_{m,l} = \mathcal{Q}(\boldsymbol{H}_{m,l})\right)_{l=1,\ldots,T}, \quad \forall m \in \mathcal{U}$$

where $\mathcal{Q}(\boldsymbol{X})$ is some quantization operator, defined later on when required. The quantized channel state information from all users is collected in the list

$$V := (V_m)_{m\in\mathcal{U}}\,.$$

If the central controller or the base stations have quantized channel state information V, the sub-optimal scheduling decision $(S_V, \boldsymbol{\pi}_V)$ can be found by solving

$$\max_{\boldsymbol{\pi}:\mathcal{S}\to\mathbb{S}^{n_t-1}} \max_{S=\{\mathcal{S}_1,\ldots,\mathcal{S}_T\}} R(P, \boldsymbol{\pi}, S, V). \tag{1.9}$$

Such that, the achievable sum-rate with quantized channel state information V at the central controller is

$$R(P, \boldsymbol{\pi}_V, S_V, H).$$

and the average achievable sum-rate with quantized channel state information V at the central controller is

$$\bar{R}_V(P) = \mathbb{E}\left[R(P, \boldsymbol{\pi}_V, S_V, H)\right].$$

Clearly, the achievable sum-rate with quantized channel state information is smaller or equal than the sum-rate with perfect channel state information.

$$R(P, \boldsymbol{\pi}_V, S_V, H) \leq R(P, \boldsymbol{\pi}_H, S_H, H).$$

Obviously, the same is true for the average sum-rates,

$$\bar{R}_V(P) \leq \bar{R}_H(P).$$

In the subsequent chapters we will explore the rate loss due to quantized channel state information under various assumptions on the quantization of the channels, the system architecture and the transmit strategies.

2 Single Cell Processing with Limited Feedback

Multiple antenna downlink technology offers the possibility of sharing the same frequency band at the same time between multiple users. If perfect channel state information is available at the base station (transmitter), the sum-rate optimal transmission technique is a combination of linear beamforming and dirty paper coding [CS03, VJG02, VT02]. Since it is difficult to implement dirty paper coding in practical systems, linear beamforming techniques have been studied extensively and shown to perform close to the optimal solution [DS05]. However, due to the rate-constrained feedback channel, obtaining channel state information at the base station remains a non-trivial task.

Over the last years, there have been a vast number of publications dealing with so-called limited feedback multi-user MIMO systems (reviewed below). In these scenarios, the base station obtains quantized channel state information via a rate-constrained feedback channel. Transmit strategies for limited feedback multi-user MIMO systems can be roughly divided in two categories. One category is based on *adaptive beamforming* where the choice of beamforming vectors is not restricted to a specific codebook. Zeroforcing beamforming is a popular adaptive beamforming strategy. The other category is based on the assumption that the transmit beamforming vectors are chosen from a fixed transmit codebook and called *fixed beamforming*.

In this chapter we consider fixed beamforming. Most of the fixed beamforming schemes require that each user reports information about its preferred transmit codebook entry. This feedback information is then used by the base station to select users for transmission. One candidate is the so-called per user unitary rate control (PU2RC) introduced in [KKL05]. In [HAH09] it is shown that PU2RC achieves the full multi-user diversity and multiplexing gain asymptotically, i.e. for a large number of users. However as pointed out by [CJKR10], the case of a large number of users is actually quiet the opposite of what next generation wireless systems aim at, namely to provide very high data rates to individual users. Therefore, we claim that for a small number of users the interference situation has to be more accurately predicted. This can not be achieved by PU2RC or other schemes based on reporting the preferred beamforming vector, see e.g. [3GP07].

Making the interference situation available to the base station is exactly the purpose of the rate approximation feedback strategy discussed in this chapter. It allows the base station to uniformly approximate the multi-user rates for *any* selection of users and *any* combination of beamforming vectors defined by a transmit codebook. The main idea is to distinguish between a transmit- and a feedback codebook. Two striking advantages come with this concept. First, the base station has now all degrees of freedom for the user selection and second, the rate allocation is more reliable due to the uniform approximation and the reliability scales with the number of feedback bits.

Related Work

An extensive survey on the limited feedback problem in MIMO systems can be found in [LHN+08]. The standard reference for point-to-point MISO systems is [KSEA03] where groundbreaking analytic expressions for the problem are derived. Reference [AYL07] evaluates the performance of point-to-point MISO systems using random vector quantization. In [SH09] is shown that random vector quantization is asymptotically optimal (i.e. the number of feedback bits, the number of transmit antennas and the number of receive antennas all go to infinity with fixed ratios) for point-to-point MIMO systems.

For multi-user MIMO systems, [Jin06] provides the standard performance analysis for the throughput degradation assuming random vector quantization. In [CJKR10] different feedback schemes are analyzed and compared under a variety of assumptions; including imperfect channel state information at the receivers and feedback delay. The major drawbacks of [Jin06, CJKR10] are that no user selection is considered. However, user selection is essential to achieve high data rates and to exploit multi-user diversity [DS05]. In [KdFG+07] different feedback schemes are proposed that enable the base station to estimate the SINR of each user and to perform user selections at the base station. Reference [TBH08] also considers zeroforcing beamforming and jointly designs the receive filters and the channel quantization to maximize the expected SINR of each user. In [DLZ07] different types of partial channel state information are assumed and the performance of dirty paper coding and zeroforcing beamforming is compared. However, all of these works [Jin06, CJKR10, KdFG+07, TBH08, DLZ07] focus on zeroforcing beamforming, usually arguing that zeroforcing enables closed form analysis.

If the choice of beamforming vectors is restricted to a codebook with orthogonal unit norm vectors, we will talk about unitary beamforming. Unitary beamforming with random orthogonal beamforming vectors was proposed in [SH05] and shown to achieve the same multi-user multiplexing gain as dirty paper coding. Based on this work different unitary beamforming algorithms with sum feedback rate constraints have been proposed

and compared in [HHA07]. In [dFKSG07] unitary beamforming with user selection is considered and a feedback protocol developed that enables the base station to compute exact SINR expressions. In [Sam06] a unitary beamforming scheme named per user unitary rate control (PU2RC) has been proposed for LTE. PU2RC uses codebooks with multiple groups of orthogonal vectors to achieve performance gains. In [ZXC09] an improved user selection scheme for PU2RC is proposed.

Contributions

We consider linear beamforming and assume that the beamforming vectors are defined by a fixed transmit codebook known to the base stations and all users, a priori. In contrast to previous work, we allow a possibly different codebook for the feedback and apply a new feedback strategy which we call *rate approximation*. Loosely speaking, using the proposed rate approximation feedback strategy the terminal selects a channel quantization vector from the feedback codebook, considering any possible scheduling decision that can be taken by the base station. As we show, this enables the base station *to approximate the user rates* rather than the *user channels*, subject to a small uniform a priori error. Then, given the feedback message, the base station is permitted to use any beamforming vector from the transmit codebook for some network oriented optimization purpose, and not just the beamforming vector dictated by the user.

In the first part of this chapter (Section 2.3) we prove that for the low to average SNR range beamforming with a fixed codebook can achieve higher rates than zeroforcing beamforming. For the rate approximation feedback strategy we analyze the rate approximation error at the base station, that is the rate error before any scheduling decision. We prove that rate error has essentially the same scaling properties compared to the zeroforcing beamforming results in [Jin06]. In fact, we find that the scaling improves with an increasing number of transmit antennas and can even be better than the scaling for zeroforcing beamforming in [Jin06]. To this end, we derive a vector quantization problem related to the rate approximation feedback strategy by replacing the chordal distance with a new distance function which inherently uses the structure of the transmit codebook. Moreover, we prove that the scaling of the rate approximation error at the base station is inherited by the achievable system sum-rate.

In the second part (Section 2.4) we highlight some of the advantages of the rate approximation feedback strategy in practical scenarios. We show how the rate approximation scheme can be naturally extended to OFDM systems. We demonstrate how feedback codebooks for arbitrary scenarios can be designed using an algorithm proposed by Linde, Buzo and Gray in [LBG80]. Using the proposed feedback method, different feedback codebooks

can be optimized beforehand and then loaded if the environment changes, for example if a user moves from indoors to outdoors). Moreover, we develop a sub-optimal feedback protocol that reduces the complexity of the rate approximation feedback strategy but still considers the transmit codebook. Finally in Section 2.5 we underline our results with system level simulations showing the benefits obtained by the proposed rate approximation feedback strategy.

2.1 System Setup and Problem Statement

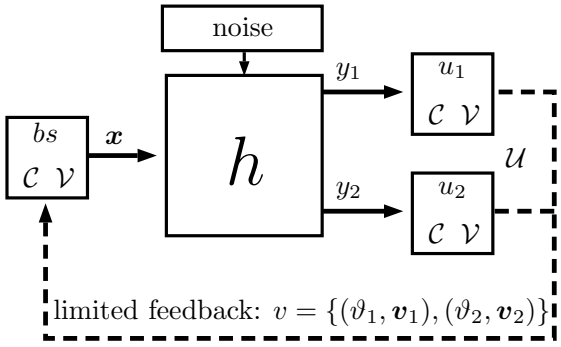

Figure 2.1: Example of a single cell system architecture with 2 users receiving independent data from a single base station. Based on quantized channel state information v the base station (bs) performs scheduling. The channel direction information $\boldsymbol{v}_m \in \mathcal{V}$ of user m is taken from a feedback codebook $\mathcal{V}$. Beamforming vectors are elements of a predefined transmit codebook $\mathcal{C}$. All terms are defined in Section 2.1.

We consider the downlink channel of a cellular network, introduced in Section 1.3, and take the following additional assumptions. We consider a single cell (base station), $T = 1$, and assume that all out-of-cell interference can be treated as additive complex Gaussian noise. In the literature such systems are frequently called multi-user MIMO systems. To simplify the notation we drop the base station index. Hence, the signal received by user m through the channel $\boldsymbol{H}_m = \boldsymbol{H}_{m,1} \in \mathbb{C}^{n_r \times n_t}$ is

$$\boldsymbol{y}_m = \boldsymbol{H}_m \boldsymbol{x} + \boldsymbol{n}_m,$$

where $\boldsymbol{n}_m \sim \mathcal{CN}(0, \boldsymbol{I}_{n_r})$ is the out-of-cell interference plus noise. If not stated otherwise we make no assumption on the channel We assume a single data stream per user and let data stream i be associated to user i. Hence, we may say that user i is scheduled for transmission implying that data stream i associated to user i is scheduled. The maximum number of

scheduled users (or data streams) is bounded by $|\mathcal{S}| \leq n_s \leq n_t$. In the single cell case of this chapter the list of scheduled data streams $S = \mathcal{S}$, and we will use $\mathcal{S}$ throughout this chapter. The beamforming vectors are taken from a finite transmit codebook $\mathcal{C} \subset \mathbb{S}^{n_t-1}$, known to the base station and all users. According to (1.2) the assignment of users to beamforming vectors is defined by the mapping

$$\boldsymbol{\pi}_{\mathcal{C}} : \mathcal{S} \to \mathcal{C},$$

that maps each user $m \in \mathcal{S}$ to an element of the transmit codebook $\mathcal{C}$. Therefore, a scheduling decision can be given by a pair $(\boldsymbol{\pi}_{\mathcal{C}}, \mathcal{S})$. Throughout this chapter we assume that the transmit codebook constitutes a tight frame (1.1) in $\mathbb{C}^{n_t}$, with frame constant A. If $A = 1$, $\mathcal{C}$ constitutes an orthonormal base and we call $\mathcal{C}$ an unitary codebook. The transmitted signal is given by the superposition

$$\boldsymbol{x} = \sum_{m \in \mathcal{S}} \sqrt{\frac{P}{|\mathcal{S}|}} \boldsymbol{\pi}_{\mathcal{C}}(m) s_m. \tag{2.1}$$

Since $\mathbb{E}\left[|s_m|^2\right] = 1$ (see Section 1.3.3 for more details), the transmitted signal fulfills an average power constraint $\mathbb{E}\left[\|\boldsymbol{x}\|_2^2\right] \leq P$. For simplicity, we assume that the receive filter $\boldsymbol{\rho}(m)$ is fixed during the feedback and transmission phase. Such that we can define the effective channel $\hat{\boldsymbol{h}}_m = \langle \boldsymbol{H}_m, \boldsymbol{\rho}(m) \rangle$ and the normalized effective channel $\boldsymbol{h}_m = \hat{\boldsymbol{h}}_m / \|\hat{\boldsymbol{h}}_m\|_2$. To simplify notation, we define the receive SNR (normalized to the number of transmit antennas n_t) of user m as

$$\lambda_m^2 := \frac{P \|\hat{\boldsymbol{h}}_m\|_2^2}{n_t},$$

and collect the set of all effective channels in the list

$$h := (\lambda_m \boldsymbol{h}_m)_{m \in \mathcal{U}}. \tag{2.2}$$

Now the SINR of user $m \in \mathcal{S}$ can be rewritten as a function of the scheduling decision $(\boldsymbol{\pi}_{\mathcal{C}}, \mathcal{S})$ and the effective channel $\lambda_m \boldsymbol{h}_m$,

$$\mathrm{SINR}_m(\boldsymbol{\pi}_{\mathcal{C}}, \mathcal{S}, \lambda_m \boldsymbol{h}_m) = \frac{\lambda_m^2 |\langle \boldsymbol{h}_m, \boldsymbol{\pi}_{\mathcal{C}}(m) \rangle|^2}{|\mathcal{S}|/n_t + \lambda_m^2 \sum_{l \in \mathcal{S} \setminus \{m\}} |\langle \boldsymbol{h}_m, \boldsymbol{\pi}_{\mathcal{C}}(l) \rangle|^2}. \tag{2.3}$$

Further, the achievable rate of user m can be rewritten as

$$r_m(\boldsymbol{\pi}_{\mathcal{C}}, \mathcal{S}, \lambda_m \boldsymbol{h}_m) = \log\left(1 + \mathrm{SINR}_m(\boldsymbol{\pi}_{\mathcal{C}}, \mathcal{S}, \lambda_m \boldsymbol{h}_m)\right), \tag{2.4}$$

and the system sum-rate for scheduling decision $(\boldsymbol{\pi}_{\mathcal{C}}, \mathcal{S})$ and channel realization h can be written as

$$R\left(\boldsymbol{\pi}_{\mathcal{C}}, \mathcal{S}, h\right) = \sum_{m \in \mathcal{S}} r_m(\boldsymbol{\pi}_{\mathcal{C}}, \mathcal{S}, \lambda_m \boldsymbol{h}_m).$$

Throughout this chapter we assume that scheduling is performed to maximize the system sum-rate. Hence, if the base station has perfect channel state information the optimal scheduling decision $(\mathcal{S}_h, \boldsymbol{\pi}_{\mathcal{C},h})$ is the solution to the optimization problem

$$\max_{\mathcal{S} \subseteq \mathcal{U}} \max_{\boldsymbol{\pi}_{\mathcal{C}}: \mathcal{S} \to \mathcal{C}} R\left(\boldsymbol{\pi}_{\mathcal{C}}, \mathcal{S}, h\right) \quad \text{subject to } |\mathcal{S}| \leq n_s. \tag{2.5}$$

Such that the system sum-rate with perfect channel state information is given by

$$R\left(\boldsymbol{\pi}_{\mathcal{C},h}, \mathcal{S}_h, h\right).$$

Our goal is to explore the rate loss due to quantized channel state information. To this end, assume that quantized channel state information at the base station is given by a channel direction information (CDI) $\boldsymbol{v}_m \in \mathcal{V}$, which is an element of the feedback codebook $\mathcal{V} \subset \mathbb{S}^{n_t - 1}$ of size $|\mathcal{V}| = 2^B$, and a channel quality information (CQI) given by a scalar $\vartheta_m \in \mathbb{R}$. The feedback protocol will be specified in the next section. We assume that the feedback codebook $\mathcal{V}$ is a priori known to all users and the base station and that the CQI is perfectly transferred to the base station. The scheduling decision $(\mathcal{S}_v, \boldsymbol{\pi}_{\mathcal{C},v})$ based on quantized channel state information

$$v := (\vartheta_m \boldsymbol{v}_m)_{m \in \mathcal{U}}$$

is the solution to the optimization problem

$$\max_{\mathcal{S} \subseteq \mathcal{U}} \max_{\boldsymbol{\pi}_{\mathcal{C}}: \mathcal{S} \to \mathcal{C}} R\left(\boldsymbol{\pi}_{\mathcal{C}}, \mathcal{S}, v\right) \quad \text{subject to } |\mathcal{S}| \leq n_s. \tag{2.6}$$

Hence, the system sum-rate with quantized channel state information is $R\left(\boldsymbol{\pi}_{\mathcal{C},v}, \mathcal{S}_v, h\right)$. Obviously the system sum-rate with quantized channel state information is smaller than the system sum-rate with perfect channel state information,

$$R\left(\boldsymbol{\pi}_{\mathcal{C},v}, \mathcal{S}_v, h\right) \leq R\left(\boldsymbol{\pi}_{\mathcal{C},h}, \mathcal{S}_h, h\right).$$

Clearly, the scheduling decisions based on quantized channel state information (2.6) should match with the scheduling decision based on perfect channel state information (2.5) as good as possible. This is the motivation for the feedback protocol developed in the next

section.

Remark 2.1. Since the precoding vectors are given by a fixed codebook, the optimization problems (2.5) and (2.6) are combinatorial problems that can be solved either by a brute force search over the user sets $\mathcal{S} \subseteq \mathcal{U}$, with $|\mathcal{S}| \leq n_s$, and the mappings $\boldsymbol{\pi}_{\mathcal{C}} : \mathcal{S} \to \mathcal{C}$ or more efficiently in a greedy fashion. Efficient algorithms to solve the scheduling problems (2.6) and (2.5) are important in practical applications. In the theoretical setting of the next sections, one can always assume that the scheduling problem is perfectly solved. In the simulations presented in Section 2.5 we compare the performance of a greedy solution and a brute force solution numerically.

2.2 Rate Approximation Feedback Strategy

In this section we develop the rate approximation feedback strategy that enables the base station to approximate the per user rates (2.4) for any scheduling decision $(\boldsymbol{\pi}_{\mathcal{C}}, \mathcal{S})$. The key idea is to let each user m minimize the maximal rate mismatch between the per user rates $r_m(\boldsymbol{\pi}_{\mathcal{C}}, \mathcal{S}, \lambda_m \boldsymbol{h}_m)$ in (2.5) and $r_m(\boldsymbol{\pi}_{\mathcal{C}}, \mathcal{S}, \vartheta_m \boldsymbol{v}_m)$ in (2.6) independent of the scheduling decision. As we will see this approach enables the base station to control the average gap between the system sum-rate based on scheduling with perfect and quantized channel state information, defined as

$$\Delta := \mathbb{E}\left[R\left(\boldsymbol{\pi}_{\mathcal{C},h}, \mathcal{S}_h, h\right) - R\left(\boldsymbol{\pi}_{\mathcal{C},v}, \mathcal{S}_v, h\right)\right].$$

The following lemma shows that to control Δ the maximal instantaneous per user rate approximation error, for some $\boldsymbol{h} \in \mathbb{C}^{n_t}$ and $\boldsymbol{v} \in \mathbb{C}^{n_t}$,

$$d(\boldsymbol{h}, \boldsymbol{v}) := \max_{\mathcal{S} \in \mathcal{S}_m} \max_{\boldsymbol{\pi}_{\mathcal{C}}: \mathcal{S} \to \mathcal{C}} |r_m(\boldsymbol{\pi}_{\mathcal{C}}, \mathcal{S}, \boldsymbol{h}) - r_m\left(\boldsymbol{\pi}_{\mathcal{C}}, \mathcal{S}, \boldsymbol{v}\right)|, \tag{2.7}$$

needs to be minimized. We defined $\mathcal{S}_m$ as the set of scheduled decisions that include user m and have cardinality not exceeding n_s,

$$\mathcal{S}_m := \{\mathcal{S} \subseteq \mathcal{U} \,:\, m \in \mathcal{S} \,\text{and}\, |\mathcal{S}| \leq n_s\}.$$

The following lemma states the upper bound on Δ.

Lemma 2.2. *Let the beamforming vectors be given by a fixed codebook $\mathcal{C} \subset \mathbb{S}^{n_t - 1}$. If the base station has quantized channel state information $v = \{\vartheta_m \boldsymbol{v}_m\}_{m \in \mathcal{U}}$, the average system*

sum-rate gap is bounded by

$$\Delta = \mathbb{E}\left[R\left(\boldsymbol{\pi}_{\mathcal{C},h}, \mathcal{S}_h, h\right) - R\left(\boldsymbol{\pi}_{\mathcal{C},v}, \mathcal{S}_v, h\right)\right] \leq 2\,\mathbb{E}\left[\sum_{m \in \mathcal{S}_h \cup \mathcal{S}_v} d(\lambda_m \boldsymbol{h}_m, \vartheta_m \boldsymbol{v}_m)\right],$$

where $(\boldsymbol{\pi}_{\mathcal{C},h}, \mathcal{S}_h)$ *is the solution to* (2.5) *and* $(\boldsymbol{\pi}_{\mathcal{C},v}, \mathcal{S}_v)$ *is the solution to* (2.6)*.*

The proof is given in Section 2.7.1. A few remarks are in place. If the worst case rate approximation error

$$\Delta_{RA} := 2\,\mathbb{E}\left[\sum_{m \in \mathcal{S}_h \cup \mathcal{S}_v} d(\lambda_m \boldsymbol{h}_m, \vartheta_m \boldsymbol{v}_m)\right] \tag{2.8}$$

is minimized, the average average system sum-rate gap Δ remains bounded by Δ_{RA}. To control Δ_{RA} each user $m \in \mathcal{U}$ needs to individually minimize the per user rate approximation error $d(\hat{\boldsymbol{h}}_m, \vartheta_m \boldsymbol{v}_m)$. Therefore, we define the following feedback strategy.

Definition 2.3 (Rate approximation feedback strategy)**.** *To determine its feedback message each user* $m \in \mathcal{U}$ *must find a tuple* $(\vartheta_m, \boldsymbol{v}_m) \in (\mathbb{R}, \mathcal{V})$ *that minimizes the per user rate approximation error*

$$\min_{\vartheta \in \mathbb{R}} \min_{\boldsymbol{v} \in \mathcal{V}} d(\lambda_m \boldsymbol{h}_m, \vartheta \boldsymbol{v}). \tag{2.9}$$

Although not apparent at this point, let us indicate some relevant properties of the rate approximation feedback strategy.

1. In the feedback decision function $d(\boldsymbol{h}, \boldsymbol{v})$ (2.5) the transmit codebook matters which seems good engineering practice as we use all available information. See Lemma 2.7 for an illustration.

2. The feedback strategy can be extended towards scenarios where the quantized channel state information must be averaged over multiple correlated channel realizations (e.g. OFDM subcarriers) (see Section 2.4.1).

3. Based on the per user rate approximation error $d(\boldsymbol{h}, \boldsymbol{v})$ feedback codebooks can be designed as described in Section 2.4.2.

In the following section we analyze the performance of a wireless network that uses the rate approximation feedback strategy. Moreover, a simpler quantization function is found which is easier to calculate than the computationally complex rate approximation error (2.7). Based on the simpler quantization function, we develop an efficient and robust feedback protocol which is presented in Section 2.4.3.

2.3 Performance Analysis

Providing good analysis techniques and results is a difficult issue. Not only should the analysis reflect the actual scenario but also give the correct tendency with respect to real system performance. One good example in this regard is given by the large number of users results, typically proving to achieve the optimal multi-user diversity gain. Another example are degrees of freedom or multiplexing gain results which prove that a particular transmit strategy achieves the optimal degrees of freedom if the SNR (i.e. transmit power) is taken to infinity. For a multi-user MIMO system with limited feedback it has been proved that for asymptotically large number of users $|\mathcal{U}|$ and asymptotically large SNR the sum-rate scales like $n_t \log\log|\mathcal{U}|$. This was shown for unitary random beamforming (i.e. the beamforming vectors are given by a random unitary codebook) [SH05], zeroforcing beamforming [YG06] and PU2RC [HAH09]. However, since the number of users is finite in a practical system and the operating point is typically in the low to average SNR range, the significance of such results can be questioned. Putting it the other way around: two methods achieving the optimal multi-user multiplexing gain might behave completely different in a practical system. Therefore our analysis is more inspired by the finite user results in [Jin06, dFKSG07, CJKR10]. First, we assume that the number of users is equal to the number of transmit antennas $|\mathcal{U}| = n_t$, all users are active $\mathcal{S} = \mathcal{U}$ and the elements of the transmit codebook is unitary $\mathcal{C}$. These assumptions enable stringent comparison to Jindal's result in [Jin06] for zeroforcing beamforming. In Section 2.3.3, we extend the results to include a user selection and codebooks that constitute a tight frame.

2.3.1 Fixed Codebook Beamforming vs. Zeroforcing Beamforming

Before analyzing the rate approximation feedback strategy, we review some basic results for zeroforcing beamforming and show (Theorem 2.6) that beamforming based on a fixed codebook can indeed outperform zeroforcing beamforming. Many papers consider zeroforcing beamforming for the performance analysis of multi-user MIMO systems; for example [Jin06, AYL07, CJKR10]. When using zeroforcing beamforming with perfect channel state information at the base station, each beamforming vector $\boldsymbol{\pi}_{ZF,h}(m) \in \mathbb{S}^{n_t-1}$ is chosen to be in the null space of the matrix $[\boldsymbol{h}_l]_{l\in\mathcal{S}\setminus\{m\}}$. If $|\mathcal{S}| \leq n_t$ and the channel vectors are random and independent, a zeroforcing beamforming solution exists with high probability. For zeroforcing beamforming with perfect channel state information at the base station the system sum-rate is given by

$$R\left(\boldsymbol{\pi}_{ZF,h}, \mathcal{S}, h\right) = \sum_{m\in\mathcal{S}} \log\left(1 + \lambda_m^2 |\langle \boldsymbol{h}_m, \boldsymbol{\pi}_{ZF,h}(m)\rangle|^2\right),$$

which is almost surely non-zero for any receive SNR $\lambda_m > 0$.

A popular feedback strategy is random vector quantization (RVQ) where $\mathcal{V}_{RVQ} = \{\boldsymbol{v}_1, \boldsymbol{v}_2, \ldots, \boldsymbol{v}_{2^B}\} \subseteq \mathbb{S}^{n_t-1}$ is a codebook of random vectors isotropically distributed on the unit sphere. In contrast to the rate approximation feedback strategy, user m chooses his feedback message to minimize the chordal distance

$$d_C(\boldsymbol{h}_m, \boldsymbol{v}) = \sqrt{1 - |\langle \boldsymbol{v}, \boldsymbol{h}_m \rangle|^2}. \tag{2.10}$$

Remark 2.4. The chordal distance aims at approximating the channel of each user as good as possible. But in contrast to the rate approximation distance (2.7), the minimum chordal distance is not capable of considering the relations between the channel and the beamforming vectors, defined by a fixed codebook.

Define $R(\boldsymbol{\pi}_{ZF,v}, \mathcal{S}, h)$ as the sum-rate with zeroforcing beamforming based on quantized channel state information

$$v_{RVQ} = \left(\boldsymbol{v}_m = \underset{\boldsymbol{v} \in \mathcal{V}_{RVQ}}{\arg\min}\, d_C(\boldsymbol{h}_m, \boldsymbol{v}) \right)_{m \in \mathcal{U}}.$$

From [Jin06] we have the following performance bound for zeroforcing beamforming with random vector quantization, which will act as a baseline for our analysis presented below.

Theorem 2.5 ([Jin06, Theorem 2])**.** *Let $\mathcal{S} = \mathcal{U} = \{1, 2, \ldots, n_t\}$. Suppose that the channels are distributed according to $\hat{\boldsymbol{h}}_{m,i} \sim \mathcal{CN}(0, 1)$, $\forall m \in \mathcal{U}$ and all $1 \leq i \leq n_t$, independent across users and antennas. Then, random vector quantization with B feedback bits per user incurs a throughput loss relative to zeroforcing beamforming with perfect channel state information according to*

$$\begin{aligned} \Delta_{RVQ} &= \mathbb{E}\left[R\left(\boldsymbol{\pi}_{ZF,h}, \mathcal{S}, h\right)\right] - \mathbb{E}\left[R(\boldsymbol{\pi}_{ZF,v}, \mathcal{S}, h)\right] \\ &< n_t \log\left(1 + P 2^{-\frac{B}{n_t - 1}}\right), \end{aligned} \tag{2.11}$$

where the expectation is taken with respect to the random channels and the random codebook.

The proof is given in [Jin06]. Before we are analyzing the performance of the rate approximation feedback strategy we assume perfect channel state information at the base station and compare the performance of zeroforcing beamforming and beamforming based on a fixed codebook. To this end, define

$$\Delta_{CSI} = \mathbb{E}\left[R\left(\boldsymbol{\pi}_{ZF,h}, \mathcal{S}, h\right) - R\left(\boldsymbol{\pi}_{\mathcal{C},h}, \mathcal{S}, h\right)\right],$$

for fixed $\mathcal{S}$. In the following theorem, the channel is modeled as isotropic fading [JG05]. In particular, we fix the channel gains $\mu_m = \|\hat{\boldsymbol{h}}_m\|_2$ for $m \in \mathcal{U}$ and let the only randomness be an independent phase ambiguity in the channel coefficients, i.e. $\hat{\boldsymbol{h}}_m = \mu_m \boldsymbol{h}_m$ where $\boldsymbol{h}_m \in \mathbb{S}^{n_t-1}$ is an isotropically distributed random complex unit vector. This assumption has no impact on the generality of the results; in fact, it only allows us to streamline the presentation throughout this proof. The following result is qualitatively known but we make it mathematically more precise.

Theorem 2.6. *If $\mathcal{U} = \mathcal{S} = \{1, 2, \ldots, n_t\}$ and each user has perfect channel state information, then for isotropic fading with any non-random $\mu_1 \geq \mu_2 \geq ... \geq \mu_{n_t}$ (i.e. non-random $\lambda_1^2 \geq \lambda_2^2 \geq ... \geq \lambda_{n_t}^2$) the rate gap between zeroforcing beamforming and beamforming with a fixed unitary codebook is bounded from above by*

$$\Delta_{CSI} \leq \sum_{m \in \mathcal{S}} \log \left(1 + \min_{\epsilon > 0} \lambda_m^2 \frac{\left(1 + \lambda_m^2\right) \frac{1}{n_t - 1} - \left(1 + \frac{\lambda_m^2}{n_t - 1}\right) \frac{c(\epsilon)(1-\epsilon)\log(n_t - m + 1)}{(1+\epsilon)^2 n_t}}{1 + \lambda_m^2} \right)$$

where $c(\epsilon) := \left(1 - e^{-(n_t - m + 1)^{\epsilon}} - \frac{1}{\epsilon n_t}\right)$.

The proof can be found in Subsection 2.7.2. Theorem 2.6 states that for some $\lambda_m \leq \lambda^*$ the rate gap Δ_{CSI} is indeed negative; this can be seen by observing that at low SNR (i.e. $\lambda_m \to 0$) for all $m < n_t$ the difference is roughly

$$\frac{1}{n_t - 1} - \frac{\log(n_t - m + 1)}{n_t} < 0$$

by choosing $c(\epsilon) = \frac{\log(\log(n_t))}{\log(n_t)}$ and n_t large enough. Thus, for low SNR beamforming based on a fixed transmit codebook can indeed outperform zeroforcing beamforming. This observation is further underlined by Figure 2.3. We stress that this is not a surprising result because zeroforcing beamforming is an altruistic beamforming scheme which does not consider the desired channel. However, the result motivates the analysis of a fixed beamforming scheme for practical scenarios which operate in a low to moderate SNR regime.

2.3.2 Rate Approximation with Unitary Transmit Codebooks

Let us first provide a rather technical bound for the per user rate approximation error (2.7).

Lemma 2.7. *Let $\mathcal{U} = \mathcal{S} = \{1, 2, \ldots, n_t\}$, the transmit codebook $\mathcal{C}$ be unitary and a subset of the feedback codebook $\mathcal{V} \subset \mathbb{S}^{n_t-1}$, $\mathcal{C} \subseteq \mathcal{V}$. Let $\boldsymbol{w}^* = \arg\max_{\boldsymbol{w} \in \mathcal{C}} |\langle \boldsymbol{h}_m, \boldsymbol{w} \rangle|^2$. If for fixed*

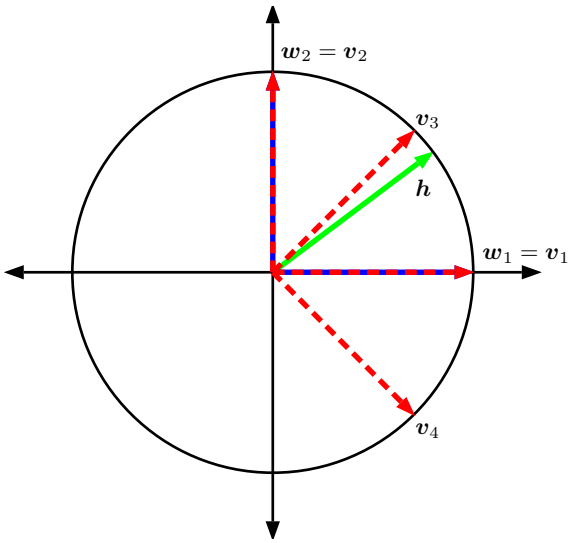

Figure 2.2: Example in $\mathbb{R}^2$, with $n_t = 2$ and $n_r = 1$. The sub-optimal feedback strategy considered in Lemma 2.7 selects $\boldsymbol{v}_1$ since $|\langle \boldsymbol{v}_1, \boldsymbol{w}^* \rangle| \geq |\langle \boldsymbol{h}, \boldsymbol{w}^* \rangle|$ must hold and in this example $\boldsymbol{w}^* = \boldsymbol{w}_1$. In contrast, if the minimum chordal distance (2.10) is used, $\boldsymbol{v}_3$ is selected since $d_C(\boldsymbol{h}, \boldsymbol{v})$ is minimized by $\boldsymbol{v} = \boldsymbol{v}_3$.

$\lambda_m \in \mathbb{R}$ and $\boldsymbol{h}_m \in \mathbb{S}^{n_t - 1}$ the feedback message is given by the vector

$$\boldsymbol{v}_m = \arg\max_{\boldsymbol{v} \in \mathcal{V}} |\langle \boldsymbol{v}, \boldsymbol{h}_m \rangle| \quad \textit{subject to} \ \max_{\boldsymbol{w} \in \mathcal{C}} |\langle \boldsymbol{v}_m, \boldsymbol{w} \rangle| \geq \max_{\boldsymbol{w} \in \mathcal{C}} |\langle \boldsymbol{h}_m, \boldsymbol{w} \rangle|$$

and the scalar ϑ_m is chosen to satisfy $\frac{\lambda_m^2 |\langle \boldsymbol{h}_m, \boldsymbol{w}^* \rangle|^2}{1 + \lambda_m^2 (1 - |\langle \boldsymbol{h}_m, \boldsymbol{w}^* \rangle|^2)} = \frac{\vartheta_m^2 |\langle \boldsymbol{v}_m, \boldsymbol{w}^* \rangle|^2}{1 + \vartheta_m^2 (1 - |\langle \boldsymbol{v}_m, \boldsymbol{w}^* \rangle|^2)}$, then

$$\begin{aligned} & d(\lambda_m \boldsymbol{h}_m, \vartheta_m \boldsymbol{v}_m) = \max_{\boldsymbol{\pi}_{\mathcal{C}} : \mathcal{S} \to \mathcal{C}} |r_m(\boldsymbol{\pi}_{\mathcal{C}}, \mathcal{S}, \lambda_m \boldsymbol{h}_m) - r_m(\boldsymbol{\pi}_{\mathcal{C}}, \mathcal{S}, \vartheta_m \boldsymbol{v}_m)| \\ & \leq \max_{\boldsymbol{w} \neq \boldsymbol{w}^*} \log \left(1 + \frac{\lambda_m^2 \left(\left| |\langle \boldsymbol{h}_m, \boldsymbol{w} \rangle|^2 - |\langle \boldsymbol{v}_m, \boldsymbol{w} \rangle|^2 \right| + \frac{\langle \boldsymbol{v}_m, \boldsymbol{w} \rangle}{\langle \boldsymbol{v}_m, \boldsymbol{w}^* \rangle} \left| |\langle \boldsymbol{v}_m, \boldsymbol{w}^* \rangle|^2 - |\langle \boldsymbol{h}_m, \boldsymbol{w}^* \rangle|^2 \right| \right)}{1 + \lambda_m^2 \left(1 - \max \left\{ |\langle \boldsymbol{h}_m, \boldsymbol{w} \rangle|^2, |\langle \boldsymbol{v}_m, \boldsymbol{w} \rangle|^2 \right\} \right)} \right). \end{aligned}$$

The proof is given in Subsection 2.7.3.

Remark 2.8. The sub-optimal feedback strategy in Lemma 2.7 supports the intuition that the rate approximation error for the best beamforming vector, taken from the codebook $\mathcal{C}$, should be set to zero by the feedback strategy. Consider the example in Figure 2.2: The sub-optimal feedback strategy considered in Lemma 2.7 selects $\boldsymbol{v}_1$ since $|\langle \boldsymbol{v}_1, \boldsymbol{w}^* \rangle| \geq |\langle \boldsymbol{h}, \boldsymbol{w}^* \rangle|$ must hold and in this example $\boldsymbol{w}^* = \boldsymbol{w}_1$. In contrast, if the minimum chordal distance (2.10) is used, $\boldsymbol{v}_3$ is selected since $d_C(\boldsymbol{h}, \boldsymbol{v})$ is minimized by $\boldsymbol{v} = \boldsymbol{v}_3$.

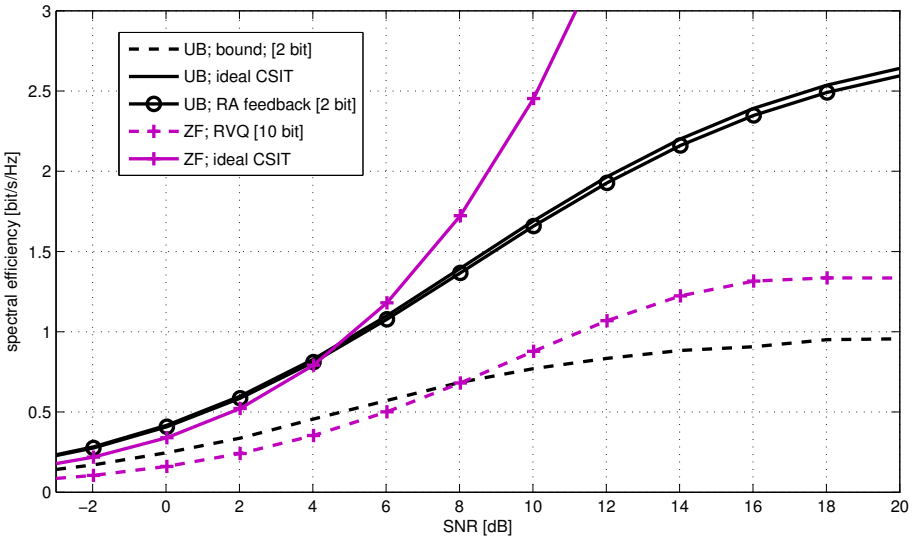

Figure 2.3: Achievable rate vs. receive SNR, comparison of zeroforcing beamforming with perfect channel state information, unitary beamforming with perfect channel state information, the rate approximation feedback strategy with unitary transmit codebooks, the unitary beamforming bound (UB; bound) is given by Corollary 2.9. Setup: $n_t = 4$, $\mathcal{U} = \mathcal{S} = \{1, 2, 3, 4\}$.

While the error term in Lemma 2.7 is not easy to access, we devise the following corollary.

Corollary 2.9. *Under the assumptions of Lemma 2.7. If $\mathcal{C} \equiv \mathcal{V}$ then*

$$\Delta_{RA} \leq 2 \sum_{m=1}^{n_t} \mathbb{E}\left[\log\left(1 + \max_{\boldsymbol{w} \neq \boldsymbol{w}^*} \frac{\lambda_m^2 |\langle \boldsymbol{h}_m, \boldsymbol{w}\rangle|^2}{1 + \lambda_m^2 (1 - |\langle \boldsymbol{h}_m, \boldsymbol{w}\rangle|^2)}\right)\right]$$

and

$$\vartheta_m^2 := \frac{\lambda_m^2 |\langle \boldsymbol{h}_m, \boldsymbol{v}_m\rangle|^2}{1 + \lambda_m^2 (1 - |\langle \boldsymbol{h}_m, \boldsymbol{v}_m\rangle|^2)}.$$

Proof. If $\mathcal{C} \equiv \mathcal{V}$, than $|\langle \boldsymbol{v}_m, \boldsymbol{w}\rangle|^2 = 0$ for all $\boldsymbol{w} \neq \boldsymbol{w}^*$. Thus, from Lemma 2.7 we have

$$d(\lambda_m \boldsymbol{h}_m, \vartheta_m \boldsymbol{v}_m) \leq \max_{\boldsymbol{w} \neq \boldsymbol{w}^*} \log\left(1 + \frac{\lambda_m^2 \left| |\langle \boldsymbol{h}_m, \boldsymbol{w}\rangle|^2 - |\langle \boldsymbol{v}_m, \boldsymbol{w}\rangle|^2 \right|}{1 + \lambda_m^2 \left(1 - |\langle \boldsymbol{h}_m, \boldsymbol{w}\rangle|^2\right)}\right).$$

Since, $\mathcal{S}_h = \mathcal{S}_v = \mathcal{S}$ the claim follows from (2.8). □

Corollary 2.9 together with Lemma 2.2 gives a first lower bound on the performance of the rate approximation feedback strategy with a unitary transmit and feedback codebook. Under the assumptions of Corollary 2.9 the bound can be given by

$$\mathbb{E}\left[R\left(\boldsymbol{\pi}_{\mathcal{C},v}, \mathcal{S}_v, h\right)\right] \geq \mathbb{E}\left[R\left(\boldsymbol{\pi}_{\mathcal{C},h}, \mathcal{S}_h, h\right)\right] - \Delta_{RA}.$$

Figure 2.3 depicts the achievable rate over the receive SNR. The rate approximation feedback strategy with a unitary transmit and feedback codebook, $\mathcal{C} = \mathcal{V}$, is compared with random vector quantization and zeroforcing beamforming. We observe that for a relevant range of SNR values (3 to 8 dB) the rate error bound for the rate approximation feedback strategy predicts a better performance then the simulated achievable rate for zeroforcing beamforming with random vector quantization; while random vector quantization requires 10 bit of feedback the rate approximation feedback strategy bound holds for $\log(n_t) = 2$ bit. In fact, the achievable rate of the rate approximation scheme with 2 bit feedback is very close to unitary beamforming with perfect channel state information.

So far, we assumed that the feedback codebook is unitary and equal to the transmit codebook $\mathcal{V} = \mathcal{C}$. We saw that the rate loss due to limited feedback is very small. However, we assumed that the number of users is equal the number of receive antennas and enabled no user selection. To enable efficient user selection the size of the feedback codebook must be increased. The following lemma shows that Δ_{RA} remains bounded when the SNR increases and that the rate error is dominated by the function

$$D_m(B) = \min_{\substack{\mathcal{V}\subset\mathbb{S}^{n_t-1}\\|\mathcal{V}|=2^B}} \mathbb{E}\left[\frac{1}{1-\tilde{\lambda}_m}\min_{0<\tilde{\vartheta}_m<1}\min_{\boldsymbol{v}\in\mathcal{V}}\max_{\boldsymbol{w}\in\mathcal{C}}\left|\tilde{\lambda}_m|\langle \boldsymbol{h}_m,\boldsymbol{w}\rangle|^2-\tilde{\vartheta}_m|\langle \boldsymbol{v},\boldsymbol{w}\rangle|^2\right|\right],$$

with $\tilde{\lambda}_m = \frac{\lambda_m^2}{1+\lambda_m^2}$ and $\tilde{\vartheta}_m = \frac{\vartheta_m^2}{1+\vartheta_m^2}$ and B the number of bits required to feed back the index of an element of the codebook $\mathcal{V}$, $|\mathcal{V}| = 2^B$.

Lemma 2.10. *Let $\mathcal{U} = \mathcal{S} = \{1, 2, \ldots, n_t\}$, the transmit codebook $\mathcal{C}$ be unitary and a subset of the feedback codebook $\mathcal{V} \subset \mathbb{S}^{n_t-1}$, $\mathcal{C} \subseteq \mathcal{V}$. If the rate approximation feedback strategy* (2.9) *is used, then*

$$\Delta_{RA} \leq 2\sum_{m=1}^{n_t}\log\left(1+\min_{\epsilon>0}\frac{(1+\epsilon)\,D_m(B)}{1+\frac{\epsilon}{n_t-1}D_m(B)}\right).$$

The proof is given in Subsection 2.7.4. The following lemma gives a fundamental bound on $D_m(B)$.

Lemma 2.11. *If the transmit codebook $\mathcal{C}$ is unitary, then*

$$D_m(B) \leq c(n_t)\mathbb{E}\left[\lambda_m^2\right]2^{-\frac{B}{n_t-1}},$$

with

$$c(n_t) = \left(\Theta(\mathcal{B}_2^{n_t-1})\binom{2n_t-2}{n_t-1}\frac{\Gamma(1+\frac{n_t-1}{2})\sqrt{n_t}}{(n_t-1)!\pi^{\frac{n_t-1}{2}}}\right)^{\frac{1}{n_t-1}} \tag{2.12}$$

and $B \geq \frac{(n_t-1)}{2}\log[(n_t-1)\sqrt{n_t-1}]$. *For* n_t-1 *small tight bounds are known for the covering density* $\Theta(\mathcal{B}_2^{n_t-1})$, *e.g.* $\Theta(\mathcal{B}_2^2) \leq 1.2091$ *(Kershner, 1939),* $\Theta(\mathcal{B}_2^3) \leq 1.4635$ *(Bambah, 1954),* $\Theta(\mathcal{B}_2^4) \leq 1.7655$ *(Delone & Ryshkov, 1963). For* $n_t - 1 \geq 3$ *the Rogers bound [B0̈4]* $\Theta(\mathcal{B}_2^{n_t-1}) < 4(n_t-1)\log(n_t-1)$ *can be used.*

The proof can be found in Subsection 2.7.5. Note that $c(n_t)$ is close to unity and falls below unity not before $n_t \geq 14$, as required for improved scaling compared to Jindal's result. As the following illustration for the case $n_t = 3$ shows, this seems to be an artifact of the proof technique.

Example 2.12. Without loss of generality, we assume the unitary transmit codebook is given by the standard ONB. We drop the user index m and define the real positive vectors $\boldsymbol{\psi} = (\psi_1, \ldots, \psi_3)$ with $\psi_n := |\langle \boldsymbol{h}, \boldsymbol{\pi}_{\mathcal{C}}(n)\rangle|^2$ and $\boldsymbol{\phi}^{\boldsymbol{v}} = (\phi_1^{\boldsymbol{v}}, \ldots, \phi_3^{\boldsymbol{v}})$ with $\phi_n^{\boldsymbol{v}} := |\langle \boldsymbol{v}, \boldsymbol{\pi}_{\mathcal{C}}(n)\rangle|^2$ for each $\boldsymbol{v} \in \mathcal{V}$. Per definition, all these vectors have unit ℓ_1-norm, $\|\boldsymbol{\psi}\|_1 = \|\boldsymbol{\phi}^{\boldsymbol{v}}\|_1 = 1$ and, hence, define points on the standard 2-simplex. Further, $\max_{\boldsymbol{\pi}_{\mathcal{C}}} |\psi_n - \phi_n^{\boldsymbol{v}}| = \|\boldsymbol{\psi} - \boldsymbol{\phi}^{\boldsymbol{v}}\|_\infty$ defines a distance between two points on the standard 2-simplex. Hence, for a given feedback codebook $\mathcal{V}$ we can define the Voronoi region around the point $\boldsymbol{\phi}^{\boldsymbol{v}}$ for a particular $\boldsymbol{v} \in \mathcal{V}$ as $V(\boldsymbol{\phi}^{\boldsymbol{v}}) = \{\boldsymbol{x} \in \mathbb{R}_+^3 : \|\boldsymbol{x} - \boldsymbol{\phi}^{\boldsymbol{v}}\|_\infty < \|\boldsymbol{x} - \boldsymbol{\phi}^{\boldsymbol{\xi}}\|_\infty, \forall \boldsymbol{\xi} \in \mathcal{V}, \boldsymbol{\xi} \neq \boldsymbol{v}\}$. If $B \in \{1, 2, 4, \ldots\}$ and $n_t = 3$, the feedback codebook can be chosen such that the Voronoi regions are 2-simplices with edge length $\tilde{\delta} \leq \sqrt{2}$. Using the symmetry of the covering and projecting the quantization points back on the coordinate axes (see Figure 2.4) we get $\max_{\boldsymbol{x} \in V(\boldsymbol{\phi}^{\boldsymbol{v}})} \|\boldsymbol{x} - \boldsymbol{\phi}^{\boldsymbol{v}}\|_\infty = \tilde{\delta}/\sqrt{8} = \delta$.

Now we can compute the volumes of the 2-simplices (the standard simplex and the scaled simplex) and proceed as in the proof of Lemma 2.11 to obtain the result

$$\delta = \max_{\boldsymbol{x} \in V(\boldsymbol{\phi}^{\boldsymbol{v}})} \|\boldsymbol{x} - \boldsymbol{\phi}^{\boldsymbol{v}}\|_\infty = 2^{-\frac{B}{n_t-1}-1}.$$

Hence, if $n_t = 3$ and Rayleigh fading is assumed (i.e. $\hat{\boldsymbol{h}}_{m,i} \sim \mathcal{CN}(0,1)$ for $i = 1, \ldots, n_t$ and $m \in \mathcal{U}$), the rate loss due to the rate-constrained feedback channel scales like

$$\begin{aligned}\Delta_{RA} \leq & 2\sum_{m=1}^{n_t} \log\left(1 + \min_{\epsilon>0} \frac{(1+\epsilon)\,\mathbb{E}\left[\frac{\tilde{\lambda}_m}{1-\tilde{\lambda}_m}\right] 2^{-\frac{B}{n_t-1}-1}}{1 + \mathbb{E}\left[\frac{\tilde{\lambda}_m}{1-\tilde{\lambda}_m}\right] \frac{\epsilon}{n_t-1} 2^{-\frac{B}{n_t-1}-1}}\right) \\ \leq & 2\sum_{m=1}^{n_t} \log\left(1 + P 2^{-\frac{B}{n_t-1}-1}\right).\end{aligned}$$

Therefore, we have an improvement of $n_t - 1$ bits in the exponential term compared to Jindal's result for zeroforcing beamforming with feedback based on minimizing the chordal distance (see [Jin06]) – under the very same assumptions.

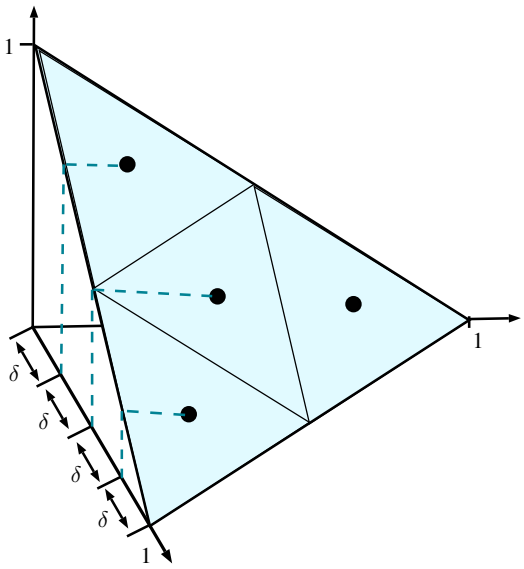

Figure 2.4: The standard 2-simplex in 3 dimensions. The projection of the quantization points $\mathcal{Q}$ on the coordinate axes implies a worst case quantization error δ.

2.3.3 Rate Approximation with User Selection and Extended Codebooks

In this subsection we assume that the elements of the transmit codebook constitute a tight frame and allow user selection at the base station.

Theorem 2.13. *Assume each element of the channel matrix are given by independent copies of $h \sim \mathcal{CN}(0,1)$. Let the transmit codebook $\mathcal{C} \subset \mathbb{S}^{n_t-1}$ and the feedback codebook $\mathcal{V} \subset \mathbb{S}^{n_t-1}$ be arbitrary. If for each transmission the base station select a subset of active users $\mathcal{S} \subseteq \mathcal{U}$, then under the rate approximation feedback strategy*

$$\Delta_{RA} \leq 4n_s \log\left(1 + Pn_t\mathbb{E}\left[\max_{\boldsymbol{w}\in\mathcal{C}} \left||\langle \boldsymbol{h}_m, \boldsymbol{w}\rangle|^2 - |\langle \boldsymbol{v}, \boldsymbol{w}\rangle|^2\right|\right]\right).$$

The proof can be found in Subsection 2.7.6. The expected value

$$\hat{D}_m(B) := \min_{\mathcal{V},|\mathcal{V}|=2^B} \mathbb{E}\left[\min_{\boldsymbol{v}\in\mathcal{V}} \max_{\boldsymbol{w}\in\mathcal{C}} \left||\langle \boldsymbol{h}_m, \boldsymbol{w}\rangle|^2 - |\langle \boldsymbol{v}, \boldsymbol{w}\rangle|^2\right|\right]$$

has been shown to be analytically tractable – in the previous section – for unitary transmit codebooks. For codebooks constituting a tight frame (see (1.1)) we devise the following corollary.

Corollary 2.14. *If the transmit codebook $\mathcal{C}$ is a tight frame, then $\hat{D}_m(B) \leq Ac(n_t)2^{-\frac{B}{n_t-1}}$, where $c(n_t)$ is defined in* (2.12) *and A is the frame constant in* (1.1).

Proof. The proof is a simple extension of Lemma 2.11. A tight frame with frame constant A can be generated by the union of A orthonormal bases $\mathcal{B}_i$, $i = 1, \ldots, A$. Hence, $\mathcal{C} = \cup_{i=1}^{A} B_i$ and therefore

$$\hat{D}_m(B) \leq A \min_{\mathcal{V},|\mathcal{V}|=2^B} \mathbb{E}\left[\min_{\boldsymbol{v}\in\mathcal{V}} \max_{i=1,\ldots,A} \max_{\boldsymbol{w}\in\mathcal{B}_i} \left||\langle \boldsymbol{h}_m, \boldsymbol{w}\rangle|^2 - |\langle \boldsymbol{v}, \boldsymbol{w}\rangle|^2\right|\right]$$

and we can proceed as in the proof of Lemma 2.11. □

2.4 Practical Considerations

This section highlights some of the advantages of the rate approximation feedback strategy in practical scenarios. The rate approximation feedback strategy is extended to systems using OFDM. We show that the rate approximation scheme can be used to implicitly averages the achievable rates over multiple OFDM subcarriers. An algorithm to generate feedback codebooks based in the channel statistics is presented. Finally, we introduce a new distance function that is less complex than the original rate approximation distance function (2.7).

2.4.1 Rate Approximation Feedback for OFDM Systems

A popular transmission technique for wideband systems is OFDM. OFDM essentially divides the frequency band in many orthogonal subcarriers. In cellular systems like LTE, the OFDM subcarriers are grouped in scheduling blocks; the smallest scheduling unit. Usually a single feedback message per scheduling block is required. The extension of the rate approximation feedback strategy to OFDM systems exploits the correlation of neighboring subcarriers and provides a single feedback message that implicitly averages the channels over a scheduling block by operating on the average achievable rate per scheduling block.

Consider a single scheduling block and collect its subcarrier indices in the set $\mathcal{F}$. For simplicity assume that all users have single antenna, $n_r = 1$. Extensions to multiple antennas are straightforward if the receive filter is fixed prior feedback. The signal received by user m on subcarrier $f \in \mathcal{F}$ can be written as

$$y_m(f) = \langle \hat{\boldsymbol{h}}_m(f), \boldsymbol{x}(f)\rangle + n_m(f),$$

where $\hat{\boldsymbol{h}}_m(f)$ is the channel, $\boldsymbol{x}(f) \in \mathbb{C}^{n_t \times 1}$ is the transmitted signal vector and $n_m(f) \sim \mathcal{CN}(0, 1)$ is additive white Gaussian noise. On all subcarriers in $\mathcal{F}$ the same users are scheduled, collected in the set $\mathcal{S}$. Each user $m \in \mathcal{S}$ is assigned to a beamforming vector

$\boldsymbol{\pi}_{\mathcal{C}}(m)$ which is also the same for all subcarriers $f \in \mathcal{F}$ and given by an element of a transmit codebook $\mathcal{C}$, similar to (2.1) the signal transmitted on subcarrier $f \in \mathcal{F}$ is

$$\boldsymbol{x}(f) = \sum_{m \in \mathcal{S}} \frac{P}{|\mathcal{S}|} \boldsymbol{\pi}_{\mathcal{C}}(m) s_m(f),$$

where $s_m(f)$ are the information symbols for user $m \in \mathcal{S}$ transmitted on subcarrier $f \in \mathcal{F}$. For simplicity, we assume an average sum-power constraint per subcarrier, i.e., the transmitted signal must satisfy $\mathbb{E}\left[\|\boldsymbol{x}(f)\|_2^2\right] \leq P$. The channels of user m are collected in the set

$$h_m(\mathcal{F}) = \left(\lambda_m(f)\boldsymbol{h}_m(f)\right)_{f \in \mathcal{F}}.$$

Such that we can extend definition (2.2) to

$$h(\mathcal{F}) = (h_m(\mathcal{F}))_{m \in \mathcal{U}}.$$

Now the average rate of user m on scheduling block $\mathcal{F}$ is

$$\bar{r}_m(\boldsymbol{\pi}_{\mathcal{C}}, \mathcal{S}, h_m(\mathcal{F})) := \frac{1}{|\mathcal{F}|} \sum_{\boldsymbol{h} \in h_m(\mathcal{F})} \log\left(1 + \mathrm{SINR}_m(\boldsymbol{\pi}_{\mathcal{C}}, \mathcal{S}, \boldsymbol{h})\right), \tag{2.13}$$

where $\mathrm{SINR}(\cdot)$ is defined in (2.3). Since we assume that user m has perfect knowledge of $h_m(\mathcal{F})$, for any potential scheduling decision $(\boldsymbol{\pi}_{\mathcal{C}}, \mathcal{S})$ user m can compute the average rate $\bar{r}_m(\boldsymbol{\pi}_{\mathcal{C}}, \mathcal{S}, h_m(\mathcal{F}))$. Therefore, instead of solving problem (2.9) to find the feedback message user m solves the problem

$$\min_{\boldsymbol{v} \in \mathcal{V}} \max_{\mathcal{S} \subseteq \mathcal{S}_m} \max_{\boldsymbol{\pi}_{\mathcal{C}}: \mathcal{S} \to \mathcal{C}} \left| \bar{r}_m(\boldsymbol{\pi}_{\mathcal{C}}, \mathcal{S}, h_m(\mathcal{F})) - r_m(\boldsymbol{\pi}_{\mathcal{C}}, \mathcal{S}, \hat{\vartheta}_m \boldsymbol{v}) \right|,$$

where $\hat{\vartheta}_m$ depends on the feedback codebook element $\boldsymbol{v}$ and the true channels $h_m(\mathcal{F})$. We define this dependency by requiring that $\hat{\vartheta}_m^2$ should be the SNR of a Gaussian channel having the same rate as if user m has the resource exclusively and uses beamforming vector $\boldsymbol{v}$, i.e., for a given $\boldsymbol{v}$ we define $\hat{\vartheta}_m$ as

$$\log(1 + \hat{\vartheta}_m^2) = \frac{1}{|\mathcal{F}|} \sum_{\boldsymbol{h} \in h_m(\mathcal{F})} \log\left(1 + |\langle \boldsymbol{h}, \boldsymbol{v} \rangle|^2\right).$$

The performance of the rate approximation scheme for OFDM systems is evaluated in the simulations in Section 2.5.

2.4.2 Feedback Codebook Design

In this section we describe how feedback codebooks for the rate approximation feedback strategy can be designed. The proposed algorithm is based on an algorithm by Linde, Buzo and Gray (LBG) [LBG80] which is an extension of the generalized Lloyd algorithm [Llo57]. A comprehensive overview of different versions of the Lloyd algorithm can be found in [GG92]. The LBG algorithm is known to converge to an optimum that is not guaranteed to be global. However, it is a practical way to design codebooks even if the statistics of the channels are unknown. The LBG algorithm can be used to generate codebooks for any given training set of sufficient size. Codebooks of arbitrary size can be generated from scratch or given codebooks can be adapted to the environment of a base station.

Our approach is inspired by [TBH08] and [MK06] who used the LBG algorithm to generate codebooks for wireless networks but with a different feedback and transmit strategy. For a given distance function $d(\boldsymbol{h}, \boldsymbol{v})$ the LBG algorithm finds the feedback codebook $\mathcal{V} = \{\boldsymbol{v}_1, \ldots, \boldsymbol{v}_N\}$ that (at least locally) minimizes the average distortion

$$D = \frac{1}{|\mathcal{T}|} \sum_{i=1}^{|\mathcal{V}|} \sum_{\boldsymbol{h} \in \mathcal{R}_i} d(\boldsymbol{h}, \boldsymbol{v}_i) \tag{2.14}$$

where $\mathcal{T} = \{\boldsymbol{h}_1, \ldots, \boldsymbol{h}_T\}$ is a possibly large set of channel realizations (i.e. training sequence) and $\mathcal{R}_i$ is the quantization region of $\boldsymbol{v}_i \in \mathcal{V}$,

$$\mathcal{R}_i = \{\boldsymbol{h} \in \mathcal{T} : d(\boldsymbol{h}, \boldsymbol{v}_i) \leq d(\boldsymbol{h}, \boldsymbol{v}_j), \forall\ j\}.$$

Another key ingredient of the LBG algorithm is the centroid condition. The centroid condition [GG92] states that the optimal codebook entry for quantization region $\mathcal{R}_i$ is

$$\min_{\boldsymbol{\zeta}_i \in \mathbb{S}^{n_t - 1}} \frac{1}{|\mathcal{R}_i|} \sum_{\boldsymbol{h} \in \mathcal{R}_i} d(\boldsymbol{h}, \boldsymbol{\zeta}_i)$$

For the rate approximation feedback strategy the distance function is given by (2.9). In this case, an analytic expression of the centroid is hard to obtain. We apply the following simplification

$$\mathrm{cent}(\mathcal{R}_i) = \arg\min_{\boldsymbol{\zeta}_i \in \mathcal{R}_i} \frac{1}{|\mathcal{R}_i|} \sum_{\boldsymbol{h} \in \mathcal{R}_i} d(\boldsymbol{h}, \boldsymbol{\zeta}_i).$$

The LBG algorithm starts by computing the centroid of the training set $\mathcal{T}$, i.e., $\mathrm{cent}(\mathcal{T})$.

Algorithm 1 LBG algorithm

1: Input: training sequence $\mathcal{T}$, desired codebook size L
2: Compute initial codebook $\mathcal{K}_0$ defined by (2.15).
3: Set: $k = 0$, $D_k = \infty$
4: **while** $|\mathcal{K}_0| < L$ **do**
5: **repeat**
6: $k = k + 1$
7: Compute the quantization regions $\mathcal{R}_i$ for $i = 1, \ldots, |\mathcal{K}_{k-1}|$.
8: Compute the new codebook

$$\mathcal{K}_k = \{\text{cent}(\mathcal{R}_1), \ldots, \text{cent}(\mathcal{R}_{|\mathcal{K}_k - 1|})$$

9: Compute the average distortion $D_k = D$ defined in (2.14).
10: **until** $(D_{k-1} - D_k)/(D_k) < \varepsilon$
11: Splitting: $\mathcal{K}_k = \mathcal{K}_k + \varepsilon \cap \mathcal{K}_k$
12: **end while**

The initial codebook is then given by

$$\mathcal{K}_0 = \{\text{cent}(\mathcal{T}) + \varepsilon, \quad \text{cent}(\mathcal{T})\} \tag{2.15}$$

Where $\varepsilon > 0$ is a design parameter that should be small. The LBG algorithm is summarized in Algorithm 1. It is executed until the desired codebook size is reached. In Figure 2.8 the performance gains with an optimized codebook are shown.

2.4.3 Decreased Complexity Rate Approximation

Mobile users usually have limited computing capabilities, therefore, solving the full rate approximation feedback problem (the min-max problem (2.9)) may not be feasible. Therefore, based on Lemma 2.10 we advise to use the sub-optimal distance function

$$d_S(\boldsymbol{h}, \boldsymbol{v}) = \max_{\boldsymbol{w} \in \mathcal{C}} \left| |\langle \boldsymbol{h}, \boldsymbol{w} \rangle|^2 - |\langle \boldsymbol{v}, \boldsymbol{w} \rangle|^2 \right|. \tag{2.16}$$

Corollary 2.9 gives some rule of thumb for computing the CQI. We define the CQI reported by user m as

$$\vartheta_m^2 = \lambda_m^2 |\langle \boldsymbol{h}_m, \boldsymbol{v}_m \rangle|^2 \tag{2.17}$$

which can also be interpreted as the effective channel of user m over the feedback codebook element $\boldsymbol{v}_m$. Note that this CQI captures two important aspects. On the one hand, if the CDI is equal to the channel direction, the user gets no penalty (i.e. $|\langle \boldsymbol{h}_m, \boldsymbol{v}_m \rangle|^2 = 1$) on the other hand, if the CDI is orthogonal to the channel direction, the effective channel is zero

Table 2.1: Configuration of channel model

Parameter	**Value**
Channel Model	SCME [BSM$^+$05]
Scenario	Urban macro
Tx antennas	4
Rx antennas	1
Tx antenna spacing	0.5λ
Antenna element positions	$(-3/4\lambda, -1/4\lambda, 1/4\lambda, 3/4\lambda)$
Angle spread	15 (high)
User velocity	30 [km/h]
Sampling frequency	7.68 [MHz]
System bandwidth	5 [MHz]
Carrier frequency	2 [GHz]
Wavelength (λ)	50 [nm]
Base station to user distance	200 [m]

(i.e. $|\langle \boldsymbol{h}_m, \boldsymbol{v}_m \rangle|^2 = 0$). Hence, the CQI (2.17) reflects the receive SNR and the quantization error, which is also in accordance with the results in [YJG07]. The performance of the proposed feedback protocol is evaluated numerically in the simulations in the next section. Later on in Lemma 4.11 we will show that if $\mathcal{C} \equiv \mathbb{S}^{n_t-1}$, the proposed distance function is equal to the chordal distance (2.10), $d_S(\boldsymbol{h}, \boldsymbol{v}) = d_C(\boldsymbol{h}, \boldsymbol{v})$.

2.5 Simulations

2.5.1 Single-Cell Simulations

In this subsection we consider single cell simulations. We assume a single antenna per user (multi-antenna users are considered in Section 2.5.2). The rate approximation feedback strategy is compared to different feedback schemes which have been discussed in the context of LTE. We demonstrate the gains which can be achieved if the feedback codebook is optimized and compare different user selection schemes.

Simulation Setup

The performance is compared using SINR based simulations. The simulation setup is given by a single 120°-sector of a cellular system. The users are uniformly distributed in $[-60°, 60°]$ and placed at a distance of 200 m to the base station. A scheduling block consists of $|\mathcal{F}| = 36$ subcarriers. The configuration of the OFDM downlink channel is chosen according to the configuration of the LTE downlink [3GP09b]. The channel is modeled

using the spatial channel model extended (SCME) [BSM+05]. Table 2.1 summarizes the configuration of the channel model. We use the high angle spread option in order to demonstrate the performance in a highly scattered environment.

We apply two different transmit codebooks. The first is the LTE codebook for transmission on four antenna ports [3GP09b]. The LTE codebook has 16 elements which result in a feedback load of 4 bits per scheduling block for the feedback of the CDI. Furthermore, it consists of four unitary groups which makes it applicable for PU2RC. The second codebook (LOS codebook) is the beamforming codebook proposed in [3GP07]. It is designed such that the "beam distance method" (as explained in 2.5.1) can be used. The codebook elements are given by line of sight channels with equidistant angles of departure. The nth component of $\boldsymbol{v}_i \in \mathcal{V}_{\text{LOS}}$ is defined as:

$$(\boldsymbol{v}_i)_n = \frac{1}{\sqrt{N}} e^{-j\frac{2\pi}{\lambda}\delta_n \sin(\theta_i)}$$

where δ_n is the position of the nth antenna element, λ is the wavelength and the line of sight angles of departure are chosen to be $\theta = [-60°, -43°, -26°, -8.5°, 8.5°, 26°, 43°, 60°]$. On top we apply tapering [Dol46], i.e., codebook elements with different amplitudes per antenna port. In the simulations we use a windowing of [0.6, 1, 1, 0.6], this results in reduced side lobes.

Considered Limited Feedback Methods

An upper bound on the performance of the rate approximation feedback strategy can be obtained by assuming perfect channel state information at the base station. In this case, the selection of users $\mathcal{S}$ and corresponding beamforming vectors $\boldsymbol{\pi}_{\mathcal{C}}$ can be performed by a brute force search over the possible user selections (at least for a small number of users) or by the greedy user selection proposed in [DS04] and [TBT07]. The theoretical upper bound is given by the dirty paper coding limit for equal power allocation over the subcarriers which is implemented using the algorithm described in [JRV+05].

A popular limited feedback scheme for scenarios with fixed beamforming vectors is PU2RC proposed in [KKL05]. PU2RC requires that the transmit codebook consists of multiple unitary groups. Each user feeds back a preferred codebook index and a CQI reflecting the SINR this user expects if all beams within its selected unitary group are used, i.e., its CQI is a worst case SINR. The performance of this approach was further investigated in [HAH09]. First, the user with the best CQI is selected. Then subsequently, the base station checks for other users who have reported a preferred codebook index in the same unitary group and selects those users with the best CQI.

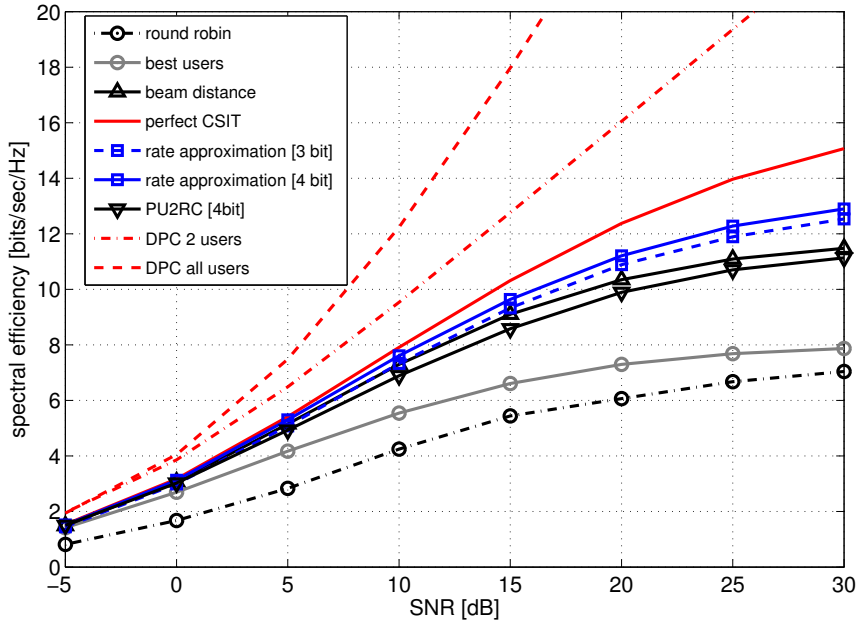

Figure 2.5: Spectral efficiency vs. averaged SNR. "DPC" denotes the dirty paper coding limit for equal power allocation over the subcarriers (using the algorithm in [JRV+05]). Setup: $|\mathcal{U}| = 8$, $|\mathcal{S}| \leq 2$, transmit codebook: LOS codebook [3 bits] (LTE codebook [4 bit] for PU2RC), rate approximation feedback codebook: LOS codebook [3 bits].

Another limited feedback scheme for fixed transmit codebooks was proposed in [3GP07]. This scheme is based on a beam distance criterion and will be termed "beam distance method". Each user reports a preferred codebook index chosen from a transmit codebook and a CQI reflecting the expected SNR. The base station selects the user with the best CQI first and blocks the beamforming vectors that are within a predefined distance to the selected beamforming vectors. Subsequently the remaining users with the best CQI are selected if their preferred beam is not blocked by a previously selected user.

To obtain a lower bound on the performance, we apply some simple user selection schemes. Each user feeds back its preferred codebook index and a CQI reflecting its SNR if this beamforming vector is used. The "best users" scheme selects a predefined number of users with the best CQI (if they reported different beamforming vectors). The "round robin" user selection selects randomly a predefined number of users that have reported different beamforming vectors.

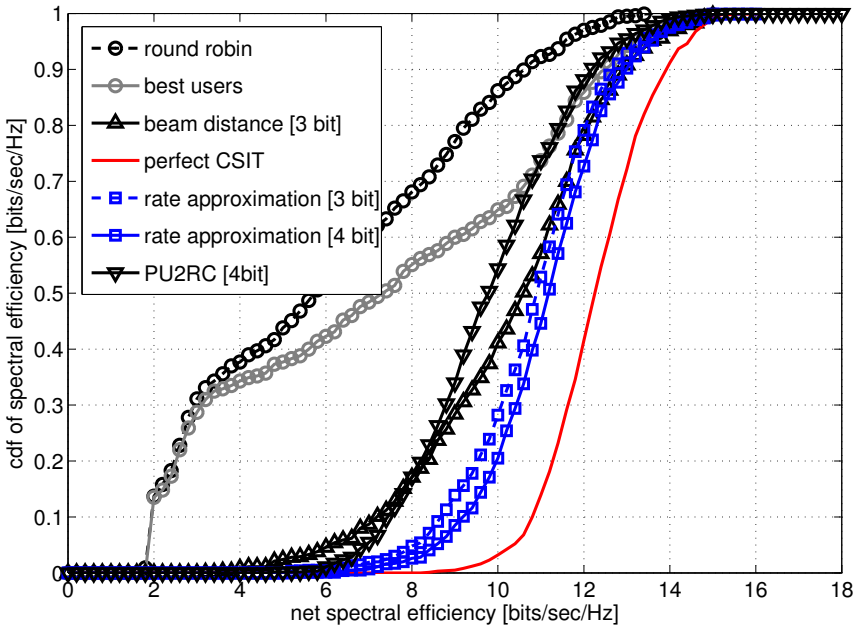

Figure 2.6: CDF of the spectral efficiency at averaged SNR of 20 dB. Setup: $|\mathcal{U}| = 8$, $|\mathcal{S}| \leq 2$, transmit codebook: LOS codebook [3 bits] (LTE codebook [4 bit] for PU2RC), feedback codebook: LOS codebook [3bit].

Simulations

We evaluate the achievable average sum-rate per unit bandwidth[1]

$$\sum_{m \in \mathcal{S}} \bar{r}_m(\boldsymbol{\pi}_{\mathcal{C}}, \mathcal{S}, h_m(\mathcal{F}))$$

where $\bar{r}_m(\boldsymbol{\pi}_{\mathcal{C}}, \mathcal{S}, h_m(\mathcal{F}))$ is defined in (2.13). Note that this implies perfect link adaption. Fig. 2.5 shows the spectral efficiency over the averaged SNR for different feedback and user selection schemes, with $|\mathcal{U}| = 8$ and $|\mathcal{S}| \leq n_s = 2$. The lower bound is given by the round robin user selection. The upper bound is given by the dirty paper coding limit for equal power allocation over the subcarriers (using the algorithm in [JRV+05]). Since in general the dirty paper coding algorithm selects all users $\mathcal{S} = \mathcal{U}$ for transmission, the figure additionally shows the dirty paper coding limit for the best subset $\mathcal{S}$ with $|\mathcal{S}| = 2$. The beam distance method which requires 3 bit for CDI feedback outperforms the PU2RC which requires 4 bit of CDI feedback. Both methods are outperformed by the rate approximation feedback strategy. Additionally, the performance of the rate approximation feedback strategy can be scaled by increasing the size of the feedback codebook (3 bits and 4 bits shown in the figure). The upper bound is given by the case with perfect channel

[1] That is the spectral efficiency in bits/sec/Hz.

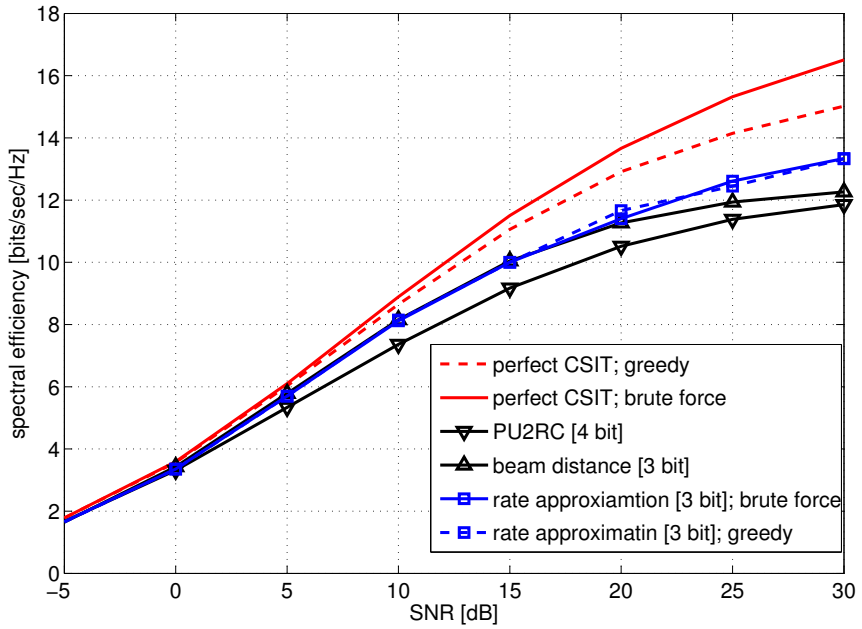

Figure 2.7: Spectral efficiency vs. averaged SNR. Comparing the brute force user selection with the greedy user selection. Setup: $|\mathcal{U}| = 10$, $|\mathcal{S}| \leq 4$, transmit codebook: LOS codebook [3 bits] (LTE codebook [4 bit] for PU2RC), feedback codebook: LOS codebook [3 bits].

state information at the base station. These observations are substantiated by Fig. 2.6 which shows the inverse cumulative distribution function (CDF) of the spectral efficiency at SNR=20 dB for the same setup.

Fig. 2.7 compares the brute force user selection with a greedy user selection. In the case of perfect channel state information at the base station, the brute force selection outperforms the greedy user selection. If we apply the rate approximation feedback strategy, the performance of both user selection algorithms is very similar. The PU2RC and the beam distance method are both outperformed by the rate approximation feedback strategy with greedy user selection.

Finally, a feedback codebook generated by the LBG algorithm, as described in Section 2.4.2, is compared to the LOS codebook. Figure 2.8 depicts the performance of the rate approximation feedback strategy with greedy user selection for two different 3 bit feedback codebooks: The LBG-optimized feedback codebook and the LOS feedback codebook. The rate approximation feedback strategy with the LOS feedback codebook already outperforms the beam distance method. With the optimized feedback codebook the performance increases by up to 5 dB, in the high SNR range. The upper bound is given by the greedy user selection with perfect channel state information at the base station.

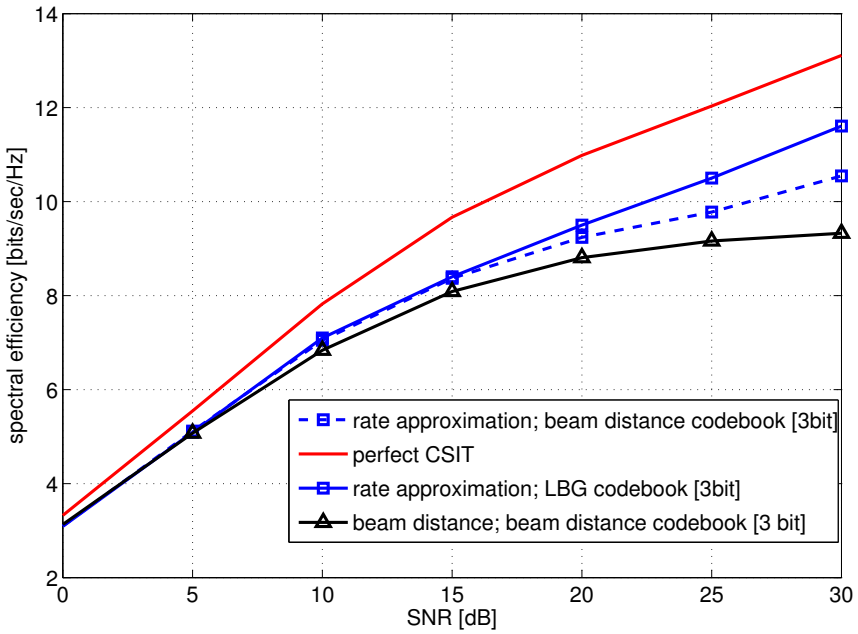

Figure 2.8: Spectral efficiency vs. averaged SNR for the rate approximation approach with greedy user selection. The LBG feedback codebook outperforms the LOS feedback codebook and the beam distance method. The upper bound is given by the greedy user selection with perfect channel state information at the base station and fixed beamforming. Setup: $|\mathcal{U}| = 10$, $|\mathcal{S}| \leq 4$, transmit codebook: LOS codebook

2.5.2 Multi-Cell Simulations

In this subsection we present multi-cell simulations for the rate approximation feedback strategy. We consider a LTE like system architecture; multiple base stations transmit to multiple users using the same spectral resources. The considered system comprises three base stations which are located at different sites but have the same network area. Figure 2.9 shows the average SINR distributions of the users over the network area. The three peaks are close to the base stations. It is assumed that all three base stations transmit with equal power on all antennas. The spectrum is divided in orthogonal subcarriers using OFDM. We use a frequency reuse factor of one, i.e., each base station uses all available subcarriers. Since no cooperation is assumed between the base stations, inter cell interference is indispensable.

The simulation parameters are given in Table 2.2, they can be summarized as follows. 3 base stations located in 3 adjacent cells and 30 users uniformly distributed over the network area; given by a radius of 250 meter around the center of the base stations. The physical layer is configured according to LTE [3GP09b]. The base stations are equipped

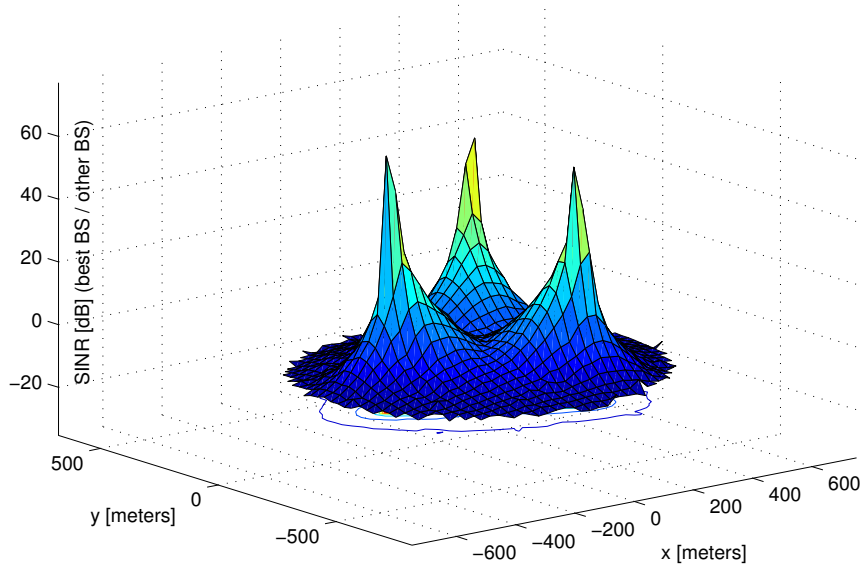

Figure 2.9: Distribution of user SINR in the LTE related simulations.

with $n_t = 4$ transmit antennas and each user is equipped with $n_r = 1$ or $n_r = 2$ receive antenna (specified in place). The transmit codebook and feedback codebook is given by the LTE codebook defined in [3GP09b] which has $N = 16$ elements. The channels are modeled by the spatial channel model extended (SCME) [BSM+05] using the urban macro scenario. In total, 600 subcarriers per base station are available. The subcarriers are clustered in groups of $F = 12$ subcarriers; in LTE one subcarrier group is denoted as physical resource block (PRB). We assume that one PRB is the smallest scheduling unit. The subcarrier indices of the scheduling block are collected in the index set $\mathcal{F}$. The average channel gain of PRB p is defined as $\sigma_p^2 := 1/|\mathcal{F}| \sum_{f\in\mathcal{F}} \|\boldsymbol{H}_{b,m}(f)\|_F^2$. Each user is assigned to that base station which has maximal average channel gain σ_p^2. Each user reports one feedback message per PRB to the base station it is assigned to.

Each of the base stations runs an independent local scheduler. In every transmission interval up to $n_s = 2$ users can be scheduled by a base station. Scheduling is performed in a greedy fashion according to [TBT07]. For simplicity we assume no delay in the channel state information report, scheduling, and transmission. The performance is evaluated based on the achievable system sum-rate per unit bandwidth,

$$\sum_{b=1}^{T} \sum_{m\in\mathcal{S}_b} \sum_{f\in\mathcal{F}} \log(1 + \mathrm{SINR}_m(\boldsymbol{\pi}_{\mathcal{C},X}, \mathcal{S}_X, \lambda_m \boldsymbol{h}_m)),$$

where SINR_m is defined in (2.3), the scheduling decision $(\boldsymbol{\pi}_{\mathcal{C},X}, \mathcal{S}_X)$ depends on the available channel state information X.

Table 2.2: Summary of simulation parameters.

Parameter	Value/Assumption
Number of base stations	3
Frequency reuse	full
Number of users $\lvert\mathcal{U}\rvert$	30 (uniformly distributed)
Number of transmit antennas n_t	4 (uncorrelated)
Number of receive antennas n_r	1 or 2 (uncorrelated)
Receiver type	maximum ratio combining
Maximum number of scheduled users n_s	2
LTE carrier frequency / bandwidth	2 GHz / 10 MHz
Number of PRB	50
Scheduling block size	1 PRB = 12 subcarriers
LTE channel model	SCME (urban macro)
Inter cell interference modeling	explicit

In the simulation we compare four different feedback strategies.

1. Perfect (average) channel state information: the base station knows the channel averaged over all subcarriers, within a scheduling block, perfectly,

$$\bar{\boldsymbol{H}}_m = \frac{1}{|\mathcal{F}|} \sum_{f \in \mathcal{F}} \boldsymbol{H}_m(f).$$

2. Minimum chordal distance: user m determines its CDI feedback by minimizing the chordal distance (2.10) to the average effective channel

$$\bar{\boldsymbol{h}}_m = \max_{\boldsymbol{u} \in \mathbb{S}^{n_t - 1}} \langle \boldsymbol{u}, \bar{\boldsymbol{H}}_m \rangle.$$

3. Rate approximation feedback strategy extended to OFDM as described above in Section 2.4.1.

4. Efficient rate approximation feedback as described in Section 2.4.3, with effective channels $\bar{\boldsymbol{h}}_m$.

Figure 2.10 depicts the CDF of the achievable rate for users with $n_r = 1$ receive antenna. The zeroforcing beamforming scheme is implemented according to [TBH08]. The PU2RC scheme is implemented according to [Sam06] and uses the same transmit codebook as is used for the rate approximation scheme. We observe that with perfect channel state information at the base station zeroforcing beamforming outperforms greedy scheduling with a fixed codebook. With partial channel state information the rate approximation

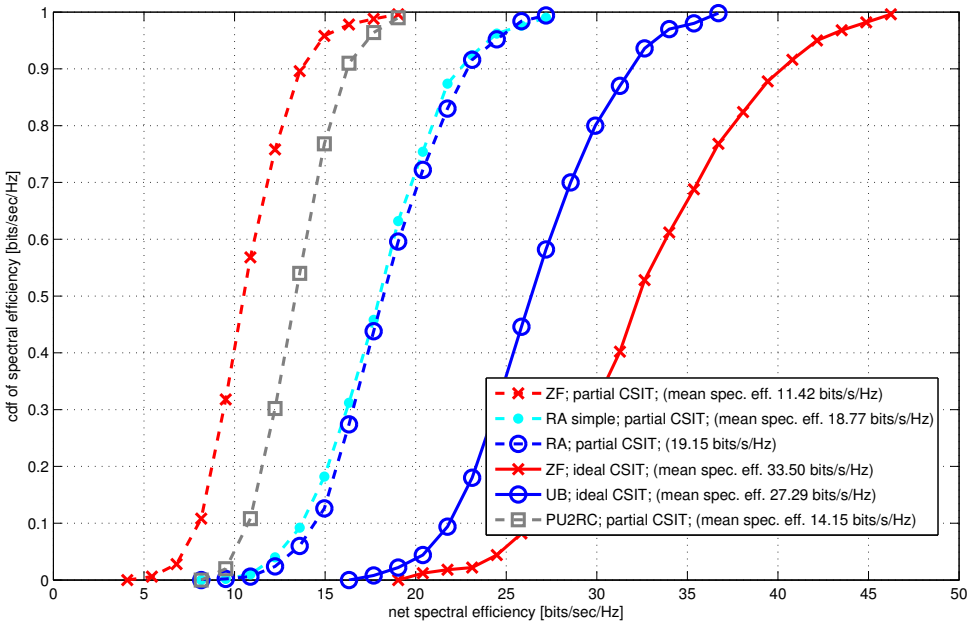

Figure 2.10: System level simulation: CDF of achievable rate for $n_r = 1$; Comparing PU2RC, zeroforcing beamforming with perfect and quantized channel state information, beamforming with a fixed codebook (UB) with perfect channel state information and the rate approximation feedback strategy.

scheme significantly outperforms zeroforcing beamforming with a gain of approximately 70%. Remarkable is also the gain of about 35% of the rate approximation scheme over PU2RC, both using the same transmit codebook. Moreover Figure 2.10 shows that rate approximation with the efficient distance function (2.16) performs very close to the full rate approximation scheme.

Figure 2.11 depicts the CDF of the achievable rate for users with $n_r = 2$ receive antennas. We observe that with perfect channel state information at the base station zeroforcing beamforming outperforms greedy user selection with a fixed codebook. With quantized channel state information the rate approximation scheme significantly outperforms all other schemes and achieves a gain of approximately 50% over zeroforcing beamforming. Remarkable is also the 35% gain of rate approximation over PU2RC, both using the same transmit codebook.

2.6 Summary and Conclusions

In this chapter we developed and analyzed the rate approximation feedback strategy. It was shown that each user can individually minimize its rate loss relative, to perfect channel state information at the base station, by selecting the feedback message that incorporates

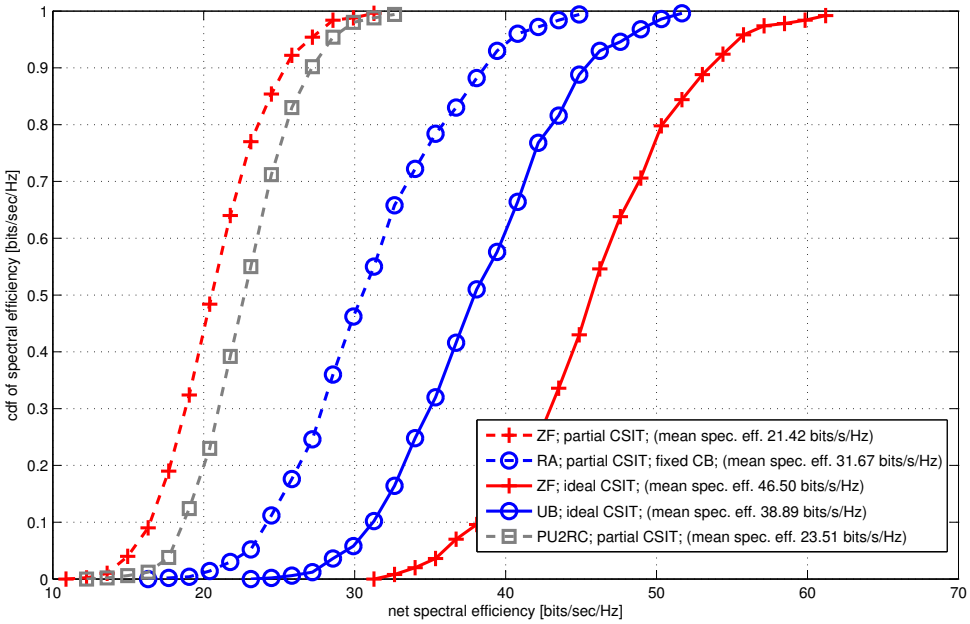

Figure 2.11: System level simulation: CDF of achievable rate for $n_r = 2$; Comparing PU2RC, zeroforcing beamforming with perfect and quantized channel state information, beamforming with a fixed codebook and perfect channel state information and the rate approximation feedback strategy.

the transmit codebook. The scaling with the number of feedback bits of the rate loss gap was derived and compared to baseline expressions for zeroforcing beamforming. It was proved that a better scaling is possible if the number of transmit antennas is sufficiently large. A remarkable result is that it is often better to reduce flexibility at the base station (by resorting the beamforming vectors to a fixed transmit codebook) in favor of being able to provide more reliable channel state information to the base station.

The proposed rate approximation feedback strategy was extended towards more practical scenarios. An Extension to OFDM was proposed, an algorithm to design feedback codebooks was presented, and reduced complexity version of the rate approximation feedback strategy was introduced. The performance was evaluated by extensive numerical simulations, showing significant gains over state of the art baseline schemes.

The rate approximation philosophy will be picked up and extended in Chapter 4 where we analyze the performance of multi-cellular systems under more general transmit strategies; including cooperated transmission by multiple base stations.

2.7 Proofs

In this section we collect all proofs of this chapter. To keep the notation simple we define the following variables.

$$\begin{aligned}
\tilde{\vartheta}_m &:= \frac{\vartheta_m^2}{\vartheta_m^2+1}, \\
\tilde{\lambda}_m &:= \frac{\lambda_m^2}{\lambda_m^2+1}, \\
\phi_{m,l}^{\boldsymbol{h}} &:= |\langle \boldsymbol{h}_m, \boldsymbol{\pi}_{\mathcal{C}}(l)\rangle|^2, \quad \forall\, m,l \in \mathcal{S}, \\
\phi_{m,l}^{\boldsymbol{v}} &:= |\langle \boldsymbol{v}_m, \boldsymbol{\pi}_{\mathcal{C}}(l)\rangle|^2, \quad \forall\, m,l \in \mathcal{S}.
\end{aligned}$$

2.7.1 Proof of Lemma 2.2

Proof. Since $(\boldsymbol{\pi}_{\mathcal{C},v}, \mathcal{S}_v)$ is the sum-rate optimal scheduling decision with quantized channel state information v, $R(\boldsymbol{\pi}_{\mathcal{C},h}, \mathcal{S}_h, v) \leq R(\boldsymbol{\pi}_{\mathcal{C},v}, \mathcal{S}_v, v)$. Thus,

$$\begin{aligned}
\Delta &= \mathbb{E}\left[R(\boldsymbol{\pi}_{\mathcal{C},h}, \mathcal{S}_h, h) - R(\boldsymbol{\pi}_{\mathcal{C},v}, \mathcal{S}_v, h)\right] \\
&= \mathbb{E}\left[R(\boldsymbol{\pi}_{\mathcal{C},h}, \mathcal{S}_h, h) - R(\boldsymbol{\pi}_{\mathcal{C},h}, \mathcal{S}_h, v) + R(\boldsymbol{\pi}_{\mathcal{C},h}, \mathcal{S}_h, v) - R(\boldsymbol{\pi}_{\mathcal{C},v}, \mathcal{S}_v, h)\right] \\
&\leq \mathbb{E}\left[R(\boldsymbol{\pi}_{\mathcal{C},h}, \mathcal{S}_h, h) - R(\boldsymbol{\pi}_{\mathcal{C},h}, \mathcal{S}_h, v) + R(\boldsymbol{\pi}_{\mathcal{C},v}, \mathcal{S}_v, v) - R(\boldsymbol{\pi}_{\mathcal{C},v}, \mathcal{S}_v, h)\right] \qquad (2.18) \\
&\leq \mathbb{E}\left[|R(\boldsymbol{\pi}_{\mathcal{C},h}, \mathcal{S}_h, h) - R(\boldsymbol{\pi}_{\mathcal{C},h}, \mathcal{S}_h, v)|\right] + \mathbb{E}\left[|R(\boldsymbol{\pi}_{\mathcal{C},v}, \mathcal{S}_v, v) - R(\boldsymbol{\pi}_{\mathcal{C},v}, \mathcal{S}_v, h)|\right] \\
&\leq 2 \cdot \mathbb{E}\left[\sum_{m \in \mathcal{S}_h \cup \mathcal{S}_v} d(\hat{\boldsymbol{h}}_m, \vartheta_m \boldsymbol{v}_m)\right],
\end{aligned}$$

where (2.18) must hold since $R(\boldsymbol{\pi}_{\mathcal{C},v}, \mathcal{S}_v, v) \geq R(\boldsymbol{\pi}_{\mathcal{C},h}, \mathcal{S}_h, v)$ by (2.6) and $d(\cdot)$ is defined in (2.7). □

2.7.2 Proof of Theorem 2.6

Proof. Define $\phi^{\boldsymbol{h}}_{m,ZF} := |\langle \boldsymbol{h}_m, \boldsymbol{\pi}_{ZF,h}(m)\rangle|^2$. For $\mathcal{S} = \{1,\dots,n_t\}$ and any mapping of beamforming vectors $\boldsymbol{\pi}_{\mathcal{C}} : \mathcal{S} \to \mathcal{C}$ we have

$$\begin{aligned}
\Delta_{\mathrm{CSI}} &\leq \mathbb{E}\left[R_{ZF}\left(\boldsymbol{\pi}_{ZF,h}, \mathcal{S}, h\right) - R\left(\boldsymbol{\pi}_{\mathcal{C}}, \mathcal{S}, h\right)\right] \\
&= \mathbb{E}\left[\sum_{m\in\mathcal{S}} \log\left(1+\lambda_m^2\phi^{\boldsymbol{h}}_{m,ZF}\right) - \log\left(1+\frac{\lambda_m^2\phi^{\boldsymbol{h}}_{m,m}}{1+\lambda_m^2\left(1-\phi^{\boldsymbol{h}}_{m,m}\right)}\right)\right] \\
&= \mathbb{E}\left[\sum_{m\in\mathcal{S}} \log\left(1+\lambda_m^2\frac{\phi^{\boldsymbol{h}}_{m,ZF} - \phi^{\boldsymbol{h}}_{m,m} + \lambda_m^2\phi^{\boldsymbol{h}}_{m,ZF}\left(1-\phi^{\boldsymbol{h}}_{m,l}\right)}{1+\lambda_m^2}\right)\right] \\
&= \mathbb{E}\left[\sum_{m\in\mathcal{S}} \log\left(1+\lambda_m^2\frac{\left(1+\lambda_m^2\right)\phi^{\boldsymbol{h}}_{m,ZF} - \left(1+\lambda_m^2\phi^{\boldsymbol{h}}_{m,ZF}\right)\phi^{\boldsymbol{h}}_{m,m}}{1+\lambda_m^2}\right)\right].
\end{aligned}$$

Since $\mathcal{C}$ is an ONB, $\boldsymbol{\pi}_{\mathcal{C}} : \mathcal{S} \to \mathcal{C}$ is a permutation on the beamforming vectors in $\mathcal{C}$. Since, $\phi^{\boldsymbol{h}}_{m,m}$ and $\phi^{\boldsymbol{h}}_{m,ZF}$ are independent random variables from Jensen's inequality we get

$$\begin{aligned}
&\mathbb{E}\left[\sum_{m\in\mathcal{S}} \log\left(1+\lambda_m^2\frac{\left(1+\lambda_m^2\right)\phi^{\boldsymbol{h}}_{m,ZF} - \left(1+\lambda_m^2\phi^{\boldsymbol{h}}_{m,ZF}\right)\phi^{\boldsymbol{h}}_{m,m}}{1+\lambda_m^2}\right)\right] \\
&\qquad \leq \sum_{m\in\mathcal{S}} \log\left(1+\lambda_m^2\frac{\left(1+\lambda_m^2\right)\mathbb{E}\left[\phi^{\boldsymbol{h}}_{m,ZF}\right] - \left(1+\lambda_m^2\mathbb{E}\left[\phi^{\boldsymbol{h}}_{m,ZF}\right]\right)\mathbb{E}\left[\phi^{\boldsymbol{h}}_{m,m}\right]}{1+\lambda_m^2}\right)
\end{aligned}$$

Due to the zeroforcing beamforming criterion, for all i, $\boldsymbol{h}_i$ and $\boldsymbol{\pi}_{ZF,h}(i)$ are independent isotropic vectors, see e.g. [Jin06]. Hence, we have that $\phi^{\boldsymbol{h}}_{m,ZF}$ is a beta distributed random variable with parameters 1 and $n_t - 2$ and expectation

$$\mathbb{E}\left[\phi^{\boldsymbol{h}}_{m,ZF}\right] = \frac{1}{n_t - 1}.$$

The expectation $\mathbb{E}\left[\phi^{\boldsymbol{h}}_{m,m}\right]$ is harder to obtain; we resort to bounding it. Suppose that without loss of generality $\mu_1 \geq \mu_2 \geq \ldots \geq \mu_{n_t}$. Since, $\boldsymbol{h}_m$ is isotropically distributed on $\mathbb{S}^{n_t-1}$ we can chose $\mathcal{C}$ as the columns the standard ONB in $\mathbb{C}^{n_t}$. Now a reasonable but sub-optimal choice of $\boldsymbol{\pi}_{\mathcal{C},h}$ can be obtained by processing the users in a greedy fashion, i.e., user m gets the beamformer

$$\boldsymbol{\pi}_{\mathcal{C},h}(m) = \operatorname*{arg\,max}_{\boldsymbol{w}\in\mathcal{J}(m)} |\langle \boldsymbol{h}_m, \boldsymbol{w}\rangle|^2,$$

where we defined the set of possible beamforming vectors as

$$\mathcal{J}(m) = \mathcal{C} \setminus \{\boldsymbol{\pi}_{\mathcal{C},h}(1), \boldsymbol{\pi}_{\mathcal{C},h}(2), \ldots, \boldsymbol{\pi}_{\mathcal{C},h}(m-1)\}.$$

Consider a fixed m, to get the image of $\boldsymbol{\pi}_{\mathcal{C},h}(m)$ we have $n_t - m + 1$ degrees of freedom. To get an explicit expression for $\mathbb{E}\left[|\langle \boldsymbol{h}_m, \boldsymbol{\pi}_{\mathcal{C},h}(m)\rangle|^2\right]$ we require the order statistics of elements of vectors uniformly distributed on the unit sphere $\mathbb{S}^{n_t-1}$. More specifically we need the expectation of $\max_{j\in\mathcal{J}\subseteq\{1,2,\ldots,n_t\}} |\hat{\boldsymbol{h}}_{m,j}|^2$, where $\hat{\boldsymbol{h}}_m \in \mathbb{C}^{n_t}$. From standard results we have the inequalities

$$\Pr\left(\max_{j\in\mathcal{J}(m)} |\hat{\boldsymbol{h}}_{m,j}|^2 \leq \sqrt{(1-\epsilon)\log\left(|\mathcal{J}(m)|\right)}\right) \leq e^{-|\mathcal{J}(m)|^{\epsilon}},$$
$$\Pr\left(\|\hat{\boldsymbol{h}}_m\|_2 \geq (1+\epsilon)\sqrt{n_t}\right) \leq \frac{1}{\epsilon n_t},$$

where $\epsilon > 0$, so that we arrive at the following expression for the expectation

$$\mathbb{E}\left[\phi^{\boldsymbol{h}}_{m,m}\right] \geq \frac{(1-\epsilon)\log(n_t - m + 1)}{(1+\epsilon)^2 n_t}\left(1 - e^{-(n_t-m+1)^{\epsilon}} - \frac{1}{\epsilon n_t}\right).$$

which proves the claim. □

2.7.3 Proof of Lemma 2.7

Proof. We use the notation defined at the beginning of this section. If $\mathcal{S} = \mathcal{U}$, $d(\lambda_m \boldsymbol{h}_m, \vartheta_m \boldsymbol{v}_m) = \max_{\boldsymbol{\pi}_{\mathcal{C}}:\mathcal{S}\to\mathcal{C}} |r_m(\boldsymbol{\pi}_{\mathcal{C}}, \mathcal{S}, \lambda_m \boldsymbol{h}_m) - r_m(\boldsymbol{\pi}_{\mathcal{C}}, \mathcal{S}, \vartheta_m \boldsymbol{v}_m)|$. Using $\mathcal{U} = \{1, 2, \ldots, n_t\}$ we get

$$\begin{aligned} r_m(\boldsymbol{\pi}_{\mathcal{C}}, \mathcal{S}, \lambda_m \cdot \boldsymbol{h}_m) - r_m(\boldsymbol{\pi}_{\mathcal{C}}, \mathcal{S}, \vartheta_m \cdot \boldsymbol{v}_m) &= \log\left(\frac{\left(\lambda_m^2 + 1\right)\left(1 + \vartheta_m^2\left(1 - \phi^{\boldsymbol{v}}_{m,m}\right)\right)}{\left(\vartheta_m^2 + 1\right)\left(1 + \lambda_m^2\left(1 - \phi^{\boldsymbol{h}}_{m,\pi(m)}\right)\right)}\right) \\ &= \log\left(\frac{1 - \tilde{\vartheta}_m \phi^{\boldsymbol{v}}_{m,m}}{1 - \tilde{\lambda}_m \phi^{\boldsymbol{h}}_{m,m}}\right) \\ &= \log\left(1 + \frac{\tilde{\lambda}_m \phi^{\boldsymbol{h}}_{m,m} - \tilde{\vartheta}_m \phi^{\boldsymbol{v}}_{m,m}}{1 - \tilde{\lambda}_m \phi^{\boldsymbol{h}}_{m,m}}\right). \end{aligned}$$

Similarly, the negative term can be written as

$$\begin{aligned} -r_m(\boldsymbol{\pi}_{\mathcal{C}}, \mathcal{S}, \lambda_m \cdot \boldsymbol{h}_m) + r_m(\boldsymbol{\pi}_{\mathcal{C}}, \mathcal{S}, \vartheta_m \cdot \boldsymbol{v}_m) &= -\log\left(\frac{1 - \tilde{\vartheta}_m \phi^{\boldsymbol{v}}_{m,m}}{1 - \tilde{\lambda}_m \phi^{\boldsymbol{h}}_{m,m}}\right) \\ &= \log\left(1 + \frac{\tilde{\vartheta}_m \phi^{\boldsymbol{v}}_{m,m} - \tilde{\lambda}_m \phi^{\boldsymbol{h}}_{m,m}}{1 - \tilde{\vartheta}_m \phi^{\boldsymbol{v}}_{m,m}}\right). \end{aligned}$$

Hence, we have the upper bound

$$\max_{\boldsymbol{\pi}_{\mathcal{C}}:\mathcal{S}\to\mathcal{C}} |r_m(\boldsymbol{\pi}_{\mathcal{C}}, \mathcal{S}, \lambda_m \boldsymbol{h}_m) - r_m(\boldsymbol{\pi}_{\mathcal{C}}, \mathcal{S}, \vartheta_m \boldsymbol{v}_m)| \tag{2.19}$$
$$\leq \max\left(\max_{\boldsymbol{\pi}_{\mathcal{C}}} \log\left(1 + \frac{\tilde{\lambda}_m \phi^{\boldsymbol{h}}_{m,m} - \tilde{\vartheta}_m \phi^{\boldsymbol{v}}_{m,m}}{1 - \tilde{\lambda}_m \phi^{\boldsymbol{h}}_{m,m}}\right), \max_{\boldsymbol{\pi}_{\mathcal{C}}} \log\left(1 + \frac{\tilde{\vartheta}_m \phi^{\boldsymbol{v}}_{m,m} - \tilde{\lambda}_m \phi^{\boldsymbol{h}}_{m,m}}{1 - \tilde{\vartheta}_m \phi^{\boldsymbol{v}}_{m,m}}\right)\right),$$

which is valid for any $\boldsymbol{v}_m \in \mathcal{V}$. Under the the assumed feedback strategy (for which always a solution exists since $\mathcal{C} \subseteq \mathcal{V}$) we get

$$\tilde{\vartheta}_m = \frac{\lambda_m^2}{\lambda_m^2 + 1} \frac{|\langle \boldsymbol{h}_m, \boldsymbol{w}^* \rangle|^2}{|\langle \boldsymbol{v}_m, \boldsymbol{w}^* \rangle|^2} = \tilde{\lambda}_m \frac{|\langle \boldsymbol{h}_m, \boldsymbol{w}^* \rangle|^2}{|\langle \boldsymbol{v}_m, \boldsymbol{w}^* \rangle|^2}$$

and finally

$$\begin{aligned}
&\max_{\boldsymbol{\pi}} \log\left(1 + \frac{\tilde{\lambda}_m \phi^{\boldsymbol{h}}_{m,m} - \tilde{\vartheta}_m \phi^{\boldsymbol{v}}_{m,m}}{1 - \tilde{\lambda}_m \phi^{\boldsymbol{h}}_{m,m}}\right) \\
&= \max_{\boldsymbol{w} \neq \boldsymbol{w}^*} \log\left(1 + \frac{\tilde{\lambda}_m |\langle \boldsymbol{h}_m, \boldsymbol{w} \rangle|^2 - \tilde{\lambda}_m \frac{|\langle \boldsymbol{h}_m, \boldsymbol{w}^* \rangle|^2}{|\langle \boldsymbol{v}_m, \boldsymbol{w}^* \rangle|^2} |\langle \boldsymbol{v}_m, \boldsymbol{w} \rangle|^2}{1 - \tilde{\lambda}_m |\langle \boldsymbol{h}_m, \boldsymbol{w} \rangle|^2}\right) \\
&\leq \max_{\boldsymbol{w} \neq \boldsymbol{w}^*} \log\left(1 + \tilde{\lambda}_m \left(\frac{\left||\langle \boldsymbol{h}_m, \boldsymbol{w} \rangle|^2 - |\langle \boldsymbol{v}_m, \boldsymbol{w} \rangle|^2\right|}{1 - \tilde{\lambda}_m |\langle \boldsymbol{h}_m, \boldsymbol{w} \rangle|^2} + \frac{\langle \boldsymbol{v}_m, \boldsymbol{w} \rangle}{\langle \boldsymbol{v}_m, \boldsymbol{w}^* \rangle} \frac{\left||\langle \boldsymbol{v}_m, \boldsymbol{w}^* \rangle|^2 - |\langle \boldsymbol{h}_m, \boldsymbol{w}^* \rangle|^2\right|}{1 - \tilde{\lambda}_m \langle \boldsymbol{h}_m, \boldsymbol{w} \rangle}\right)\right),
\end{aligned}$$

and for the other term since $|\langle \boldsymbol{h}_m, \boldsymbol{w}^* \rangle|^2 \leq |\langle \boldsymbol{v}_m, \boldsymbol{w}^* \rangle|^2$ we have

$$\begin{aligned}
&\max_{\boldsymbol{\pi}} \log\left(1 + \frac{\tilde{\vartheta}_m \phi^{\boldsymbol{v}}_{m,m} - \tilde{\lambda}_m \phi^{\boldsymbol{h}}_{m,m}}{1 - \tilde{\vartheta}_m \phi^{\boldsymbol{v}}_{m,m}}\right) \\
&\leq \max_{\boldsymbol{w} \neq \boldsymbol{w}^*} \log\left(1 + \frac{\tilde{\lambda}_m \frac{|\langle \boldsymbol{h}_m, \boldsymbol{w}^* \rangle|^2}{|\langle \boldsymbol{v}_m, \boldsymbol{w}^* \rangle|^2} |\langle \boldsymbol{v}_m, \boldsymbol{w} \rangle|^2 - \tilde{\lambda}_m |\langle \boldsymbol{h}_m, \boldsymbol{w} \rangle|^2}{1 - \tilde{\lambda}_m \frac{|\langle \boldsymbol{h}_m, \boldsymbol{w}^* \rangle|^2}{|\langle \boldsymbol{v}_m, \boldsymbol{w}^* \rangle|^2} |\langle \boldsymbol{v}_m, \boldsymbol{w} \rangle|^2}\right) \\
&\leq \max_{\boldsymbol{w} \neq \boldsymbol{w}^*} \log\left(1 + \tilde{\lambda}_m \left(\frac{\left||\langle \boldsymbol{h}_m, \boldsymbol{w} \rangle|^2 - |\langle \boldsymbol{v}_m, \boldsymbol{w} \rangle|^2\right|}{1 - \tilde{\lambda}_m |\langle \boldsymbol{v}_m, \boldsymbol{w} \rangle|^2} + \frac{\langle \boldsymbol{v}_m, \boldsymbol{w} \rangle}{\langle \boldsymbol{v}_m, \boldsymbol{w}^* \rangle} \frac{\left||\langle \boldsymbol{v}_m, \boldsymbol{w}^* \rangle|^2 - |\langle \boldsymbol{h}_m, \boldsymbol{w}^* \rangle|^2\right|}{1 - \tilde{\lambda}_m |\langle \boldsymbol{v}_m, \boldsymbol{w} \rangle|^2}\right)\right).
\end{aligned}$$

□

2.7.4 Proof of Lemma 2.10

Proof. We use the notation defined at the beginning of this section. According to (2.9), for $\mathcal{S} = \mathcal{U}$, the rate approximation feedback strategy aims on minimizing

$$\max_{\boldsymbol{\pi}_{\mathcal{C}}} |r_m(\boldsymbol{\pi}_{\mathcal{C}}, \mathcal{S}, \lambda_m \boldsymbol{h}_m) - r_m(\boldsymbol{\pi}_{\mathcal{C}}, \mathcal{S}, \vartheta \boldsymbol{v})|$$

over $\vartheta \in \mathbb{R}$ and $\boldsymbol{v} \in \mathcal{V}$. Therefore, from (2.19) and Jensen's inequality we have

$$\Delta R_{\mathrm{RA}} \leq \sum_{m=1}^{n_t} \log\left(1 + \mathbb{E}\left[\min_{\substack{1>\tilde{\vartheta}_m>0 \\ \boldsymbol{v}\in\mathcal{V}}} \max_{\boldsymbol{\pi}_{\mathcal{C}}} \frac{\left|\tilde{\lambda}_m \phi^{\boldsymbol{h}}_{m,m} - \tilde{\vartheta}_m \phi^{\boldsymbol{v}}_{m,m}\right|}{1 - \tilde{\lambda}_m \phi^{\boldsymbol{h}}_{m,m}}\right]\right) + \sum_{m=1}^{n_t} \log\left(1 + \mathbb{E}\left[\min_{\substack{1>\tilde{\vartheta}_m>0 \\ \boldsymbol{v}\in\mathcal{V}}} \max_{\boldsymbol{\pi}_{\mathcal{C}}} \frac{\left|\tilde{\lambda}_m \phi^{\boldsymbol{h}}_{m,m} - \tilde{\vartheta}_m \phi^{\boldsymbol{v}}_{m,m}\right|}{1 - \tilde{\vartheta}_m \phi^{\boldsymbol{v}}_{m,m}}\right]\right). \tag{2.20}$$

Let us re-write the first term on the right side of (2.20). We first exploit that whenever $\max_{\boldsymbol{\pi}_{\mathcal{C}}} |\phi^{\boldsymbol{h}}_{m,m}| \geq 1 - \epsilon, \epsilon \leq 1/2$, then by Lemma 2.7 the error can be uniformly bounded from above by

$$\frac{\tilde{\lambda}_m \epsilon}{1 - \tilde{\lambda}_m \epsilon} = \frac{\lambda_m^2 \epsilon}{1 + \lambda_m^2 (1 - \epsilon)} \leq \frac{\lambda_m^2 \epsilon}{1 + \lambda_m^2 \epsilon},$$

and since $\max_{\boldsymbol{\pi}_{\mathcal{C}}} |\phi^{\boldsymbol{h}}_{m,m}| \geq \frac{1}{n_t}$ and $(1 - \epsilon) \leq \frac{\epsilon}{n_t - 1}$ for $\epsilon \leq 1 - \frac{1}{n_t}$ we have for $\max_{\boldsymbol{\pi}_{\mathcal{C}}} |\phi^{\boldsymbol{h}}_{m,m}| \geq \max(0, 1 - \epsilon)$

$$\frac{\tilde{\lambda}_m \epsilon}{1 - \tilde{\lambda}_m \epsilon} \leq \frac{\lambda_m^2 \epsilon}{1 + \lambda_m^2 \frac{\epsilon}{n_t - 1}} = \frac{\tilde{\lambda}_m \epsilon}{1 + \tilde{\lambda}_m \left(\frac{\epsilon}{n_t - 1} - 1\right)},$$

for any $\epsilon > 0$ (even that for $\epsilon > 1$). On the other hand, we have for $\max_{\boldsymbol{\pi}_{\mathcal{C}}} |\phi^{\boldsymbol{h}}_{m,m}| < \max(0, 1 - \epsilon)$

$$\begin{aligned} \frac{\left|\tilde{\lambda}_m \phi^{\boldsymbol{h}}_{m,m} - \tilde{\vartheta}_m \phi^{\boldsymbol{v}}_{m,m}\right|}{1 - \tilde{\lambda}_m \phi^{\boldsymbol{h}}_{m,m}} &\leq \frac{\left|\tilde{\lambda}_m \phi^{\boldsymbol{h}}_{m,m} - \tilde{\vartheta}_m \phi^{\boldsymbol{v}}_{m,m}\right|}{1 - \tilde{\lambda}_m + \tilde{\lambda}_m \epsilon} \\ &\leq \frac{\left|\tilde{\lambda}_m \phi^{\boldsymbol{h}}_{m,m} - \tilde{\vartheta}_m \phi^{\boldsymbol{v}}_{m,m}\right|}{1 + \tilde{\lambda}_m \left(\frac{\epsilon}{n_t - 1} - 1\right)}, \end{aligned}$$

Hence, we can write for some pair $\boldsymbol{h}_m, \boldsymbol{v}_m$

$$\frac{\left|\tilde{\lambda}_m \phi^{\boldsymbol{h}}_{m,m} - \tilde{\vartheta}_m \phi^{\boldsymbol{v}}_{m,m}\right|}{1 - \tilde{\lambda}_m \phi^{\boldsymbol{h}}_{m,m}} \leq \frac{\max\left\{\tilde{\lambda}_m \epsilon, \left|\tilde{\lambda}_m \phi^{\boldsymbol{h}}_{m,m} - \tilde{\vartheta}_m \phi^{\boldsymbol{v}}_{m,m}\right|\right\}}{1 + \tilde{\lambda}_m \left(\frac{\epsilon}{n_t - 1} - 1\right)}$$

and set

$$\tilde{\lambda}_m \epsilon = \min_{\substack{1>\tilde{\vartheta}_m>0 \\ \boldsymbol{v}\in\mathcal{V}}} \max_{\boldsymbol{\pi}} \left|\tilde{\lambda}_m \phi^{\boldsymbol{h}}_{m,m} - \tilde{\vartheta}_m \phi^{\boldsymbol{v}}_{m,m}\right| = \left|\tilde{\lambda}_m \phi^{\boldsymbol{h}}_{m,m^*} - \tilde{\vartheta}^*_m \phi^{\boldsymbol{v}^*}_{m,m^*}\right|,$$

where we defined $\phi^{\boldsymbol{h}}_{m,m^*} := |\langle \boldsymbol{h}_m, \boldsymbol{\pi}^*(m)\rangle|^2$ and $\phi^{\boldsymbol{v}^*}_{m,m^*} := |\langle \boldsymbol{v}^*, \boldsymbol{\pi}^*(m)\rangle|^2$, yields

$$\min_{\substack{1>\tilde{\vartheta}_m>0\\ \boldsymbol{v}\in\mathcal{V}}} \max_{\boldsymbol{\pi}} \frac{\left|\tilde{\lambda}_m\phi^{\boldsymbol{h}}_{m,m} - \tilde{\vartheta}_m\phi^{\boldsymbol{v}}_{m,m}\right|}{1-\tilde{\lambda}_m\phi^{\boldsymbol{h}}_{m,m}} \leq \frac{\left|\tilde{\lambda}_m\phi^{\boldsymbol{h}}_{m,m^*} - \tilde{\vartheta}^*_m\phi^{\boldsymbol{v}^*}_{m,m^*}\right|}{1-\tilde{\lambda}_m + \frac{1}{n_t-1}\left|\tilde{\lambda}_m\phi^{\boldsymbol{h}}_{m,m^*} - \tilde{\vartheta}^*_m\phi^{\boldsymbol{v}^*}_{m,m^*}\right|}.$$

Equivalently, for the second term on the right side of (2.20) we have

$$\begin{aligned}\frac{\left|\tilde{\lambda}_m\phi^{\boldsymbol{h}}_{m,m} - \tilde{\vartheta}_m\phi^{\boldsymbol{v}}_{m,m}\right|}{1-\tilde{\vartheta}_m\phi^{\boldsymbol{v}}_{m,m}} &\leq \frac{\max\left\{\tilde{\lambda}_m\epsilon, \left|\tilde{\lambda}_m\phi^{\boldsymbol{h}}_{m,m} - \tilde{\vartheta}_m\phi^{\boldsymbol{v}}_{m,m}\right|\right\}}{1-\tilde{\lambda}_m\phi^{\boldsymbol{h}}_{m,m}+\tilde{\lambda}_m\phi^{\boldsymbol{h}}_{m,m}-\tilde{\vartheta}_m\phi^{\boldsymbol{v}}_{m,m}}\\ &\leq \frac{\max\left\{\tilde{\lambda}_m\epsilon, \left|\tilde{\lambda}_m\phi^{\boldsymbol{h}}_{m,m} - \tilde{\vartheta}_m\phi^{\boldsymbol{v}}_{m,m}\right|\right\}}{1+\tilde{\lambda}_m\left(\frac{\max\left\{\epsilon-\left|\tilde{\lambda}_m\phi^{\boldsymbol{h}}_{m,m}-\tilde{\vartheta}_m\phi^{\boldsymbol{v}}_{m,m}\right|,0\right\}}{n_t-1}-1\right)}.\end{aligned}$$

Setting $\epsilon = (1+\epsilon')\left|\tilde{\lambda}_m\phi^{\boldsymbol{h}}_{m,m^*} - \tilde{\vartheta}^*_m\phi^{\boldsymbol{v}^*}_{m,m^*}\right|$, $\epsilon'>0$, since the error term is still increasing in ϵ, yields

$$\min_{\substack{1>\tilde{\vartheta}_m>0\\ \boldsymbol{v}\in\mathcal{V}}} \max_{\boldsymbol{\pi}_{\mathcal{C}}} \frac{\left|\tilde{\lambda}_m\phi^{\boldsymbol{h}}_{m,m} - \tilde{\vartheta}_m\phi^{\boldsymbol{v}}_{m,m}\right|}{1-\tilde{\vartheta}_m\phi^{\boldsymbol{v}}_{m,m}} \leq \frac{(1+\epsilon')\left|\tilde{\lambda}_m\phi^{\boldsymbol{h}}_{m,m^*} - \tilde{\vartheta}^*_m\phi^{\boldsymbol{v}^*}_{m,m^*}\right|}{1-\tilde{\lambda}_m + \frac{\epsilon'}{n_t-1}\left|\tilde{\lambda}_m\phi^{\boldsymbol{h}}_{m,m^*} - \tilde{\vartheta}^*_m\phi^{\boldsymbol{v}^*}_{m,m^*}\right|},$$

expanding the fraction with $(1-\tilde{\lambda}_m)$ and applying Jensen's inequality proves the claim. □

2.7.5 Proof of Lemma 2.11

Proof. Consider an arbitrary but fixed user $m \in \mathcal{U}$ and, without loss of generality, assume the transmit codebook $\mathcal{C}$ is given by the standard ONB. Define the vector $\boldsymbol{\psi}_m = \left(|\langle \boldsymbol{h}_m, \boldsymbol{\pi}_{\mathcal{C}}(1)\rangle|^2, \ldots, |\langle \boldsymbol{h}_m, \boldsymbol{\pi}_{\mathcal{C}}(n_t)\rangle|^2\right)$. Since, $\|\boldsymbol{h}_m\| = 1$ from the Parseval's identity follows that $\|\boldsymbol{\psi}_m\|_1 = 1$ and, therefore, any $\boldsymbol{\psi}_m$ corresponds to a point on the $d := n_t - 1$ dimensional simplex defined by $\mathcal{K}_d = \{\boldsymbol{x} \in \mathbb{R}^{d+1} : x_i > 0,\, i = 1, \ldots, n_t \text{ and } \|\boldsymbol{x}\|_1 = 1\}$, which has edge length $\sqrt{2}$. Similarly, each element of the feedback codebook $\boldsymbol{v} \in \mathcal{V}$ defines a point $\boldsymbol{q} \in \mathcal{K}_d$ on the d-simplex, collected in the set $\mathcal{Q} \subset \mathcal{K}_d$, with $|\mathcal{Q}| = |\mathcal{V}| = 2^B$. Setting $\tilde{\vartheta}_m = \tilde{\lambda}_m$ the function $D_m(B)$ can be bounded from above by

$$D_m(B) \leq \mathbb{E}\left[\lambda_m^2\right] \max_{\boldsymbol{x}\in\mathcal{K}_d} \min_{\boldsymbol{q}\in\mathcal{Q}} \|\boldsymbol{x}-\boldsymbol{q}\|_\infty.$$

Now we show that $\delta := \max_{\boldsymbol{x}\in\mathcal{K}_d} \min_{\boldsymbol{q}\in\mathcal{Q}} \|\boldsymbol{x}-\boldsymbol{q}\|_\infty$ can be bounded from above by $c(n_t)2^{-\frac{B}{(n_t-1)}}$, with $c(n_t)$ a constant. Consider the cubes $\mathcal{B}^{n_t}_\infty(\boldsymbol{y};\delta) := \{\boldsymbol{x} \in \mathbb{R}^{n_t} : \|\boldsymbol{y}-\boldsymbol{x}\|_\infty \leq \delta\}$. If $\boldsymbol{y} \in \mathcal{K}_d$, then the intersection of the centered cubes $\mathcal{B}^{n_t}_\infty(\boldsymbol{y};\delta)$ with $\mathcal{K}_d$ is a

polytope with $2d$ facets. Let $\mathcal{B}_2^d(\delta) := \{\boldsymbol{x} \in \mathbb{R}^d : \|\boldsymbol{x}\|_2 \leq \delta\}$ be the balls with radius δ that are inscribed in this polytopes. Hence, to upperbound the number of centered cubes $\mathcal{B}_\infty^{n_t}(\boldsymbol{y}; \delta)$, with $\boldsymbol{y} \in \mathcal{K}_d$, required to cover the simplex $\mathcal{K}_d$ we need to compute the number of balls $\mathcal{B}_2^d(\delta)$ required to cover $\mathcal{K}_d$. Let the number of balls $\mathcal{B}_2^d(\delta)$ required to cover the simplex $\mathcal{K}^d$ be given by the covering number $N(\mathcal{K}_d, \mathcal{B}_2^d(\delta))$. The covering number $N(\mathcal{A}, \mathcal{B})$ is defined as the number of convex bodies $\mathcal{B}$ in $\mathbb{R}^d$ required to cover a convex body $\mathcal{A}$ in $\mathbb{R}^d$. Using the Rogers-Zong Lemma [RZ97] the covering number can be bounded from above by

$$N(\mathcal{A}, \mathcal{B}) \leq \Theta(\mathcal{B}) \frac{\mathrm{vol}(\mathcal{A} - \mathcal{B})}{\mathrm{vol}(\mathcal{B})}, \tag{2.21}$$

where $\mathrm{vol}(\cdot)$ is a function that computes the volume and $\Theta(\mathcal{B}) \geq 1$ is the covering density of $\mathcal{B}$; if $\mathbb{R}^d$ can be tiled by translates of $\mathcal{B}$ then $\Theta(\mathcal{B}) = 1$; if the covering has some overlap then $\Theta(\mathcal{B}) > 1$. Now we can use the Rogers-Shephard inequality [RS57], which states that

$$\mathrm{vol}(\mathcal{A} - \mathcal{B})\mathrm{vol}(\mathcal{A} \cap \mathcal{B}) \leq \binom{2d}{d} \mathrm{vol}(\mathcal{A})\mathrm{vol}(\mathcal{B}). \tag{2.22}$$

Assuming that $\mathrm{vol}(\mathcal{A} \cap \mathcal{B}) = \mathrm{vol}(\mathcal{B})$ we get from (2.21) and (2.22) that the covering number $N(\mathcal{A}, \mathcal{B})$ is upper bounded by

$$N(\mathcal{A}, \mathcal{B}) \leq \Theta(\mathcal{B}) \binom{2d}{d} \frac{\mathrm{vol}(\mathcal{A})}{\mathrm{vol}(\mathcal{B})}. \tag{2.23}$$

Now we can apply this bound to our problem. The volumes of the d-simplex $\mathcal{K}_d$ and the balls $\mathcal{B}_2^d(\delta)$ are $\mathrm{vol}(\mathcal{K}_d) = \frac{\sqrt{d+1}}{d!}$ and $\mathrm{vol}(\mathcal{B}_2^d(\delta)) = \frac{\pi^{d/2}}{\Gamma(1+d/2)}\delta^d$, where $\Gamma(\cdot)$ is the gamma function. Hence, the covering number can be bounded from above by

$$N(\mathcal{K}_d, \mathcal{B}_2^d(\delta)) = N(\frac{1}{\delta}\mathcal{K}_d, \mathcal{B}_2^d(1)) \leq \Theta(\mathcal{B}_2^d(1)) \binom{2d}{d} \frac{\Gamma(1 + d/2)\sqrt{d+1}}{d!\pi^{d/2}} \cdot \frac{1}{\delta^d}.$$

Solving for δ and using $2^B \leq N(\mathcal{K}_d, \mathcal{B}_2^d(\delta)) =$ we get

$$\delta \leq \left(\Theta(\mathcal{B}_2^d) \binom{2n_t - 2}{n_t - 1} \frac{\Gamma(1 + \frac{n_t - 1}{2})\sqrt{n_t}}{(n_t - 1)!\pi^{\frac{n_t-1}{2}}} \right)^{\frac{1}{n_t - 1}} 2^{-\frac{B}{n_t - 1}}.$$

Finally, for (2.23) to be valid we need to ensure that $\mathrm{vol}(\mathcal{K}_d \cap \mathcal{B}_2^d(\delta)) = \mathrm{vol}(\mathcal{B}_2^d(\delta))$ or, in other words, δ is smaller than the inradius of the inscribed circle of the simplex. According to Klamkin [KT79] for a regular simplex the inradius equals the circumradius divided by $n_t - 1$. Finally, the circumradius can be shown by the volume ratio and Stirlings formula to be greater than $\sqrt{n_t - 1}$, which completes the proof. □

2.7.6 Proof of Theorem 2.13

Proof. We use the notation defined at the beginning of this section. Recall that

$$\Delta_{RA} = 2\,\mathbb{E}\left[\sum_{m\in\mathcal{S}_h\cup\mathcal{S}_v} d(\lambda_m \boldsymbol{h}_m, \vartheta_m \boldsymbol{v}_m)\right].$$

We take an approach similar to Lemma 2.7 and use the same notation. For an arbitrary but fixed $m \in \mathcal{S}_h \cup \mathcal{S}_v$ we have

$$\begin{aligned}
&r_m(\boldsymbol{\pi}_{\mathcal{C}}, \mathcal{S}, \lambda_m \boldsymbol{h}_m) - r_m(\boldsymbol{\pi}_{\mathcal{C}}, \mathcal{S}, \vartheta_m \boldsymbol{v}_m) \\
&= \log\left(\frac{\frac{|\mathcal{S}|}{n_t} + \lambda_m^2 \sum_{l\in\mathcal{S}} \phi_{m,l}^{\boldsymbol{h}}}{\frac{|\mathcal{S}|}{n_t} + \lambda_m^2 \sum_{l\in\mathcal{S}\setminus\{m\}} \phi_{m,l}^{\boldsymbol{h}}}\right) - \log\left(\frac{\frac{|\mathcal{S}|}{n_t} + \vartheta_m^2 \sum_{l\in\mathcal{S}} \phi_{m,l}^{\boldsymbol{v}}}{\frac{|\mathcal{S}|}{n_t} + \vartheta_m^2 \sum_{l\in\mathcal{S}\setminus\{m\}} \phi_{m,l}^{\boldsymbol{v}}}\right) \\
&= \log\left(\frac{\frac{|\mathcal{S}|}{n_t} + \lambda_m^2 \sum_{l\in\mathcal{S}} \phi_{m,l}^{\boldsymbol{h}}}{\frac{|\mathcal{S}|}{n_t} + \vartheta_m^2 \sum_{l\in\mathcal{S}} \phi_{m,l}^{\boldsymbol{v}}}\right) + \log\left(\frac{\frac{|\mathcal{S}|}{n_t} + \vartheta_m^2 \sum_{l\in\mathcal{S}\setminus\{m\}} \phi_{m,l}^{\boldsymbol{v}}}{\frac{|\mathcal{S}|}{n_t} + \lambda_m^2 \sum_{l\in\mathcal{S}\setminus\{m\}} \phi_{m,l}^{\boldsymbol{h}}}\right).
\end{aligned}$$

Setting $\vartheta_m^2 = \lambda_m^2$ we get

$$\begin{aligned}
&r_m(\boldsymbol{\pi}_{\mathcal{C}}, \mathcal{S}, \lambda_m \boldsymbol{h}_m) - r_m(\boldsymbol{\pi}_{\mathcal{C}}, \mathcal{S}, \lambda_m \boldsymbol{v}_m) \\
&= \log\left(1 + \frac{n_t\lambda_m^2}{|\mathcal{S}|} \frac{\sum_{l\in\mathcal{S}} \phi_{m,l}^{\boldsymbol{h}} - \phi_{m,l}^{\boldsymbol{v}}}{1 + \lambda_m^2 \sum_{l\in\mathcal{S}} \phi_{m,l}^{\boldsymbol{v}}}\right) + \log\left(1 + \frac{n_t\lambda_m^2}{|\mathcal{S}|} \frac{\sum_{l\in\mathcal{S}\setminus\{m\}} \phi_{m,l}^{\boldsymbol{v}} - \phi_{m,l}^{\boldsymbol{h}}}{1 + \lambda_m^2 \sum_{l\in\mathcal{S}\setminus\{m\}} \phi_{m,l}^{\boldsymbol{h}}}\right) \\
&\le \log\left(1 + \frac{n_t\lambda_m^2}{|\mathcal{S}|} \left|\sum_{l\in\mathcal{S}} \phi_{m,l}^{\boldsymbol{h}} - \phi_{m,l}^{\boldsymbol{v}}\right|\right) + \log\left(1 + \frac{n_t\lambda_m^2}{|\mathcal{S}|} \left|\sum_{l\in\mathcal{S}\setminus\{m\}} \phi_{m,l}^{\boldsymbol{h}} - \phi_{m,l}^{\boldsymbol{v}}\right|\right) \\
&\le \log\left(1 + \frac{n_t\lambda_m^2}{|\mathcal{S}|} |\mathcal{S}| \max_{\boldsymbol{\pi}_{\mathcal{C}}} \left|\phi_{m,m}^{\boldsymbol{h}} - \phi_{m,m}^{\boldsymbol{v}}\right|\right) + \log\left(1 + \frac{n_t\lambda_m^2}{|\mathcal{S}|} |\mathcal{S}\setminus\{m\}| \max_{\boldsymbol{\pi}_{\mathcal{C}}} \left|\phi_{m,m}^{\boldsymbol{h}} - \phi_{m,m}^{\boldsymbol{v}}\right|\right) \\
&\le 2\log\left(1 + n_t\lambda_m^2 \max_{\boldsymbol{\pi}_{\mathcal{C}}} \left|\phi_{m,m}^{\boldsymbol{h}} - \phi_{m,m}^{\boldsymbol{v}}\right|\right) \\
&= 2\log\left(1 + P\|\hat{\boldsymbol{h}}_m\|_2^2 \max_{\boldsymbol{\pi}_{\mathcal{C}}} \left|\phi_{m,m}^{\boldsymbol{h}} - \phi_{m,m}^{\boldsymbol{v}}\right|\right).
\end{aligned}$$

The lower bound on $-(r_m(\boldsymbol{\pi}_{\mathcal{C}}, \mathcal{S}, \lambda_m \boldsymbol{h}_m) - r_m(\boldsymbol{\pi}_{\mathcal{C}}, \mathcal{S}, \vartheta_m \boldsymbol{v}_m))$ can be obtained in a similar manner. Taking expectations and using Jensen's inequality we obtain

$$\begin{aligned}
&\mathbb{E}\left[r_m(\boldsymbol{\pi}_{\mathcal{C}}, \mathcal{S}, \lambda_m \boldsymbol{h}_m) - r_m(\boldsymbol{\pi}_{\mathcal{C}}, \mathcal{S}, \lambda_m \boldsymbol{v}_m)\right] \\
&\qquad\qquad \le 2\log\left(1 + \mathbb{E}\left[P\|\hat{\boldsymbol{h}}_m\|_2^2 \max_{\boldsymbol{\pi}_{\mathcal{C}}} \left|\phi_{m,m}^{\boldsymbol{h}} - \phi_{m,m}^{\boldsymbol{v}}\right|\right]\right).
\end{aligned}$$

Since $\max_{\boldsymbol{\pi}_\mathcal{C}} |\phi^{\boldsymbol{h}}_{m,m} - \phi^{\boldsymbol{v}}_{m,m}|$ depends only on the channel directions $\boldsymbol{h}_m$, it is independent of the channel magnitude $\|\hat{\boldsymbol{h}}_m\|_2$. Using the independence and $\mathbb{E}\left[\|\hat{\boldsymbol{h}}_m\|_2^2\right] = n_t$ we get

$$\mathbb{E}\left[r_m(\boldsymbol{\pi}_\mathcal{C}, \mathcal{S}, \lambda_m \boldsymbol{h}_m) - r_m(\boldsymbol{\pi}_\mathcal{C}, \mathcal{S}, \lambda_m \boldsymbol{v}_m)\right] \leq 2 \log\left(1 + P n_t \mathbb{E}\left[\max_{\boldsymbol{\pi}_\mathcal{C}} \left|\phi^{\boldsymbol{h}}_{m,m} - \phi^{\boldsymbol{v}}_{m,m}\right|\right]\right).$$

Since the number of elements in the sum (2.8) are bounded by $2n_s$ the claim follows. □

3 Degrees of Freedom of Cellular Systems

A key challenge in wireless networks is interference. Over many decades, treating interference as noise has been seen as one of the best options to handle interfering signals with weak to moderate strength. In recent years, a technique called interference alignment has become a popular research topic. Interference alignment refers to techniques where the transmit and receive parameters are chosen such that interfering signals cast overlapping shadows at the corresponding receivers. In the landmark paper [CJ08] interference alignment was used to show that, in a fading environment, the degrees of freedom of the K-user interference channel is $K/2$. Hence, every user is able to access half of the spectrum free from interference. The degrees of freedom measure the number of signaling dimension that can be accessed free from interference. In fact, the notion of degrees of freedom has shown to be a useful metric for a better understanding of the interference problem in wireless networks. For example, in cooperative cellular systems the degrees of freedom can give a hint for user scheduling and beamforming design.

Many interference alignment schemes [Sye10, NGJV12], including the scheme used in [CJ08], use long symbol extensions (in time or frequency) to approach arbitrarily close to the optimal degrees of freedom. Instead of coding over time or frequency extensions the optimal degrees of freedom can also be achieved by coding over signal levels [MGMAK09]. However, interference alignment over limited signaling dimensions is a long standing open problem. Progress was made in [BCT11] where, for symmetric interference channels (i.e. all nodes have the same number of antennas and transmit/receive the same number of data streams), necessary and sufficient conditions for the feasibility of interference alignment were found. Recently the same authors [BCT14] have shown that for the K-User MIMO interference channel with no symbol extensions (i.e. diversity is only achieved through multiple antennas) the maximum number of degrees of freedom is bounded by 2 which is in stark contrast to the $K/2$ degrees of freedom result for fading channels.

Related Work

The downlink or uplink of a cellular system can be modeled as multiple mutually interfering broadcast or multiple access channels, respectively. To the best of our knowledge, interference alignment for cellular systems was first considered in [ST08] where an inter-

ference alignment scheme termed subspace interference alignment was proposed. The idea is to align all interference to a subspace of the receive space such that each receiver has at least one interference free dimension. The degrees of freedom of cellular systems with single antenna users are characterized in [PL09, PL11]. Further, in [SLZ10] the degrees of freedom of a two-cell cellular system with multiple base station antennas are characterized. Further results on the two-cell scenario have been found in [SLL$^+$11, SY13]. In [NMAC14] is shown that if the cells are divided in orthogonal sectors and interference from neighboring cells is the only interference, then the optimal degrees of freedom $K/2$ can be achieved – even without symbol extensions.

Analytic solutions for the interference alignment problem in the MIMO interference channel are only know for a very few special cases, e.g., the "toy example" in [CJ08]. Therefore, iterative algorithms that find an approximate interference alignment solutions have been considered. In [GCJ08, PH11] different algorithms have been proposed that possibly achieve interference alignment in the interference channel. The algorithms are based on alternating the optimization of receive filters and transmit precoders. These algorithms cannot directly be applied to cellular systems; at least, if the algorithms are applied to cellular systems, they have a very poor convergence behavior. In [ZBH11] algorithms that are based on alternating optimization are proposed for cellular systems. In [YJK10] the notion of proper systems has been introduced for the MIMO interference channel. The proper condition is a necessary condition for the feasibility of interference alignment. The concept was extended to symmetric multi-antenna cellular systems in [ZBH11], partially connected cellular systems in [GG11] and general multi-antenna cellular systems in [LY13].

Contributions

The contributions of this chapter can be summarized as follows. We characterize the degrees of freedom of fully connected symmetric cellular systems (defined below) for certain system setups and under different assumptions on the channels. First, we assume a fading environment and allow a asymptotically large number of symbol extensions. Next, we find sufficient conditions for the feasibility of interference alignment, if the number of symbol extensions is limited. Finally we assume that the transmission must be performed over constant channels (i.e. no symbol extensions are possible); here we find a sufficient condition for the feasibility of interference alignment. Based on the insight achieved by the analysis, we propose different algorithms which possibly achieve the optimal degrees of freedom. The algorithms are based on alternating the optimization of the transmit precoders and receive filters. The first algorithm aims on aligning the out-of-cell inter-

ference at each receiver in a subspace of the available receive space. It is inspired by the minimum interference leakage algorithm proposed for the interference channel in [GCJ08] and the subspace interference alignment scheme for cellular systems in [ST08]. Our second algorithm aims on directly maximizing the SINR of all receivers. A similar algorithms was independently reported in [ZBH11], but in contrast to [ZBH11] we allow symbol extensions over time or frequency and include a user selection. Therefore, our algorithm is able to operate in more general system setups. Finally our findings are underlined by extensive simulations. First, we consider a Wyner-like channel model to validate the analytic results. Then, we use a LTE related channel model to evaluate the performance of the proposed algorithms in practical scenarios.

3.1 System Setup

The system is modeled according to Section 1.3. To streamline the presentation we specify some of the assumptions and introduce shorthand notations. We assume that the number of base stations is lager than one, $T > 1$, and that each base station provides wireless service to a disjoint set of users, i.e., $\mathcal{U}_b \cap \mathcal{U}_l = \emptyset$ for all base stations $b \neq l$. We focus on symmetric cellular systems which are defined as follows.

Definition 3.1. *A cellular system, with T base stations each equipped with n_t antennas and K users per cell each equipped with n_r antennas is denoted a $\big((T, n_t) \times (K, n_r)\big)$ symmetric cellular system.*

We assume that $\mu \in \mathbb{N}$ symbol extensions are used for the transmission of a codeword. Therefore, the downlink channel from base station l to user $m \in \mathcal{U}_b$ is given by $\boldsymbol{H}_{m,l} \in \mathbb{C}^{\mu n_r \times \mu n_t}$ which has a block diagonal structure with μ blocks. Each non-zero element of the channel matrix $\boldsymbol{H}_{m,l}$ is given by independent copies of a continuous distributed random variable, and to avoid degenerated channel conditions we assume that these values are bounded between a non-zero minimum and and a finite maximum. The signal vector received by user $m \in \mathcal{U}_b$ is

$$\boldsymbol{y}_m = \boldsymbol{H}_{m,b}\boldsymbol{x}_b + \sum_{\substack{l=1 \\ l \neq b}}^{B} \boldsymbol{H}_{m,l}\boldsymbol{x}_l + \boldsymbol{n}_m \in \mathbb{C}^{\mu n_r},$$

with $\boldsymbol{n}_m \sim \mathcal{CN}(0, \boldsymbol{I}_{\mu n_r})$. The transmitted signal vector $\boldsymbol{x}_b \in \mathbb{C}^{\mu n_t \times 1}$ is constructed by a linear combination of multiple data streams. Assume that $\mathcal{S}_b$ data streams are scheduled

for transmission by base station b. Precoding matrix $\boldsymbol{V}_b \in \mathbb{C}n_t \times |\mathcal{S}_b|$ is given by

$$\boldsymbol{V}_b = [\boldsymbol{\pi}(i)]_{i \in \mathcal{S}_b}.$$

Such that the signal received by user m can be written as

$$\boldsymbol{y}_m = \sum_{b=1}^{T} \boldsymbol{H}_{m,b} \boldsymbol{V}_b \boldsymbol{s}_b + \boldsymbol{n}_m,$$

where $\boldsymbol{s}_b = \left[\frac{\mu P}{|\mathcal{S}_b|} s_i\right]_{i \in \mathcal{S}_b}^T$ is the vector of data symbols transmitted by base station b. As described in Section 1.3.3, the data symbols are modeled as complex Gaussian, $s_i \sim \mathcal{CN}(0,1)$, and power allocation between data streams is uniform. Hence, the signal transmitted over μ symbol extensions satisfies an average power constraint, $\mathbb{E}\left[\|\boldsymbol{x}_b\|_2^2\right] \leq \mu P$. To decode its intended data streams $\mathcal{R}_m \subseteq \mathcal{S}$ user m uses the receive filter

$$\boldsymbol{U}_m = [\boldsymbol{\rho}(i)]_{i \in \mathcal{R}_m}.$$

Such that the estimated data symbols of receiver m can be written as the vector

$$\hat{\boldsymbol{s}}_m = \boldsymbol{U}_m^H \boldsymbol{y}_m.$$

3.2 Degrees of Freedom of Cellular Systems

The degrees of freedom characterize the system sum-rate of a cellular system, if the transmit power P is taken to infinity. Let the scheduled data streams S be fixed. For asymptotically large transmit power P the ergodic system sum-rate with perfect channel state information, defined in (1.8), can be approximated by

$$\bar{R}_H(P) = d \log(P) + o(\log(P)),$$

where d are the degrees of freedom of the cellular system, defined as

$$d := \sum_{b=1}^{T} d_b = \lim_{P \to \infty} \frac{\bar{R}(P)}{\log(P)}.$$

Intuitively, the degrees of freedom can be seen as the number of interference free parallel data streams that can be transmitted in a wireless system.

When analyzing the degrees of freedom, the assumptions made about the channel model are crucial. One possibility is to assume that it is possible to encode the signal over many (possibly an infinite number) independent channel realizations. This coding strategy was considered in the landmark paper by Cadambe and Jafar [CJ08]. Another line of research assumes that the signal must be encoded over a single channel realization. Yet another possibility is to assume that the coding can be preformed over a small finite number of channel realizations. In the following we evaluate the degrees of freedom of cellular networks for each of these assumptions.

3.2.1 Degrees of Freedom with Varying Channels

In this subsection we assume that coding can be performed over many independent channel realizations. First, we consider single antenna users, then the degrees of freedom for users with multiple antennas follow from the single antenna case. The results are extension to cellular systems of results in [CJ08, GJ10] for the interference channel. The following corollary characterizes the degrees of freedom of certain system setups for symmetric cellular systems with single antenna users.

Corollary 3.2. *Assume a varying channel and let the channel coefficients be independent and drawn from a continuous distribution. Let $T > 1$ and assume a $\big((T, n_t) \times (K, 1)\big)$ symmetric cellular system.*

i) If $TK \leq n_t$, then $d = TK$.

ii) If $K < n_t < TK$ and n_t/K is an integer, then $d = \frac{TKn_t}{K+n_t}$.

iii) If $K \geq n_t$, then then $d = \frac{TKn_t}{K+n_t}$.

The proof is given in Section 3.6.1. We stress that similar results have been recently reported in [PL11]. The degrees of freedom for users with multiple receive antennas can now be characterized as follows.

Corollary 3.3. *Assume a $\big((T, n_t) \times (K, n_r)\big)$ symmetric cellular system and a varying channel and let the channel coefficients be independent and drawn from a continuous distribution. If $R = \frac{\max(n_t, Kn_r)}{\min(n_t, Kn_r)}$ is an integer, the degrees of freedom are partially characterized as follows.*

i) If $T > R$, then $d = \frac{Tn_tKn_r}{Kn_r+n_t}$.

ii) If $T \leq R$ and $Kn_r \leq n_t$, then $d = TKn_r$.

iii) If $T \leq R$ and $Kn_r > n_t$, then $\frac{Tn_tKn_r}{Kn_r+n_t} \leq d \leq Tn_t$.

The proof is given in Section 3.6.2.

Coordination Versus Joint Transmission.

In [3GP09a] the 3GPP defined further advancements for LTE including coordinated scheduling/beamforming and joint processing/transmission. From our point of view, a $\big((T, n_t) \times (K, n_r)\big)$ cellular system using joint transmission can be seen as a broadcast channel with Tn_t transmit antennas and TK users with n_r receive antennas each. Hence, using joint transmission a cellular system has

$$d_{\mathrm{BC}} = \min(Tn_t, TKn_r)$$

degrees of freedom [Jaf05]. On the other hand, from Corollary 3.3 we know that – for K sufficiently large – a symmetric cellular system operating in a coordinated scheduling mode (i.e. using interference alignment) achieves at least $d = \frac{Tn_tKn_r}{Kn_r+n_t}$ degrees of freedom. Hence, for a large number of users K we observe that

$$\lim_{K\to\infty} d_{\mathrm{BC}} = \lim_{K\to\infty} d = Tn_t.$$

We conclude that with increasing number of users a symmetric cellular system operating in coordinated scheduling mode can achieve the same degrees of freedom as a symmetric cellular system operating in joint transmission mode.

3.2.2 Degrees of Freedom with a Limited Number of Symbol Extensions

Corollary 3.2 and 3.3 state the maximal degrees of freedom of a symmetric cellular system, if an asymptotically large number of symbol extensions and data streams is available. However, in practical systems the number of symbol extensions and data streams is limited. Therefore, the following question arises: How many symbol extensions μ are required to guarantee interference free transmission in a $\big((T, n_t) \times (K, n_r)\big)$ cellular system with one data stream per user? For simplicity, we consider a single data stream per user. However, extensions to multiple data streams are possible.

Mathematically, this means we have to find transmit precoding vectors $\boldsymbol{\pi}$ and receive filters $\boldsymbol{\rho}$ such that the following conditions can be fulfilled.

$$\boldsymbol{\rho}(j)^H \boldsymbol{H}_{k,b} \boldsymbol{\pi}(i) = 0, \quad \forall k \in \mathcal{U}_b, \forall b \in [1, T] \text{ and } \forall\, j \in \mathcal{R}_k, \forall i \in \mathcal{S}_b \text{ with } i \neq j, \tag{3.1}$$

$$\boldsymbol{\rho}(i)^H \boldsymbol{H}_{k,b} \boldsymbol{\pi}(i) > 0, \quad \forall i \in \mathcal{R}_k, \forall k \in \mathcal{U}_b \text{ and } \forall\, b \in [1, T] \tag{3.2}$$

If these so-called interference alignment conditions are fulfilled, all receivers can null all interference and receive an interference free signal. Therefore, if conditions (3.1) and (3.2)

can be fulfilled, we say that interference alignment is feasible and the system is called proper. More precisely:

Definition 3.4. *A cellular system for which a set of transmit precoding vectors $\boldsymbol{\pi}$ and receive filters $\boldsymbol{\rho}$ exists, such that the interference alignment conditions* (3.1) *and* (3.2) *can be fulfilled, is called a proper cellular system.*

The notion of proper systems was introduced in [YJK10] for the MIMO interference channel. Recently, [ZBH11] considered $\big((T, n_t) \times (K, n_r)\big)$ cellular systems, with no symbol extensions $\mu = 1$ and a single stream per user $|\mathcal{R}_k| = 1$, and found necessary conditions for the existence of transmit precoders and receive filters such that the interference alignment conditions (3.1) and (3.2) can be fulfilled. Since we consider (orthogonal) symbol extensions, every cellular system can be turned into a proper cellular system by increasing the number of symbol extensions μ. However, we stress that not every proper cellular system achieves the maximal degrees of freedom. The following corollary follows from [ZBH11]; it states a necessary condition for a proper cellular system with symbol extensions.

Corollary 3.5. *Assume a $\big((T, n_t) \times (K, n_r)\big)$ symmetric cellular system and let the channel coefficients be independent and drawn from a continuous distribution. If the number of data streams per user $|\mathcal{R}_k| = 1$ for all $k \in \mathcal{U}$ and*

$$\mu \geq \frac{KT + 1}{n_t + n_r} \text{ and} \tag{3.3}$$

$$\mu \geq \frac{K}{n_t} \text{ and} \tag{3.4}$$

$$\mu \geq \frac{K + 1}{n_r}, \tag{3.5}$$

then the cellular system is proper according to Definition (3.4)*.*

The proof is given in Section 3.6.3.

3.2.3 Degrees of Freedom without Symbol Extensions

In this subsection we consider the problem of finding interference alignment solutions for a single channel realization. This scenario is frequently also termed the constant channel case (see e.g. [CJ08]). To establish the feasibility of interference alignment with constant channels we consider $\big((T, n_t) \times (K, n_r)\big)$ symmetric cellular systems and assume that in each transmission all users $\mathcal{U}_b$ are scheduled. We assume that the number of antennas is equal at all nodes $N = n_t = n_r$, and for each user the same number of data streams is assigned, $\delta := |\mathcal{R}_k| = |\mathcal{R}_m|$ for all $k, m \in \mathcal{U}$. The results in this section are extensions of the feasibility results for MIMO interference channels in [BCT11] and [RLL12].

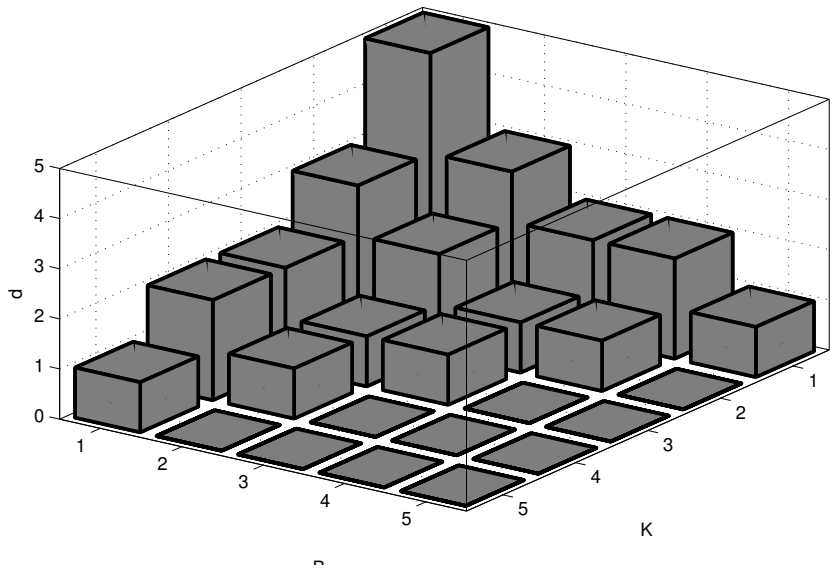

Figure 3.1: Feasibility of interference alignment for a symmetric cellular system with B base stations, K users per base station, d data streams per user and 5 antennas per node.

Corollary 3.6. *Let the number of base stations T, the number of users per base station K and the number of data streams per user δ be fixed and let the number of transmit antennas be equal to the number of receive antennas $N = n_t = n_r$. For independent channel coefficients drawn from a continuous distribution, the interference alignment problem is feasible if*

$$N \geq \frac{\delta(KT+1)}{2}.$$

The corollary is proved in Section 3.6.4. The following corollary follows directly from the Corollary 3.6.

Corollary 3.7. *Under the assumptions of Corollary 3.6*

$$\delta \leq \frac{2N}{TK+1}$$

degrees of freedom are achievable for each user.

We conclude that the total degrees of freedom of a symmetric cellular system with N antennas at each node and constant channels are bounded by

$$d \leq \frac{2NTK}{TK+1}.$$

Figure 3.1 depicts the feasible degrees of freedom for $N = 5$ transmit and receive antennas and a different number of base stations T and users K.

3.3 Interference Alignment Algorithms

In this section we present two algorithms that find sub-optimal solutions to the scheduling problem (1.7) or (1.9) (depending on the available channel state information). The algorithms exploit the duality of cellular systems. Due to the reciprocity of the wireless channel, a set of precoding vectors and receive filters achieving interference alignment in the downlink also achieve interference alignment in the uplink, if the roles of the precoder and receive filter are swapped. We stress that alternating optimization of transmit and receive parameters has been applied beforehand to wireless networks. For example [RFLT98, SCR05] considered the joint beamforming and power control problem with individual SINR constraints. Recently [GCJ08] showed that through alternating optimization interference alignment solutions for the MIMO interference channel can be found. Another (yet related) line of research was carried out in [SKB09], where power control with active link protection was considered and results from [BCP00] were extended to the axiomatic interference model of [Yat95]. In fact, it turns out that such power control schemes are requiered to prove convergence (of the objective function) of the SINR maximization algorithm presented below.

Below we introduce a centralized interference alignment algorithm for proper cellular systems (according to Definition 3.4). Then, we introduce an improved algorithm which aims on maximizing the SINR of individual users and includes a user selection. The latter algorithm does not require the systems to be proper and can be applied to arbitrary cellular systems. Later on, in Chapter 4 we introduce a distributed interference alignment algorithm that significantly reduces the feedback load by feeding back the effective channel vector instead of the entire channel matrix.

3.3.1 Centralized System Architecture

If the uplink and downlink use the same frequency band, forward and backward training can be used to obtain channel state information at the transmitters and receivers. However, cellular systems usually use different frequency bands for uplink and downlink transmissions; therefore feedback of channel state information is required. Figure 3.2 depicts an example of a centralized system architecture with feedback. Scheduling is performed by a central controller which receives channel state information through a feedback channel.

To acquire channel state information each base station b transmits orthogonal common pilots which are used by all users m to measure the channels H_m. Each user m quan-

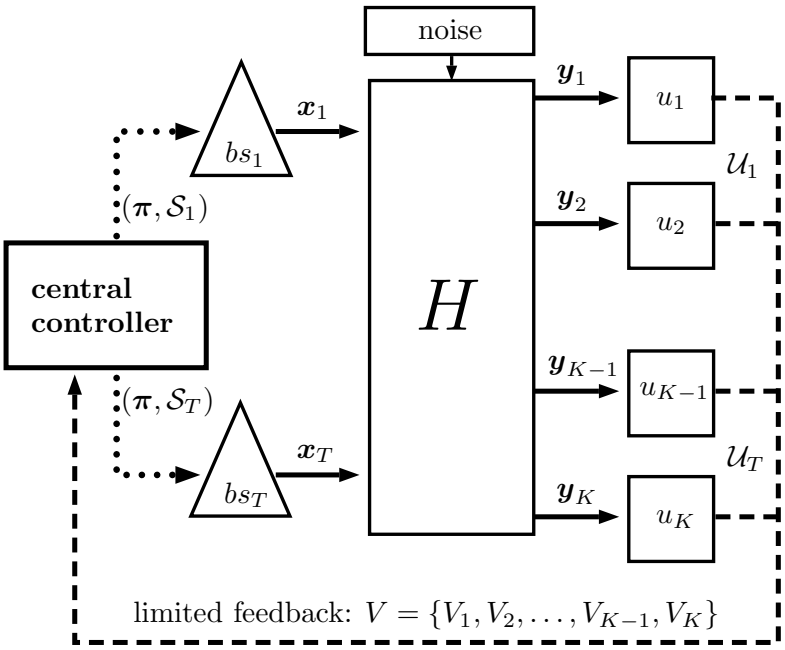

Figure 3.2: Centralized system architecture. Each user u_m feeds back quantized channel state information V_m to a central controller. Based on the available channel state information $V = \{V_1, \ldots, V_K\}$ the central controller performs scheduling and distributes the scheduling decision to the base stations $bs_1, \ldots, bs_T$.

tizes and feeds back the measured channels $V_m = (\tilde{\boldsymbol{H}}_{m,b} = \mathcal{Q}(\boldsymbol{H}_{m,b}))_{b=1,\ldots,T}$ such that the central controller has knowledge of all quantized channels $V = (V_m)_{m \in \mathcal{U}}$. Based on this quantized channel state information the central controller performs scheduling and distributes the scheduling decision among all base stations. Finally, orthogonal dedicated (i.e. precoded) pilots are transmitted by all base stations such that each user $m \in \mathcal{S}$ can estimate the effective channel $\boldsymbol{H}_{m,l}\boldsymbol{\pi}(i)$ and compute the receive filters $\boldsymbol{\rho}(i)$, for all $i \in \mathcal{R}_m$. The algorithms presented in the subsequent subsections alternates between the optimization of the receive filters and transmit precoders. The alternating optimization algorithm is summarized as follows:

i) *Initialization:* Select an arbitrary transmit precoder $\boldsymbol{V}_b \in \mathbb{C}^{n_t \times K}$, for all base stations $b = 1, \ldots, T$.

ii) *Receive filter optimization:* For fixed transmit precoders optimize the receive filter $\boldsymbol{\rho}(k) \in \mathbb{C}^{n_r}$, for all users k.

iii) *Transmit precoder optimization:* For fixed receive filters optimize the transmit precoder $\boldsymbol{V}_b \in \mathbb{C}^{n_t \times K}$, for all base stations $b = 1, \ldots, T$.

iv) *Iteration:* start from ii) until a termination condition is satisfied (e.g. maximum number of iterations, minimum residual interference).

3.3.2 Iterative Out-of-Cell Interference Minimization

Consider a proper cellular system $\big((T, n_t) \times (K, n_r)\big)$ with $|\mathcal{R}_k| = 1$ data streams per user k and let all users be scheduled, $\mathcal{S}_b = \mathcal{U}_b$. (In Section 3.3.3 below we extend the algorithm to systems which do not need to be proper by including a user selection and using a different objective function when optimizing the precoders and receive filters.) The receive filters and transmit precoders are optimized to minimize all interference. The approach is inspired by the iterative interference alignment algorithm for the interference channel [GCJ08] and the interference alignment scheme for cellular systems described in [ST08]. Our goal is to minimize the out-of-cell interference by finding receive filters $\boldsymbol{U}_k \in \mathbb{C}^{n_r \times |\mathcal{R}_k|}$ and a transmit subspace $\tilde{\boldsymbol{V}}_b \in \mathbb{C}^{n_t \times |\mathcal{S}_b|}$. The intra-cell interference is handled by an additional zeroforcing precoder. The precoder for stream $i \in \mathcal{S}_b$ is given by $\boldsymbol{\pi}(i) = \tilde{\boldsymbol{V}}_b \boldsymbol{w}_i$, where $\boldsymbol{w}_i \in \mathbb{C}^{|\mathcal{S}_b|}$ is the zeroforcing precoder.

Receive Filter Optimization

The goal of the receive filter optimization is to pick the receive subspace with minimum out-of-cell interference. Assume that all transmit precoders $\boldsymbol{V}_b$, $b = 1, \ldots, T$, are fixed, then the receive filter that minimizes the out-of-cell interference of data stream $k \in \mathcal{R}_k = \{k\}$ is given by

$$\boldsymbol{\rho}(k) = \nu_{\min} \left(\sum_{\substack{l=1 \\ l \neq b}}^{T} \tilde{\boldsymbol{H}}_{k,l} \boldsymbol{V}_l \big(\tilde{\boldsymbol{H}}_{k,l} \boldsymbol{V}_l \big)^H \right), \tag{3.6}$$

where $\nu_{\min}(\boldsymbol{X})$ is defined as the eigenvector corresponding to the smallest magnitude eigenvalue of the matrix $\boldsymbol{X}$. In the receive filter optimization no intra-cell interference is considered. Intra-cell interference is considered only in the beamformer optimization. This approach ensures that the intra-cell interference gets aligned with the out-of-cell interference.

Transmit Subspace Optimization

The transmit precoder optimization is performed in the reciprocal network. In the reciprocal network the channel from user k to base station l is given by $\overleftarrow{\boldsymbol{H}}_{b,k} = \big(\tilde{\boldsymbol{H}}_{k,b}\big)^H$. The transmit precoders are given by the receive filters in the forward network, $\overleftarrow{\boldsymbol{V}}_k = \boldsymbol{U}_k$. The

receive subspace that minimizes the out-of-cell interference at base station b is given by

$$\overleftarrow{\boldsymbol{U}}_b = \nu_{\min}^{[|\mathcal{U}_b|]} \left(\sum_{\substack{l=1 \\ l \neq b}}^{B} \sum_{k \in \mathcal{U}_l} \overleftarrow{\boldsymbol{H}}_{l,k} \overleftarrow{\boldsymbol{V}}_k \left(\overleftarrow{\boldsymbol{H}}_{l,k} \overleftarrow{\boldsymbol{V}}_k \right)^H \right),$$

where $\nu_{\min}^{[n]}(\boldsymbol{X})$ is defined as the eigenvectors corresponding to the n smallest magnitude eigenvalues of the matrix $\boldsymbol{X}$. The transmit subspace with minimum out-of-cell interference is then given by $\tilde{\boldsymbol{V}}_b = \overleftarrow{\boldsymbol{U}}_b$.

Zeroforcing of Intra-Cell Interference

After iterating between the optimization of the receive filters and the transmit subspaces, intra-cell interference is handled by an additional zeroforcing step. For each user $m \in \mathcal{U}_b$ base station b picks a zeroforcing precoding vector based on $\tilde{\boldsymbol{H}}_{k,b} \tilde{\boldsymbol{V}}_b$, for all $k \in \mathcal{U}_b \setminus \{m\}$. The zeroforcing precoding vector $\boldsymbol{w}_m \in \mathbb{S}^{|\mathcal{U}_b|-1}$ is picked from the null space of

$$\boldsymbol{w}_m \in \ker \left([\boldsymbol{\xi}_k]_{k \in \mathcal{U}_b \setminus \{m\}} \right),$$

with $\boldsymbol{\xi}_k = \left(\boldsymbol{\rho}(k)^H \tilde{\boldsymbol{H}}_{k,b} \tilde{\boldsymbol{V}}_b \right)^T \in \mathbb{C}^{|\mathcal{U}_b|}$ and $\ker(X)$ the null space of the matrix $\boldsymbol{X}$. Finally, the transmit precoder used by base station b is given by

$$\boldsymbol{V}_b = \left[\tilde{\boldsymbol{V}}_b \boldsymbol{w}_k \right]_{k \in \mathcal{U}_b}. \tag{3.7}$$

In the simulations presented in Section 3.4 we show that if interference alignment is feasible, the algorithm finds an interference alignment solution with high probability.

Convergence of the Residual Interference

The convergence of the residual interference using the minimum interference algorithm can be proved in a similar manner as the proof of convergence in [GCJ08] for the K-user interference channel. Key observations are the following. First, the out-of-cell interference is monotonically decreased when computing the receive filter (3.6). Second, the transmit beamformer computation (3.7) decreases the out-of-cell interference and nulls all intra-cell interference. Note that even if the residual interference converges to a local minimum, it is not guaranteed that the algorithm converges to a unique solution.

Algorithm 2 - Outer loop: Receive filter optimization and iteration

1: Set $\boldsymbol{\pi}(i) = 1/\sqrt{N}[1, 1, \ldots, 1]^T$ for all $i \in \mathcal{U}$ and $\mathcal{S}_b = \emptyset$ for all b.
2: **repeat**
3: **for** $b = 1$ to T and all $k \in \mathcal{U}_b$ **do**
4: **if** $k \in \mathcal{S}_b$ **then**
5: Compute receive filter $\boldsymbol{\rho}(k)$ according to (3.8).
6: **else**
7: Receive filter is $\boldsymbol{\rho}(k) = \tilde{\boldsymbol{H}}_{k,b}\boldsymbol{\pi}(k)$.
8: **end if**
9: **end for**
10: **Inner loop:** User selection and precoder optimization (Input: $\boldsymbol{\rho}$. Output: $\mathcal{S}_b$ and $\boldsymbol{\pi}$).
11: **until** some termination condition is satisfied.

3.3.3 Iterative SINR Maximization with User Selection

The algorithm presented in this subsection can handle cellular systems with an arbitrary number of users U. For the ease of presentation we assume a single data stream per user an let user i be associated with data stream i. For each transmission interval the central controller selects a subset of users $\mathcal{S}_b \subseteq \mathcal{U}$ for transmission. Users are selected to maximize the approximated sum rate $R(P, \boldsymbol{\pi}, S, V)$. However, finding the optimal user selection is computationally not tractable, therefore we apply a greedy user selection that starts with no selected users and adds a new user – if this increases the approximated sum rate $R(P, \boldsymbol{\pi}, S, V)$ – every time the transmit precoders are updated. The receive filters and transmit precoders are optimized to maximize the achievable rate of each user. The approach is inspired by the maximum SINR algorithm proposed for the interference channel in [GCJ08]. However, cellular systems differ from the interference channel since intra-cell and out-of-cell interference occurs and the intra-cell interference is observed through the same channel as the desired signal. For cellular systems we have found that the best convergence behavior can be achieved if intra-cell interference is considered only in the optimization of the transmit precoders. Another algorithm that aims on maximizing the SINR was recently proposed in [ZBH11]. In contrast to the algorithm proposed here [ZBH11] considers intra-cell interference only at the receivers and required an additional orthogonality constraint at the transmitters.

For the ease of presentation, the algorithm is split in an outer loop and an inner loop. For fixed receive filters the inner loop performs the user selection and the optimization of transmit precoders. The outer loop optimizes the receive filters for a fixed set of users and fixed precoders. The outer loop is summarized in Algorithm 2. It is performed until some termination condition is satisfied, e.g. a maximum number of iterations is reached.

Algorithm 3 - Inner loop: User selection and precoder optimization

Input: $\boldsymbol{u}_k$ for all $k \in \mathcal{U}$
Set: $\mathcal{S}_b = \emptyset$ for all b
repeat
  for $b = 1$ to T **do**
    for $k \in \mathcal{U}_b \setminus \mathcal{S}_b$ **do**
      $\mathcal{T}_b = \{k\} \cup \mathcal{S}_b$
      Compute precoder for potential new user and all other users selected by that base station $\boldsymbol{\pi}(k) = \overleftarrow{\boldsymbol{\rho}}(k)$ for all $k \in \mathcal{T}_b$.
      Update precoder of all previously selected users $\boldsymbol{\pi}(m) = \overleftarrow{\boldsymbol{\rho}}(m)$ for all $l \neq b$ and all $m \in \mathcal{S}_l$.
      Compute achievable system sum-rate $R(P, \boldsymbol{\pi}, S, V)$ with $S = (\mathcal{S}_1, \ldots, \mathcal{S}_{b-1}, \mathcal{T}_b, S_{b+1}, \ldots, \mathcal{S}_T)$.
    end for
    Add one new user if sum rate increases.
  end for
until No new users added at any base station b.

In the outer loop all base stations are processed in an arbitrary ordering and the optimal receive filters $\boldsymbol{\rho}(k)$ are computed as described below. If no users are selected by a base station, isotropic interference from that base station is assumed, i.e., it is assumed the base station transmits with the precoding vector $\boldsymbol{V}_b = 1/\sqrt{N}[1, 1, \ldots, 1]^T$. The inner loop is summarized in Algorithm 3. It comprises of the user selection and the computation of transmit precoders. In every iteration step the inner loop starts with no selected users. All base stations are processed in an arbitrary ordering until no new users are added to the system. For each base station b a new user is added, if this increases the system sum rate. Each time a user is added to the system all precoders are updated such that the new interference situation is considered.

Receive Filter Optimization

The receive filter optimization is performed as follows. Assume that all transmit precoders $\boldsymbol{V}_b$, $b = 1, \ldots, T$ are fixed. The receive filter for user $k \in \mathcal{S}$ is then given by

$$\boldsymbol{\rho}(k) = \nu_{\max}\big(\boldsymbol{\Theta}_{k,b}^{-1}\boldsymbol{G}_{k,b}\big), \tag{3.8}$$

where $\nu_{\max}(\boldsymbol{X})$ is defined as the eigenvector corresponding to the largest magnitude eigenvalue of the matrix $\boldsymbol{X}$. The gain covariance matrix is defined as

$$\boldsymbol{G}_{b,k} = \tilde{\boldsymbol{H}}_{k,b}\boldsymbol{\pi}(k)\big(\tilde{\boldsymbol{H}}_{k,b}\boldsymbol{\pi}(k)\big)^H$$

and the out-of-cell interference plus noise covariance matrix is defined as

$$\boldsymbol{\Theta}_{k,b} = \sum_{\substack{l=1 \\ l\neq b}}^{T} \tilde{\boldsymbol{H}}_{k,b}\boldsymbol{V}_l\big(\tilde{\boldsymbol{H}}_{k,b}\boldsymbol{V}_l\big)^H + \boldsymbol{I}_{\mu n_r}.$$

We stress that in the receive filter optimization no intra-cell interference is considered.

Transmit Precoder Optimization

The transmit precoder optimization is performed on the (virtual) reciprocal network. The receive filter (in the reciprocal network) for user k is given by

$$\overleftarrow{\boldsymbol{\rho}}(k) = \nu_{\max}\left(\overleftarrow{\boldsymbol{\Theta}}_{b,k}^{-1}\overleftarrow{\boldsymbol{G}}_{b,k}\right).$$

The interference plus noise covariance matrix is defined as

$$\overleftarrow{\boldsymbol{\Theta}}_{b,k} = \sum_{l=1}^{T}\sum_{j\in\mathcal{S}_l\setminus\{k\}} \overleftarrow{\boldsymbol{H}}_{l,k}\overleftarrow{\boldsymbol{\pi}}(k)\big(\overleftarrow{\boldsymbol{H}}_{l,k}\overleftarrow{\boldsymbol{\pi}}(k)\big)^H + \boldsymbol{I}_{\mu n_t}$$

and the gain covariance matrix is defined as

$$\overleftarrow{\boldsymbol{G}}_{b,k} = \overleftarrow{\boldsymbol{H}}_{b,k}\overleftarrow{\boldsymbol{\pi}}(k)\big(\overleftarrow{\boldsymbol{H}}_{b,k}\overleftarrow{\boldsymbol{\pi}}(k)\big)^H.$$

Finally, the transmit precoder for user k is given by $\boldsymbol{\pi}(k) = \overleftarrow{\boldsymbol{\rho}}(k)$.

3.4 Simulations

First we validate the results in Section 3.2. Then we consider a more practical scenario to further evaluate the performance of the algorithms described in Section 3.3.

3.4.1 Numerical Evaluation

In this subsection we validate the results of Section 3.2. We consider the Wyner-like channel model [Wyn94]. All channels are given by $\boldsymbol{H}_{k,b} = \alpha_{k,b}\hat{\boldsymbol{H}}_{k,b}$. The elements of $\hat{\boldsymbol{H}}_{k,b}$ are drawn from a complex Gaussian distribution with zero mean and variance $(2n_t n_r)^{-1/2}$

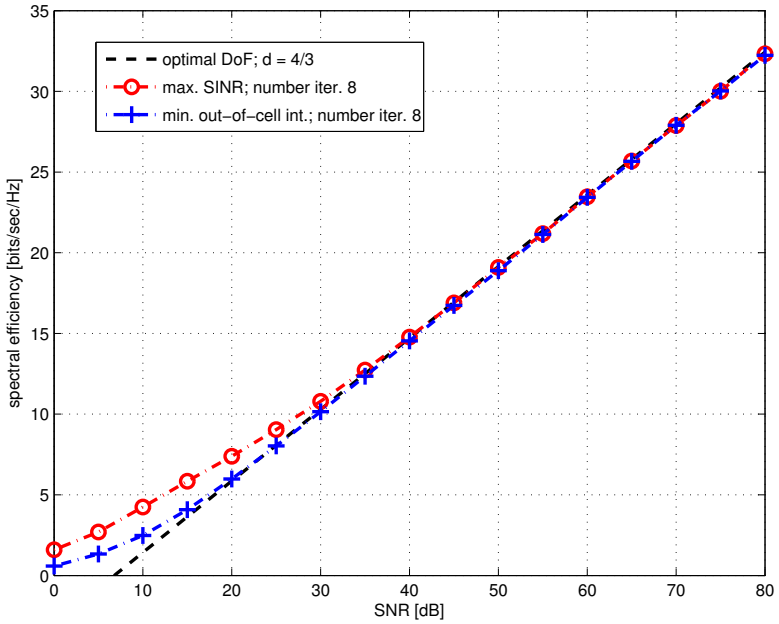

Figure 3.3: $\big((2,1)\times(2,1)\big)$ cellular system; spectral efficiency vs. SNR; $\mu = 3$ symbol extensions the proposed algorithms achieve the optimal degrees of freedom $d = 4/3$.

such that $\mathbb{E}\left[\|\hat{\boldsymbol{H}}_{k,b}\|_F^2\right] = 1$. The channel gain between base station b and user k is modeled by $\alpha_{k,b} \in \mathbb{R}_+$. In the simulations $\alpha_{k,b} = 1$ was chosen for all b and all k. We assume perfect channel state information at the central controller and a single data stream per user. We apply the out-of-cell interference minimization algorithm and the SINR maximization algorithm without user selection, i.e., all users are scheduled and only the receive filters and precoders are optimized. As a baseline we consider local zeroforcing, i.e., each base station selects the transmit precoder under the zeroforcing constrained, considering only users within the same cell. The receive beamforming vector is given by the SINR maximizing solution.

$\big((2,1)\times(2,1)\big)$ Cellular System

Consider a $\big((2,1)\times(2,1)\big)$ symmetric cellular system. From Corollary 3.6 we know that interference alignment is feasible $\mu \geq 2.5$. If we chose $\mu = 3$ each user has a three dimensional receive space but also receives three interfering streams. Thus, to enable each user to cancel all interference, the interference must be aligned in two dimensions at each user. If interference alignment can be achieved, the maximal degrees of freedom are $d = 4/3$.

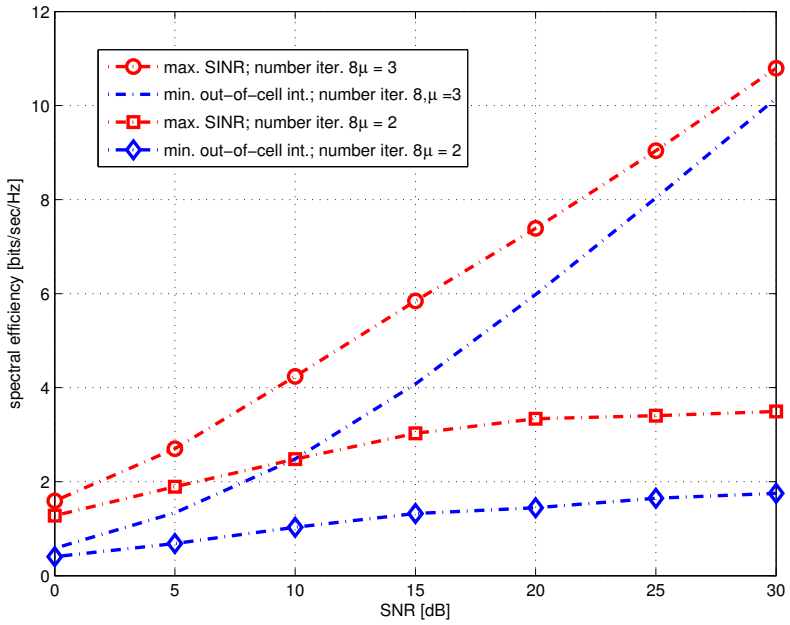

Figure 3.4: $\big((2,1)\times(2,1)\big)$ cellular system; spectral efficiency vs. SNR; $\mu = 3$ and $\mu = 2$ symbol extensions; with $\mu < 3$ the optimal degrees of freedom cannot be achieved.

Figure 3.3 shows that the cellular max SINR algorithm and the min out-of-cell interference algorithm are not interference limited at high SNR and achieve the maximal degrees of freedom. The dashed black graph shows the 3/4 slope; the offset was chosen arbitrarily. Figure 3.4 depicts the performance of the proposed algorithms if $\mu = 2$ symbol extensions are used, i.e. interference alignment is not feasible. It can be observed that with $\mu = 2$ the spectral efficiency becomes interference limited at high SNR.

In Figure 3.5 we compare the proposed algorithms with local zeroforcing. We observe that local zeroforcing is interference limited and is clearly outperformed by the proposed algorithms. A remarkable result is that one iteration is sufficient to achieve a significant gain over the zeroforcing performance. If we increase the number of iterations, the performance of the min out-of-cell interference algorithm increases only slightly but the cellular max SINR algorithm increases its performance significantly.

$\big((3,5)\times(3,5)\big)$ Cellular System

From Corollary 3.6 we know that in a $\big((3,5)\times(3,5)\big)$ cellular system interference alignment is feasible if $\mu \geq 1$. We chose $\mu = 1$ and make the following observation: At each receiver the interference from 8 unintended signals must be aligned in at least 4 dimensions of the 5 dimensional receive space. From Corollary 3.3 we have that $45/4 \leq d \leq 15$, but to

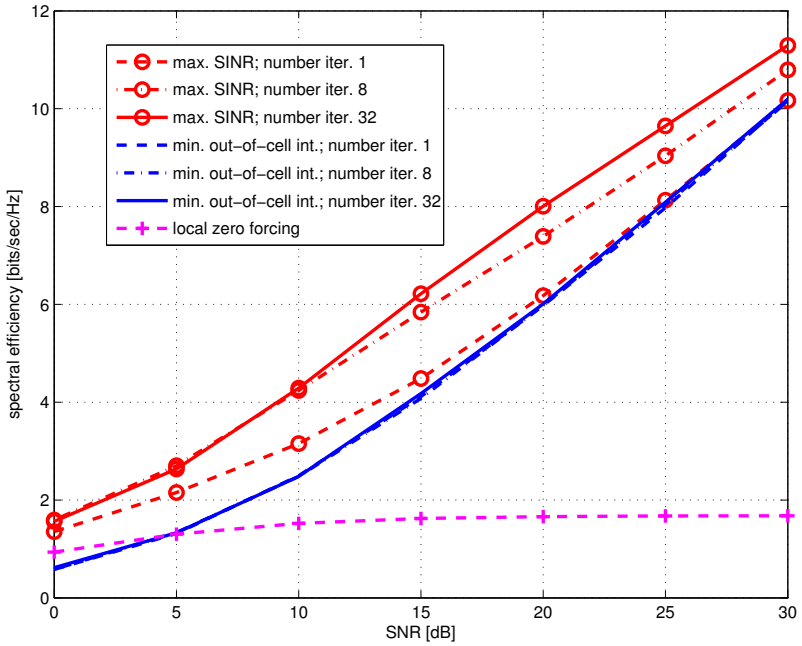

Figure 3.5: $\big((2,1) \times (2,1)\big)$ cellular system with $\mu = 3$; spectral efficiency vs. SNR; proposed algorithms outperform local zero forcing beamforming.

achieve the optimal degrees of freedom we require multiple data streams per user and an increasing number of symbol extensions. With a single stream per user and no symbol extensions the maximal degrees of freedom are $d = TK = 9$.

$\big((3,4) \times (2,2)\big)$ Cellular System

In a $\big((3,4) \times (2,2)\big)$ cellular system interference alignment is feasible if the number of symbol extensions $\mu \geq 7/6$. Hence, if we chose $\mu = 1$ we expect that the performance becomes interference limited at high SNR. Figure 3.7 shows a comparison of the proposed algorithms with local zeroforcing. We observe that the max SINR algorithm and the min out-of-cell interference algorithm are interference limited at high SNR. The cellular max SINR algorithm clearly outperforms local zeroforcing and the min out-of-cell interference algorithm outperforms local zeroforcing if SNR is higher than 10 dB. We conclude that even if the proposed algorithms cannot guarantee interference free transmissions for arbitrary cellular systems, a significant gain over non-cooperating schemes can be achieved.

3.4.2 LTE Related Simulations

In this subsection we consider SINR based simulations. The system setup is in accordance with the LTE specifications [3GP09b] and summarized in Table 3.1. The simulation setup

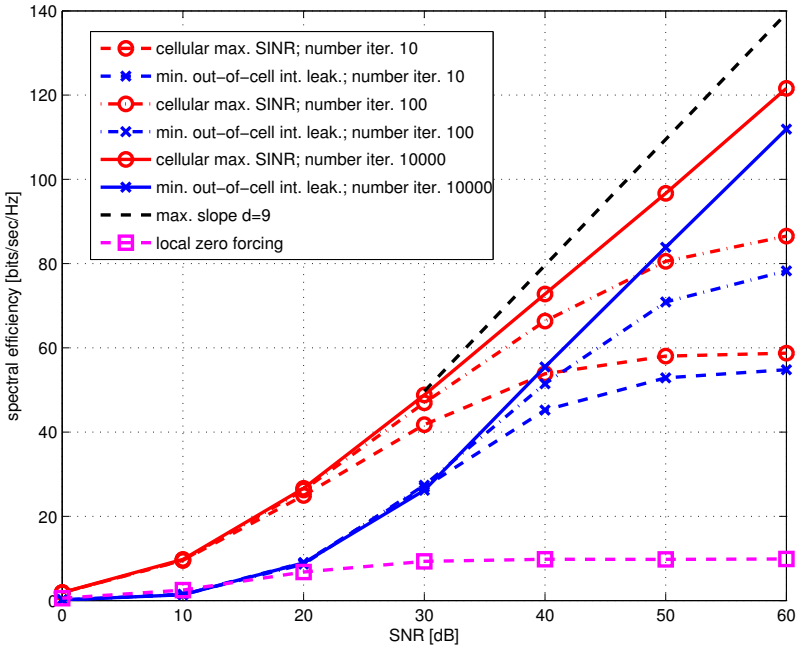

Figure 3.6: $\big((3,5)\times(3,5)\big)$ cellular system; spectral efficiency vs. SNR; comparison of the minimum out-of-cell interference algorithm and the cellular max SINR algorithm for different number of iterations. Both algorithms achieve the maximal degrees of freedom.

is essentially similar to the setup used in Section 2.5.2. The channels are modeled using the SCME [BSM+05]. The cluster of cooperating base stations comprises three base stations which are located at different sites but have the same network area. Figure 2.9 shows the average SINR distribution over the network area. The three peaks are close to the base station locations. Channel state information is assumed to be averaged over one scheduling block. One scheduling block comprises of 12 adjacent subcarriers. Therefore, the transmit precoders and receive filters are computed per scheduling block.

We compare the SINR maximization algorithm with user selection (Subsection 3.3.3) with two baseline schemes. The first baseline is given by local zeroforcing and block diagonalization with greedy user selection. Using local zeroforcing each base station nulls all intra-cell interference but takes no steps to minimize the out-of-cell interference. The user selection is performed in a greedy fashion [TBT07]. The second baseline is block diagonalization. When using block diagonalization each scheduled user is connected to all (three) base stations. The detailed algorithm is described in [SSH04]. Block diagonalization is a joint transmission scheme and therefore requires data sharing between the base stations.

In Figure 3.8 we assume perfect channel state information and compare the system spectral efficiency of the proposed SINR maximization algorithm with local zeroforcing

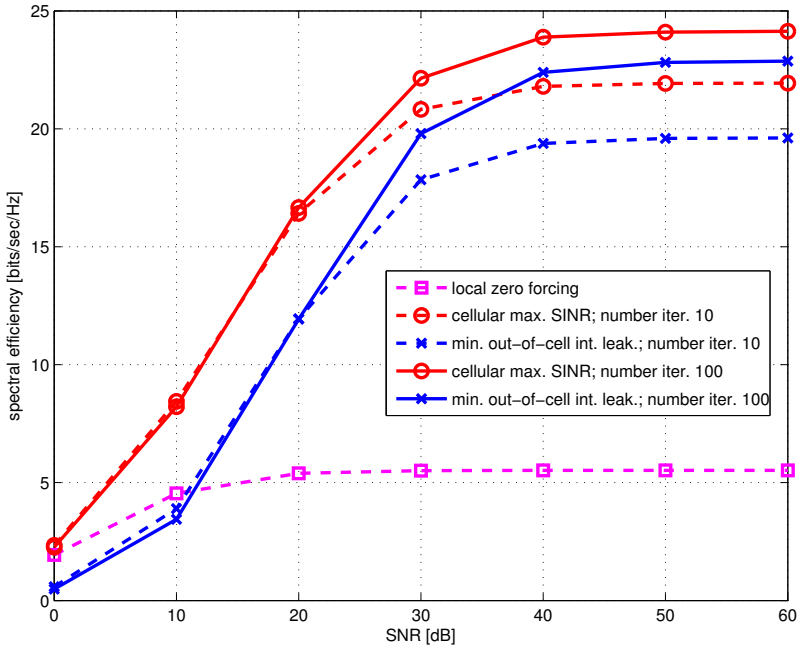

Figure 3.7: $\big((3,4)\times(2,2)\big)$ cellular system with $\mu = 1$; spectral efficiency vs. SNR; comparing the proposed algorithms with local zeroforcing beamforming.

and block diagonalization. We observe that block diagonalization performs about 10 bit/s/Hz better than the proposed scheme which performs about 15 bit/s/Hz better than local zeroforcing. We conclude that with perfect channel state information we can observe a significant *cooperation gain*.

Now we consider quantized channel state information at the base stations. Assume each user quantizes its channel in the time-domain; an approach proposed for LTE in [Wil10]. To do so, we assume that most significant $n_p = 6$ channel taps lie within the first $n_{cp} = 100$ samples. The real and imaginary parts of each of the n_p channel taps is quantized using n_B bits. Further, we assume that a user reports a feedback message every $T_{FB} = 0.5$ ms. Thus, the feedback rate is

$$R_{FB} = \frac{n_t n_r}{T_{FB}}(\log_2(n_{cp}) + 2n_p n_B) \text{ bit/s/user}.$$

Figure 3.9 shows the mean spectral efficiency of the feedback rate. We observe that at a relevant feedback rate (i.e. $R_{FB} < 5$ Mbit/s/user) the proposed max SINR algorithm performs close to block diagonalization. This is a remarkable result since the requirements on the backhaul network are significantly smaller than with block diagonalization which requires data sharing. In the regime of very small feedback rates the rate approximation scheme discussed in Chapter 2 gives the best performance.

Table 3.1: Summary of simulation parameters.

Parameter	Description
Scenario	FDD Downlink
Number BS	3
Number UE	30
Antenna configuration	BS: 4 Tx Ant.; MS: 2 Rx Ant. uniform linear array ($\lambda/2$ spacing)
Carrier Frequency	2.1 GHz, 10 MHz bandwidth
Scheduling block size	1 PRB
Number streams per user	1
Modulation and Coding	ideal link adaptation
Pilot/control overhead	not taken into account
Feedback	per scheduling block
Channel model	SCME: urban macro (3 km/h, high angular spread)
Scheduling	frequency selective SDMA.
Max. users per SB	4 (MU-MIMO mode)
Receiver	linear receiver with ideal channel state information
Intra-cell/Out-of-cell interference	fully modeled

3.5 Summary and Conclusions

We considered cellular systems which are a natural extension of the interference channel. The degrees of freedom of certain cellular systems and under different assumptions on the channel statistics have been derived. Conditions for the feasibility of interference alignment for systems with symbol extension have been found. The insights obtained in the analysis motivated us to propose different algorithms for the optimization of beamforming vectors and receive filters. One of the algorithms includes a greedy user selection, which exploits the multi-user diversity of cellular systems. In the simulations we showed that in certain scenarios the optimal degrees of freedom can be achieved with the proposed algorithms. We demonstrated that even if the optimal degrees of freedom can not be achieved – in some scenarios – an interference free transmission can be guaranteed. For other scenarios, we saw that even if an interference free transmission can not possible the proposed algorithms have huge advantages, in terms of sum rate, over uncoordinated schemes. We demonstrated by LTE related simulations that – in a practical scenario – the proposed algorithms performs very close to joint transmission schemes that require data sharing. In Chapter 4 we will further evaluate the performance degradation of coordinated transmit strategies due quantized channel state information feedback.

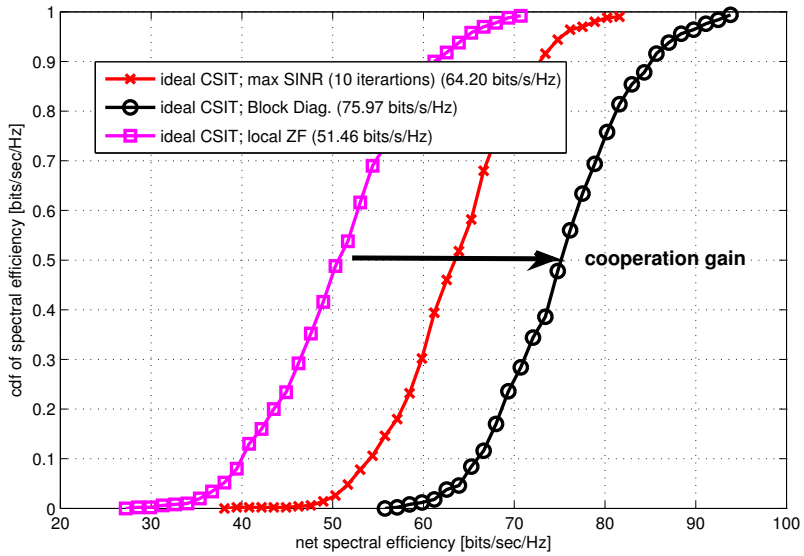

Figure 3.8: CDF of system spectral efficiency; ideal channel state information; comparing the proposed max SINR algorithm with local zeroforcing and block diagonalization.

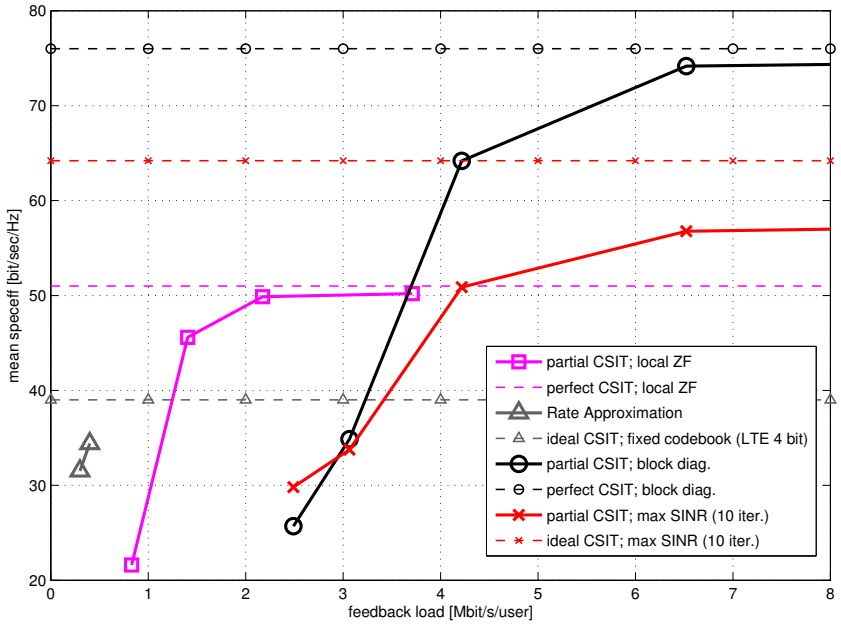

Figure 3.9: Mean spectral efficiency vs. feedback load [Mbit/sec/user]; comparison of different transmit strategies.

3.6 Proofs

3.6.1 Proof of Corollary 3.2

Proof. We consider the three cases $TK \leq n_t$, $K < n_t < TK$ and $n_t \leq K$ separately.

Case $TK \leq n_t$: Each base station has more antennas than users in the system, hence, the degrees of freedom are bounded from bellow by $d \geq TK$, which can be achieved by zeroforcing at the base station. The outer bound is obtained by allowing all users and all base stations to cooperate. Hence, the outer bound is given by the degrees of freedom of the $Tn_t \times TK$ point-to-point MIMO channel [Jaf05], that is, $d \leq TK$. Since the inner and outer bound are the same, the claim $d = TK$ if $TK \leq n_t$ follows.

Case $K < n_t < TK$: If n_t/K is an integer the inner bound is given by the degrees of freedom of the TK user $n_t/K \times 1$ interference channel, that is, each user communicates with n_t/K antennas of its assigned base station. Using [GJ10, Theorem 3] we obtain the inner bound $d \geq \frac{n_t TK}{n_t+K}$. The outer bound follows by allowing cooperation between users in the same cell, which yields the T user $n_t \times K$ interference channel. Applying [GJ10, Theorem 1] the degrees of freedom are bounded from above by $d \leq \frac{n_t TK}{n_t+K}$.

Case $K \geq n_t$: The outer bound can be proved in a similar manner as the degrees of freedom outer bound for the X-channel in [CJ09]. Due to the duality of the degrees of freedom in the uplink and downlink of cellular systems [ST08] it is sufficient to show the degrees of freedom for the uplink. To this end define the set of messages

$$\mathcal{W}^{[l,b]} = \{W_i : \forall\, i \in \mathcal{U}_b\} \cup \{W_i : \forall\, i \in \mathcal{S}_l \subseteq \mathcal{U}_l, |\mathcal{S}_l| = n_t\}\,,$$

that is, n_t messages W_i that originate from users in cell l plus all messages that are intended for base station b. See Figure 3.10 for an example.

Now we compute the degrees of freedom of a cellular system where all messages that are not in $\mathcal{W}^{[l,b]}$ are eliminated. Obviously, this assumption cannot reduce the rate achieved by the remaining messages. Subsequent, the outer bound of the total degrees of freedom follows by summing these partial outer bounds over all cells b and $l \neq b$.

Fix some pair (b, l) with $l \neq b$. Consider any reliable coding scheme such that base station b can decode and subtract all messages $W_i \in \mathcal{W}^{[l,b]}$ with $i \in \mathcal{U}_b$ from the received signal. Now, if we reduce the noise at base station b this base station can also decode the messages $W_i \in \mathcal{W}^{[l,b]}$ with $k \in \mathcal{S}_l$, $l \neq b$. This has transformed the cellular system into a MAC with messages $\mathcal{W}^{[l,b]}$. Hence, the degrees of freedom of the cellular system with

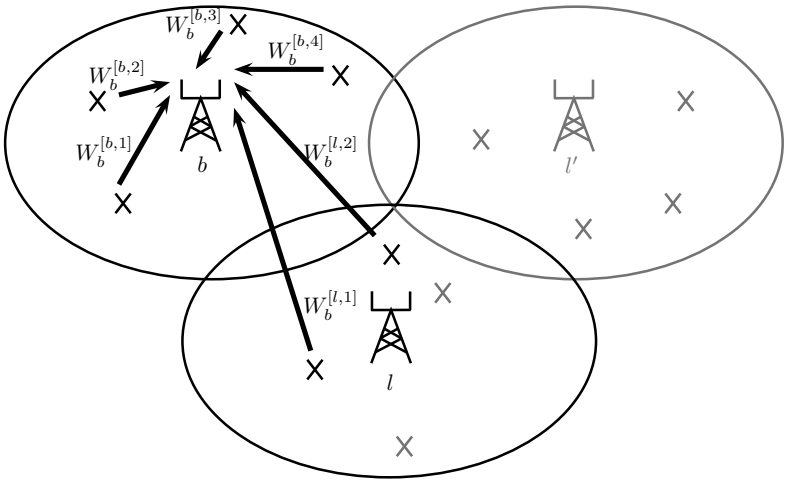

Figure 3.10: Example of message set $\mathcal{W}^{[l,b]}$ for a $\big((3,2)\times(4,1)\big)$ cellular system. Base station b decodes all messages from the users in $\mathcal{U}_b$ and additionally decodes the messages $W_l^{[l,1]}$ and $W_l^{[l,2]}$ from users in cell l.

reduced noise and messages $\mathcal{W}^{[l,b]}$ is upper bounded by

$$\sum_{i\in\mathcal{U}_b} d_{b,i} + \sum_{k\in\mathcal{S}_l} d_{l,k} \leq n_t.$$

Summing the last inequality over all b and $l \neq b$ and using $d = \sum_{b=1}^{T}\sum_{i\in\mathcal{U}_b} d_{b,i}$ we obtain the outer bound,

$$\begin{aligned}
&\sum_{b=1}^{T}\sum_{\substack{l=1\\l\neq b}}^{T}\left(\sum_{i\in\mathcal{U}_b} d_{b,i} + \sum_{k\in\mathcal{S}_l} d_{l,k}\right) \leq T(T-1)n_t \\
\Leftrightarrow\ &(T-1)d + \sum_{b=1}^{T}\sum_{l\neq b}^{T}\sum_{k\in\mathcal{S}_l} d_{l,k} \leq T(T-1)n_t
\end{aligned}$$

Since, $d_{l,k} = d_{l,k'}$ for all $k, k' \in \mathcal{U}_l$ we can sum the last inequality over all $k' \in \mathcal{U}_l$ and obtain the outer bound

$$\begin{aligned}
\Leftrightarrow K(T-1)d + (T-1)n_t d &\leq T(T-1)Kn_t \\
\Leftrightarrow Kd + n_t d &\leq TKn_t \\
\Leftrightarrow d &\leq \frac{TKn_t}{K+n_t}.
\end{aligned}$$

The achievable scheme can be summarized as follows. n_t users in cell 1 and n_t users in cell 2 define the interference subspace at each base station $b = 1, \ldots, T$. All remaining users align their interference in this interference subspace. Further, we require that the two interference subspaces at base station $b = 3, \ldots, T$ have an overlap of sufficient size, as depicted in Figure 3.13. Then, as we will show, for any $n \in \mathbb{N}$ the achievable scheme achieves the degrees of freedom

$$\delta(n) = \frac{2n_t^2(n+1)^\Gamma + 2n_t(K-n_t)n^\Gamma + (T-2)n_tKn^\Gamma}{2n_t(n+1)^\Gamma + (K-n_t)n^\Gamma}, \tag{3.9}$$

where the parameter Γ must be careful chosen, as shown below. Taking $n \to \infty$ yields the degrees of freedom of the achievable scheme

$$d = \lim_{n\to\infty} \delta(n) = \frac{TKn_t}{K+n_t}.$$

Next the achievable scheme is described in details. The uplink channel between some base station (receiver) b and user (transmitter) $m \in \mathcal{U}_l$ is denoted as $\bar{\boldsymbol{H}}_b^{l,m}$. Let the total number of dimensions available at each transmitter be

$$\mu_n = 2n_t(n+1)^\Gamma + (K-n_t)n^\Gamma,$$

that is, $\bar{\boldsymbol{H}}_b^{l,m} \in \mathbb{C}^{\mu_n n_t \times \mu_n}$, for all m, b, l. We stress that this notation is somewhat inconsistent with the notation used in this thesis but it will simplify the readability the proof significantly. In cell $b = 1, 2$ a subset of n_t users, collected in the index set $\hat{\mathcal{U}}_b \subseteq \mathcal{U}_b$, transmits $n_t(n+1)^\Gamma$ streams using the precoder

$$\bar{\boldsymbol{V}}^{[b,\varkappa]} = \boldsymbol{V}_1 \in \mathbb{C}^{\mu_n \times n_t(n+1)^\Gamma}, \text{ with } \varkappa \in \hat{\mathcal{U}}_i.$$

All remaining users $m \in \mathcal{U}_l \setminus \hat{\mathcal{U}}_l$ with $l = 1, 2, \ldots, T$ transmit $n_t n^\Gamma$ streams using the precoder

$$\bar{\boldsymbol{V}}^{[l,m]} = \boldsymbol{V}_2 \in \mathbb{C}^{\mu_n \times n_t n^\Gamma}.$$

Hence, at base station $b = 1, 2$ the intended signals span $n_t^2(n+1)^\Gamma + (K-n_t)n_tn^\Gamma$ dimensions and at base station $b = 3, \ldots, T$ the intended signals span Kn_tn^Γ dimensions.

Consequently, at the base stations $1, 2$ all interference must align in a $n_t\mu_n - n_t^2(n+1)^\Gamma - (K-n_t)n_tn^\Gamma = n_t^2(n+1)^\Gamma$ dimensional subspace and at base stations $3, \ldots, T$ all interference must align in a $n_t\mu_n - Kn_tn^\Gamma = 2n_t^2(n+1)^\Gamma - n_t^2n^\Gamma$ dimensional subspace. If we require the following conditions on the precoders $\boldsymbol{V}_1$ and $\boldsymbol{V}_2$, interference alignment can be achieved as required.

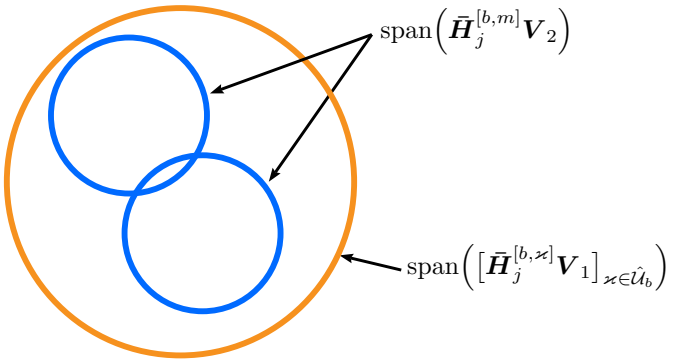

Figure 3.11: Alignment condition **C1**: The users $\varkappa \in \hat{\mathcal{U}}_b$ in cells $b = 1, 2$ span an interference subspace at all base stations $j = 1, 2, \ldots, T$, $j \neq b$, in which the interference subspace spanned by the users $m \in \mathcal{U}_b \setminus \hat{\mathcal{U}}_b$ aligns.

C1 At all base stations $j = 1, 2, \ldots, T$ the interference generated by the users $m \in \mathcal{U}_b \setminus \hat{\mathcal{U}}_b$, with $b = 1, 2$, $b \neq j$, must align with the interference generated by the users $\varkappa \in \hat{\mathcal{U}}_b$,

$$\text{span}\left(\bar{\boldsymbol{H}}_j^{[b,m]}\boldsymbol{V}_2\right) \subseteq \text{span}\left(\left[\bar{\boldsymbol{H}}_j^{[b,\varkappa]}\boldsymbol{V}_1\right]_{\varkappa\in\hat{\mathcal{U}}_b}\right)$$

C2 The interference at base stations $j = 1, \ldots, T$ generated by the users $m \in \mathcal{U}_i$ in cell $i = 3, 4, \ldots, T$, with $i \neq j$, must align with the interference subspace spanned by the users $\varkappa \in \hat{\mathcal{U}}_b$ with $b = 1, 2$ and $b \neq j$. That is,

$$\text{span}\left(\bar{\boldsymbol{H}}_j^{[i,m]}\boldsymbol{V}_2\right) \subseteq \text{span}\left(\left[\bar{\boldsymbol{H}}_j^{[b,\varkappa]}\boldsymbol{V}_1\right]_{\varkappa\in\hat{\mathcal{U}}_b}\right)$$

An example of the interference subspace alignment according to conditions **C1** and **C2** are depicted in Figure 3.11 and 3.12, respectively.

According to condition **C1** and **C2** at base stations $b = 1, 2$ the interference occupies $n_t^2(n+1)^\Gamma$ dimensions, which leaves the required $n_t^2(n+1)^\Gamma + n_t(K - n_t)n^\Gamma$ dimensions for the intended signals.

To obtain the Kn_tn^Γ dimensional interference free subspace at base station $i = 3, \ldots, T$ we need one extra alignment condition. Due to condition **C1** and **C2** we can guarantee that all interference is aligned in a $2n_t^2(n+1)^\Gamma$ dimensional subspace. To achieve the required Kn_tn^Γ interference free dimensions we need that $n_t^2n^\Gamma$ interfering signals from users $\hat{\mathcal{U}}_1$ align with the interfering signals from users $\hat{\mathcal{U}}_2$.

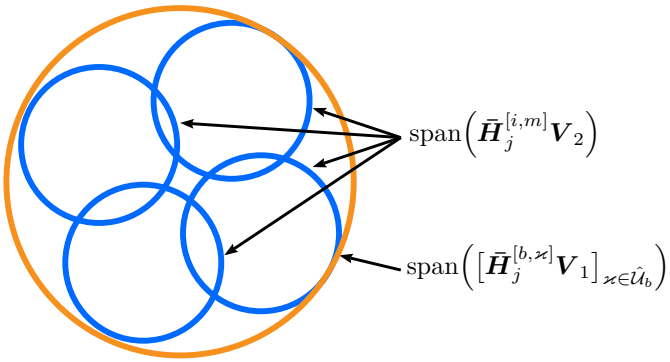

Figure 3.12: Alignment condition **C2**: for all $j = 1, \ldots, T$ the interference subspace of the users $m \in \mathcal{U}_i$ in cell $i = 3, 4, \ldots, T$, with $i \neq j$, aligns with the interference generated by the users $\varkappa \in \hat{\mathcal{U}}_b$ in cell $b = 1, 2$ with $b \neq j$.

Figure 3.13 depicts an example of the required alignment. To achieve this alignment we proceed as follows. We write $\boldsymbol{V}_1 = \left[\boldsymbol{V}_1^+ \boldsymbol{V}_1^-\right]$, where $\boldsymbol{V}_1^+ \in \mathbb{C}^{\mu_n \times n_t n^\Gamma}$ and $\boldsymbol{V}_1^- \in \mathbb{C}^{\mu_n \times n_t((n+1)^\Gamma - n^\Gamma)}$. Now we require that

$$\text{span}\left(\bar{\boldsymbol{H}}_j^{[1,m]}\boldsymbol{V}_1^+\right) \subseteq \text{span}\left(\left[\bar{\boldsymbol{H}}_j^{[2,\varkappa]}\boldsymbol{V}_1\right]_{\varkappa\in\hat{\mathcal{U}}_b}\right),$$

for all $m \in \hat{\mathcal{U}}_1$.

Note that conditions **C1** and **C2** can be rewritten as

$$\begin{aligned}
&\text{span}\left(\bar{\boldsymbol{H}}_j^{[i,m]}\boldsymbol{V}_2\right) \subseteq \text{span}\left(\left[\bar{\boldsymbol{H}}_j^{[b,\varkappa]}\boldsymbol{V}_1\right]_{\varkappa\in\hat{\mathcal{U}}_b}\right)\\
\Leftrightarrow &\text{span}\left(\left[\bar{\boldsymbol{H}}_j^{[b,\varkappa]}\right]^{-1}_{\varkappa\in\hat{\mathcal{U}}_b}\bar{\boldsymbol{H}}_j^{[i,m]}\boldsymbol{V}_2\right) \subseteq \text{span}\left(\boldsymbol{I}_{n_t}\otimes\boldsymbol{V}_1\right)\\
\Leftrightarrow &\text{span}\left(\boldsymbol{T}_j^{[b,im]}\boldsymbol{V}_2\right) \subseteq \text{span}\left(\boldsymbol{I}_{n_t}\otimes\boldsymbol{V}_1\right),
\end{aligned}$$

where

$$\boldsymbol{T}_j^{[b,im]} = \left[\boldsymbol{T}_{j,1}^{[b,im]}, \ldots, \boldsymbol{T}_{j,n_t}^{[b,im]}\right]^T = \left[\bar{\boldsymbol{H}}_j^{[b,\varkappa]}\right]^{-1}_{\varkappa\in\hat{\mathcal{U}}_b}\bar{\boldsymbol{H}}_j^{[i,m]}$$

and $\boldsymbol{T}_{j,o}^{[b,im]}$ are diagonal matrices.

Hence, from **C1** we have that $\text{span}\left(\boldsymbol{T}_{j,o}^{[b,bm]}\boldsymbol{V}_2\right) \subseteq \text{span}\left(\boldsymbol{V}_1\right)$, for all $i = 1, \ldots, n_t$. Without loss of generality we fix $b = 2$, $m = 1$, $j = 1$, $o = 1$, set $\text{span}\left(\boldsymbol{V}_1^+\right) = \text{span}\left(\boldsymbol{T}_{1,1}^{[2,21]}\boldsymbol{V}_2\right)$ and claim the condition

C3

$$\text{span}\left(\bar{\boldsymbol{H}}_j^{[1,m]}\boldsymbol{T}_{1,1}^{[2,21]}\boldsymbol{V}_2\right) \subseteq \text{span}\left(\left[\bar{\boldsymbol{H}}_j^{[2,\varkappa]}\boldsymbol{V}_1\right]_{\varkappa\in\hat{\mathcal{U}}_b}\right)$$

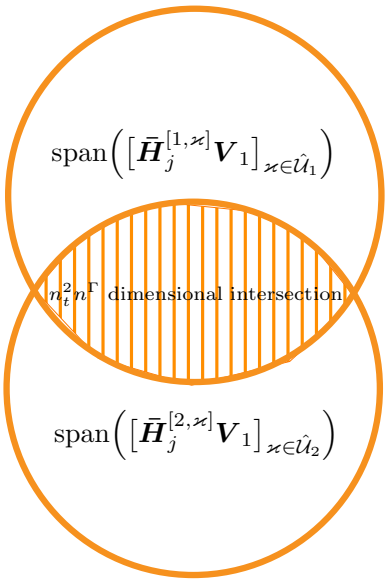

Figure 3.13: Interference alignment at receivers $j = 3, \ldots, T$ the interference subspace defined by base station 1 and 2 has an overlap of at least $n_t^2 n^\Gamma$ dimensions.

for all $m \in \hat{\mathcal{U}}_1$ and all $j = 3, \ldots, T$.

This condition together with **C1** and **C2** implies that the interference at base stations $b = 3, \ldots, T$ lies in a $2n_t^2(n+1)^\Gamma - n_t^2 n^\Gamma$ dimensional subspace.

If we are able to find precoders $\boldsymbol{V}_1$ and $\boldsymbol{V}_2$ such that **C1**, **C2** and **C3** are fulfilled, $\delta(n)$ in (3.9) is achievable. Note that from **C1** we have $L_1 = 2(T-1)(K-n_t)$ conditions, **C2** we have $L_2 = 2K\big((T-2)+(T-3)\big)$ conditions and from **C3** we have $L_3 = n_t(T-2)$ conditions. Hence, we have $n_t(L_1+L_2+L_3)$ conditions of the form

$$\mathrm{span}\left(\boldsymbol{\Upsilon}_g \boldsymbol{V}_2\right) \subseteq \mathrm{span}\left(\boldsymbol{V}_1\right), \quad g = 1, \ldots, n_t(L_1+L_2+L_3),$$

where $\boldsymbol{\Upsilon}_g = \boldsymbol{T}_{j,n}^{[b,im]}$ as defined above. Now we can chose $\Gamma = n_t(L_1+L_2+L_3)$ and use [CJ09, Lemma 2] to construct the precoders $\boldsymbol{V}_1$ and $\boldsymbol{V}_2$ such that **C1**, **C2** and **C3** are fulfilled.

Finally, it remains to show that all received signals are linearly independent. This can easily be seen by checking if the conditions in [CJ09, Lemma 1] are fulfilled. □

3.6.2 Proof of Corollary 3.3

Proof. Case $T > R$: The outer bound follows by allowing cooperation among the users in a cell and using the degrees of freedom outer bound for the T user $KM \times n_t$ interference

channel [GJ10, Theorem 1] which yields

$$d \leq \frac{Tn_tKn_r}{Kn_r + n_t}.$$

The inner bound follows from Corollary 3.2 by considering a $\big((T, n_t) \times (Kn_r, 1)\big)$ cellular system and noting that $TKn_r > n_t$ due to the assumption $T > R$. Hence, we have

$$d \geq \frac{Tn_tKn_r}{Kn_r + n_t}.$$

Case $T \leq R$ and $Kn_r \leq n_t$: The outer bound is obtained by allowing cooperation among the receivers and among the transmitters, which cannot decrease the degrees of freedom. Therefore the degrees of freedom are bounded from above by the degrees of freedom of the point-to-point $Tn_t \times TKn_r$ MIMO channel. By assumption $TKn_r \leq n_t \leq Tn_t$ and therefore $d \leq TKn_r$. The inner bound is obtained by considering the $\big((T, n_t) \times (Kn_r, 1)\big)$ cellular system and using Corollary 3.2. Since, by assumption $TKn_r \leq n_t$ we have $d \geq TKn_r$.

Case $T \leq R$ and $Kn_r > n_t$: The outer bound follows by allowing cooperation among the receivers and using the outer bound for the inference channel [GJ10, Theorem 1], $d \leq \frac{Tn_tKn_r}{Kn_r+n_t}$. The inner bound follows by considering the $\big((T, n_t) \times (Kn_r, 1)\big)$ cellular system and using Corollary 3.2, $d \geq \frac{Tn_tKn_r}{Kn_r+n_t}$. □

3.6.3 Proof of Corollary 3.5

Proof. The claim can be proved in a similar manner as the proof of a proper cellular system, with $\mu = 1$, in [ZBH11].

To prove condition (3.3) we count the number of equations and the number of variables, eliminating superfluous variables. Then, we use Bezout's Theorem which states that a system of multivariate polynomial equations is solvable if and only if the number of equations does not exceed the number of variables.

Condition (3.4) must hold since each base station must be able to transmit K independent signals simultaneously. Therefore, $\mu N \geq K$ must hold.

Condition (3.5) must hold since each user will receive at least K independent signals from one interfering base station, but must be able to decode its desired data stream. □

3.6.4 Proof of Corollary 3.6

The proof is strongly inspired by [BCT11] and [RLL12] who proved the feasibility of interference alignment for the interference channel. To prove Corollary 3.6 we use basic

results from algebraic geometry. A good introduction to algebraic geometry can be found in [Sha95]. The following theorem is essential in the proof of Corollary 3.6.

Theorem 3.8. *(Dimension of fibres [Sha95]) Let $f : X \to Y$ be a regular map between irreducible varieties. Suppose that f is surjective: $f(X) = Y$, and that* $\dim X = n$, $\dim Y = m$. *Then $m \leq n$, and*

1. *$\dim F \geq n - m$ for any $y \in Y$ and for any component F of the fibre $f^{-1}(y)$;*
2. *there exists a nonempty open subset $U \subset Y$ such that* $\dim f^{-1}(y) = n - m$ *for $y \in U$.*

A proof can be found in [Sha95].

For a cellular system the vector space of all interfering channel is given as follows. The interfering channels experienced by an arbitrary but fixed user $k \in \mathcal{S}_b$ are

$$\mathcal{H}_{b,k} = \mathbb{C}^{n_r \times n_t} \times \prod_{\substack{l=1 \\ l \neq b}}^{T} \mathbb{C}^{n_r \times n_t},$$

where $\prod_{n=1}^{n_t} X_n$ is the Cartesian product of the vector spaces X_n. Note that in contrast to the interference channel results in [BCT11, RLL12] we also need to consider the direct channels $\boldsymbol{H}_{b,k}^{[b]}$. The first term corresponds to the intra-cell interference and the second term corresponds to the out-of-cell interference. The vector space of all interfering channels is given by

$$\mathcal{H} = \prod_{b=1}^{T} \prod_{k=1}^{K} \mathcal{H}_{b,k} = \prod_{b=1}^{T} \prod_{k=1}^{K} \prod_{l=1}^{T} \mathbb{C}^{n_r \times n_t},$$

which is an irreducible variety and has dimension $\dim \mathcal{H} = TKTn_t n_r$. The vector space of all possible transmit precoding and receive filter matrices (i.e. the strategy space) can be defined as product of Grassmannians $\mathcal{G}(d, n)$, i.e.,

$$\mathcal{S} = \prod_{b=1}^{T} \prod_{k=1}^{K} \mathcal{G}(d, n_t) \times \prod_{b=1}^{T} \prod_{k=1}^{K} \mathcal{G}(d, n_r),$$

which has dimension $\dim \mathcal{S} = TK(d(n_r - d) + d(n_t - d))$ (see [Sha95, Example 5, pg. 68]). Now we define $\mathcal{I} \subseteq \mathcal{S} \times \mathcal{H}$ as the set of all (s, h) such $s \in \mathcal{S}$ is a feasible strategy for the channel realization $h \in \mathcal{H}$. The following lemma gives the dimensions of $\mathcal{I}$.

Lemma 3.9. *Let the number of base stations T, the number of users per base station K and the number of streams per user d be fixed and let the number of transmit antennas be equal the number of receive antennas $N = n_t = n_r$, then $\mathcal{I}$ is a irreducible variety with*

dimension

$$\dim \mathcal{I} = 2dTK(N-d) + TK\left(T(N^2 - Kd^2) + d^2\right).$$

Proof. The proof is a simple extension of [BCT11, Lemma 6] and omitted. □

Now we can prove Corollary 3.6.

Proof of Corollary 3.6. Define the regular map

$$q : \mathcal{I} \to \mathcal{H} \text{ and its inverse } q^{-1} : \mathcal{H} \to \mathcal{I}.$$

If for a given $h \in \mathcal{H}$ the interference alignment problem at hand has a solution, then

$$\dim\, q^{-1}(h) \geq 0 \tag{3.10}$$

must hold.

Let $\mathcal{Z}_0 = q(\mathcal{I})$ and let $\mathcal{Z}$ denote the closure of $\mathcal{Z}_0$, then by definition $q : \mathcal{I} \to \mathcal{Z}$ is dominant. Hence, from [Sha95, Theorem 7, pg. 76] we have

$$\begin{aligned} \dim\, q^{-1}(h) &\geq \dim\, \mathcal{I} - \dim\, \mathcal{Z} \\ \Rightarrow \dim\, \mathcal{Z} &\geq \dim\, \mathcal{I} - \dim\, q^{-1}(h) \end{aligned}$$

Therefore, if

$$\dim\, q^{-1}(h) = TK\big(d^2(1-TK) + 2d(N-d)\big), \tag{3.11}$$

we have

$$\dim\, \mathcal{Z} \geq \dim\, \mathcal{I} - \dim\, q^{-1}(h) = \dim \mathcal{H}.$$

Since $\mathcal{Z} \subseteq \mathcal{H}$ and $\mathcal{H}$ is irreducible we have $\mathcal{Z} = \mathcal{H}$ from which follows that $q : \mathcal{I} \to \mathcal{H}$ is dominant. Now, to check that $q^{-1}(h)$ has the required dimensions (3.11) we can use [BCT11, Lemma 8]. Finally, solving (3.10) for N the claim follows

$$N \geq \frac{d(KT+1)}{2}.$$

□

4 Coordinated Processing with Limited Feedback

Coordinated processing of signals by multiple network nodes is regarded as a key design element in future cellular networks. In the downlink of cellular systems coordinated processing strategies can be divided in two categories: i) Joint coherent transmission from multiple transmitters; which is usually referred to as network MIMO. ii) Coordinated beamforming by multiple transmitters. In theory coherent transmission (network MIMO) from multiple base stations to multiple users promises vast gains in achievable rates [KFV06, GHH+10, MF11]. In practice a high capacity backhaul network is required that enables data sharing and the exchange of control messages. Industrial field trials show rather disappointing throughput gains [IDM+11]. The main limiting factors are the bandwidth and latency requirements on the backhaul network, and the problem of efficiently acquiring and sharing channel state information [RC09].

Coordinated beamforming requires no message sharing and therefore the requirements on the backhaul network are much more relaxed. In recent years interference alignment schemes have attracted much attention, see for example [CJ08, MGMAK09, GG11, NGJV12, BCT14, NMAC14]. Interference alignment is a coordinated beamforming technique which essentially aligns the signaling spaces so that multiple interfering signals appear as a single one or at least cast overlapping shadows at the receivers. In Chapter 3 we discussed different interference alignment schemes. The scheme used in [CJ08] requires long symbol extensions and a fast fading environment. Therefore, coordinated linear beamforming schemes that exploit spatial diversity are considered to be a good candidate for future cellular systems [IDM+11] and gained much attention in recent years [ZHG09, HPC10, DY10]. However, the acquisition and sharing of channel state information is still a formidable challenge to enable coordinated linear beamforming. Interference alignment with limited feedback has been considered in [TB09, EAH12, EALH12] for the interference channel and in [LSHC12] for cellular systems. In [TG09] interference alignment with imperfect (noisy) channel state information at the receivers and transmitters was considered. Even though analytic treatment of the limited feedback problem has made significant progress in the past, many results focus on the large SNR regime; essen-

tially carrying out system degrees of freedom analysis. For example, degrees of freedom analysis with limited feedback was provided for the broadcast channel in [Jin06], for interference channel [RG12, EAH12] and for network MIMO in [dKG12]. However, the degrees of freedom approach cannot really account for the throughput degradation experienced in practice. The main reasons are: i) The large SNR regime where achieving degrees of freedom is optimal is considered. The primary goal in this regime is interference mitigation instead of signal enhancement. ii) No user selection is considered. iii) Ideal link adaptation is assumed. Altogether, this renders the performance analysis too optimistic and motivates extended analysis of the limited feedback problem.

Now, the question is: How can we get reliable estimates of the performance degradation due to limited feedback. In this chapter we take a step forward towards a more realistic answer to this question. Our approach is universal in the sense that we do not consider a specific transmit strategy. By considering cellular systems which in fact can be modeled as multiple interfering broadcast channels our results also hold for the interference channel and the broadcast channel, which are special cases of the interfering broadcast channel. In particular our findings can be summarized as follows.

- We introduce a new metric for the performance evaluation which better captures the achievable rate degradation due to limited feedback. The metric is defined per user instead of sum-rate.

- We calculate an upper bound on the achievable rate degradation for any scheduling decision, any beamforming strategy, and any SNR regime which is a useful performance benchmark for the design of systems.

- We derive a lower and upper bound on the the achievable rate degradation for interference alignment.

- We introduce a distributed iterative interference alignment algorithm which achieves the optimal scaling for any SNR regime. The main idea is that instead of sending the complete channel matrix each user fixes a receive filter and feeds back a quantized version of the effective channel.

- We show that the proposed distributed approach is favorable over centralized approaches in terms of performance, convergence speed and computational complexity. Even if the algorithm requires feedback for every iteration step, the overall feedback compared to a centralized approach can be significantly reduced.

4.1 Problem Formulation

A comprehensive description of the system model is given in Section 1.3. We review some of the assumptions and specify some others, then we state the problem. We consider cellular networks with T base stations each equipped with n_t antennas and U users each equipped with n_r antennas. Each base station b provides wireless service to a disjoint set of users $\mathcal{U}_b$, i.e., $\mathcal{U}_b \cap \mathcal{U}_s = \emptyset$ for all $b \neq s$. For simplicity, we assume a single data stream per user and no symbol extensions. Let data stream i be associated to user i such that we can say that user i is scheduled for transmission implying that data stream i associated to user i is scheduled. The base stations are grouped in coordination clusters and all T base stations are within the same cluster. In an ideal world the cluster would be coordinated by a central controller. The central controller receives channel state information from all users, performs scheduling and distributes the scheduling decision among all base stations. Figure 3.2 on page 66 depicts an example of this ideal centralized system setup. If full channel state information is available at the central controller (as it would be the case in an ideal world), the sum-rate optimal scheduling decision $(S_H, \boldsymbol{\pi}_H)$ is the solution to the optimization problem

$$\max_{\substack{S=\{\mathcal{S}_1,\ldots,\mathcal{S}_T\} \\ \mathcal{S}_i \subseteq \mathcal{U}_i}} \max_{\boldsymbol{\pi}:\mathcal{S}\to\mathbb{S}^{n_t-1}} R(P, \boldsymbol{\pi}, S, H), \tag{4.1}$$

where $R(P, \boldsymbol{\pi}, \mathcal{S}, H)$ is defined in (1.6) and the domain of $\boldsymbol{\pi}$ is $\mathcal{S} = \mathcal{S}_1 \cup \ldots \cup \mathcal{S}_T$. Hence, with perfect channel state information at a central controller the achievable system sum-rate is $R(P, \boldsymbol{\pi}_H, \mathcal{S}_H, H)$.

However, in practice a central controller needs to receive quantized channel state information through a rate-constrained feedback channel. Based on quantized channel state information V the scheduling decision $(\boldsymbol{\pi}_V, \mathcal{S}_V)$ is found by solving the problem

$$\max_{\substack{S=\{\mathcal{S}_1,\ldots,\mathcal{S}_T\} \\ \mathcal{S}_i \subseteq \mathcal{U}_i}} \max_{\boldsymbol{\pi}:\mathcal{S}\to\mathbb{S}^{n_t-1}} R\left(P, \boldsymbol{\pi}, \mathcal{S}, V\right), \tag{4.2}$$

instead of problem (4.1). Such that the achievable system sum-rate with quantized channel state information is $R(P, \boldsymbol{\pi}_V, \mathcal{S}_V, H)$. In general, the achievable system sum-rate with quantized channel state information is smaller or equal the achievable system sum-rate with perfect channel state information, $R(P, \boldsymbol{\pi}_V, \mathcal{S}_V, H) \leq R(P, \boldsymbol{\pi}_H, \mathcal{S}_H, H)$. In Section 4.2 we explore this performance degradation caused by quantized channel state information. We find an universal upper bound on the performance degradation which holds for any receive and transmit strategy, incorporates user selection and is valid for any SNR regime.

Solving optimization problem (4.1) or (4.2) is in general not feasible. In the previous

chapter we discussed centralized iterative algorithms that find sub-optimal solutions to this scheduling problems. However, a centralized system architecture requires a backhaul network which provides high data rates and very low delays. Such that the feasibility of a centralized system architecture can at least be questioned. In this chapter we go one step further and claim that connecting all base stations to a central controller may not be required. We present a distributed iterative algorithm that significantly reduces the feedback overhead. Based on the universal rate gap bound (devised in the next section) we evaluate its performance degradation with respect to the feedback overhead.

4.2 Universal Rate Loss Gap Analysis

In this section we present a universal upper bound for the rate loss due to quantized channel state information. The bound is universal in the sense that it holds for any receive and transmit strategy, incorporates user selection and is valid for any SNR regime. Before we state our result we review some of the related results.

4.2.1 Related Work

For interference alignment, a limited feedback scheme for the K-user interference channel is proposed in [RG12], and it is shown that the throughput loss due to the channel quantization scales like

$$\mathbb{E}\left[r_m(P, \boldsymbol{\pi}_{\mathrm{IA},H}, S_{IC}, H) - r_m(P, \boldsymbol{\pi}_{\mathrm{IA},V}, S_{IC}, H)\right] < \log\left(1 + P2^{-\frac{B}{N_g}+1}\right), \tag{4.3}$$

where $N_g = 2n_r((K-1)n_t - n_r)$ is the real dimension of the Grassmannian manifold and $S_{IC} = (\{1\}, \{2\}, \ldots, \{K\})$ is the user selection. In [KV10] similar results have been obtained for a system using OFDM. An in depth treatment of the scaling law analysis using Grassmannian manifolds can be found in [Kri11]. In [LSHC12] the uplink of a cellular system with two base stations and four users was considered and it was shown that the rate gap scaling is exactly as the scaling for zeroforcing beamforming with RVQ in Theorem 2.5. As we will see this result cannot be generalized to systems with more than two cells. In Section 2.3.1 we reviewed some of the related results for the broadcast channel. In particular, Theorem 2.5 provided by [Jin06] gives the scaling of the rate gap for zeroforcing beamforming with RVQ. Based on the rate gap [Jin06] found a scaling law for the number of feedback bits that guarantees that the optimal number of degrees of freedom can be achieved. This result has been recently generalized by [dKG12] who considered joint transmission in a multi-cellular system. However, to characterize the performance degradation experienced in practice one cannot rely completely on a degrees

of freedom analysis; when considering degrees of freedom implicitly the infinite SNR regime is considered. In this section we take a different approach. We show that the scaling law in Theorem 2.5 is to optimistic, if we consider more general systems and a different but more realistic metric. On the other hand, we will see that the scaling laws (4.3) can be significantly improved if we use a different feedback strategy.

4.2.2 Performance Metric

Assume that channel state information is not only used to perform scheduling (i.e. precoding and user selection) but is also for link adaptation. If the controller has only quantized channel state information, each of these tasks causes a rate loss compared to the performance with perfect channel state information. Therefore, we define the following per user performance metric

$$\begin{aligned}\Delta r_m &:= \max\{r_m(P, \boldsymbol{\pi}_H, S_H, H) - r_m(P, \boldsymbol{\pi}_V, S_V, H), r_m(P, \boldsymbol{\pi}_H, S_H, H) - r_m(P, \boldsymbol{\pi}_V, S_V, V)\} \\ &= r_m(P, \boldsymbol{\pi}_H, S_H, H) - \min\{r_m(P, \boldsymbol{\pi}_V, S_V, H), r_m(P, \boldsymbol{\pi}_V, S_V, V)\}. \end{aligned} \tag{4.4}$$

Because of the per user formulation Δr_m is not necessarily positive for all H. The rate loss gap Δr_m captures basically two cases. First, if $r_m(P, \boldsymbol{\pi}_V, S_V, H) > r_m(P, \boldsymbol{\pi}_V, S_V, V)$ the rate gap is $r_m(P, \boldsymbol{\pi}_H, S_H, H) - r_m(P, \boldsymbol{\pi}_V, S_V, V)$. Thus, the rate gap captures the rate loss due to beamforming, scheduling and link adaptation based on quantized channel state information since it is assumed that the base station transmits with a rate $r_m(P, \boldsymbol{\pi}_V, S_V, V)$. Second, if $r_m(P, \boldsymbol{\pi}_V, S_V, H) < r_m(P, \boldsymbol{\pi}_V, S_V, V)$, the rate gap is $r_m(P, \boldsymbol{\pi}_H, S_H, H) - r_m(P, \boldsymbol{\pi}_V, S_V, H)$ and describes the rate loss due to beamforming and scheduling based on quantized channel state information. In the later, we do not consider link adaptation, since even if allocation of a rate $r_m(P, \boldsymbol{\pi}_V, S_V, V) > r_m(P, \boldsymbol{\pi}_V, S_V, H)$ causes an outage event with high probability in practice mechanisms like automatic repeat requests are used to handle such events. As we will see Δr_m is strong enough to address some of the drawbacks of the conventional analysis and leads to indeed different results.

The following lemma sets the basis for our analysis; it allows us to bound the expected value of the rate gap $\mathbb{E}[\Delta r_m]$ in terms of the *same* scheduling decisions.

Lemma 4.1. *Let $(S_H, \boldsymbol{\pi}_H)$ denote the scheduling decision under perfect channel state information H according to* (4.1)*. Let $(S_V, \boldsymbol{\pi}_V)$ be the scheduling decision under quantized channel state information V according to* (4.2)*. Assume that the random channels $\boldsymbol{H}_{m,l}$ are independent and identically distributed for all $m \in \mathcal{U}$ and all $l = 1, \ldots, T$, then for*

any fixed user $m \in \mathcal{U}$ the expected rate gap $\mathbb{E}[\Delta r_m]$ is bounded by

$$\begin{aligned}\mathbb{E}\left[\max\left\{r_m(P,\boldsymbol{\pi}_V,S_V,H)-r_m(P,\boldsymbol{\pi}_V,S_V,V),0\right\}\right] &\\ \leq \mathbb{E}\left[\Delta r_m\right] &\\ \leq 3\,\mathbb{E}\left[\max_{\substack{S=\{\mathcal{S}_1,\ldots,\mathcal{S}_T\}\\ \mathcal{S}_i\subseteq\mathcal{U}_i}}\ \max_{\boldsymbol{\pi}:\mathcal{S}\to\mathbb{S}^{n_t-1}}\left|r_m(P,\boldsymbol{\pi},S,H)-r_m(P,\boldsymbol{\pi},S,V)\right|\right].&\end{aligned}$$

The proof can be found in Section 4.7.1. We offer some brief remarks.

Remark 4.2. The upper bound in Lemma 4.1 is also true, if we consider the rate gap $r_m(P,\boldsymbol{\pi}_H,S_H,H)-r_m(P,\boldsymbol{\pi}_V,S_V,H)$ which is more in line with the results for zero forcing and interference alignment (4.3) discussed above.

Remark 4.3. The lower and upper bounds in Lemma 4.1 are tight if $H = V$. On the other hand, if there is no correlation between H and V, the bound can be arbitrarily loose. However, since we assume that V is a "good" approximation of H the bounds in Lemma 4.1 can be assumed to be reasonably tight.

Remark 4.4. Even though we assumed achievable rates, it is possible to consider extensions of this lemma for different or more general utility functions. In addition, the assumptions on the channel distribution may be relaxed but they are required in the following.

4.2.3 Main Result

Our first result is an universal upper bound on the expected rate gap $\mathbb{E}[\Delta r_m]$ defined in (4.4). It is based on the following feedback strategy. For fixed receive filters $\boldsymbol{\rho}(m)$ each user $m \in \mathcal{U}$ quantizes and feeds back the effective channels $\hat{\boldsymbol{h}}_{m,l} := (\boldsymbol{H}_{m,l})^H\boldsymbol{\rho}(m)$ to base station l. We stress that each base station requires only local channel state information, i.e., it needs not to know the channel between some other base station and any user. The normalized effective channels

$$\boldsymbol{h}_{m,l} := \frac{\hat{\boldsymbol{h}}_{m,l}}{\|\hat{\boldsymbol{h}}_{m,l}\|_2}$$

are quantized by a random codebook $\mathcal{V}_m \subset \mathbb{S}^{n_t-1}$, with 2^B isotropically distributed elements. Each user $m \in \mathcal{U}$ uses an independent copy of the random codebook which ensures with high probability that the feedback messages from different users are linearly independent. User m quantizes its normalized effective channels $\boldsymbol{h}_{m.l}$, for all $l = 1,\ldots,T$, by minimizing the chordal distance $d_C(\boldsymbol{h}_{m,l},\boldsymbol{v})$, defined in (2.10),

$$\boldsymbol{v}_{m,l} := \operatorname*{arg\,min}_{\boldsymbol{v}\in\mathcal{V}_m} d_C(\boldsymbol{h}_{m,l},\boldsymbol{v}), \tag{4.5}$$

For simplicity we assume that base station l knows the channel norm $\mu_{m,l} := \|\hat{\boldsymbol{h}}_{m,l}\|_2$, for all $m \in \mathcal{U}$ perfectly. After base station l has received a feedback message from each user $m \in \mathcal{U}$ it has local channel state information

$$V^l := \left(\hat{\boldsymbol{v}}_{m,l} = \mu_{m,l}\boldsymbol{v}_{m,l}\right)_{m\in\mathcal{U}}. \tag{4.6}$$

Such that the quantized channel state information distributed in the system can be collected in the list $V = (V^l)_{l=1,\ldots,T}$.

Now we are ready to prove our man result. The following theorem holds for any receive and transmit strategy, incorporates user selection and is valid for any SNR regime.

Theorem 4.5. *Assume that the elements of random channels $\boldsymbol{H}_{m,l}$ are independent and identically distributed for all $m \in \mathcal{U}$ and all $l = 1, \ldots, T$. Let the transmit beamformer $\boldsymbol{\pi}$ and the user selection $\mathcal{S}$ be arbitrary but fixed. If each user $m \in \mathcal{U}$ uses RVQ (4.5) with B bits per base station feedback link and each base station l has instantaneous knowledge of $\mu_{m,l}$, for all $m \in \mathcal{U}$,*

$$\begin{aligned}&\mathbb{E}\left[|r_m(P, \boldsymbol{\pi}, S, H) - r_m(P, \boldsymbol{\pi}, S, V)|\right]\\ &\quad\leq 2\log\left(1 + \frac{P}{2}\left[T\left(T-1\right)\mathbb{E}\left[\mu_{m,1}^4\right]2^{-\frac{B}{n_t-1}} + 2^{-\frac{B}{2(n_t-1)}}\left(\mathbb{E}^{\frac{1}{4}}\left[\mu_{m,1}^8\right] + T\mathbb{E}^{\frac{1}{2}}\left[\mu_{m,1}^2\right]\right)\right]\right),\end{aligned}$$

holds for any SNR P.

The proof is presented in Section 4.7.2. According to Remark 4.2 the upper bound in Theorem 4.5 can indeed be regarded as generalizations of Jindal's result (2.11) and the result for interference alignment (4.3). Some more remarks are in place.

Remark 4.6. In contrast to the previous results results (2.11) and (4.3) we obtain a different scaling for the RVQ scheme (4.5). It is significantly better than the result (4.3) for interference alignment with Grassmannian feedback but requires two times more feedback bits than the result (2.11) for the broadcast channel with zero forcing.

4.3 Distributed Interference Alignment with Quantized Channel State Information

We assume that each base station and all users are equipped with $N = n_t = n_r$ antennas. This assumption enables us to use Corollary 3.6 and to select users such that interference alignment is possible. However, if $n_t \neq n_r$ feasibility of interference alignment can be ensured in a different way, e.g., increasing the number of users step by step. As we

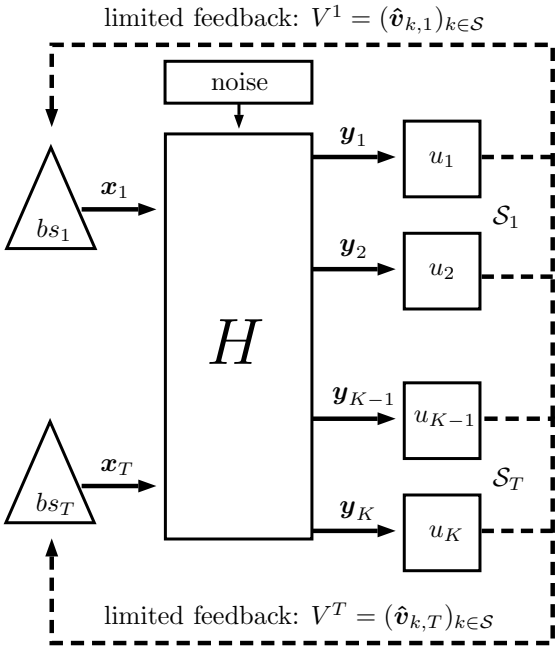

Figure 4.1: Distributed system architecture. Each scheduled user u_m, $m \in \mathcal{S}$, feeds back quantized channel state information $\hat{\boldsymbol{v}}_{m,l} = \mu_{m,l}\boldsymbol{v}_{m,l}$ to base station l. Based on local channel state information $V^l = (\mu_{m,l}\boldsymbol{v}_{m,l})_{m\in\mathcal{S}}$ each base station l computes the precoders $\boldsymbol{\pi}(m)$, $m \in \mathcal{S}_l$, and transmits dedicated pilots to initiate the next iteration step.

will see, the distributed algorithm makes efficient use of quantized channel state information. Figure 4.1 depicts an example of the distributed system architecture. The minimum interference algorithm with user selection and quantized channel state information is summarized in Algorithm 4. At the beginning of each transmission frame, orthogonal common pilots are transmitted so that all users m can measure the channel matrices $\boldsymbol{H}_{m,b}$ for all b. Knowledge of the channel matrices $\boldsymbol{H}_{m,b}$ is required by the users to compute the effective channels; common pilots must be retransmitted in intervals depending on the coherence time of the channel. Next, the user selection is performed and then the iterative optimization of transmit precoders and receive filters is executed. In each iteration, after the transmit precoders have been optimized every base station transmits dedicated pilots on orthogonal resources such that each user $m \in \mathcal{S}$ can measure the effective channels $\boldsymbol{H}_{m,l}\boldsymbol{\pi}(m)$, for all $m \in \mathcal{S}_l$ and all $l = 1, \ldots, T$. Based on the measured effective channels each user optimizes its receive filter and feeds back the effective channels $(\boldsymbol{H}_{m,l})^H\boldsymbol{u}_m$, which requires knowledge of $\boldsymbol{H}_{m,l}$. A detailed description of each step is given now.

Algorithm 4 minimum interference algorithm with user selection

Begin of transmission frame:
Transmit common pilots to all users and make an estimate $\boldsymbol{H}_{m,b}$, with $b = 1, \ldots, T$ and $m \in \mathcal{U}$.
Each base station $b = 1, \ldots, T$ selects $\mathcal{S}_b \subseteq \mathcal{U}$ according to (4.7).
Set $\boldsymbol{\pi}(m) = 1/\sqrt{n_t}(1, 1, \ldots, 1)^T$ for all $m \in \mathcal{S}$.
repeat
Each base station $b = 1, \ldots, T$ transmits dedicated pilots.
for $b = 1, \ldots, T$ **do**
Compute receive filter matrix $\boldsymbol{u}_m$, for all $m \in \mathcal{S}_b$, according to (3.6).
Quantize and feed back the effective channels $\hat{\boldsymbol{v}}_{m,l}$, for all $m \in \mathcal{S}_b$, $l = 1, \ldots, T$, according to (4.6).
end for
for $b = 1, \ldots, T$ **do**
Compute beamforming vectors $\boldsymbol{\pi}(m)$, for all $m \in \mathcal{S}_b$, according to (4.8).
end for
until termination condition is satisfied (e.g. maximum number of iterations, minimum residual interference, ...).
End of transmission frame

User Selection

If the channel coefficients are independent and drawn from a continuous distribution we can apply Corollary 3.6 to ensure that interference alignment is feasible. According to Corollary 3.6 spatial interference alignment is feasible if the number of active users per base station is bounded by

$$|\mathcal{S}_b| \leq \frac{1}{T}(2n_t - 1), \ b = 1, \ldots, T. \tag{4.7}$$

Therefore, at the beginning of every transmission frame each base station selects $\lfloor \frac{1}{T}(2n_t - 1) \rfloor$ users. The users can be selected according to some metric, e.g, maximum fairness, maximum channel gain or the user selection can be defined by higher layers.

Receive Filter Optimization Based on Perfect Channel State Information

The receive filters are optimized by the users in a distributed manner. During the receive filter optimization all transmit precoders $\boldsymbol{\pi}$ are fixed. In the first iteration it is assumed that each base station transmits with a beamforming vector $1/\sqrt{n_t}(1, 1, \ldots, 1)^T$. Based on dedicated pilots each user $m \in \mathcal{S}$ measures the effective channels $\boldsymbol{H}_{m,l}\boldsymbol{\pi}(m)$, $l = 1, \ldots, T$, $l \neq b$, $m \in \mathcal{S}_l$. and computes the receive filter $\boldsymbol{\rho}(m)$ according to (3.6). Next each user $m \in \mathcal{S}$ feeds back the effective channels $(\boldsymbol{H}_{m,l})^H \boldsymbol{\rho}(m)$.

Feedback of Effective Channels

In each iteration step all scheduled users $m \in \mathcal{S}$ feed back quantized channel state information to all base stations. For fixed receive filters $\boldsymbol{\rho}(m)$ each user $m \in \mathcal{S}$ quantizes and feeds back the effective channels $\hat{\boldsymbol{h}}_{m,l}$ to base station l. Such that in each iteration base station l gets an update of the local channel state information V^l (4.6). Based on V^l base station l updates the precoders $\boldsymbol{\pi}(m)$ for all $m \in \mathcal{S}_l$.

Distributed Transmit Precoder Optimization Based on Quantized Channel State Information

The transmit precoder optimization is performed by each base station independently and is based on quantized local channel state information V_l. Similar to the centralized algorithm (Section 3.3.2) the transmit precoders are computed in two steps. First, the transmit subspace which causes minimum out-of-cell interference is determined. Second, the intra-cell interference is canceled by a zero forcing step.

Consider the reciprocal network, the reciprocal precoded channel from user m in cell b to base station l is given by $\overleftarrow{\boldsymbol{v}}_{m,l} = \hat{\boldsymbol{v}}_{m,l}$. For base station b the receive subspace (in the reciprocal system) which causes minimum out-of-cell interference is given by

$$\boldsymbol{\Pi}_b = \nu_{\min}^{|\mathcal{S}_b|}\big(\overleftarrow{\boldsymbol{\Theta}}_b\big) \in \mathbb{C}^{n_t \times |\mathcal{S}_b|},$$

where $\nu_{\min}^{N}(\boldsymbol{X})$ is defined as the eigenvectors corresponding to the N smallest magnitude eigenvalues of the Hermitian matrix $\boldsymbol{X}$. The interference covariance matrix $\overleftarrow{\boldsymbol{\Theta}}_b$ is defined as

$$\overleftarrow{\boldsymbol{\Theta}}_b = \sum_{\substack{l=1 \\ l \neq b}}^{T} \sum_{m \in \mathcal{S}_l} \overleftarrow{\boldsymbol{v}}_{m,b} (\overleftarrow{\boldsymbol{v}}_{m,b})^H.$$

Finally, the intra-cell interference is canceled by an additional zero forcing step. The zero forcing precoder $\boldsymbol{w}_{m,b} \in \mathbb{C}^{|\mathcal{S}_b|}$ for user m in cell b is chosen from the null space of the effective channels $\boldsymbol{v}_{k,b}^H \boldsymbol{\Pi}_b$, with $k \in \mathcal{S}_b$ and $k \neq m$ such that the transmit precoder for user $m \in \mathcal{S}_b$ is given by

$$\boldsymbol{\pi}(m) = \boldsymbol{\Pi}_b \boldsymbol{w}_{m,b}. \tag{4.8}$$

After each base station l has determined the precoding vectors for all $m \in \mathcal{S}_l$ it transmits dedicated pilots such that the next iteration can be initiated by the users.

In the next section we are going to analyze the rate loss gap of the distributed interference alignment algorithm with respect to the centralized solution with full channel state

information. In Section 4.5 we compare the algorithms numerically and demonstrate that the distributed algorithm significantly reduces the feedback load.

4.4 Rate Loss Gap Analysis for Distributed Interference Alignment

Together with Lemma 4.1 we have the following corollary which tailors Theorem 4.5 to the distributed interference alignment algorithm described in Section 4.3 (Algorithm 4).

Corollary 4.7. *Under the assumptions of Theorem 4.5, in any iteration of Algorithm 4 the average rate loss per user is upper bounded by*

$$\begin{aligned}\mathbb{E}\left[\Delta r_m\right] &\leq 6\log\left(1+\frac{P}{2}\left[T^2 n_r^2 2^{-\frac{B}{n_t-1}}+(n_r+T)2^{-\frac{B}{2(n_t-1)}}\right]\right)\\ &\leq 3P\left(T^2 n_r^2 2^{-\frac{B}{n_t-1}}+(n_r+T)2^{-\frac{B}{2(n_t-1)}}\right).\end{aligned}$$

The prove is devised to Section 4.7.3. The following theorem shows that the scaling $2^{-\frac{B}{2(n_t-1)}}$ can not be improved if we consider interference alignment with RVQ and link adaptation. In particular it can not be improved for the distributed interference alignment algorithm (Algorithm 4) described in Section 4.3,

Theorem 4.8. *Under the assumptions of Theorem 4.5, for sufficiently high SNR the average rate loss is bounded from below by*

$$\begin{aligned}\mathbb{E}\left[\Delta r_m\right] \geq \max_{c_1>0}\frac{1}{c_1}&\left(1-\frac{n_t^2\left(n_t+1\right)}{4\sqrt{c_1}\left(n_t-1\right)2^{-n_t}}\right)\\ &\mathbb{E}\left[\log\left(1+\frac{c_1 P\mathbb{E}\left[\mu_{m,b}^2\right]}{|\mathcal{S}_b|\left(1+P\mathbb{E}\left[\mu_{m,b}^2\right]\right)}\sqrt{\frac{4\cdot 2^{-n_t}n_t-1}{n_t^2\left(n_t+1\right)}}2^{\frac{-B}{2(n_t-1)}}\right)\right]\\ &-\log\left(1+PT\sqrt{\mathbb{E}\left[\mu_{m,b}^4\right]}2^{\frac{-B}{n_t-1}}\right)\end{aligned}$$

where $|\mathcal{S}_b|$ satisfies the interference alignment feasibility condition (4.7)*, for all $b=1,\ldots,T$, with equality. In particular, for some $c_2>0$*

$$\mathbb{E}\left[\Delta r_m\right] \geq c_2\log\left(1+\frac{P\mathbb{E}\left[\mu_{m,b}^2\right]}{|\mathcal{S}_b|\left(1+P\mathbb{E}\left[\mu_{m,b}^2\right]\right)}2^{\frac{-B}{2(n_t-1)}}\right)+o\left(2^{\frac{-B}{(n_t-1)}}\right)$$

holds.

The proof can be found in Section 4.7.4. Note that the lower bound is bounded in P. Therefore, it can not be used for degrees of freedom analysis where P is taken to infinity. But, Theorem 4.8 shows that the scaling $2^{(-B/(2(n_t-1)))}$ cannot be improved for finite SNR P.

4.5 Simulations

Baseline

As a baseline scheme we consider the centralized interference alignment algorithm described in Subsection 3.6. The baseline scheme requires a central processing unit which has global (quantized) channel state information. Each user m quantizes and feeds back the channel matrix $\boldsymbol{H}_{m,l}$, for all $l = 1, \ldots, T$, to the central processing unit. To quantize the channel matrices, we apply a scalar quantization or a vector quantization scheme.

Scalar Quantization Each user maps each element of the channel matrix to an element of a scalar feedback codebook with 2^{B_s} elements. Scalar quantization (SQ) leads to a feedback load of $2Tn_tn_rB_s$ bits per user and per feedback message. As we will see, the feedback and control overhead is significantly larger than for the proposed distributed algorithm.

Vector Quantization Vector quantization (VQ) is a popular quantization scheme for multi-antenna channels. As a baseline we consider the following scheme which was also used in [KMLL12] and [KV10]. Each user m quantizes the channel matrices $\boldsymbol{H}_{m,l}$, for all $l = 1, \ldots, K$, by applying RVQ on the vector $\mathrm{vec}(\boldsymbol{H}_{m,l})$, where $\mathrm{vec}(\boldsymbol{X})$ stacks the columns of the matrix $\boldsymbol{X}$ one over the other.

Simulation Setup

In the simulations we consider a cellular network with $T = 3$ base stations and $U = 9$ users. Each node is equipped with $n_t = n_r = 5$ antennas. Hence, according to Corollary 3.6 interference alignment is feasible if each base station b serves $|\mathcal{S}_b| = 3$ users. For the minimum interference algorithm (Algorithm 4) each base station is assigned randomly to three users. Power allocation is assumed to be uniform. The channels are modeled according to the Wyner-like channel model described in Section 3.4.1.

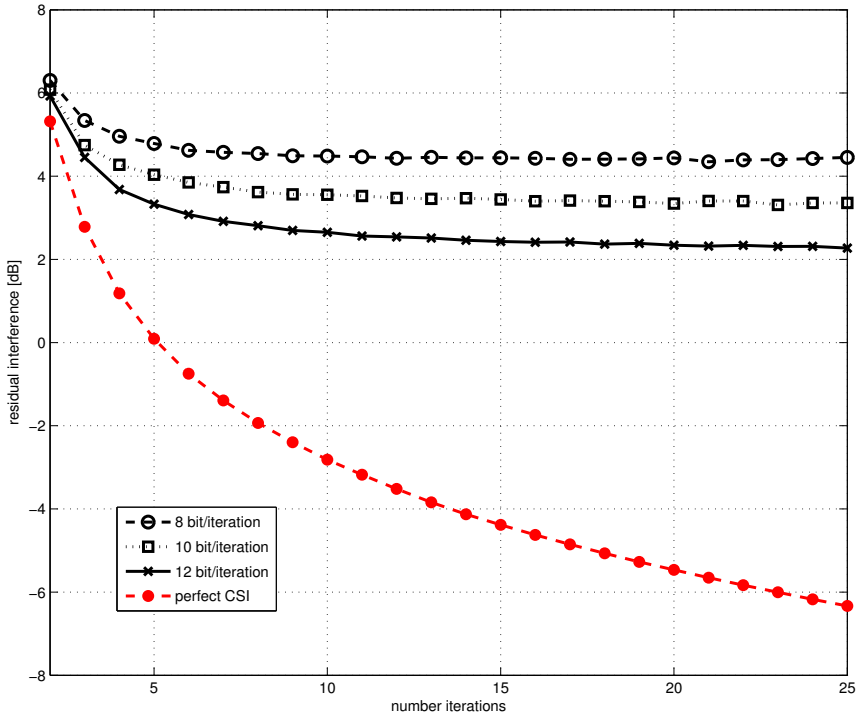

Figure 4.2: Spectral efficiency over SNR. Convergence of the proposed minimum interference algorithm (MIA – Algorithm 4). Observation: The proposed algorithm converges quickly.

Simulation Results

First, we investigate the convergence of the proposed Algorithm 4. Figure 4.2 depicts the residual interference of Algorithm 4. We observe that with quantized channel state information the residual interference converges rapidly to its minimum of approximately 4.5 dB, 3.5 dB and 2.5 dB for 8, 10 and 12 bit per user per iteration, respectively. In contrast, with ideal channel state information the residual interference keeps decreasing with the number of iterations. We conclude that with quantized channel state information the number of iterations can be kept low (≈ 5 iterations) without losing a significant part of the performance that can be achieved with more iterations. Hence, the algorithm seems to be well suited for practical applications where a small number of iterations is mandatory.

This observation is further supported by Figure 4.3 which depicts the spectral efficiency over the SNR for the minimum interference algorithm (Algorithm 4). Each user uses an independent random codebook with 2^{16} isotropic elements. Again, we observe that the proposed interference alignment algorithm converges rapidly, i.e., going from 4 to 6 iterations the performance is increased only slightly. This is a remarkable result since a small number of iterations keeps the feedback load small.

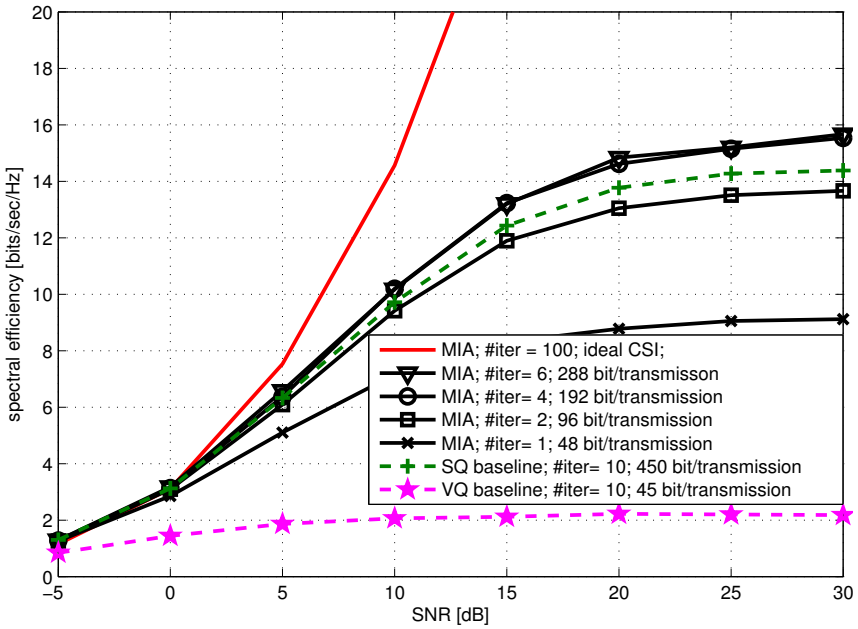

Figure 4.3: Spectral efficiency over SNR. Convergence of the proposed minimum interference algorithm (MIA – Algorithm 4). The proposed algorithm converges quickly and outperforms the base line with less than half the number of feedback bits and iterations.

In addition, Figure 4.3 shows the performance of the SQ baseline and VQ baseline schemes as defined above. Due to the centralized approach the feedback load of these schemes does not increase with the number of iterations. After 10 iterations the baseline schemes have converged. The SQ baseline is clearly outperformed by the minimum interference algorithm with 4 iterations and 192 bit feedback load per user and per transmission. That is, with the iterative minimum interference algorithm we require less than half the number feedback bits to outperform the SQ baseline. The VQ base line with a 15 bit random codebook (45 bit feedback per transmission per user) performs very poorly. To obtain a better performance significantly larger codebooks are required. However, computing the feedback decision for larger codebooks becomes quickly infeasible.

4.6 Conclusion and Future Work

We introduced an improved metric for the performance evaluation of the interfering broadcast channel. The improved metric captures the throughput degradation due to quantized channel state information by modelling the beamformer offset and the link adaptation problem. We obtained the rate loss scaling laws with the number of feedback bits and

showed that they are different from existing ones. We provided an distributed iterative interference alignment algorithm and corresponding feedback strategies which achieve the derived scaling laws and significantly reduces the feedback load compared to centralized algorithms.

The considered performance metric takes a step towards a more realistic assessment of the performance degradation in practical systems by modelling also the link adaption problem based on quantized channel state information. However, for an even more realistic assessment of the performance degradation other metrics are also of interest. For example extension to outage probability or outage rates would be interesting.

4.7 Proofs

4.7.1 Proof of Lemma 4.1

Proof. First we need to show that $\mathbb{E}\left[r_m(P, \boldsymbol{\pi}_H, \mathcal{S}_H, V)\right] \leq \mathbb{E}\left[r_m(P, \boldsymbol{\pi}_V, \mathcal{S}_V, V)\right]$ which does not trivially follow from the sum-rate maximization (4.2). To see this assume that $\mathbb{E}\left[r_m(P, \boldsymbol{\pi}_H, \mathcal{S}_H, V)\right] > \mathbb{E}\left[r_m(P, \boldsymbol{\pi}_V, \mathcal{S}_V, V)\right]$ for some user m. Since $\mathbb{E}\left[r_m(P, \boldsymbol{\pi}_H, \mathcal{S}_H, V)\right] = \mathbb{E}\left[r_l(P, \boldsymbol{\pi}_H, \mathcal{S}_H, V)\right]$ and $\mathbb{E}\left[r_m(P, \boldsymbol{\pi}_V, \mathcal{S}_V, V)\right] = \mathbb{E}\left[r_l(P, \boldsymbol{\pi}_V, \mathcal{S}_V, V)\right]$ for all $m, l \in \mathcal{U}$, it follows from the symmetry of the system that $\mathbb{E}\left[r_m(\boldsymbol{\pi}_H, \mathcal{S}_H, V)\right] > \mathbb{E}\left[r_m(P, \boldsymbol{\pi}_V, \mathcal{S}_V, V)\right]$ for all $m \in \mathcal{U}$. Hence, we have

$$\mathbb{E}\left[\sum_{m\in\mathcal{U}} r_m(P, \boldsymbol{\pi}_V, \mathcal{S}_V, V)\right] < \mathbb{E}\left[\sum_{m\in\mathcal{U}} r_m(P, \boldsymbol{\pi}_H, \mathcal{S}_H, V)\right],$$

which contradicts with the definition of $\mathcal{S}_V$ and $\boldsymbol{\pi}_V$ given in (4.2). Therefore,

$$\mathbb{E}\left[r_m(P, \boldsymbol{\pi}_H, \mathcal{S}_H, V)\right] \leq \mathbb{E}\left[r_m(P, \boldsymbol{\pi}_V, \mathcal{S}_V, V)\right], \tag{4.9}$$

must hold for all $m \in \mathcal{U}$. In a similar manner we can show that

$$\mathbb{E}\left[r_m(P, \boldsymbol{\pi}_V, \mathcal{S}_V, H)\right] \leq \mathbb{E}\left[r_m(P, \boldsymbol{\pi}_H, \mathcal{S}_H, H)\right] \tag{4.10}$$

holds for all $m \in \mathcal{U}$. Inequalities (4.9) and (4.10) state that in expectation the sum-rate optimal scheduling decision maximizes also the individual per user rates. To prove the upper bound we write $\mathbb{E}\left[\Delta r_m\right]$ as

$$\begin{aligned}\mathbb{E}\left[\Delta r_m\right] = \mathbb{E}[r_m(P, \boldsymbol{\pi}_H, \mathcal{S}_H, H) - r_m(P, \boldsymbol{\pi}_V, \mathcal{S}_V, H) + \\ \max\{r_m(P, \boldsymbol{\pi}_V, \mathcal{S}_V, H) - r_m(P, \boldsymbol{\pi}_V, \mathcal{S}_V, V), 0\}].\end{aligned}$$

The first term can be bounded by

$$\begin{aligned}&\mathbb{E}[r_m(P, \boldsymbol{\pi}_H, \mathcal{S}_H, H) - r_m(P, \boldsymbol{\pi}_V, \mathcal{S}_V, H)] \\ &= \mathbb{E}[r_m(P, \boldsymbol{\pi}_H, \mathcal{S}_H, H) - r_m(P, \boldsymbol{\pi}_V, \mathcal{S}_V, V) + r_m(P, \boldsymbol{\pi}_V, \mathcal{S}_V, V) - r_m(P, \boldsymbol{\pi}_V, \mathcal{S}_V, H)] &(4.11)\\ &\leq \mathbb{E}[r_m(P, \boldsymbol{\pi}_H, \mathcal{S}_H, H) - r_m(P, \boldsymbol{\pi}_H, \mathcal{S}_H, V) + r_m(P, \boldsymbol{\pi}_V, \mathcal{S}_V, V) - r_m(P, \boldsymbol{\pi}_V, \mathcal{S}_V, H)] &(4.12)\\ &\leq 2\mathbb{E}[\max_{\mathcal{S}\subseteq U} \max_{\boldsymbol{\pi}:\mathcal{S}\to\mathbb{S}^{n_t-1}} |r_m(P, \boldsymbol{\pi}, \mathcal{S}, H) - r_m(P, \boldsymbol{\pi}, \mathcal{S}, V)|].\end{aligned}$$

Equation (4.11) holds since we simply added a $0 = -r_m(P, \boldsymbol{\pi}_V, \mathcal{S}_V, V) + r_m(P, \boldsymbol{\pi}_V, \mathcal{S}_V, V)$. The first inequality (4.12) holds according to (4.9). Further by (4.10) we have $\mathbb{E}[r_m(P, \boldsymbol{\pi}_H, \mathcal{S}_H, H) -$

$r_m(P, \boldsymbol{\pi}_V, \mathcal{S}_V, H)] \geq 0$. Since

$$\mathbb{E}[\max\{r_m(P, \boldsymbol{\pi}_H, \mathcal{S}_H, H) - r_m(P, \boldsymbol{\pi}_V, \mathcal{S}_V, V), 0\}] \leq \mathbb{E}[\max_{\mathcal{S}\subseteq U} \max_{\boldsymbol{\pi}:\mathcal{S}\to\mathbb{S}^{n_t-1}} |r_m(P, \boldsymbol{\pi}, \mathcal{S}, H) - r_m(P, \boldsymbol{\pi}, \mathcal{S}, V)|].$$

is also true the upper bounds follows. Since according to (4.10)

$$\mathbb{E}[r_m(P, \boldsymbol{\pi}_H, \mathcal{S}_H, H) - r_m(P, \boldsymbol{\pi}_V, \mathcal{S}_V, H)] \geq 0,$$

the lower bound follows by setting the first term in (4.4) equal to 0.

□

4.7.2 Proof of Theorem 4.5

Before proving Theorem 4.5 we prove two lemmas which are required in the proof.

Lemma 4.9. *Let $\boldsymbol{x} \in \mathbb{S}^{n_t-1}$ be an independent isotropic random vector and $\mathcal{V} = (\boldsymbol{v}_1, ..., \boldsymbol{v}_{2^B}) \subset \mathbb{S}^{n_t-1}$ be a collection of 2^B independent isotropic random vectors. If we define*

$$Z := \min_{\boldsymbol{v}\in\mathcal{V}}(1 - |\langle \boldsymbol{x}, \boldsymbol{v}\rangle|^2),$$

then for some $n \geq 1$ we have

$$\left(\frac{n_t - 1}{n_t} 2^{\frac{-B}{n_t-1}}\right)^n \leq \mathbb{E}[Z^n] \leq \left(2^{\frac{-B}{n_t-1}}\right)^n \leq \left(\frac{n_t}{n_t - 1}\mathbb{E}[Z]\right)^n.$$

Proof. Since $1 - |\langle \boldsymbol{x}, \boldsymbol{v}\rangle|^2$ is beta distributed with parameters $n_t - 1$ and 1 [Jin06], Z is the minimum of 2^B beta$(n_t - 1, 1)$ distributed random variables. Therefore, $\mathbb{E}[Z] \geq \frac{n_t-1}{n_t} 2^{\frac{-B}{n_t-1}}$ (see e.g. [Jin06]) and by Jensen's inequality we get the lower bound

$$\mathbb{E}[Z^n] \geq \mathbb{E}[Z]^n = \left(\frac{n_t - 1}{n_t} 2^{\frac{-B}{n_t-1}}\right)^n.$$

For the upper bound we use [AYL07, Lemma 1] which states that $\Pr(Z > x) = \left(1 - x^{n_t-1}\right)^{2^B}$. Thus, $\Pr(Z^n > x) = \Pr\left(Z > x^{1/n}\right) = \left(1 - x^{\frac{n_t-1}{n}}\right)^{2^B}$, with $n \geq 1$, and therefore

$$\mathbb{E}[Z^n] \leq \left(2^{\frac{-B}{n_t-1}}\right)^n.$$

Using, $\mathbb{E}[Z] \geq \frac{n_t-1}{n_t} 2^{\frac{-B}{n_t-1}}$ once more the second upper bound follows. □

Let us now define the following metric.

Definition 4.10.

$$\omega\left(\boldsymbol{x},\boldsymbol{y}\right) := \max_{\boldsymbol{w}\in\mathbb{S}^{n_t-1}} \left| |\langle \boldsymbol{x},\boldsymbol{w}\rangle|^2 - |\langle \boldsymbol{y},\boldsymbol{w}\rangle|^2 \right| \tag{4.13}$$

As we will see, this metric essentially dictates the rate loss gap in Theorem 4.5. We have the following lemma, which shows that this metric is equal to the chordal distance.

Lemma 4.11. *Let $\boldsymbol{x}\in\mathbb{S}^{n_t-1}$ and $\boldsymbol{y}\in\mathbb{S}^{n_t-1}$ be unit norm vectors, then*

$$\max_{\boldsymbol{w}\in\mathbb{S}^{n_t-1}} \left| |\langle \boldsymbol{x},\boldsymbol{w}\rangle|^2 - |\langle \boldsymbol{y},\boldsymbol{w}\rangle|^2 \right| = \sqrt{1-|\langle \boldsymbol{x},\boldsymbol{y}\rangle|^2}.$$

Proof. We have

$$\left| |\langle \boldsymbol{x},\boldsymbol{w}\rangle|^2 - |\langle \boldsymbol{y},\boldsymbol{w}\rangle|^2 \right| = \left| \boldsymbol{w}^H(\boldsymbol{x}\boldsymbol{x}^H - \boldsymbol{y}\boldsymbol{y}^H)\boldsymbol{w} \right|.$$

Consider the matrix $\boldsymbol{A} := \boldsymbol{x}\boldsymbol{x}^H - \boldsymbol{y}\boldsymbol{y}^H$. Since $\operatorname{rank}(\cdot)$ is a subadditive function we have that the matrix $\boldsymbol{A}$ has maximum rank of two and, therefore, has only two non-zero eigenvalues λ_1 and λ_2. But the matrix $\boldsymbol{A}$ is trace-less as well

$$\operatorname{Tr}(\boldsymbol{A}) = \lambda_1 + \lambda_2 = \operatorname{Tr}(\boldsymbol{x}\boldsymbol{x}^H - \boldsymbol{y}\boldsymbol{y}^H) = \|\boldsymbol{x}\|_2^2 - \|\boldsymbol{y}\|_2^2 = 0. \tag{4.14}$$

Therefore, $\lambda_1 = -\lambda_2$ must hold. On the other hand, we get from the Frobenius norm $\|\boldsymbol{A}\|_F^2 = \operatorname{Tr}(\boldsymbol{A}^H\boldsymbol{A})$ that

$$\begin{aligned}\operatorname{Tr}(\boldsymbol{A}^H\boldsymbol{A}) &= \lambda_1^2 + \lambda_2^2 = \|\boldsymbol{x}\|_2^4 + \|\boldsymbol{y}\|_2^4 - 2|\langle \boldsymbol{x},\boldsymbol{y}\rangle|^2 \\ &= 2(1-|\langle \boldsymbol{x},\boldsymbol{y}\rangle|^2)\end{aligned}$$

Thus, using $\lambda_1 = -\lambda_2$ we get for the two non-zero eigenvalues

$$|\lambda_1| = |\lambda_2| = \sqrt{1-|\langle \boldsymbol{x},\boldsymbol{y}\rangle|^2}, \tag{4.15}$$

which proves the claim. □

We are now ready to prove Theorem 4.5.

Proof. Fix the user selection $\mathcal{S}$ and the transmit beamformers $\boldsymbol{\pi}$. Denote the optimal receive filter as $\boldsymbol{u}_m^*$ with respect to the collection H, we have $\hat{\boldsymbol{h}}_{m,b} = (\boldsymbol{H}_{m,b})^H\boldsymbol{u}_m^*$, $\mu_{m,b} = \|\hat{\boldsymbol{h}}_{m,b}\|_2$ and $\boldsymbol{h}_{m,b} = \hat{\boldsymbol{h}}_{m,b}/\mu_{m,b}$ for all $b = 1,...,T$. Hence, the achievable rate of user $m\in\mathcal{S}_b$ is

$$r_m(P,\boldsymbol{\pi},\mathcal{S},H) = \log\left(1 + \frac{\frac{P\mu_{m,b}^2}{|\mathcal{S}_b|}|\langle \boldsymbol{h}_{m,b},\boldsymbol{\pi}(m)\rangle|^2}{1+\sum_{l=1}^{T}\sum_{\substack{k\in\mathcal{S}_l\\k\neq m}}\frac{P\mu_{m,l}^2}{|\mathcal{S}_l|}|\langle \boldsymbol{h}_{m,l},\boldsymbol{\pi}(k)\rangle|^2}\right).$$

Since the base station does not know the channels H it must use the imperfect channel state information $V = \{\hat{\boldsymbol{v}}_{m,b} = \mu_{m,b}\boldsymbol{v}_{m,b} : m \in \mathcal{U}, b = 1, \ldots, T\}$. Based on V the base station estimates the rates achievable by user m as

$$r_m(P, \boldsymbol{\pi}, \mathcal{S}, V) = \log\left(1 + \frac{\frac{P\mu_{m,b}^2}{|\mathcal{S}_b|}|\langle \boldsymbol{v}_{m,b}, \boldsymbol{\pi}(m)\rangle|^2}{1 + \sum_{l=1}^{T}\sum_{\substack{k\in\mathcal{S}_l \\ k\neq m}} \frac{P\mu_{m,l}^2}{|\mathcal{S}_l|}|\langle \boldsymbol{v}_{m,l}, \boldsymbol{\pi}(k)\rangle|^2}\right).$$

For the ease of presentation, we define the following variables (index m omitted),

$$\Phi_{b,k} := \frac{P\mu_{m,b}^2}{|\mathcal{S}_b|}|\langle \boldsymbol{h}_{m,b}, \boldsymbol{\pi}(k)\rangle|^2 \tag{4.16}$$

$$\Psi_{b,k} := \frac{P\mu_{m,b}^2}{|\mathcal{S}_b|}|\langle \boldsymbol{v}_{m,b}, \boldsymbol{\pi}(k)\rangle|^2 \tag{4.17}$$

$$\Delta_{b,k} := \Phi_{b,k} - \Psi_{b,k}$$

$$\Psi_\Sigma = \left(1 + \sum_{l=1}^{T}\sum_{k\in\mathcal{S}_l}\Psi_{l,k}\right)^{-1}$$

$$\Phi_\Sigma = \left(1 + \sum_{l=1}^{T}\sum_{\substack{k\in\mathcal{S}_l \\ k\neq m}}\Phi_{l,k}\right)^{-1}.$$

Equation (4.16) and (4.17) can be interpreted as the effective received SNR of user m through the channels $\boldsymbol{h}_{m,b}$ and $\boldsymbol{v}_{m,b}$, respectively. Further, define $\delta := |r_m(P, \boldsymbol{\pi}, \mathcal{S}, H) - r_m(P, \boldsymbol{\pi}, \mathcal{S}, V)|$, which can bounded from above by

$$\begin{aligned}
\delta \leq & \max_{\mathcal{S}\subseteq U}\max_{\boldsymbol{\pi}:\mathcal{S}\to\mathbb{S}^{n_t-1}} |r_m(P, \boldsymbol{\pi}, \mathcal{S}, H) - r_m(P, \boldsymbol{\pi}, \mathcal{S}, V)| \\
&= \max_{\mathcal{S}\subseteq U}\max_{\boldsymbol{\pi}:\mathcal{S}\to\mathbb{S}^{n_t-1}} \left|\log\left(\frac{1 + \sum_{l=1}^{T}\sum_{k\in\mathcal{S}_l}\Phi_{l,k}}{1 + \sum_{l=1}^{T}\sum_{k\in\mathcal{S}_l}\Psi_{l,k}}\right) + \log\left(\frac{1 + \sum_{l=1}^{T}\sum_{\substack{k\in\mathcal{S}_l \\ k\neq m}}\Psi_{l,k}}{1 + \sum_{l=1}^{T}\sum_{\substack{k\in\mathcal{S}_l \\ k\neq m}}\Phi_{l,k}}\right)\right| \\
&= \max_{\mathcal{S}\subseteq U}\max_{\boldsymbol{\pi}:\mathcal{S}\to\mathbb{S}^{n_t-1}} \left|\log\left(1 + \sum_{l=1}^{T}\sum_{k\in\mathcal{S}_l}\Psi_\Sigma\Delta_{l,k}\right) + \log\left(1 + \sum_{l=1}^{T}\sum_{\substack{k\in\mathcal{S}_l \\ k\neq m}}\Phi_\Sigma\left(-\Delta_{l,k}\right)\right)\right|.
\end{aligned}$$

Using $\log(1+a)+\log(1+b) \leq 2\log\left(1+\frac{1}{2}(a+b)\right)$, with $a, b > -1$, yields

$$\begin{aligned}
\delta &\leq \max_{\mathcal{S}\subseteq U} \max_{\boldsymbol{\pi}:\mathcal{S}\to\mathbb{S}^{n_t-1}} \left| \log\left(1+\sum_{l=1}^{T}\sum_{k\in\mathcal{S}_l} \Psi_\Sigma \cdot \Delta_{l,k}\right) \right. \\
&\quad \left. + \log\left(1+\sum_{l=1}^{T}\sum_{k\in\mathcal{S}_l} \Phi_\Sigma \cdot (-\Delta_{l,k}) + \sum_{l=1}^{T} \Phi_\Sigma \cdot \Delta_{l,m}\right) \right| \\
&= 2 \max_{\mathcal{S}\subseteq U} \max_{\boldsymbol{\pi}:\mathcal{S}\to\mathbb{S}^{n_t-1}} \left| \log\left(1+\frac{1}{2}(\Psi_\Sigma - \Phi_\Sigma)\sum_{l=1}^{T}\sum_{k\in\mathcal{S}_l} \Delta_{l,k} + \frac{1}{2}\sum_{l=1}^{T} \Phi_\Sigma \cdot \Delta_{l,m}\right) \right| \\
&\leq 2 \max_{\mathcal{S}\subseteq U} \max_{\boldsymbol{\pi}:\mathcal{S}\to\mathbb{S}^{n_t-1}} \log\left(1+\frac{1}{2}|\Psi_\Sigma - \Phi_\Sigma| \left|\sum_{l=1}^{T}\sum_{k\in\mathcal{S}_l} \Delta_{l,k}\right| + \frac{1}{2}\sum_{l=1}^{T}|\Delta_{l,m}|\right).
\end{aligned}$$

Since

$$\Psi_\Sigma - \Phi_\Sigma = \frac{1}{\Psi_\Sigma^{-1}\Phi_\Sigma^{-1}}\left(\sum_{l=1}^{T}\sum_{\substack{k\in\mathcal{S}_l \\ k\neq m}} \Phi_{l,k} - \sum_{l=1}^{T}\sum_{k\in\mathcal{S}_l} \Psi_{l,k}\right) \leq \frac{1}{\Psi_\Sigma^{-1}\Phi_\Sigma^{-1}}\sum_{l=1}^{T}\sum_{k\in\mathcal{S}_l}|\Delta_{l,k}|$$

holds, we have the result

$$\begin{aligned}
\delta &\leq 2 \max_{\mathcal{S}\subseteq U} \max_{\boldsymbol{\pi}:\mathcal{S}\to\mathbb{S}^{n_t-1}} \log\left(1+\frac{1}{2}\left(\sum_{l=1}^{T}\sum_{k\in\mathcal{S}_l}|\Delta_{l,k}|\right)^2 + \frac{1}{2}\sum_{l=1}^{T}|\Delta_{l,m}|\right) \\
&\leq 2\log\left(1+\frac{1}{2}\max_{\mathcal{S}\subseteq U}\sum_{l_1=1}^{T}\sum_{k_1\in\mathcal{S}_{l_1}}\sum_{l_2=1}^{T}\sum_{k_2\in\mathcal{S}_{l_2}} \max_{\boldsymbol{\pi}:\mathcal{S}\to\mathbb{S}^{n_t-1}}|\Delta_{l_1,k_1}| \max_{\boldsymbol{\pi}:\mathcal{S}\to\mathbb{S}^{n_t-1}}|\Delta_{l_2,k_2}| \right. \\
&\quad \left. + \frac{1}{2}\sum_{l=1}^{T}\max_{\boldsymbol{\pi}:\mathcal{S}\to\mathbb{S}^{n_t-1}}|\Delta_{l,m}|\right).
\end{aligned}$$

Now, observe that

$$\begin{aligned}
\max_{\boldsymbol{\pi}:\mathcal{S}\to\mathbb{S}^{n_t-1}}|\Delta_{l,k}| &= \frac{P\mu_{m,l}^2}{|\mathcal{S}_l|}\max_{\boldsymbol{\pi}:\mathcal{S}\to\mathbb{S}^{n_t-1}}\left||\langle \boldsymbol{h}_{m,l}, \boldsymbol{\pi}(k)\rangle|^2 - |\langle \boldsymbol{v}_{m,l}, \boldsymbol{\pi}(k)\rangle|^2\right| \\
&= \frac{P\mu_{m,l}^2}{|\mathcal{S}_l|}\max_{\boldsymbol{x}\in\mathbb{S}^{n_t-1}}\left||\langle \boldsymbol{h}_{m,l}, \boldsymbol{x}\rangle|^2 - |\langle \boldsymbol{v}_{m,l}, \boldsymbol{x}\rangle|^2\right| \\
&= \frac{P\mu_{m,l}^2}{|\mathcal{S}_l|}\omega\left(\boldsymbol{h}_{m,l}, \boldsymbol{v}_{m,l}\right),
\end{aligned}$$

where $\omega(\cdot,\cdot)$ was defined in (4.13) and the last term $\frac{P\mu_{m,b}^2}{|\mathcal{S}_b|}\omega\left(\boldsymbol{h}_{m,l}, \boldsymbol{v}_{m,l}\right)$ is actually inde-

pendent of k. Taking expectation and applying Jensen's inequality we obtain

$$\delta \leq 2\log\Bigg(1+\frac{P}{2}\sum_{l_1=1}^{T}\sum_{l_2=1}^{T}\mathbb{E}\left[\mu_{m,l_1}^2\omega\left(\boldsymbol{h}_{m,l_1},\boldsymbol{v}_{m,l_1}\right)\mu_{m,l_2}^2\omega\left(\boldsymbol{h}_{m,l_2},\boldsymbol{v}_{m,l_2}\right)\right] + \frac{P}{2}\sum_{l=1}^{T}\mathbb{E}\left[\mu_{m,l}^2\omega\left(\boldsymbol{h}_{m,l},\boldsymbol{v}_{m,l}\right)\right]\Bigg). \quad (4.18)$$

Now, for $l_1 \neq l_2$ we have from the Cauchy-Schwarz inequality

$$\begin{aligned}\mathbb{E}\left[\mu_{m,l_1}^2\omega\left(\boldsymbol{h}_{m,l_1},\boldsymbol{v}_{m,l_1}\right)\mu_{m,l_2}^2\omega\left(\boldsymbol{h}_{m,l_2},\boldsymbol{v}_{m,l_2}\right)\right] &= \mathbb{E}\left[\mu_{m,l_1}^2\omega\left(\boldsymbol{h}_{m,l_1},\boldsymbol{v}_{m,l_1}\right)\right]\mathbb{E}\left[\mu_{m,l_2}^2\omega\left(\boldsymbol{h}_{m,l_2},\boldsymbol{v}_{m,l_2}\right)\right]\\ &\leq \mathbb{E}^{\frac{1}{2}}\left[\mu_{m,l_1}^4\right]\mathbb{E}^{\frac{1}{2}}\left[\omega^2\left(\boldsymbol{h}_{m,l_1},\boldsymbol{v}_{m,l_1}\right)\right]\mathbb{E}^{\frac{1}{2}}\left[\mu_{m,l_2}^4\right]\mathbb{E}^{\frac{1}{2}}\left[\omega^2\left(\boldsymbol{h}_{m,l_2},\boldsymbol{v}_{m,l_2}\right)\right] \quad (4.19)\end{aligned}$$

and for $l_1 = l_2$ we have from the Cauchy-Schwarz inequality

$$\begin{aligned}\mathbb{E}\left[\mu_{m,l_1}^4\omega^2\left(\boldsymbol{h}_{m,l_1},\boldsymbol{v}_{m,l_1}\right)\right] &\leq \mathbb{E}\left[\mu_{m,l_1}^4\omega\left(\boldsymbol{h}_{m,l_1},\boldsymbol{v}_{m,l_1}\right)\right]\\ &\leq \mathbb{E}^{\frac{1}{4}}\left[\mu_{m,l_1}^8\right]\mathbb{E}^{\frac{1}{2}}\left[\omega^2\left(\boldsymbol{h}_{m,l_1},\boldsymbol{v}_{m,l_1}\right)\right]. \quad (4.20)\end{aligned}$$

Using Lemma 4.11 and Lemma 4.9 we get

$$\mathbb{E}\left[\omega^2\left(\boldsymbol{h}_{m,l},\boldsymbol{v}_{m,l}\right)\right] = \mathbb{E}\left[\min_{\boldsymbol{v}\in\mathcal{V}}\left(1-|\langle\boldsymbol{h}_{k,l},\boldsymbol{v}\rangle|^2\right)\right] < 2^{\frac{-B}{n_t-1}}. \quad (4.21)$$

Such that, the claim follows by plugging (4.19), (4.20) and (4.21) in (4.18). □

4.7.3 Proof of Corollary 4.7

Proof: Using Lemma 4.1 we have

$$\mathbb{E}\left[\Delta r_m\right] \leq 3\,\mathbb{E}\left[\max_{\mathcal{S}\subseteq U}\max_{\boldsymbol{\pi}:\mathcal{S}\to\mathbb{S}^{n_t-1}}\left|r_m(P,\boldsymbol{\pi},\mathcal{S},H)-r_m(P,\boldsymbol{\pi},\mathcal{S},V)\right|\right].$$

Now, we can use Theorem 4.5 and obtain

$$\begin{aligned}&\mathbb{E}\left[\Delta r_m\right]\\ &\leq 6\log\left(1+\frac{P}{2}\left[T\left(T-1\right)\mathbb{E}\left[\mu_{m,1}^4\right]2^{-\frac{B}{n_t-1}}+2^{-\frac{B}{2(n_t-1)}}\left(\mathbb{E}^{\frac{1}{4}}\left[\mu_{m,1}^8\right]+T\mathbb{E}^{\frac{1}{2}}\left[\mu_{m,1}^2\right]\right)\right]\right)\end{aligned}$$

When optimizing the beamformers using Algorithm 4 all receive filters are fixed. Thus, we can compute the expected values

$$\begin{aligned}\mathbb{E}\left[\mu_{m,1}^2\right] &= \mathbb{E}\left[\|(\boldsymbol{H}_{m,1})^H \boldsymbol{u}_m\|_2^2\right] = \mathbb{E}\left[(\boldsymbol{u}_m)^H \boldsymbol{H}_{m,1}(\boldsymbol{H}_{m,1})^H \boldsymbol{u}_m\right] = 1 \\ \mathbb{E}\left[\mu_{m,1}^4\right] &\leq \mathbb{E}\left[\left(\sum_{i=1}^{n_t} \|\boldsymbol{h}_i\|_2^2\right)^2\right] \leq n_r^2 \\ \mathbb{E}^{\frac{1}{4}}\left[\mu_{m,1}^8\right] &\leq n_r,\end{aligned}$$

where $\boldsymbol{h}_i$ is the ith column of $\boldsymbol{H}_{m,1}$ and we used the Cauchy-Schwarz inequality and the fact that $n_t \sum_{i=1}^{n_t} \|\boldsymbol{h}_i\|_2^2$ is chi-squared distributed with $n_t n_r$ degrees of freedom. ■

4.7.4 Proof of Theorem 4.8

The following lemma allows us to bound the expected value of certain concave functions from below. The lemma is a partial reverse of Jensen's inequality when certain conditions on the moments are fulfilled; more precisely, if $\left(1 - \sqrt{\frac{\mathbb{E}[z^2]}{c_1 \mathbb{E}[z]^2}}\right) \geq c_3$ holds, with $c_1 > 0$ and $c_3 \neq 0$ being constants. Note that this is exactly the case for the quantization error, as we will see in the proof of Theorem 4.8.

The following lemma is a partial reverse of Jensen's inequality for super linear functions. The lemma will be useful since $\log(1+x)$ is a super linear function.

Lemma 4.12. *If $f : \mathbb{R} \to \mathbb{R}$ is superlinear, then for any constant $c_1 > 0$ and any random variable $z > 0$,*

$$\mathbb{E}\left[f(z)\right] \geq \frac{f(c_1 \mathbb{E}\left[z\right])}{c_1} \left(1 - \sqrt{\frac{\mathbb{E}\left[z^2\right]}{c_1 \mathbb{E}\left[z\right]^2}}\right)$$

holds.

Proof. By assumption $f(z)$ is superlinear and therefore $f(0) = 0$. Thus, for any x and y and any $t \in [0,1]$, $f(tx + (1-t)y) \geq tf(x) + (1-t)f(y)$. Setting $x = 0$ and $y = z^*$, $f((1-t)z^*) \geq \frac{z^*}{z^*}(1-t)f(z^*)$. Hence, for any $0 \leq z \leq z^*$,

$$\frac{f(z)}{z} \geq \frac{f(z^*)}{z^*} \tag{4.22}$$

For any $z^* > 0$ we have

$$\begin{aligned}
\mathbb{E}[f(z)] &\geq \mathbb{E}[f(z)\mathbb{I}\{z \leq z^*\}] \\
&= \mathbb{E}\left[\frac{f(z)}{z} z \mathbb{I}\{z \leq z^*\}\right] \\
&\geq \frac{f(z^*)}{z^*}\mathbb{E}[z\mathbb{I}\{z \leq z^*\}] \qquad (4.23) \\
&= \frac{f(z^*)}{z^*}\mathbb{E}[z(1 - \mathbb{I}\{z > z^*\})] \\
&= \frac{f(z^*)}{z^*}\left(\mathbb{E}[z] - \mathbb{E}[z\mathbb{I}\{z > z^*\}]\right) \\
&\geq \frac{f(z^*)}{z^*}\left(\mathbb{E}[z] - \sqrt{\mathbb{E}[z^2]}\sqrt{\mathbb{E}[\mathbb{I}\{z > z^*\}]}\right) \qquad (4.24) \\
&= \frac{f(z^*)}{z^*}\mathbb{E}[z]\left(1 - \sqrt{\frac{\mathbb{E}[z^2]}{\mathbb{E}[z]^2}}\sqrt{\Pr(z > z^*)}\right) \\
&\geq \frac{f(z^*)}{z^*}\mathbb{E}[z]\left(1 - \sqrt{\frac{\mathbb{E}[z^2]}{\mathbb{E}[z]\, z^*}}\right). \qquad (4.25)
\end{aligned}$$

Inequality (4.23) follows from (4.22), (4.24) follows from the Cauchy-Schwarz inequality and (4.25) follows from Markov's inequality. If we choose $z^* = c_1\mathbb{E}[z]$ the claim follows. □

The following lemma is a modification of Lemma 4.11.

Lemma 4.13. *Let $\boldsymbol{x} \in \mathbb{S}^{n_t-1}$ and $\boldsymbol{y} \in \mathbb{S}^{n_t-1}$ be unit norm vectors. If $\boldsymbol{w}$ is uniformly distributed on the unit sphere $\mathbb{S}^{n_t-1}$ and $m \geq 2$, then*

$$\frac{4 \cdot 2^{-n_t}}{n_t(n_t+1)}\left(1 - |\langle \boldsymbol{x}, \boldsymbol{y}\rangle|^2\right)^{\frac{m}{2}} \leq \mathbb{E}\left[\max\left\{|\langle \boldsymbol{x}, \boldsymbol{w}\rangle|^2 - |\langle \boldsymbol{y}, \boldsymbol{w}\rangle|^2, 0\right\}^m\right] \leq \left(1 - |\langle \boldsymbol{x}, \boldsymbol{y}\rangle|^2\right)^{\frac{m}{2}}$$

holds.

Proof. We have

$$\left||\langle \boldsymbol{x}, \boldsymbol{w}\rangle|^2 - |\langle \boldsymbol{y}, \boldsymbol{w}\rangle|^2\right| = \left|\boldsymbol{w}^H(\boldsymbol{x}\boldsymbol{x}^H - \boldsymbol{y}\boldsymbol{y}^H)\boldsymbol{w}\right|.$$

Consider the eigen-decomposition of the Hermitian matrix $\boldsymbol{A} := \boldsymbol{x}\boldsymbol{x}^H - \boldsymbol{y}\boldsymbol{y}^H = \boldsymbol{Q}\boldsymbol{\Lambda}\boldsymbol{Q}^H$. Since, $\boldsymbol{A}$ has maximum rank of 2, it has at most two non-zero eigenvalues. Therefore, the diagonal matrix $\boldsymbol{\Lambda}$ can be written as $\boldsymbol{\Lambda} = \operatorname{diag}(\lambda_1, \lambda_2, 0, \ldots, 0)$, with $\lambda_1 \leq \lambda_2$. Since, $\boldsymbol{Q}$ is a Hermitian matrix, with columns given by the eigenvectors of $\boldsymbol{A}$, and $\boldsymbol{w}$ is uniformly distributed on $\mathbb{S}^{n_t-1}$, the following is true

$$\mathbb{E}\left[\left(\boldsymbol{w}^H\boldsymbol{A}\boldsymbol{w}\right)^m\right] = \mathbb{E}\left[\left(\boldsymbol{w}^H\boldsymbol{\Lambda}\boldsymbol{w}\right)^m\right].$$

According to (4.14) $\lambda_1 = -\lambda_2$. Thus, we have

$$\begin{aligned}
\mathbb{E}\left[\max\left\{\boldsymbol{w}^H\boldsymbol{A}\boldsymbol{w},0\right\}^m\right] &= \mathbb{E}\left[\max\left\{\lambda_1|w_1|^2-\lambda_1|w_2|^2,0\right\}^m\right] \\
&\geq \lambda_1^m\mathbb{E}\left[\max\left\{2|w_1|^2-1,0\right\}^m\right] &(4.26)\\
&= \lambda_1^m\mathbb{E}\left[(2|w_1|^2-1)^m \,\middle|\, |w_1|^2\geq 1/2\right] &(4.27)\\
&= \lambda_1^m\int_{\sqrt{1/2}}^1 (2\varepsilon^2-1)^m\, d\mu(\varepsilon). &(4.28)
\end{aligned}$$

Inequality (4.26) holds since $\|\boldsymbol{w}\|_2 = 1$ and therefore $|w_1|^2+|w_2|^2\leq 1$. Equation (4.27) is true because $2|w_1|^2-1$ is non-negative only for $|w_1|^2\geq 1/2$. In (4.28) $\mu(\varepsilon)$ is the Haar-measure of $\{\boldsymbol{w}\in\mathbb{S}^{n_t-1} : |w_1|\leq\varepsilon\}$. Now we apply a result by Rudin [Rud80, page 15 equation (2)] for functions on the sphere $\mathbb{S}^{n_t-1}$ in one parameter. We have, for some function $f:\mathbb{R}\to\mathbb{R}$ and a normalized measure $\sigma(\mathbb{S}^{n_t-1})=1$,

$$\begin{aligned}
\int_{\mathbb{S}^{n_t-1}} f(\sigma)\, d\sigma &= \frac{n_t-1}{\pi}\int_0^{2\pi} d\Theta\int_0^1 (1-r^2)^{n_t-2} f(r) r\, dr \\
&= 2(n_t-1)\int_0^1 (1-r^2)^{n_t-2} f(r) r\, dr. &(4.29)
\end{aligned}$$

By setting $f(r) := \lambda_1^m(2r^2-1)^m\chi_{\left[\sqrt{1/2},1\right]}(r)$, where $\chi_I(x)$ is the characteristic function, the lower bound is proved as follows. Plugging $f(r)$ in (4.29) and using (4.28) we have

$$\begin{aligned}
\mathbb{E}\left[\max\left\{\boldsymbol{w}^H\boldsymbol{A}\boldsymbol{w},0\right\}^m\right] &\geq \lambda_1^m\int_{\sqrt{1/2}}^1 (2r^2-1)^m \underbrace{2(n_t-1)(1-r^2)^{n_t-2} r\, dr}_{d\mu(r)} \\
&= \lambda_1^m(n_t-1)\int_{1/2}^1 (2u-1)^m(1-u)^{n_t-2}\, du &(4.30)\\
&= \lambda_1^m(n_t-1)\int_{1/2}^1 (2(u-1)+1)^m(1-u)^{n_t-2}\, du \\
&= \lambda_1^m(n_t-1)\int_0^{1/2} (1-2v)^m v^{n_t-2}\, dv &(4.31)\\
&= 4\lambda_1^m\frac{2^{-n_t}}{n_t(n_t+1)}. &(4.32)
\end{aligned}$$

Equation (4.30) is obtained by substituting $u=r^2$ and in (4.31) we substituted $v=1-u$. Finally, (4.32) follows by solving the integral. Using (4.15) in the proof of Lemma 4.11, which states that the largest eigenvalue of A is $\lambda_1 = \sqrt{1-|\langle\boldsymbol{x},\boldsymbol{y}\rangle|^2}$, the lower bound is obtained.

The upper bound follows, since $0 \leq \max\left\{|w_1|^2 - |w_2|^2, 0\right\}^m \leq 1$ holds for any $\boldsymbol{w} \in \mathbb{S}^{n_t-1}$. Therefore, $\mathbb{E}\left[\max\left\{\boldsymbol{w}^H \boldsymbol{A}\boldsymbol{w}, 0\right\}^m\right] = \lambda_1^m \mathbb{E}\left[\max\left\{|w_1|^2 - |w_2|^2, 0\right\}^m\right] \leq \lambda_1^m$ together with (4.15) proves the upper bound. □

Now we are ready to prove Theorem 4.8.

Proof. Consider an arbitrary but fixed user $m \in \mathcal{S}_b$ where $|\mathcal{S}_b|$ is non-random and fulfills the feasibility condition (4.7), for all $b = 1, ..., T$, with equality. Define an interference alignment solution $\boldsymbol{\pi}_{\mathrm{IA}}$ as $|\langle \boldsymbol{v}_{m,b}, \boldsymbol{\pi}_{\mathrm{IA}}(k)\rangle|^2 = 0$, for all $b = 1, \ldots, T$ and $k \in \mathcal{S} \setminus \{m\}$. For sufficiently high SNR, $R(P, \boldsymbol{\pi}_{\mathrm{IA}}, S, V)$ achieves the optimal capacity scaling (4.2). Thus, we can use Lemma 4.1 and get

$$\mathbb{E}\left[\Delta r_m\right] \geq \mathbb{E}\left[\max\left\{r_m(P, \boldsymbol{\pi}_{\mathrm{IA}}, \mathcal{S}, H) - r_m(P, \boldsymbol{\pi}_{\mathrm{IA}}, \mathcal{S}, V), 0\right\}\right],$$

with

$$r_m(P, \boldsymbol{\pi}_{\mathrm{IA}}, \mathcal{S}, H) = \log\left(1 + \frac{\frac{P\mu_{m,b}^2}{|\mathcal{S}_b|}|\langle \boldsymbol{h}_{m,b}, \boldsymbol{\pi}_{\mathrm{IA}}(m)\rangle|^2}{1 + \sum_{l=1}^{T}\sum_{\substack{k\in\mathcal{S}_l \\ k\neq m}} \frac{P\mu_{m,l}^2}{|\mathcal{S}_l|}|\langle \boldsymbol{h}_{m,l}, \boldsymbol{\pi}_{\mathrm{IA}}(k)\rangle|^2}\right)$$

$$r_m(P, \boldsymbol{\pi}_{\mathrm{IA}}, \mathcal{S}, V) = \log\left(1 + \frac{P}{|\mathcal{S}_b|}\mu_{m,b}^2|\langle \boldsymbol{v}_{m,b}, \boldsymbol{\pi}_{\mathrm{IA}}(m)\rangle|^2\right).$$

Similar to (4.16) and (4.17) we define the following variables (index m omitted)

$$\Phi_{b,k}^* = \frac{P\mu_{m,b}^2}{|\mathcal{S}_b|}|\langle \boldsymbol{h}_{m,b}, \boldsymbol{\pi}_{\mathrm{IA}}(k)\rangle|^2$$

$$\Psi_{b,k}^* = \frac{P\mu_{m,b}^2}{|\mathcal{S}_b|}|\langle \boldsymbol{v}_{m,b}, \boldsymbol{\pi}_{\mathrm{IA}}(k)\rangle|^2$$

$$\Delta_{b,k}^* = \frac{|\mathcal{S}_b|}{P\mu_{m,b}^2}\max\left\{\Phi_{b,k}^* - \Psi_{b,k}^*, 0\right\},$$

which can be interpreted as the effective receive SNR of user m for the IA solution. Using this notation the rate gap can be written in compact form,

$$\Delta r_m(P, \boldsymbol{\pi}_H, \boldsymbol{\pi}_V) \geq \max\left\{\log\left(1 + \sum_{l=1}^{T}\sum_{k\in\mathcal{S}_l}\Phi_{l,k}^*\right) - \log\left(1 + \sum_{l=1}^{T}\sum_{\substack{k\in\mathcal{S}_l \\ k\neq m}}\Phi_{l,k}^*\right) - \log\left(1 + \Psi_{b,m}^*\right), 0\right\}$$

and since $\max\{a-b-c,0\} \geq \max\{a-b,0\} - c$ for $c > 0$, the rate gap for user m is bounded from below by

$$\begin{aligned}\Delta r_m(P, \boldsymbol{\pi}_H, \boldsymbol{\pi}_V) &\geq \log\left(1 + \frac{\max\left\{\Phi^*_{l,m} - \Psi^*_{b,m}, 0\right\}}{1 + \Psi^*_{b,m}}\right) - \log\left(1 + \sum_{l=1}^{T} \sum_{\substack{k \in \mathcal{S}_l \\ k \neq m}} \Phi^*_{l,k}\right) \\ &\geq \underbrace{\log\left(1 + \frac{P\mu^2_{m,b}}{|\mathcal{S}_b|\left(1 + P\mu^2_{m,b}\right)}\Delta^*_{b,m}\right)}_{:=\mathcal{A}} - \underbrace{\log\left(1 + \sum_{l=1}^{T} \sum_{\substack{k \in \mathcal{S}_l \\ k \neq m}} \Phi^*_{l,k}\right)}_{:=\mathcal{B}}. \end{aligned} \tag{4.33}$$

To bound $\mathbb{E}\left[\Delta r_m(P, \boldsymbol{\pi}_H, \boldsymbol{\pi}_V)\right]$ from below, we will derive a lower bound on the expected value of $\mathcal{A}$ and an upper bound on the expected value of $\mathcal{B}$.

We start with the upper bound for $\mathcal{B}$. Since, $\boldsymbol{\pi}_{IA}$ is an interference alignment solution according to V, we have $|\langle \boldsymbol{h}_{m,b}, \boldsymbol{\pi}_{\mathrm{IA}}(k)\rangle|^2 \leq Z$, for $k \neq m$, where $Z = \min_{\boldsymbol{v} \in \mathcal{V}}(1 - |\langle \boldsymbol{h}_{k,l}, \boldsymbol{v}\rangle|^2)$ is the quantization error (defined in Lemma 4.9) under RVQ. By Lemma 4.9 and the Cauchy-Schwarz inequality we have

$$\mathbb{E}\left[\Phi^*_{l,k}\right] \leq \frac{P}{|\mathcal{S}_l|}\sqrt{\mathbb{E}\left[\mu^4_{m,b}\right]}\sqrt{\mathbb{E}\left[Z^2\right]} \leq \frac{P}{|\mathcal{S}_l|}\sqrt{\mathbb{E}\left[\mu^4_{m,b}\right]}2^{\frac{-B}{n_t - 1}}, \ \forall k \neq m, l.$$

Using Jensen's inequality and $\frac{|\mathcal{S}_l|-1}{|\mathcal{S}_l|} \leq 1$, for all l, we obtain the upper bound

$$\mathbb{E}\left[\mathcal{B}\right] \leq \log\left(1 + TP\sqrt{\mathbb{E}\left[\mu^4_{m,b}\right]}2^{\frac{-B}{n_t - 1}}\right). \tag{4.34}$$

To lower bound $\mathcal{A}$ we define the positive random variable

$$Y := \left(\Delta^*_{b,m}\right)^2 = \max\left\{|\langle \boldsymbol{h}_{m,b}, \boldsymbol{\pi}_{\mathrm{IA}}(k)\rangle|^2 - |\langle \boldsymbol{v}_{m,b}, \boldsymbol{\pi}_{\mathrm{IA}}(k)\rangle|^2, 0\right\}^2,$$

where the mapping between Y and $\Delta^*_{b,m}$ is bijective, since $\Delta^*_{b,m}$ is positive per definition. Taking expectation conditioned on $\mu_{m,b}$ and $\boldsymbol{h}_{m,b}$ (denoted $\mathbb{E}\left[\cdot|\mu_{m,b}, \boldsymbol{h}_{m,b}\right] := \mathbb{E}_{|\mu,\boldsymbol{h}}\left[\cdot\right]$) and

using Lemma 4.12 with the concave function $f(x) = \log(1+\sqrt{x})$ we get

$$\begin{aligned}
\mathbb{E}_{|\mu,\boldsymbol{h}}[\mathcal{A}] &= \mathbb{E}_{|\mu,\boldsymbol{h}}\left[\log\left(1+\frac{P\mu_{m,b}^2}{|\mathcal{S}_b|\left(1+P\mu_{m,b}^2\right)}\Delta_{b,m}^*\right)\right] \\
&= \mathbb{E}_{|\mu,\boldsymbol{h}}\left[\log\left(1+\frac{P\mu_{m,b}^2}{|\mathcal{S}_b|\left(1+P\mu_{m,b}^2\right)}\sqrt{Y}\right)\right] \\
&\geq \frac{1}{c_1}\left(1-\sqrt{\frac{\mathbb{E}_{|\mu,\boldsymbol{h}}[Y^2]}{c_1\mathbb{E}_{|\mu,\boldsymbol{h}}[Y]^2}}\right)\log\left(1+c_1\frac{P\mu_{m,b}^2}{|\mathcal{S}_b|\left(1+P\mu_{m,b}^2\right)}\sqrt{\mathbb{E}_{|\mu,\boldsymbol{h}}(Y)}\right).
\end{aligned}$$

It remains to compute the first and second moment of Y. Since, conditioned on $\mu_{m,b}$ and $\boldsymbol{h}_{m,b}$ the beamformer $\boldsymbol{\pi}_{\mathrm{IA}}(m)$ is isotropic distributed, we have by Lemma 4.13 (first step, $n=2$) and Lemma 4.9 (last step)

$$\begin{aligned}
\mathbb{E}_{|\mu,\boldsymbol{h}}(Y) &= \mathbb{E}_{|\mu,\boldsymbol{h}}\left[\max\left\{|\langle\boldsymbol{h}_{m,b},\boldsymbol{\pi}_{\mathrm{IA}}(m)\rangle|^2-|\langle\boldsymbol{v}_{m,b},\boldsymbol{\pi}_{\mathrm{IA}}(m)\rangle|^2,0\right\}^2\right] \\
&\geq \frac{4\cdot 2^{-n_t}}{n_t(n_t+1)}\mathbb{E}_{|\mu,\boldsymbol{h}}\left[\min_{\boldsymbol{v}\in\mathcal{V}}(1-|\langle\boldsymbol{h}_{m,b},\boldsymbol{v}\rangle|^2)\right] \\
&= \frac{4\cdot 2^{-n_t}}{n_t(n_t+1)}\mathbb{E}_{|\mu,\boldsymbol{h}}(Z) \\
&\geq \frac{4\cdot 2^{-n_t}}{n_t(n_t+1)}\frac{n_t-1}{n_t}2^{\frac{-B}{n_t-1}}.
\end{aligned}$$

Again by Lemma 4.13 (first step) and Lemma 4.9 (second step) we have

$$\mathbb{E}_{|\mu,\boldsymbol{h}}\left(Y^2\right) \leq \mathbb{E}_{|\mu,\boldsymbol{h}}\left[Z^2\right] \leq \left(\frac{n_t}{n_t-1}\mathbb{E}_{|\mu,\boldsymbol{h}}[Z]\right)^2.$$

Such that,

$$\begin{aligned}
\mathbb{E}_{|\mu,\boldsymbol{h}}[\mathcal{A}] \geq \frac{1}{c_1}&\left(1-\frac{n_t^2(n_t+1)}{4\sqrt{c_1}(n_t-1)2^{-n_t}}\right) \\
&\log\left(1+\frac{c_1P\mu_{m,b}^2}{|\mathcal{S}_b|\left(1+P\mu_{m,b}^2\right)}\sqrt{\frac{4\cdot 2^{-n_t}(n_t-1)}{n_t^2(n_t+1)}}2^{\frac{-B}{2(n_t-1)}}\right). \quad (4.35)
\end{aligned}$$

Plugging (4.35) and (4.34) in (4.33) and taking expectation with respect to $\mu_{m,b}$ the claim follows. □

5 Rate Estimation Based on Compressed Measurements

With a rapidly growing number of devices current centralized signaling strategies lead to a massive consumption and inefficient use of spectral resources. Different concepts are currently discussed to cope with the tremendous increase of mutually interfering signals. One of the most disruptive changes could be the enhancement of the centralized system architecture towards an ad-hoc networking technologies. In order to overcome the limits of unassisted ad-hoc networking technologies, researchers have recently turned their attention towards network-assisted device-to-device (D2D) communication, which promises more efficient spectrum utilization, higher reliability and quality of service (QoS) support, while providing D2D discovery support, synchronization and security [DRW+09, FDM+12, LLAH15]. In particular, the design aspects of D2D communication are currently discussed in 3GPP, where the feasibility and the architecture enhancements of so called proximity services (ProSe) are under discussion [3GP13], [3GP14]. Thereby, D2D links can operate in in-band mode and out-band mode. While the in-band D2D mode utilizes the same spectral resources as cellular users that transmit their data via base stations in the traditional cellular mode, the out-band D2D mode allocates cellular users and D2D links to different frequency bands. We focus on in-band D2D communication and assume that all users are in-coverage, which means that each user is connected to some base station. As an underlay to cellular networks, in-band D2D communication can be seen as a network-assisted interference channel, in which D2D transmissions reuse cellular resources while being assisted by base stations.

Network-assisted D2D communication poses some fundamental challenges that include transmission mode selection, robust interference management and feedback design. The underlying problems are aggravated by the lack of channel state information[1] at different locations in a network. There is in particular a vital need for timely and accurate channel state information that can be used by the network controller to facilitate reliable D2D discovery and QoS-aware scheduling. In other words, when establishing D2D links and

[1] Notice that channel state information is used in a broad sense and does not necessarily mean the full channel knowledge. In particular, channel state information may also refer to the information about achievable rates.

allocating cellular resources to them, the network controller must have enough channel state information to ensure that the QoS demands of all cellular and D2D users (e.g. expressed in terms of some minimum data rate requirements) are guaranteed once in-band D2D links are established. This requires the development of measurement-based feedback protocols that enable the network controller to acquire the required channel state information in a highly efficient way and with it to open the door toward D2D communication as an underlay to cellular networks.

Contributions

We develop and study a sensing and reconstruction strategy for the estimation of achievable rates based on compressed non-adaptive measurements (which we call compressive rate estimation). The developed protocol exploits collisions in an interference channel to obtain compressed non-adaptive measurements from linear random projections. The proposed protocol combines the estimation from compressed measurements with coded access to reduce the number of pilot-based measurements that need to be fed back to estimate the achievable rates (and to make timely and robust decisions) at a central controller. We apply methods from compressed sensing and sparse approximation [CRT06]. Since, a major drawback of compressed sensing based techniques is that they require highly complex decoders, we also consider linear estimation methods which require significantly less complexity. As we will see the advantages of the proposed protocol are three-fold. First, by applying the concept of coded access we are able to significantly reduce the pilot contamination in the network. Second, the feedback overhead is reduced since a much smaller number of measurements needs to be quantized and fed back. Third, most of the complexity required to estimate the achievable rates is imposed on the central controller.

Related Work

Sparse approximation is a compression technique where a signal is approximated by a sparse representation. Nowadays, sparse approximation is widely used in many standards like JPEG, MPEG, and MP3. The classical approach to compress a bandlimited signal is to take a huge number of samples at a rate given by the Nyquist-Shannon sampling theorem and then find a sparse representation, effectively throwing away a large number of the taken measurements. However, in [CRT06, Don06] it was shown that a signal having a sparse representation can be recovered from a small number of non-adaptive linear measurements. Based on these works a huge number of sensing and recovery techniques for different data models have been published in recent years. A significant amount of work has been done on the theoretical frontier, see for example [HN06, CR07, RSV08, CP11, FR13].

An endless number of applications has been envisioned, including channel estimation and applications to wireless sensor networks. In [QAN10] a compressive sensing based feedback resource reduction protocol for MIMO broadcast channels was proposed. In [KKT12] systems with a very large number antennas (i.e. massive MIMO) where considered and a compressed sensing based feedback protocol for spatially correlated antenna arrays was proposed. In [DBWB10] a framework for what they call compressive signal processing was developed. The idea of compressive signal processing is to extract certain information from measurements instead of first reconstructing the full data. The problem of pilot signals that contaminate the available resources was identified in [CRP10] as a crucial problem in networks with many antennas (or nodes) that use pilot signals channel acquisition schemes.

5.1 System Setup and Problem Formulation

We consider a cellular network with a large number of users and multiple base stations that are controlled by the same central network controller. Each user corresponds to a transmitter-receiver pair and we assume there are $N > 1$ transmitters that access the (wireless) channel to transfer independent data to N receivers. The users (transmitter-receiver pairs) are indexed in an arbitrary but fixed order with indices from the set $\mathcal{N} = \{1, 2, \dots N\}$.[2] In contrast to the previous chapters we assume a single antenna per node. All transmitters are controlled by the same central controller. We adopt a discrete-time flat-fading channel model; described in Section 1.3.1. In a given time slot (time index dropped) the channel from transmitter j to receiver i is given by the transfer function $h_{i,j} \in \mathbb{C}$. The vector of channel coefficients from all transmitters to receiver i is defined as

$$\boldsymbol{h}_i := (h_{i,1}, \dots, h_{i,N})^T \in \mathbb{C}^N$$

and the matrix of all channel coefficients as $\boldsymbol{H} := (\boldsymbol{h}_1, \dots, \boldsymbol{h}_N)$. The nodes are grouped in G groups user $\mathcal{G}_g$, $g = 1, 2, \dots, G$. Nodes within the same group are co-located; the channels from node i to all nodes $j \in \mathcal{G}_g$ are given by

$$h_{i,j} = a_{i,g} b_{i,j} \in \mathbb{C}, \tag{5.1}$$

where $b_{j,i} \sim \mathcal{CN}(0, 1)$ denotes the small scale fading coefficient and $a_{j,g}$ denotes the distance dependent path loss coefficient between node j and group g. We stress that a similar channel model was used in [HTC12] to model large cellular networks with co-located users.

[2] We also use $\mathcal{N}$ to refer to transmitters, receivers and transmissions (i.e., users scheduled for transmissions). According to this, transmission $i \in \mathcal{N}$ is the transmission from transmitter $i \in \mathcal{N}$ to receiver $i \in \mathcal{N}$

Depending on the path loss coefficients and the size of each group the channel matrix has some structure. In the following, of particular interest will scenarios where a large number of path loss components is zero, i.e., if many $a_{i,g} = 0$, the channel vector $\boldsymbol{h}_i$, fr all $i \in \mathcal{G}_g$ is sparse.

Let a subset $\mathcal{S} \subseteq \mathcal{N}$ of transmissions be scheduled, then the signal received by receiver $i \in \mathcal{S}$ is

$$y_i = h_{i,i}s_i + \sum_{j \in \mathcal{S}\setminus\{i\}} h_{i,j}s_j + n_i, \tag{5.2}$$

where $s_j \in \mathbb{C}$ is the complex data symbol transmitted by transmitter j and $n_i \sim \mathcal{CN}(0, \sigma_i^2)$ is additive noise at receiver i. We consider Gaussian codes such that the transmitted data symbols can be modeled as i.i.d. complex Gaussian random variables with $\mathbb{E}[s_j] = 0$ and $\mathbb{E}\left[|s_j|^2\right] = P$, where P is the average power constraint of any node; for simplicity we consider no power control. The SINR of receiver $i \in \mathcal{S}$, defined in (1.3), can now be rewritten as

$$\mathrm{SINR}_i(P, \mathcal{S}, \boldsymbol{h}_i) = \frac{P|h_{i,i}|^2}{\sigma_i^2 + \sum_{j \in \mathcal{S}\setminus\{i\}} P|h_{i,j}|^2}.$$

For the data transmission phase we assume that each user can track its channel perfectly. For fixed channels $\boldsymbol{h}_i$, and scheduling decision $\mathcal{S}$ an achievable rate for transmission i (from transmitter i to receiver i) is defined as

$$r_i(P, \mathcal{S}, \boldsymbol{h}_i) = \log\left(1 + \mathrm{SINR}_i(P, \mathcal{S}, \boldsymbol{h}_i)\right).$$

We stress that even if in the following the achievable rate will act as utility function, extensions of the presented methods and results to other utility function are possible.

5.1.1 Problem Statement

Figure 5.1 depicts the envisioned system architecture. The network is controlled by a central controller. The central controller obtains channel state information from all receivers. Depending on the services the network provides, the tasks of the central controller can be manifold. For many tasks knowledge of the achievable rates $r_i(P, \mathcal{S}, \boldsymbol{h}_i)$ for some scheduling decision $\mathcal{S}$ is essential. Such rate estimates can for example be used to perform scheduling, link adaption or proximity discovery and pairing for D2D communications. If the central controller has perfect channel state information it can easily compute the achievable rate $r_i(P, \mathcal{S}, \boldsymbol{h}_i)$ for any scheduling decision $\mathcal{S}$. However, obtaining perfect channel state information is impossible in practical applications.

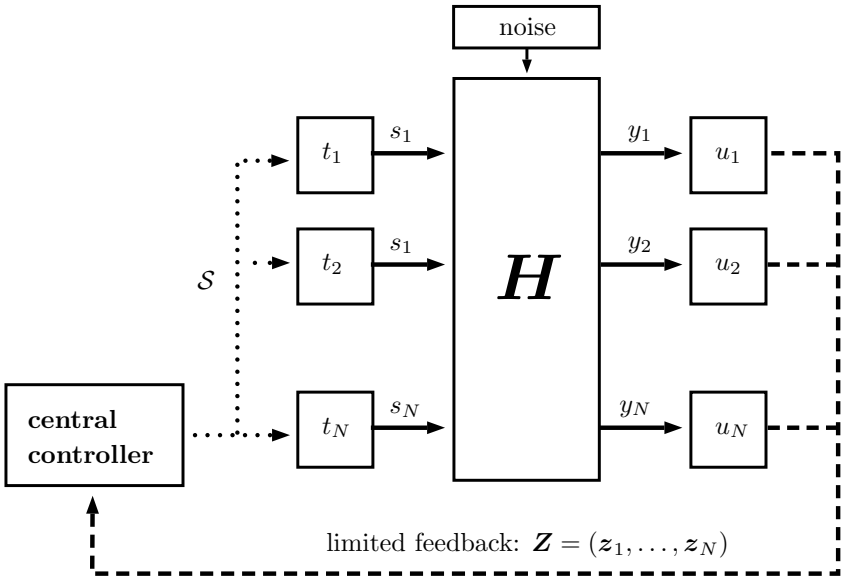

Figure 5.1: Interference network controlled by a central controller. Based on feedback information from the receivers the central controller performs scheduling and distributes the scheduling decision.

In Section 5.2 we present a measurement and feedback protocol that provides the central controller with quantized and compressed channel state information $\boldsymbol{z}_i = f(\boldsymbol{h}_i) + \boldsymbol{\mu}_i$, for each receiver $i \in \mathcal{N}$, where $f : \mathbb{C}^N \to \mathbb{C}^M$ is a linear function that compresses ($M < N$) the channel state information and $\boldsymbol{\mu}_i$ is additive (quantization) noise. Based on $\boldsymbol{z}_i$ the central controller estimates the achievable rates for any scheduling decision $\mathcal{S}$ by a function

$$\gamma_i(P, \mathcal{S}, \boldsymbol{z}_i).$$

To make reliable decisions based on the estimated rates the rate gap

$$\Delta_i := |r(P, \mathcal{S}, \boldsymbol{h}_i) - \gamma(P, \mathcal{S}, \boldsymbol{z}_i)|,$$

must be bounded (and small) for any scheduling decision $\mathcal{S}$.

5.2 Rate Estimation Based on Compressed Measurements

In this section we introduce a channel measurement and feedback protocol and a linear and a non-linear rate estimation function. The measurement and rate estimation protocol is summarized in Table 5.1.

Table 5.1: Measurement and rate estimation protocol.

Central controller	Transmit synchronization signal.
Transmitters	Transmit sequences of M pilot signals.
Receivers	Measure superpositions of pilot signals. Quantize measurements and feed back to the central controller.
Central controller	Estimate rates based on quantized compressed linear measurements.

5.2.1 Random Channel Measurement

To enable efficient channel measurements all transmitters simultaneously transmit a sequence of M pilot signals. The sequence transmitted by transmitter i is denoted as $\boldsymbol{\phi}_i \in \mathbb{C}^M$ and all sequences transmitted by all transmitters are collected in the measurement matrix $\boldsymbol{\Phi} = (\boldsymbol{\phi}_1, \ldots, \boldsymbol{\phi}_N) \in \mathbb{C}^{M \times N}$. According to (5.2) the vector of all M signals received by node i can be written as

$$\boldsymbol{y}_i = \boldsymbol{\Phi}\boldsymbol{h}_i + \boldsymbol{n}_i \in \mathbb{C}^M.$$

To feed back the vector of channel measurements $\boldsymbol{y}_i$ to the network controller each receiver i uses a quantization operator $\mathcal{Q} : \mathbb{C}^M \to \mathbb{C}^M$. For simplicity we assume that $\mathcal{Q}(\boldsymbol{y}_i) = \boldsymbol{y}_i + \bar{\boldsymbol{n}}_i$, where $\bar{\boldsymbol{n}}_i$ is additive noise independent of $\boldsymbol{y}_i$. We assume an error and delay free feedback channel from all nodes to the network controller, such that the channel state information at the network controller is

$$\boldsymbol{z}_i = f(\boldsymbol{y}_i) + \boldsymbol{\mu}_i = \boldsymbol{\Phi}\boldsymbol{h}_i + \boldsymbol{\mu}_i, \tag{5.3}$$

where we defined the additive noise term $\boldsymbol{\mu}_i = \bar{\boldsymbol{n}}_i + \boldsymbol{n}_i$, that collects the measurement and quantization noise and is assumed to be independent of the measurements $f(\boldsymbol{y}_i)$. Further we define the matrix of all quantized channel measurements, known to the network controller, as $\boldsymbol{Z} := (\boldsymbol{z}_1, \ldots, \boldsymbol{z}_N) \in \mathbb{C}^{M \times N}$.

5.2.2 Rate Estimation

Based on the compressed and quantized measurements the achievable rate $r_i(P, \mathcal{S}, \boldsymbol{h}_i)$ of link i is estimated by the central controller with the function

$$\gamma_i(P, \mathcal{S}, \boldsymbol{z}_i) = \log\left(1 + \frac{P\beta(\boldsymbol{z}_i, i)}{1 + \sum_{j \in \mathcal{S}\setminus\{i\}} P\beta(\boldsymbol{z}_i, j)}\right), \tag{5.4}$$

which is a function of the estimated SINR $\frac{P\beta(\boldsymbol{z}_i,i)}{1+\sum_{j\in\mathcal{S}\setminus\{i\}}P\beta(\boldsymbol{z}_i,j)}$. Since the SINR is a function of the channel gains $|h_{i,j}|^2$ it is sufficient if the central controller has estimates of the channel gains instead of the complex channel coefficients. The estimated channel gain between receiver i and transmitter j is given by the function

$$|\hat{h}_{i,j}|^2 = \beta(\boldsymbol{z}_i, j).$$

In the subsequent sections we compare the performance of different functions $\beta(\boldsymbol{z}_i, j)$. One class of functions is given by *linear channel gain estimation functions*:

Definition 5.1. *A linear channel gain estimation function is given by*

$$\beta_l(\boldsymbol{z}_i, j) = |\langle \boldsymbol{\Psi}\boldsymbol{z}_i, \boldsymbol{e}_j\rangle|^2,$$

where the matrix $\boldsymbol{\Psi} \in \mathbb{C}^{N\times M}$ depends on the measurement matrix $\boldsymbol{\Phi}$ and $\boldsymbol{e}_j$ is the jth column of the identity matrix $\boldsymbol{I}_N$.

Another class of functions is given by *non-linear channel gain estimation functions*:

Definition 5.2. *A non-linear channel gain estimation function is given by*

$$\beta_{nl}(\boldsymbol{z}_i, j) = |\langle \alpha(\boldsymbol{z}_i), \boldsymbol{e}_j\rangle|^2$$

where $\alpha : \mathbb{C}^M \to \mathbb{C}^N$ is some non-linear function.

5.3 Rate Gap Analysis

5.3.1 Concentration of Measure

The concentration of measure phenomenon is a power full tool. For an in depth treatment we refer the reader to [Led05]. A concise introduction can be found in [Tao12]. Throughout this chapter we assume that the elements of the measurement matrix $\boldsymbol{\Phi}$ are chosen at random and impose the following two conditions. First, the matrix is normalized such that the expected value of the random variable $\|\boldsymbol{\Phi}\boldsymbol{a}\|_2^2$ satisfies

$$\mathbb{E}\left[\|\boldsymbol{\Phi}\boldsymbol{a}\|_2^2\right] = \|\boldsymbol{a}\|_2^2, \forall \boldsymbol{a} \in \mathbb{C}^N.$$

Second, we assume that for any $\boldsymbol{a} \in \mathbb{C}^N$ the random variable $\|\boldsymbol{\Phi}\boldsymbol{a}\|_2^2$ is strongly concentrated around its expected value,

$$\Pr\left(\left|\|\boldsymbol{\Phi}\boldsymbol{a}\|_2^2 - \|\boldsymbol{a}\|_2^2\right| > \varepsilon\|\boldsymbol{a}\|_2^2\right) \leq c_0 e^{-\gamma(\varepsilon)} \tag{5.5}$$

where $c_0 > 0$ is a constant, and $\gamma(\varepsilon)$ is a function that depends on the distribution of $\boldsymbol{\Phi}$. Examples of measurement matrices that satisfy the concentration inequality (5.5) are matrices with elements that are sub-Gaussian distributed (see e.g. [Ver10]). A random variable X is called sub-Gaussian if there exists a constant $c > 0$ such that the moment generating function can be bounded by

$$\mathbb{E}\left[\exp(Xt)\right] \leq \exp(c^2 t^2/2). \tag{5.6}$$

Examples of sub-Gaussian random variables are the normal distribution, and all bounded distributions. In particular, if the elements of $\boldsymbol{\Phi} \in \mathbb{C}^{M\times N}$ are distributed according to $\phi_{i,j} \sim \mathcal{CN}(0, 1/M)$, then $\mathbb{E}\left[\boldsymbol{\Phi}^H\boldsymbol{\Phi}\right] = \boldsymbol{I}_N$, and $\mathbb{E}\left[\|\boldsymbol{\Phi}\boldsymbol{a}\|_2^2\right] = \boldsymbol{a}^H\mathbb{E}\left[\boldsymbol{\Phi}^H\boldsymbol{\Phi}\right]\boldsymbol{a} = \|\boldsymbol{a}\|^2$. Moreover, it can be shown (see e.g. [Dav11]) that

$$\Pr\left(\left|\|\boldsymbol{\Phi}\boldsymbol{a}\|_2^2 - \|\boldsymbol{a}\|_2^2\right| > \varepsilon\|\boldsymbol{a}\|_2^2\right) \leq 2\exp\left(-\varepsilon^2 M\frac{1-\ln(2)}{2}\right). \tag{5.7}$$

Moreover, the following result will be useful in our analysis. Let $\boldsymbol{a}$ be a random vector with elements $a_i \sim \mathcal{CN}(0,1)$. Then, for all $t > 0$,

$$\Pr\left(\|\boldsymbol{a}\|_2^2 - \mathbb{E}\left[\|\boldsymbol{a}\|_2^2\right] > t\right) \leq \exp(-t^2/2). \tag{5.8}$$

In fact, this is a special case of the concentration of measure theorem for Lipschitz functions, see [FR13, Theorem 8.40].

5.3.2 Preliminary Result

First, we introduce a general result that enables us to bound Δ_i independent of the estimation function. To simplify the notation we define the channel gain $x_{i,j} := |h_{i,j}|^2$, the vector of channel gains $\boldsymbol{x}_i := (x_{i,1}, \ldots, x_{i,N})^T$ and the matrix of channel gains $\boldsymbol{X} := (\boldsymbol{x}_1, \ldots, \boldsymbol{x}_N)$. In a similar manner we define the estimated channel gains as $\hat{x}_{i,j} := \beta(\boldsymbol{z}_i, j)$, the vector of estimated channel gains $\hat{\boldsymbol{x}}_i := (\hat{x}_{i,1}, \ldots, \hat{x}_{i,N})^T$ and the matrix of estimated channel gains $\hat{\boldsymbol{X}} := (\hat{\boldsymbol{x}}_1, \ldots, \hat{\boldsymbol{x}}_N)$.

Lemma 5.3. *Let the achievable rates $r(P, \mathcal{S}, \boldsymbol{h}_i)$ be estimated by $\gamma_i(P, \mathcal{S}, \boldsymbol{z}_i)$ defined in (5.4). For any scheduling decision $\mathcal{S}$, with $|\mathcal{S}| \leq n$, and any channel gain estimation $\hat{x}_{i,j} = \beta(\boldsymbol{z}_i, j)$,*

$$\Delta_i = |r_i(P, \mathcal{S}, \boldsymbol{h}_i) - \gamma_i(P, \mathcal{S}, \boldsymbol{z}_i)| \leq 2P\sum_{j\in\mathcal{S}} |x_{i,j} - \hat{x}_{i,j}|,$$

holds simultaneously for all $i \in \mathcal{S}$.

To control Δ_i we need to control $\sum_{l\in\mathcal{N}} \left||h_{i,l}|^2 - |\hat{h}_{i,l}|^2\right|$ based on the measurements $\boldsymbol{z}_i = \boldsymbol{\Phi}\boldsymbol{h}_i + \boldsymbol{\mu}_i$, defined in (5.3). Hence, it is not necessary that we recover the vectors $\boldsymbol{h}_i$, for all i. Instead, recovery of the vectors $\boldsymbol{x}_i$ is sufficient. We stress that this is different from classical estimation theory (see e.g. [Lue68]) where based on the measurements $\boldsymbol{z}_i$ minimization of the error $\|\boldsymbol{h}_i - \hat{\boldsymbol{h}}_{\boldsymbol{i}}\|_2^2 = \sum_{l\in\mathcal{N}} |h_{i,l} - \hat{h}_{i,l}|^2$ is considered.

5.3.3 Non-Linear Rate Estimation

In this subsection we study a non-linear channel gain estimation function that uses concepts from compressed sensing to exploit the sparsity of the channels. More precisely, we assume that the channel vectors are compressible, that is, for some $i \in \mathcal{N}$ the channel vector $\boldsymbol{h}_i$ is sparse or has at least fast decaying magnitudes. Compressibility of a given vector can be quantified by calculating

$$\sigma_k(\boldsymbol{x})_p := \min_{\hat{\boldsymbol{x}}\in\Sigma_k} \|\boldsymbol{x} - \hat{\boldsymbol{x}}\|_p,$$

where $\Sigma_k := \{\boldsymbol{x} \in \mathbb{C}^N : \mathrm{supp}(\boldsymbol{x}) \leq k\}$ the set of all k-sparse vectors. The function α, defined in Definition 5.2, is given by the solution to the convex optimization problem

$$\alpha(\boldsymbol{z}_i) = \underset{\boldsymbol{x}\in\mathbb{C}^N}{\arg\min} \|\boldsymbol{x}\|_1 \quad \text{subject to} \quad \|\boldsymbol{\Phi}\boldsymbol{x} - \boldsymbol{z}_i\|_2 \leq \xi. \tag{5.9}$$

The parameter ξ must be chosen such that $\|\boldsymbol{\mu}_i\|_2 \leq \xi$.

We will first review some basic results from compressed sensing and then show how these results can be applied to obtain bounds on Δ_i. Compressed sensing recovering results can be divided in uniform and nonuniform recovery results. A uniform recovery result means that one can recover all k-sparse vectors – with high probability – from linear measurements with the same matrix. Nonuniform recovery means that a fixed k-sparse vector can be recovered with a randomly drawn measurement matrix, with high probability. Uniform recovery results are obviously stronger since they imply nonuniform recovery. To streamline the presentation we consider only uniform recovery. One class of uniform recovery results are based on the restricted isometry property (RIP) of the measurement matrix $\boldsymbol{\Phi}$. The RIP is defined as follows.

Definition 5.4. *An $M \times N$ matrix $\boldsymbol{\Phi}$ satisfies the RIP of order $k \geq 1$, if there exists $0 \leq \delta_k$ such that the inequality*

$$(1 - \delta_k)\|\boldsymbol{x}\|_2^2 \leq \|\boldsymbol{\Phi}\boldsymbol{x}\|_2^2 \leq (1 + \delta_k)\|\boldsymbol{x}\|_2^2,$$

holds for all $\boldsymbol{x} \in \Sigma_k$. *The smallest number* $\delta_k = \delta_k(\boldsymbol{\Phi})$ *is called the restricted isometry constant of the matrix* $\boldsymbol{\Phi}$.

Many ensembles of random matrices are known to satisfy the RIP with high probability. An important class of random matrices are matrices with elements that are i.i.d. sub-Gaussian distributed. In particular, if $X \sim \mathcal{CN}(0, \sigma^2)$, then $\mathbb{E}\left[\exp(Xt)\right] \leq \exp(\sigma^2 t^2/2)$ and therefore, according to (5.6), X is sub-Gaussian[3].

For concreteness we assume that the elements of $\boldsymbol{\Phi}$ are distributed complex Gaussian $\phi_{i,j} \sim \mathcal{CN}(0, 1/M)$. In fact, this assumption enables us to explicitly compute most of the constants that would otherwise depend on the distribution of $\boldsymbol{\Phi}$. We stress that more general results for sub-Gaussian measurement matrices can be found for example in [EK12, FR13] and references therein. The following theorem which is proved in [FR13, Theorem 9.27] enables us to bound the RIP constant of $\boldsymbol{\Phi}$. To be self contained, we state the theorem in our notation.

Theorem 5.5 ([FR13, Theorem 9.27])**.** *Let* $\boldsymbol{\Phi}$ *be a random* $M \times N$ *matrix with i.i.d. elements distributed according to* $\phi_{i,j} \sim \mathcal{CN}(0, 1/M)$. *Assume that*

$$M \geq 2\eta^{-2}\left(k \ln(eN/k) + \ln(2\varepsilon^{-1})\right),$$

with $\eta, \varepsilon \in (0, 1)$. *Then the RIP constant* δ_k *of* $\boldsymbol{\Phi}$ *satisfies*

$$\delta_k \leq 2\left(1 + \frac{1}{\sqrt{2\ln(eN/k)}}\right)\eta + \left(1 + \frac{1}{\sqrt{2\ln(eN/k)}}\right)^2 \eta^2,$$

with probability $1 - \varepsilon$.

As pointed out by [FR13, Remark 9.28] the statement of the last theorem can be simplified by using $\delta_k \leq \delta \leq C_1\eta$ with $C_1 = 2(1 + \sqrt{1/2}) + (1 + \sqrt{1/2})^2$ such that $M \geq 2C_1^2\delta^{-2}\left(k \ln(eN/k) + \ln(2\varepsilon^{-1})\right)$ yields $\delta_k \leq \delta$. According to Lemma 5.3 we need to control $\|\boldsymbol{x}_i - \hat{\boldsymbol{x}}_i\|_2$ to control the rate gap Δ_i. If the measurement matrix satisfies the RIP of order k with $\delta_k < 1/3$, the following theorem provides an error estimate.

Theorem 5.6 ([CZ13, Theorem 3.3])**.** *Suppose* $\boldsymbol{\Phi}$ *satisfies the RIP of order* k *with* $\delta_k < 1/3$. *Let the measurements be given by* $\boldsymbol{z} = \boldsymbol{\Phi}\boldsymbol{h} + \boldsymbol{\mu}$, *according to* (5.3), *with* $\|\boldsymbol{\mu}\|_2 \leq \xi$. *Then for any* $\boldsymbol{h} \in \mathbb{C}^N$ *the solution* $\hat{\boldsymbol{h}} = \alpha(\boldsymbol{z})$ *to* (5.9) *obeys*

$$\|\boldsymbol{h} - \hat{\boldsymbol{h}}\|_2 \leq C_2(\delta_k)\frac{\sigma_k(\boldsymbol{h}_i)_1}{\sqrt{k}} + 2C_3(\delta_k)\xi, \tag{5.10}$$

[3] In fact, strictly sub-Gaussian since $c^2 = \sigma^2$.

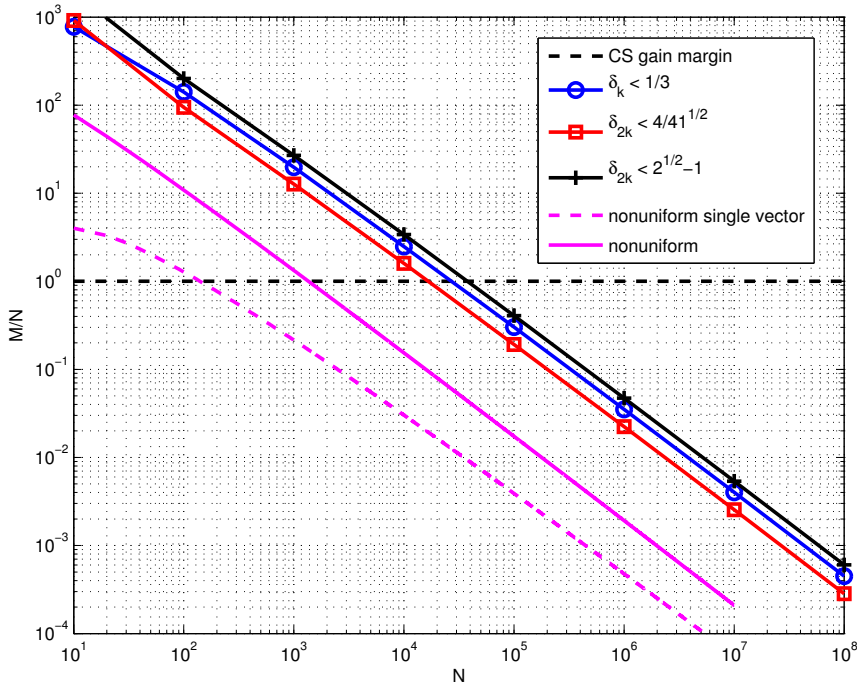

Figure 5.2: Bounds on compression ratio M/N over system size N. Maximal compression to achieve perfect reconstruction with probability $\varepsilon = 0.9$ fixed sparsity $k = 10$.

where $C_2(\delta) = \frac{2\sqrt{2}(2\delta+\sqrt{(1-3\delta)\delta})+2(1-3\delta)}{1-3\delta}$ *and* $C_3(\delta) = \frac{\sqrt{2(1+\delta)}}{1-3\delta}$ *are constants.*

The theorem is proved in [CZ13, Theorem 3.3]. We stress that many similar error bounds for Problem 5.9 and related problems are known. The probably most popular error bound was provided in the seminal paper [CRT06], which requires that the measurement matrix has a RIP constant $\delta_{2k} \leq \sqrt{2} - 1$. A better error bound is given in [FR13, Theorem 6.12] where $\delta_{2k} \leq 4/\sqrt{41}$ is required. Figure 5.2 depicts the system size N over the compression ratio M/N for different RIP constants. The number of measurements is evaluated according to Theorem 5.5. To obtain significantly reduced number of measurements the number of links N must be large. Figure 5.2 includes also bounds on the number of measurements for non-uniform recovery. Non-uniform recovery results give a error bounds for much smaller system sizes N. However, we stress that the RIP is only a sufficient condition for recovery. From Theorem 5.5, Theorem 5.6 and Lemma 5.3 we devise the following corollary.

Corollary 5.7. *Let* $\mathbf{\Phi}$ *be a random* $M \times N$ *matrix with i.i.d. elements distributed according to* $\phi_{i,j} \sim \mathcal{CN}(0, 1/M)$. *Suppose the measurements are given by* $\boldsymbol{z}_i = \mathbf{\Phi}\boldsymbol{h}_i + \boldsymbol{\mu}_i$, *according*

to (5.3)*, with* $\|\boldsymbol{\mu}\|_2 \leq \xi$*. If*

$$M \geq 2C_1^2\delta^{-2}\left(k\ln(eN/k) + \ln(2\varepsilon^{-1})\right),$$

with $\delta \leq \delta_{2k} < 1/3$ *and* $\|\boldsymbol{h}_i\|_2 \leq a_i$ *then for all* $\{\boldsymbol{h}_i\}_{i\in\mathcal{N}}$ *the solutions* $\{\hat{\boldsymbol{h}}_i\}_{i\in\mathcal{N}}$ *to* (5.9) *obey*

$$Pr(\exists i \in \mathcal{N} : \Delta_i > 2Pq(\boldsymbol{h}_i,\xi)(2a_i + q(\boldsymbol{h}_i,\xi))) \leq \varepsilon,$$

with $q(\boldsymbol{h}_i,\xi) = C_2(\delta_k)\frac{\sigma_k(\boldsymbol{h}_i)_1}{\sqrt{k}} + 2C_3(\delta_k)\xi$ *and* $C_2(\delta), C_3(\delta) > 0$ *as in Theorem 5.6.*

The proof is given in Section 5.6.2. We present some brief remarks. If the number of measurements are in the order of $\mathcal{O}(k\ln(eN/k)$ and for all $i \in \mathcal{N}$ the channels $\boldsymbol{h}_i$ are k-sparse (i.e. $\sigma_k(\boldsymbol{h}_i)_1 = 0$), then the rate estimation error Δ_i remains bounded. Moreover, in the noiseless case ($\xi = 0$) perfect recovery can be achieved. However, for both cases the system size N must be sufficiently large as said before and illustrated in Figure 5.2.

5.3.4 Linear Rate Estimation

In this subsection we derive bounds on the rate gap Δ_i for linear channel gain estimation functions. First, we prove a general theorem that is valid for any linear estimation function defined in Definition 5.1 and any ensemble of measurement matrices that satisfies the concentration of measure inequality (5.5). We have the following general result, which is the main result in this chapter.

Theorem 5.8. *Let channel state information be given by any linear estimation function* $\beta(\boldsymbol{z}_i, j) = |\langle \boldsymbol{\Psi}\boldsymbol{z}_i, \boldsymbol{e}_j\rangle|^2$*, with* $\boldsymbol{\Psi} = \boldsymbol{\Phi}^H\boldsymbol{A}$ *where* $\boldsymbol{A}$ *is any positive semi-definite matrix. If* $\boldsymbol{\Phi}$ *fulfills the concentration inequality* (5.5) *and the number of active transmissions is bounded by* $1 \leq |\mathcal{S}| \leq n$*, then for any fixed* $\boldsymbol{h}_i$ *and any* $u_0 \geq 0$*,* $e_0 \geq 0$ *and* $\varepsilon \geq 0$*,*

$$\begin{aligned} Pr\left(\exists i \in \mathcal{N} : \Delta_i > 2P\left(4\|\boldsymbol{h}_i\|_2^2\sqrt{n}(1+u_0)\varepsilon + e_0\right)\right) \\ \leq 4nN\exp(-\gamma(\varepsilon)) + NPr(s_{\max}(\boldsymbol{\Psi}\boldsymbol{\Phi}) > u_0) + \\ \sum_{i\in\mathcal{N}} Pr(\|\boldsymbol{\Psi}\boldsymbol{e}\|_2(\|\boldsymbol{\Psi}\boldsymbol{e}\|_2 + 2\|\boldsymbol{\Psi}\boldsymbol{\Phi}\boldsymbol{h}_i\|_2) > e_0). \end{aligned}$$

The prove is deferred to Section 5.6.3. Clearly the bound depends on the choice of $\boldsymbol{\Psi}$ and the distribution of $\boldsymbol{\Phi}$. The latter determines the function $\gamma(\varepsilon)$. However the theorem is rather general and enables the evaluation of different linear estimation functions, different assumptions on the channels and different distributions of the measurement matrix $\boldsymbol{\Phi}$.

As an illustration we assume that the channel vectors are k-sparse, $\boldsymbol{h}_i \in \Sigma_k$ for all i, and consider the following estimation function and measurement matrix. Let the elements

of $\mathbf{\Phi}$ be distributed complex Gaussian and define the linear estimation function as

$$\beta_l(\boldsymbol{z}_i, j) = |\langle \mathbf{\Phi}^+ \boldsymbol{z}_i, \boldsymbol{e}_j \rangle|^2, \tag{5.11}$$

where $\mathbf{\Phi}^+$ is defined as the pseudo inverse $\mathbf{\Phi}^+ = \mathbf{\Phi}^H(\mathbf{\Phi}\mathbf{\Phi}^H)^{-1}$, for $M < N$. We devise the following corollary.

Corollary 5.9. *Under the assumptions of Theorem 5.8. Let $M < N$. Suppose that the elements of $\mathbf{\Phi}$ are distributed $\phi_{i,j} \sim \mathcal{CN}(0, 1/M)$. Let $\beta_l(\boldsymbol{z}_i, j) = |\langle \mathbf{\Phi}^+ \boldsymbol{z}_i, \boldsymbol{e}_j \rangle|^2$. Assume that $\|\boldsymbol{e}\|_2 = 0$ and for all $i \in \mathcal{N}$ we have $\boldsymbol{h}_i$ is k-sparse, and $\boldsymbol{h}_{i,j} \sim \mathcal{CN}(0, 1)$ for all $j \in supp(\boldsymbol{h}_i)$. We have*

$$Pr\left(\exists i \in \mathcal{N} : \Delta_i > 16P\sqrt{\frac{\kappa n}{M}}\left(\sqrt{2}\ln\left(\frac{4nN+1}{\varepsilon}\right) + k\sqrt{\ln\left(\frac{4nN+1}{\varepsilon}\right)}\right)\right) \leq \varepsilon,$$

with $\kappa = 2/(1 - \log(2))$.

The proof is given in Section 5.6.4. A few remarks are in place. For fixed transmit powers P, a fixed system size N, a given error probability ε and a fixed number of active links n, the rate estimation error scales with $\sqrt{1/M}$, which is also in accordance with the estimation results in [DWB06, Theorem 4.1], where essentially the same scaling is achieved. As was be expected the linear decoding function is not able to achieve perfect recovery (for $M < N$). Perfect recovery can only be achieved by the compressed sensing based decoder but comes at the cost of additional complexity. However, the simulations in the next section show that the linear decoder performs quiet well applied to a small systems.

5.4 Application: Proximity Discovery and Pairing

A subset $\mathcal{N}_1 \subseteq \mathcal{N}$ is used to refer to so-called cellular users that have been scheduled for (cellular) transmissions via some base stations. As a result, the remaining users with indices in $\mathcal{N}_2 = \mathcal{N} \setminus \mathcal{N}_1$ have been identified as potential D2D users. For concreteness but without loss of generality, we assume that the cellular users transmit in the downlink channel. As a result, if $i \in \mathcal{N}_1$ is a cellular user, then the ith transmitter is a base station, while the ith receiver is a wireless device.

In what follows, we assume that each receiver i has a rate (or quality-of-service) requirement $\bar{r}_i$ and we define a feasible scheduling decision as follows.

Definition 5.10 (Feasible scheduling decision)**.** *Given a channel matrix $\boldsymbol{H}$, we say that a scheduling decision $\mathcal{S}$ is feasible if $r(\boldsymbol{h}_i, \mathcal{S}) \geq \bar{r}_i$ holds for each $i \in \mathcal{S}$.*

It is important to emphasize that $r(\boldsymbol{h}_i, \mathcal{S}) \geq \bar{r}_i$ is assumed to hold for each $i \in \mathcal{N}_1 \subset \mathcal{S}$. In other words, we assume that the requirements of cellular users are satisfied and $\mathcal{N}_1$ is a feasible scheduling decision. As far as the remaining D2D users in $\mathcal{N} \setminus \mathcal{N}_1$ are concerned, the network controller may schedule them to be paired with the transmissions in $\mathcal{N}_1$, provided that (i) D2D devices are in proximity to each other (see below) and the resulting scheduling decision is feasible in the sense of Definition 5.10.

5.4.1 Proximity discovery and pairing with perfect channel state information

Two main steps towards establishing a D2D communication are proximity discovery and pairing. In the following we use the following definition.

Definition 5.11 (Proximity)**.** *Given some channel realization, we say that two nodes are in proximity to each other if the achievable rate between the two nodes fulfills a given rate requirement.*

Ideally, proximity discovery and pairing should be based on the achievable rates. If the network controller had perfect instantaneous knowledge of the channel matrix $\boldsymbol{H}$, it could compute the achievable rates $r(\boldsymbol{h}_i, \mathcal{S}), i \in \mathcal{N}$ for any scheduling decision $\mathcal{S} \subseteq \mathcal{N}$. Thus, proximity discovery can be performed as follows.

Definition 5.12 (Proximity discovery with perfect channel state information)**.** *Assuming that the network controller has perfect knowledge of $\boldsymbol{h}_i$ for some $i \in \mathcal{N} \setminus \mathcal{N}_1$, we say that transmitter and receiver i are in proximity if $i \in \mathcal{N}_2$ where*

$$\mathcal{N}_2 = \{i \in \mathcal{N} \setminus \mathcal{N}_1 : r(P, \{i\}, \boldsymbol{h}_i) \geq \bar{r}_i\}\,.$$

Therefore, $\mathcal{N}_2$ is the set of all transmitter-receiver pairs that are in proximity.

After performing proximity discovery, the network controller decides if additional D2D transmissions $\mathcal{N}_2$ are paired with the cellular transmissions $\mathcal{N}_1$. The optimal scheduling decision with rate constraints is found by solving the following optimization problem. Under the assumption of perfect channel state information at the network controller, the scheduling decision $\mathcal{S} \subseteq \mathcal{N}_1 \cup \mathcal{N}_2$ is a solution to

$$\begin{aligned} &\max_{\mathcal{X} \subseteq \mathcal{N}_2} \sum_{i \in \mathcal{X} \cup \mathcal{N}_1} r(P, \mathcal{X} \cup \mathcal{N}_1, \boldsymbol{h}_i) \\ &\text{subject to } r(P, \mathcal{X} \cup \mathcal{N}_1, \boldsymbol{h}_i) \geq \bar{r}_i \text{ for all } i \in \mathcal{X} \cup \mathcal{N}_1\,. \end{aligned}$$

Since $\mathcal{N}_1$ is assumed to be feasible decision scheduling, the problem in (5.4.1) has always a solution in the sense that if no D2D user can be paired with cellular users, then $\mathcal{S} = \mathcal{N}_1$ is

the feasible scheduling decision. Note that since $\mathcal{N}_1$ is given, solving the pairing decision problem provides a feasible scheduling decision $\mathcal{S}$.

5.4.2 Proximity discovery and pairing with compressed channel state information

The rationale behind the definition of the rate gap in (5.1.1) comes from the rate requirements. In particular, if $\Delta_i \leq \lambda$ for some known $\lambda > 0$, then the network controller can reliably perform proximity discovery by identifying pairs of transmitters and receivers that are in proximity and wish to communicate with each other.

Definition 5.13 (Proximity discovery with compressed channel state information)**.** *Assuming that the network controller has compressed compressed channel state information $\boldsymbol{z}_i$ for some $i \in \mathcal{N} \setminus \mathcal{N}_1$, we say that transmitter and receiver i are in proximity if $i \in \hat{\mathcal{N}}_2$ where*

$$\hat{\mathcal{N}}_2 = \{i \in \mathcal{N} \setminus \mathcal{N}_1 : \gamma(P, \{i\}, \boldsymbol{z_i}) \geq \bar{r}_i + \lambda\}\,.$$

Hence, for a given rate estimation strategy the network controller needs to be able to compute bounds of the rate gap Δ_i, for all $i \in \mathcal{S}$ and any possible scheduling decision $\mathcal{S}$. The scheduling decision $\hat{\mathcal{S}}$ based on estimated rates is found by solving

$$\begin{aligned} &\max_{\mathcal{X} \subseteq \hat{\mathcal{N}}_2} \sum_{i \in \mathcal{X} \cup \mathcal{N}_1} \gamma(P, \mathcal{X} \cup \mathcal{N}_1, \boldsymbol{z}_i,) \\ &\text{subject to } \gamma(P, \mathcal{X} \cup \mathcal{N}_1, \boldsymbol{z}_i) \geq \bar{r}_i + \lambda \text{ for all } i \in \mathcal{X} \cup \mathcal{N}_1. \end{aligned} \tag{5.12}$$

The objective of the network controller is to make reliable pairing decisions or, equivalently, scheduling decisions based on partial channel state information $\boldsymbol{Z} = (\boldsymbol{z}_1, \ldots, \boldsymbol{z}_N)$. Reliable decisions are those decisions that give a feasible scheduling decision according Definition 5.10.

5.4.3 Simulations

We consider a cellular system with 1 base station and 25 users. Every node has a single antenna. The channels are modeled according to (5.1). We compare two setups: i) 5 groups of 5 users each, the path loss coefficients are chosen as $10^{z/10}$, with z uniformly distributed in $[0, 1]$. ii) 25 users all in the same group and path loss coefficient is $a_{i,g} = 1$ for all i, g, i.e., all channels are i.i.d. complex Gaussian distributed. The rate requirement is set to $\bar{r} = 1/10 \log(1 + P)$. Problem 5.9 was solved using the Tfocs toolbox [BCG11].

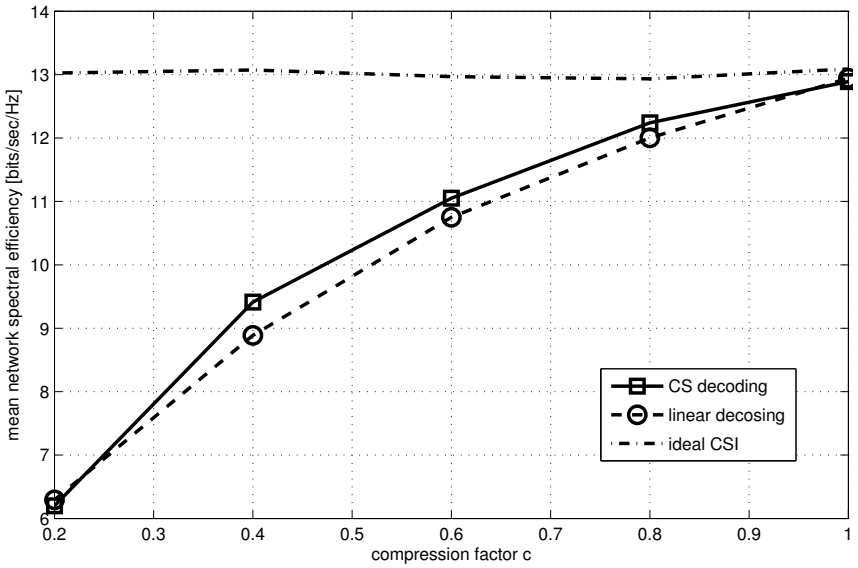

Figure 5.3: Average sum-rate over compression factor M/N; Setup: 25 users, 1 base station, perfect feedback channel (no feedback and quantization noise), single group; channel matrix i.i.d. Gauss and not compressible. Comparison of linear and non-linear rate estimation.

We compare the solution to problem (5.12) for the non-linear compressed sensing estimation function (5.9) and the linear estimation function (5.11). In the simulations $\lambda = 0$, since the analytic results do not give tight bounds for systems with $N = 25$. Nevertheless the results in Figure 5.3 show that linear estimation performs very close to the much more complex compressed sensing based estimation. Figure 5.4 shows that if the channel matrix is compressible the compressed sensing estimation function performs better than the linear estimation function. Since the considered systems are quiet small it is expected that the gain of compressed sensing increases for larger systems.

5.5 Conclusions and Future Work

We developed a channel sensing and reconstruction protocol that enables the central controller to estimate the achievable rates based on compressed non-adaptive measurements. The scaling of the estimation error at the central controller has been analyzed for linear and non-linear decoding functions. Scaling results for the non-linear decoding function where shown to follow from well known compressed sensing results. However, for a small to moderate system size N the compressed sensing results do not provide reasonable performance bounds. For linear decoding functions we derived a general result which can be used to analyze the performance of a variety of linear decoding functions and measure-

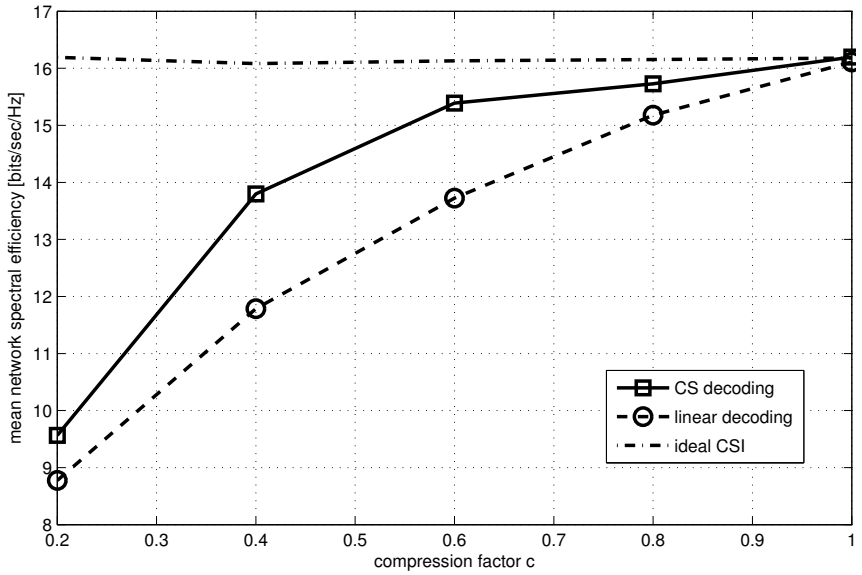

Figure 5.4: Average sum-rate over compression factor M/N; Setup: 25 users, 1 base station, perfect feedback channel (no feedback and quantization noise), 5 group of 5 users each; channel matrix compressible, single group; channel matrix i.i.d. Gauss and not compressible. Comparison of linear and non-linear rate estimation.

ment matrices. For a linear decoding function based on the pseudo inverse and Gaussian measurement matrices we investigated the scaling of the rate estimation error with the number of measurements.

The measurement protocol is based on a few simplifications which render the direct application in practical systems rather difficult. For example, the assumption of perfect time and frequency synchronization is hard (if not impossible) to achieve in distributed networks with a huge number of devices. To this end, the analog coding developed in [GS13] can be used to relax the requirements on the synchronization.

Future work may also include the exploration of different linear and non-linear decoding functions. To this end, Theorem 5.8 provides a good basis to evaluate different linear decoding functions. For non-linear decoding functions applications of matrix recovery and other compressed sensing related approaches are a promising research direction. Extensions to other network architectures are another prospective direction. Coordinated transmission techniques where groups of devices (or antennas) are jointly transmitting with beamforming vectors $\boldsymbol{w}$ given by some finite codebook can be analyzed with the proposed framework by estimating $|\langle \boldsymbol{h}_i, \boldsymbol{w} \rangle|$.

5.6 Proofs

5.6.1 Proof of Lemma 5.3

Proof. Since $x_{i,j} = |h_{i,j}|^2$ the rate gap Δ_i can rewritten as

$$\begin{aligned}
\Delta_i &= \left| \log\left(1 + \frac{p_j x_{i,j}}{1 + \sum_{l\in\mathcal{S}\setminus\{i\}} p_l x_{i,l}}\right) - \log\left(1 + \frac{p_j \hat{x}_{i,j}}{1 + \sum_{l\in\mathcal{S}\setminus\{i\}} p_l \hat{x}_{i,l}}\right)\right| \\
&= \left| \log\left(\frac{1 + \sum_{l\in\mathcal{S}} p_l x_{i,l}}{1 + \sum_{l\in\mathcal{S}} p_l \hat{x}_{i,l}}\right) + \log\left(\frac{1 + \sum_{l\in\mathcal{S}\setminus\{i\}} p_l \hat{x}_{i,l}}{1 + \sum_{l\in\mathcal{S}\setminus\{i\}} p_l x_{i,l}}\right)\right| \\
&= \left| \log\left(1 + \frac{\sum_{l\in\mathcal{S}} p_l (x_{i,l} - \hat{x}_{i,l})}{1 + \sum_{l\in\mathcal{S}} p_l \hat{x}_{i,l}}\right) + \log\left(1 + \frac{\sum_{l\in\mathcal{S}\setminus\{i\}} p_l (\hat{x}_{i,l} - x_{i,l})}{1 + \sum_{l\in\mathcal{S}\setminus\{i\}} p_l x_{i,l}}\right)\right| \\
&\leq \left| \log\left(1 + \frac{\sum_{l\in\mathcal{S}} p_l (x_{i,l} - \hat{x}_{i,l})}{1 + \sum_{l\in\mathcal{S}} p_l \hat{x}_{i,l}}\right)\right| + \left|\log\left(1 + \frac{\sum_{l\in\mathcal{S}\setminus\{i\}} p_l (\hat{x}_{i,l} - x_{i,l})}{1 + \sum_{l\in\mathcal{S}\setminus\{i\}} p_l x_{i,l}}\right)\right| \\
&\leq 2\log\left(1 + \sum_{l\in\mathcal{S}} p_l |x_{i,l} - \hat{x}_{i,l}|\right),
\end{aligned}$$

where the first inequality follows from the triangle inequality and the second inequality follows from Jensen's inequality and the fact that the denominators are positive. Since, $\log(1+x) \leq x$ is a good bound for small positive $x \geq 0$ and by assumption $p_j \leq P$, for all j, we obtain the first claim

$$\Delta_i \leq 2P \sum_{l\in\mathcal{S}} |x_{i,l} - \hat{x}_{i,l}|.$$

□

5.6.2 Proof of Corollary 5.7

Proof. Using Lemma 5.3, the Cauchy-Schwarz inequality and the reverse triangle inequality we get

$$\begin{aligned}
\Delta_i &\leq 2P \sum_{j\in\mathcal{S}} |x_{i,j} - \hat{x}_{i,j}| \\
&\leq 2P \sum_{j\in\mathcal{N}} |(|h_{i,j}| - |\hat{h}_{i,j}|)(|h_{i,j}| + |\hat{h}_{i,j}|)| \\
&\leq 2P \left\|\boldsymbol{h}_i - \hat{\boldsymbol{h}}_i\right\|_2 \left\||\boldsymbol{h}_i| + |\hat{\boldsymbol{h}}_i|\right\|_2 \\
&\leq 2P \left\|\boldsymbol{h}_i - \hat{\boldsymbol{h}}_i|\right\|_2 \left(2\|\boldsymbol{h}_i\|_2 + \left\|\boldsymbol{h}_i - \hat{\boldsymbol{h}}_{\boldsymbol{i}}\right\|_2\right).
\end{aligned} \tag{5.13}$$

By assumption $M \geq 2C_1^2\delta^{-2}\left(k\ln(eN/k)+\ln(2\varepsilon^{-1})\right)$, with $\delta < 1/3$, such that $\boldsymbol{\Phi}$ satisfies the RIP with probability at least $1-\varepsilon$. Hence, we can use Theorem 5.6 and plug (5.10) in (5.13). Finally, defining $q(\boldsymbol{h}_i,\xi) = C_2(\delta_k)\frac{\sigma_k(\boldsymbol{h}_i)_1}{\sqrt{k}} + 2C_3(\delta_k)\xi$ the claim follows. □

5.6.3 Proof of Theorem 5.8

We develop the prove Theorem 5.8 in several steps.

Lemma 5.14. *Let X and Y be two non-negative real random variables. If $f : \mathbb{R}\times\mathbb{R}\to\mathbb{R}$ is monotonically increasing and $y_0 > 0$ is a positive constant, then*

$$Pr\left(f(X,Y) > \varepsilon\right) \leq \min_{y_0\geq 0} Pr\left(f(X,y_0) > \varepsilon\right) + Pr\left(Y > y_0\right).$$

Proof. First assume that the random variable Y is bounded by $Y > y_0$. In this case the claim is trivially true, since $\Pr\left(Y > y_0\right) = 1$. Therefore, assume that $\Pr\left(Y \leq y_0\right) > 0$. For any arbitrary but fixed $y_0 \geq 0$ we have,

$$\begin{aligned}
\Pr\left(f(X,Y) > \varepsilon\right) &= 1 - \Pr\left(f(X,Y) \leq \varepsilon | Y \leq y_0\right) - \Pr\left(f(X,Y) \leq \varepsilon | Y > y_0\right) \\
&\leq 1 - \Pr\left(f(X,Y) \leq \varepsilon | Y \leq y_0\right) \\
&\leq 1 - \Pr\left(f(X,y_0) \leq \varepsilon | Y \leq y_0\right) \\
&= 1 - \frac{\Pr\left(\{f(X,y_0) \leq \varepsilon\} \cap \{Y \leq y_0\}\right)}{\Pr\left(Y \leq y_0\right)} \\
&= 1 - \frac{1 - \Pr\left(\{f(X,y_0) > \varepsilon\} \cup \{Y > y_0\}\right)}{\Pr\left(Y \leq y_0\right)} \qquad (5.14) \\
&\leq 1 - \frac{1 - \Pr\left(f(X,y_0) > \varepsilon\right) - \Pr\left(Y > y_0\right)}{\Pr\left(Y \leq y_0\right)} \qquad (5.15) \\
&\leq \Pr\left(f(X,y_0) > \varepsilon\right) + \Pr\left(Y > y_0\right),
\end{aligned}$$

where (5.14) follows from De Morgan's law and (5.15) follows from the union bound. □

Lemma 5.15. *Let $\mathcal{V} = \{\boldsymbol{v}_1,\ldots,\boldsymbol{v}_n\} \subset \mathbb{S}^{N-1}$ be an arbitrary but fixed set of mutually orthogonal vectors ($n \leq N$), $\boldsymbol{\Psi} = \boldsymbol{\Phi}^H\boldsymbol{A} \in \mathbb{C}^{N\times M}$ and $\boldsymbol{A} \in \mathbb{C}^{M\times M}$ be a positive semi-definite matrix. If $\boldsymbol{w} = \boldsymbol{\Phi}\boldsymbol{u} + \boldsymbol{e}$ and $\boldsymbol{\Phi}$ is a $M \times N$ random matrix that satisfies the concentration inequality* (5.5) *and $0 \leq \delta < 1$, then for any fixed $\boldsymbol{u} \in \mathbb{C}^N$ and $\boldsymbol{e} \in \mathbb{C}^M$*

$$\begin{aligned}
Pr\left(\left|\sum_{i=1}^{n} |\langle \boldsymbol{u},\boldsymbol{v}_i\rangle|^2 - |\langle \boldsymbol{\Psi}\boldsymbol{w},\boldsymbol{v}_i\rangle|^2\right| > 4\|\boldsymbol{u}\|_2^2\sqrt{n}(1+u_0)\varepsilon + e_0\right) &\leq 4n\exp(-\gamma(\varepsilon)) \\
&+ Pr(s_{\max}(\boldsymbol{\Psi}\boldsymbol{\Phi}) > u_0) + Pr(\|\boldsymbol{\Psi}\boldsymbol{e}\|_2(\|\boldsymbol{\Psi}\boldsymbol{e}\|_2 + 2\|\boldsymbol{\Psi}\boldsymbol{\Phi}\boldsymbol{u}\|_2) > e_0)
\end{aligned}$$

holds, where $\gamma(\varepsilon)$ depends on the distribution of $\boldsymbol{\Phi}$ and $u_0 \geq 0$ is a positive constant.

Proof. Rewriting, using the triangle inequality, Parseval's identity and the Cauchy-Schwartz inequality we get

$$\begin{aligned}
&\sum_{i=1}^{n} \left| |\langle \boldsymbol{u}, \boldsymbol{v}_i \rangle|^2 - |\langle \boldsymbol{\Psi}(\boldsymbol{\Phi}\boldsymbol{u} + \boldsymbol{e}), \boldsymbol{v}_i \rangle|^2 \right| \\
&= \sum_{i=1}^{n} \left| |\langle \boldsymbol{u}, \boldsymbol{v}_i \rangle|^2 - |\langle \boldsymbol{\Psi}\boldsymbol{\Phi}\boldsymbol{u}, \boldsymbol{v}_i \rangle|^2 - |\langle \boldsymbol{\Psi}\boldsymbol{e}, \boldsymbol{v}_i \rangle|^2 - 2\Re\left(\langle \boldsymbol{\Psi}\boldsymbol{e}, \boldsymbol{v}_i \rangle \overline{\langle \boldsymbol{\Psi}\boldsymbol{\Phi}\boldsymbol{u}, \boldsymbol{v}_i \rangle} \right) \right| \\
&\leq \sum_{i=1}^{n} \left| |\langle \boldsymbol{u}, \boldsymbol{v}_i \rangle|^2 - |\langle \boldsymbol{\Psi}\boldsymbol{\Phi}\boldsymbol{u}, \boldsymbol{v}_i \rangle|^2 \right| + \sum_{i=1}^{n} |\langle \boldsymbol{\Psi}\boldsymbol{e}, \boldsymbol{v}_i \rangle|^2 + 2|\langle \boldsymbol{\Psi}\boldsymbol{e}, \boldsymbol{v}_i \rangle \langle \boldsymbol{\Psi}\boldsymbol{\Phi}\boldsymbol{u}, \boldsymbol{v}_i \rangle| \\
&\leq \sum_{i=1}^{n} \left| |\langle \boldsymbol{u}, \boldsymbol{v}_i \rangle|^2 - |\langle \boldsymbol{\Psi}\boldsymbol{\Phi}\boldsymbol{u}, \boldsymbol{v}_i \rangle|^2 \right| + \sum_{i=1}^{n} |\langle \boldsymbol{\Psi}\boldsymbol{e}, \boldsymbol{v}_i \rangle|^2 + 2\sqrt{\sum_{i=1}^{n} |\langle \boldsymbol{\Psi}\boldsymbol{e}, \boldsymbol{v}_i \rangle|^2 \sum_{i=1}^{n} |\langle \boldsymbol{\Psi}\boldsymbol{\Phi}\boldsymbol{u}, \boldsymbol{v}_i \rangle|^2} \\
&\leq \sum_{i=1}^{n} \left| |\langle \boldsymbol{u}, \boldsymbol{v}_i \rangle|^2 - |\langle \boldsymbol{\Psi}\boldsymbol{\Phi}\boldsymbol{u}, \boldsymbol{v}_i \rangle|^2 \right| + \|\boldsymbol{\Psi}\boldsymbol{e}\|_2 (\|\boldsymbol{\Psi}\boldsymbol{e}\|_2 + 2\|\boldsymbol{\Psi}\boldsymbol{\Phi}\boldsymbol{u}\|_2).
\end{aligned}$$

Applying Lemma 5.14 we get for any $0 \leq e_0$

$$\begin{aligned}
&\Pr\left(\sum_{i=1}^{n} \left| |\langle \boldsymbol{u}, \boldsymbol{v}_i \rangle|^2 - |\langle \boldsymbol{\Psi}\boldsymbol{w}, \boldsymbol{v}_i \rangle|^2 \right| > \varepsilon' \right) \\
&\leq \Pr\left(\sum_{i=1}^{n} \left| |\langle \boldsymbol{u}, \boldsymbol{v}_i \rangle|^2 - |\langle \boldsymbol{\Psi}\boldsymbol{\Phi}\boldsymbol{u}, \boldsymbol{v}_i \rangle|^2 \right| + e_0 > \varepsilon' \right) + \Pr\left(\|\boldsymbol{\Psi}\boldsymbol{e}\|_2 (\|\boldsymbol{\Psi}\boldsymbol{e}\|_2 + 2\|\boldsymbol{\Psi}\boldsymbol{\Phi}\boldsymbol{u}\|_2) > e_0 \right).
\end{aligned} \tag{5.16}$$

Hence, we are left with the first term. If $\|\boldsymbol{u}\|_2 = 0$, the claim is trivially true. Therefore assume $\|\boldsymbol{u}\|_2 > 0$ and define $\bar{\boldsymbol{u}} := \boldsymbol{u}/\|\boldsymbol{u}\|_2$. We start by deriving the following bound

$$\begin{aligned}
\sum_{i=1}^{n} \left| |\langle \boldsymbol{u}, \boldsymbol{v}_i \rangle|^2 - |\langle \boldsymbol{\Psi}\boldsymbol{\Phi}\boldsymbol{u}, \boldsymbol{v}_i \rangle|^2 \right| &= \|\boldsymbol{u}\|_2^2 \sum_{i=1}^{n} \left| \left(|\langle \bar{\boldsymbol{u}}, \boldsymbol{v}_i \rangle| - |\langle \boldsymbol{\Psi}\boldsymbol{\Phi}\bar{\boldsymbol{u}}, \boldsymbol{v}_i \rangle| \right) \left(|\langle \bar{\boldsymbol{u}}, \boldsymbol{v}_i \rangle| + |\langle \boldsymbol{\Psi}\boldsymbol{\Phi}\bar{\boldsymbol{u}}, \boldsymbol{v}_i \rangle| \right) \right| \\
&\leq \|\boldsymbol{u}\|_2^2 \max_{i=1,\ldots,n} \left| |\langle \bar{\boldsymbol{u}}, \boldsymbol{v}_i \rangle| - |\langle \boldsymbol{\Psi}\boldsymbol{\Phi}\bar{\boldsymbol{u}}, \boldsymbol{v}_i \rangle| \right| \sum_{i=1}^{n} \left(|\langle \bar{\boldsymbol{u}}, \boldsymbol{v}_i \rangle| + |\langle \boldsymbol{\Psi}\boldsymbol{\Phi}\bar{\boldsymbol{u}}, \boldsymbol{v}_i \rangle| \right)
\end{aligned} \tag{5.17}$$

Next, we bound the sum and the maximum independently. For the sum we have

$$\sum_{i=1}^{n}\left(|\langle\bar{\boldsymbol{u}},\boldsymbol{v}_i\rangle|+|\langle\boldsymbol{\Psi}\boldsymbol{\Phi}\bar{\boldsymbol{u}},\boldsymbol{v}_i\rangle|\right)\leq\left(\sqrt{n\sum_{i=1}^{n}|\langle\bar{\boldsymbol{u}},\boldsymbol{v}_i\rangle|^2}+\sqrt{n\sum_{i=1}^{n}|\langle\boldsymbol{\Psi}\boldsymbol{\Phi}\bar{\boldsymbol{u}},\boldsymbol{v}_i\rangle|^2}\right) \tag{5.18}$$

$$\leq\sqrt{n}\left(1+\|\boldsymbol{\Psi}\boldsymbol{\Phi}\bar{\boldsymbol{u}}\|_2\right) \tag{5.19}$$

where (5.18) follows from the Cauchy-Schwarz inequality and (5.19) follows from the Parseval's identity. By assumption $\boldsymbol{\Psi}=\boldsymbol{\Phi}^H\boldsymbol{A}=\boldsymbol{\Phi}^H\boldsymbol{A}^{1/2}\boldsymbol{A}^{1/2}$, where $\boldsymbol{A}^{1/2}$ is the principal square root of $\boldsymbol{A}$, therefore the maximum in (5.17) can be written as

$$\max_{i=1,\dots,n}\Big||\langle\bar{\boldsymbol{u}},\boldsymbol{v}_i\rangle|-|\langle\boldsymbol{\Psi}\boldsymbol{\Phi}\bar{\boldsymbol{u}},\boldsymbol{v}_i\rangle|\Big|=\max_{i=1,\dots,n}\Big||\langle\bar{\boldsymbol{u}},\boldsymbol{v}_i\rangle|-|\langle\boldsymbol{A}^{1/2}\boldsymbol{\Phi}\bar{\boldsymbol{u}},\boldsymbol{A}^{1/2}\boldsymbol{\Phi}\boldsymbol{v}_i\rangle|\Big|.$$

Thus, the polarization identity and the triangle inequality can be used to get,

$$\begin{aligned}
&\Big||\langle\bar{\boldsymbol{u}},\boldsymbol{v}_i\rangle|-|\langle\boldsymbol{A}^{1/2}\boldsymbol{\Phi}\bar{\boldsymbol{u}},\boldsymbol{A}^{1/2}\boldsymbol{\Phi}\boldsymbol{v}_i\rangle|\Big|\leq\Big|\langle\bar{\boldsymbol{u}},\boldsymbol{v}_i\rangle-\langle\boldsymbol{A}^{1/2}\boldsymbol{\Phi}\bar{\boldsymbol{u}},\boldsymbol{A}^{1/2}\boldsymbol{\Phi}\boldsymbol{v}_i\rangle\Big|\\
&=\frac{1}{4}\Big|\|\bar{\boldsymbol{u}}+\boldsymbol{v}_i\|_2^2-\|\bar{\boldsymbol{u}}-\boldsymbol{v}_i\|_2^2+i\|\bar{\boldsymbol{u}}+i\boldsymbol{v}_i\|_2^2-i\|\bar{\boldsymbol{u}}-i\boldsymbol{v}_i\|_2^2\\
&\quad-\|\boldsymbol{A}^{1/2}\boldsymbol{\Phi}(\bar{\boldsymbol{u}}+\boldsymbol{v}_i)\|_2^2+\|\boldsymbol{A}^{1/2}\boldsymbol{\Phi}(\bar{\boldsymbol{u}}-\boldsymbol{v}_i)\|_2^2-i\|\boldsymbol{A}^{1/2}\boldsymbol{\Phi}(\bar{\boldsymbol{u}}+i\boldsymbol{v}_i)\|_2^2+i\|\boldsymbol{A}^{1/2}\boldsymbol{\Phi}(\bar{\boldsymbol{u}}-i\boldsymbol{v}_i)\|_2^2\Big|\\
&\leq\frac{1}{4}\Big(\Big|\|\bar{\boldsymbol{u}}+\boldsymbol{v}_i\|_2^2-\|\boldsymbol{A}^{1/2}\boldsymbol{\Phi}(\bar{\boldsymbol{u}}+\boldsymbol{v}_i)\|_2^2\Big|+\Big|\|\boldsymbol{A}^{1/2}\boldsymbol{\Phi}(\bar{\boldsymbol{u}}-\boldsymbol{v}_i)\|_2^2-\|\bar{\boldsymbol{u}}-\boldsymbol{v}_i\|_2^2\Big|\\
&\quad+\Big|i\|\bar{\boldsymbol{u}}+i\boldsymbol{v}_i\|_2^2-i\|\boldsymbol{A}^{1/2}\boldsymbol{\Phi}(\bar{\boldsymbol{u}}+i\boldsymbol{v}_i)\|_2^2\Big|+\Big|i\|\boldsymbol{A}^{1/2}\boldsymbol{\Phi}(\bar{\boldsymbol{u}}-i\boldsymbol{v}_i)\|_2^2-i\|\bar{\boldsymbol{u}}-i\boldsymbol{v}_i\|_2^2\Big|\Big)\\
&\leq\max\Big\{\Big|\|\bar{\boldsymbol{u}}+\boldsymbol{v}_i\|_2^2-\|\boldsymbol{A}^{1/2}\boldsymbol{\Phi}(\bar{\boldsymbol{u}}+\boldsymbol{v}_i)\|_2^2\Big|,\Big|\|\boldsymbol{A}^{1/2}\boldsymbol{\Phi}(\bar{\boldsymbol{u}}-\boldsymbol{v}_i)\|_2^2-\|\bar{\boldsymbol{u}}-\boldsymbol{v}_i\|_2^2\Big|,\\
&\qquad\Big|i\|\bar{\boldsymbol{u}}+i\boldsymbol{v}_i\|_2^2-i\|\boldsymbol{A}^{1/2}\boldsymbol{\Phi}(\bar{\boldsymbol{u}}+i\boldsymbol{v}_i)\|_2^2\Big|,\Big|i\|\boldsymbol{A}^{1/2}\boldsymbol{\Phi}(\bar{\boldsymbol{u}}-i\boldsymbol{v}_i)\|_2^2-i\|\bar{\boldsymbol{u}}-i\boldsymbol{v}_i\|_2^2\Big|\Big\}\\
&=:M_i,
\end{aligned}$$

for any i. Therefore, the maximum can be bounded from above by

$$\max_{i=1,\dots,n}\Big||\langle\bar{\boldsymbol{u}},\boldsymbol{v}_i\rangle|-|\langle\boldsymbol{\Psi}\boldsymbol{\Phi}\bar{\boldsymbol{u}},\boldsymbol{v}_i\rangle|\Big|\leq\max_{i=1,\dots,n}M_i \tag{5.20}$$

Substituting the bounds (5.20) and (5.19) in (5.17), taking probability with respect to $\boldsymbol{\Phi}$

and applying Lemma 5.14,

$$\Pr\left(\sum_{i=1}^{n}\left||\langle \boldsymbol{u},\boldsymbol{v}_i\rangle|^2-|\langle \boldsymbol{\Psi\Phi u},\boldsymbol{v}_i\rangle|^2\right|>\varepsilon'-e_0\right)\leq \Pr\left(\|\boldsymbol{u}\|_2^2\sqrt{n}\,(1+\|\boldsymbol{\Psi\Phi}\bar{\boldsymbol{u}}\|_2)\max_{i=1,\dots,n}M_i>\varepsilon'-e_0\right)$$
$$\leq \min_{u_0\geq 0}\Pr\left(\|\boldsymbol{u}\|_2^2\sqrt{n}\,(1+u_0)\max_{i=1,\dots,n}M_i>\varepsilon'-e_0\right)+\Pr\left(\|\boldsymbol{\Psi\Phi}\bar{\boldsymbol{u}}\|_2>u_0\right).$$

Using the union bound over all $4n$ terms in $\max_{i=1,\dots,n}M_i$ we get

$$\Pr\left(\sum_{i=1}^{n}\left||\langle \boldsymbol{u},\boldsymbol{v}_i\rangle|^2-|\langle \boldsymbol{\Psi\Phi u},\boldsymbol{v}_i\rangle|^2\right|>\varepsilon'-e_0\right)$$
$$\leq \min_{u_0\geq 0}4n\Pr\left(\|\boldsymbol{u}\|_2^2\sqrt{n}\,(1+u_0)\left|\|\bar{\boldsymbol{u}}+\boldsymbol{v}_i\|_2^2-\|\boldsymbol{A}^{1/2}\boldsymbol{\Phi}(\bar{\boldsymbol{u}}+\boldsymbol{v}_i)\|_2^2\right|>\varepsilon'-e_0\right)+\Pr\left(\|\boldsymbol{\Psi\Phi}\bar{\boldsymbol{u}}\|_2>u_0\right).$$

for an arbitrary but fixed $i\in[1,n]$. Rearranging and using the concentration inequality (5.5) we obtain,

$$\Pr\left(\sum_{i=1}^{n}\left||\langle \boldsymbol{u},\boldsymbol{v}_i\rangle|^2-|\langle \boldsymbol{\Psi\Phi u},\boldsymbol{v}_i\rangle|^2\right|>\varepsilon'-e_0\right)$$
$$\leq \min_{u_0\geq 0}4n\Pr\left(\left|\|\bar{\boldsymbol{u}}+\boldsymbol{v}_i\|_2^2-\|\boldsymbol{A}^{1/2}\boldsymbol{\Phi}(\bar{\boldsymbol{u}}+\boldsymbol{v}_i)\|_2^2\right|>\frac{\varepsilon'-e_0}{\|\boldsymbol{u}\|_2^2\sqrt{n}\,(1+u_0)}\right)+\Pr\left(\|\boldsymbol{\Psi\Phi}\bar{\boldsymbol{u}}\|_2>u_0\right)$$

$$\leq \min_{u_0\geq 0}4n\exp\left(-\gamma\left(\frac{\varepsilon'-e_0}{\|\bar{\boldsymbol{u}}+\boldsymbol{v}_i\|_2^2\|\boldsymbol{u}\|_2^2\sqrt{n}(1+u_0)}\right)\right)+\Pr\left(\|\boldsymbol{\Psi\Phi}\bar{\boldsymbol{u}}\|_2>u_0\right)$$
$$\leq \min_{u_0\geq 0}4n\exp\left(-\gamma\left(\frac{\varepsilon'-e_0}{4\|\boldsymbol{u}\|_2^2\sqrt{n}(1+u_0)}\right)\right)+\Pr\left(\|\boldsymbol{\Psi\Phi}\bar{\boldsymbol{u}}\|_2>u_0\right).$$

The last inequality holds since $\|\bar{\boldsymbol{u}}+\boldsymbol{v}_i\|_2^2\leq 4$. Since $\Pr\left(\|\boldsymbol{\Psi\Phi}\bar{\boldsymbol{u}}\|_2>u_0\right)\leq\Pr\left(s_{\max}(\boldsymbol{\Psi\Phi})>u_0\right)$ the claim follows from the last equation and (5.16), with $\varepsilon'=\varepsilon 4\|\boldsymbol{u}\|_2^2\sqrt{n}(1+u_0)+e_0$. □

Now we are ready to prove Theorem 5.8.

Proof of Theorem 5.8. Since $|h_{i,j}|^2=\langle \boldsymbol{h}_i,\boldsymbol{e}_j\rangle|^2$ and $|\hat{h}_{i,j}|^2=|\langle\hat{\boldsymbol{h}}_i,\boldsymbol{e}_j\rangle|^2$ we can apply Lemma 5.15 and Lemma 5.3, and obtain

$$\Pr\left(\Delta_i>\varepsilon 8P\|\boldsymbol{h}_i\|_2^2\sqrt{n}(1+u_0)+2Pe_0\right)\leq 4n\exp\left(-\gamma\left(\varepsilon\right)\right)$$
$$+\Pr\left(s_{\max}(\boldsymbol{\Psi\Phi})>u_0\right)+\Pr\left(\|\boldsymbol{\Psi e}\|_2(\|\boldsymbol{\Psi e}\|_2+2\|\boldsymbol{\Psi\Phi h}_i\|_2)>e_0\right).$$

Using the union bound over all $i \in \mathcal{N}$ we get

$$\Pr\left(\exists i \in \mathcal{N} : \Delta_i > \varepsilon 8P\|\boldsymbol{h}_i\|_2^2\sqrt{n}(1+u_0) + 2Pe_0\right) \leq 4nN\exp\left(-\gamma\left(\varepsilon\right)\right) + N\Pr\left(s_{\max}(\boldsymbol{\Psi}\boldsymbol{\Phi}) > u_0\right) + \sum_{i\in\mathcal{N}} \Pr\left(\|\boldsymbol{\Psi}\boldsymbol{e}\|_2(\|\boldsymbol{\Psi}\boldsymbol{e}\|_2 + 2\|\boldsymbol{\Psi}\boldsymbol{\Phi}\boldsymbol{h}_i\|_2) > e_0\right).$$

Setting $c_1 = 8P\|\boldsymbol{h}_i\|_2^2\sqrt{n}$ and $c_2 = 2P$ the claim follows. □

5.6.4 Proof of Corollary 5.9

Proof. For an arbitrary but fixed $\boldsymbol{h}_i$. Setting $e_0 = 0$, we have

$$\Pr\left(\|\boldsymbol{\Psi}\boldsymbol{e}\|_2(\|\boldsymbol{\Psi}\boldsymbol{e}\|_2 + 2\|\boldsymbol{\Psi}\boldsymbol{\Phi}\boldsymbol{u}\|_2) > e_0\right) = 0.$$

Since $\boldsymbol{\Phi}^+\boldsymbol{\Phi}$ is a projector (i.e. Hermitian and idempotent) $s_{\max}(\boldsymbol{\Phi}^+\boldsymbol{\Phi}) = 1$, and therefore we can set $u_0 = 1$ and obtain $\Pr\left(s_{\max}(\boldsymbol{\Psi}\boldsymbol{\Phi}) > 1\right) = 0$. Hence, using (5.7) we get from Theorem 5.8

$$\Pr\left(\exists i \in \mathcal{N} : \Delta_i > 16P\|\boldsymbol{h}_i\|_2^2\sqrt{n}\varepsilon')\right) \leq 4nN\exp\left(-M\varepsilon'^2/\kappa\right),$$

with $\kappa = \frac{2}{1-\ln(2)}$. Since $\boldsymbol{h}_i$ is also random we can use Lemma 5.14 and get

$$\Pr\left(\exists i \in \mathcal{N} : \Delta_i > 16Ph_0\sqrt{n}\varepsilon')\right) \leq 4nN\exp\left(-M\varepsilon'^2/\kappa\right) + \Pr\left(\|\boldsymbol{h}_i\|_2^2 > h_0\right).$$

By assumption we have $\mathbb{E}\left[\|\boldsymbol{h}_i\|_2^2\right] = k$. Thus, (5.8) gives,

$$\Pr\left(\|\boldsymbol{h}_i\|_2^2 > h_0\right) = \Pr\left(\|\boldsymbol{h}_i\|_2^2 > t + k\right) \leq \exp(-t^2/2).$$

Hence, if we set $h_0 = t + k$ and $t = \sqrt{2M\varepsilon'^2/\kappa}$,

$$\Pr\left(\exists i \in \mathcal{N} : \Delta_i > 16P\sqrt{n}(\sqrt{2M\varepsilon'^2/\kappa} + k)\varepsilon')\right) \leq (4nN+1)\exp\left(-M\varepsilon'^2/\kappa\right).$$

Finally, setting $\varepsilon = (4nN+1)\exp\left(-M\varepsilon'^2/\kappa\right)$ the claim follows. □

Publication List

[1] Jan Schreck, Peter Jung, Gerhard Wunder, Michael Ohm, and Hans-Peter Mayer. Limited feedback in multiuser MIMO-OFDM systems based on rate approximation. In *IEEE Global Telecommunications Conference (GLOBECOM)*, pages 1–6, November 2009.

[2] Jan Schreck, Peter Jung, and Gerhard Wunder. Approximation of multiuser rates in MIMO-OFDM downlink systems. In *14th International OFDM-Workshop*, 2009.

[3] Gerhard Wunder, Jan Schreck, Peter Jung, Howard Huang, and Reinaldo Valenzuela. A new robust transmission technique for the multiuser MIMO downlink. In *IEEE International Symposium on Information Theory (ISIT)*, pages 2123–2127, 2010.

[4] Gerhard Wunder and Jan Schreck. A robust and efficient transmission technique for the LTE downlink. In *44th Annual Asilomar Conference on Signals, Systems, and Computers*, 2010.

[5] Gerhard Wunder, Jan Schreck, Peter Jung, Howard Huang, and Reinaldo Valenzuela. Rate approximation: A new paradigm for multiuser MIMO downlink communications. In *IEEE International Conference on Communications (ICC)*, 2010.

[6] Gerhard Wunder, Peter Jung, and Jan Schreck. Multiuser MIMO systems using codebook tailored limited feedback protocol. In *IEEE ITG Workshop on Smart Antennas (WSA)*, March 2012.

[7] Gerhard Wunder, Jan Schreck, and Peter Jung. Nearly doubling the throughput of multiuser MIMO systems using codebook tailored limited feedback protocol. *IEEE Transactions on Wireless Communications*, 11(11):3921–3931, 2012.

[8] Peter Jung, Jan Schreck, Michael Ohm, and Gerhard Wunder. Method for resource allocation, radio communication system, base station, and mobile station thereof, September 2011. US Patent Application 13/131,729.

[9] Peter Jung, Jan Schreck, and Gerhard Wunder. Method for resource allocation in a radio communication system, October 2011. European Patent Specification EP2378688A1.

[10] Gerhard Wunder and Jan Schreck. Feedback information transmission and scheduling in a radio access network, November 2012. EP Patent Application EP20110305647.

[11] Jan Schreck and Gerhard Wunder. Iterative interference alignment for cellular systems. In *2011 International ITG Workshop on Smart Antennas (WSA)*, pages 1–8, February 2011.

[12] Jan Schreck and Gerhard Wunder. Distributed interference alignment in cellular systems: Analysis and algorithms. In *IEEE European Wireless 2011*, pages 1–8, Vienna, 2011.

[13] Jan Schreck and Gerhard Wunder. Iterative interference alignment for cellular systems with user selection. In *IEEE International Conference on Acoustics, Speech and Signal Processing (ICASSP)*, pages 1–4, 2012.

[14] Jan Schreck and Gerhard Wunder. Interference alignment over limited dimensions for cellular networks: Feasibility and algorithms. In *2012 International ITG Workshop on Smart Antennas (WSA)*, pages 352–358, March 2012.

[15] Gerhard Wunder, Supreeth Raghuprakash, Peter Jung, and Jan Schreck. Multi-user MIMO multi-cell systems: Finite SNR rate loss analysis. In *IEEE ITG Workshop on Smart Antennas (WSA)*, 2013.

[16] Jan Schreck, Gerhard Wunder, and Peter Jung. Distributed interference alignment with limited feedback for cellular networks. In *International Workshop on Emerging Technologies for LTE-Advanced and Beyond-4G at IEEE Globecom*, pages 1–6, Atlanta, December 2013.

[17] Jan Schreck, Gerhard Wunder, and Perter Jung. Robust iterative interference alignment for cellular networks with limited feedback. *IEEE Transactions on Wireless Communications*, 14(2):882–894, Feb 2015.

[18] Jan Schreck, Peter Jung, and Sławomir Stańczak. On channel state feedback for two-hop networks based on low rank matrix recovery. In *IEEE International Conference on Communications (ICC)*, pages 5–10, 2013.

[19] Jan Schreck, Peter Jung, and Sławomir Stańczak. Compressive rate estimation with applications to device-to-device communications. *IEEE Transactions on Wireless Communications*, 2014. submitted for publication, `http://arxiv.org/abs/1504.07365`.

[20] Jan Schreck, Peter Jung, and Gerhard Wunder. Compressed sensing based channel state feedback for cooperating MIMO-OFDM systems. In *16th International OFDM Workshop*, pages 1–5, Hamburg, Germany, August 2011.

[21] Jan Schreck and Sławomir Stanczak, Stańczak. On SINR balancing for a two-hop downlink channel. In *Asilomar Conference on Signals, Systems, and Computers*, pages 1–5, November 2012.

Bibliography

[3GP07] 3GPP R1-073937. Comparison aspects of fixed and adaptive beamforming for LTE downlink. In *3GPP TSG RAN WG1*, number R1-073937. Alcatel-Lucent, 2007.

[3GP09a] 3GPP TR 36.814. Further advancements for E-UTRA physical layer aspects. Evolved Universal Terrestrial Radio Access (E-UTRA), 2009.

[3GP09b] 3GPP TS 36.201. LTE physical layer - general description, 2009.

[3GP13] 3GPP. 3rd Generation Partnership Project; Technical Specification Group Services and System Aspects; Feasibility study for Proximity Services (ProSe) (Release 12). Technical report, 3GPP TR 22.803, 2013.

[3GP14] 3GPP. 3rd Generation Partnership Project; Technical Specification Group Services and System Aspects; Study on architecture enhancements to support Proximity-based Services (ProSe). Technical report, 3GPP TR 23.703, 2014.

[Ala98] S. Alamouti. A simple transmit diversity technique for wireless communications. *IEEE Journal on Selected Areas in Communications*, 16(8):1451–1458, Oct 1998.

[AYL07] C. Au-Yeung and D. Love. On the performance of random vector quantization limited feedback beamforming in a MISO system. *IEEE Transactions on Wireless Communications*, 6(2):458–462, February 2007.

[BÖ4] K. Böröczky. *Finite packing and covering.* Cambridge University Press, 2004.

[BCG11] S. Becker, E. Candes, and M. Grant. Tfocs: Flexible first-order methods for rank minimization. In *Low-rank Matrix Optimization Symposium, SIAM Conf. on Optimization*, 2011.

[BCP00] N. Bambos, S. C. Chen, and G. J. Pottie. Channel access algorithms with active link protection for wireless communication networks with power control. *Networking, IEEE/ACM Transactions on*, 8(5):583–597, 2000.

[BCT11] G. Bresler, D. Cartwright, and D. Tse. Feasibility of interference alignment for the MIMO interference channel: The symmetric square case. In *2011 IEEE Information Theory Workshop*, pages 447–451. IEEE, October 2011.

[BCT14] G. Bresler, D. Cartwright, and D. Tse. Feasibility of interference alignment for the MIMO interference channel. *IEEE Transactions on Information Theory*, 60(9):5573–5586, 2014.

[BSM+05] D. S. Baum, J. Salo, M. Milojevic, P. Kyösti, and J. Hansen. MATLAB implementation of the interim channel model for beyond-3g systems (SCME). `http://radio.tkk.fi/en/research/rf_applications_in_mobile_communication/radio_channel/scm.html`, May 2005.

[Cas96] M. Castells. *The information age: Economy, society, and culture. Volume I: The rise of the network society.* Blackwell, 1996.

[Cis14] Cisco. Cisco visual networking index: Global mobile data traffic forecast update, 2013 – 2018. Technical report, Cisco, 2014.

[CJ08] V. R. Cadambe and S. A. Jafar. Interference alignment and degrees of freedom of the K-user interference channel. *IEEE Transactions on Information Theory*, 54(8):3425–3441, August 2008.

[CJ09] V. R. Cadambe and S. A. Jafar. Interference alignment and the degrees of freedom of wireless X networks. *IEEE Transactions on Information Theory*, 55(9):3893–3908, September 2009.

[CJKR10] G. Caire, N. Jindal, M. Kobayashi, and N. Ravindran. Multiuser MIMO achievable rates with downlink training and channel state feedback. *IEEE Transactions on Information Theory*, 56(6):2845–2866, June 2010.

[CP11] E. Candès and Y. Plan. A probabilistic and ripless theory of compressed sensing. *Information Theory, IEEE Transactions on*, 57(11):7235–7254, 2011.

[CR07] E. Candès and J. Romberg. Sparsity and incoherence in compressive sampling. *Inverse Problems*, 23(3):969–985, June 2007.

[CRP10] G. Caire, S. A. Ramprashad, and H. Papadopoulos. Rethinking network MIMO: Cost of CSIT, performance analysis, and architecture comparisons. In *Information Theory and Applications Workshop (ITA), 2010*, pages 1–10, Jan 2010.

[CRT06] E. J. Candes, J. K. Romberg, and T. Tao. Stable signal recovery from incomplete and inaccurate measurements. *Communications on pure and applied mathematics*, 59(8):1207–1223, 2006.

[CS03] G. Caire and S. Shamai. On the achievable throughput of a multiantenna gaussian broadcast channel. *Information Theory, IEEE Transactions on*, 49(7):1691–1706, July 2003.

[CZ13] T. T. Cai and A. Zhang. Sharp RIP bound for sparse signal and low-rank matrix recovery. *Applied and Computational Harmonic Analysis*, 35(1):74–93, July 2013.

[Dav11] M. Davenport. Concentration of measure for sub-gaussian random variables. *OpenStax CNX*, pages 1–5, 2011.

[DBWB10] M. Davenport, P. Boufounos, M. Wakin, and R. Baraniuk. Signal processing with compressive measurements. *Selected Topics in Signal Processing, IEEE Journal of*, 4(2):445–460, April 2010.

[dFKSG07] R. de Francisco, M. Kountouris, D. T. M. Slock, and D. Gesbert. Orthogonal linear beamforming in MIMO broadcast channels. In *2007 IEEE Wireless Communications and Networking Conference*, pages 1210–1215, March 2007.

[dKG12] P. de Kerret and D. Gesbert. Degrees of freedom of the network MIMO channel with distributed CSI. *IEEE Transactions on Information Theory*, 58(11):6806–6824, 2012.

[DLZ07] P. Ding, D. J. Love, and M. D. Zoltowski. Multiple antenna broadcast channels with shape feedback and limited feedback. *IEEE Transactions on Signal Processing*, 55(7):3417–3428, July 2007.

[Dol46] C. Dolph. A current distribution for broadside arrays which optimizes the relationship between beam width and side-lobe level. *Proceedings of the IRE*, 34(6):335–348, 1946.

[Don06] D. Donoho. Compressed sensing. *IEEE Transactions on Information Theory*, 52(4):1289–1306, April 2006.

[DRW+09] K. Doppler, M. Rinne, C. Wijting, C. B. Riberio, and K. Hugl. D2D communications underlaying an LTE cellular network. *IEEE Communications Magazine*, 7(12):42–49, December 2009.

[DS04] G. Dimic and N. Sidropoulos. Low-complexity downlink beamforming for maximum sum capacity. In *IEEE International Conference on Acoustics, Speech, and Signal Processing*, volume 4, pages iv–701–iv–704 vol.4, May 2004.

[DS05] G. Dimic and N. Sidiropoulos. On downlink beamforming with greedy user selection: Performance analysis and a simple new algorithm. *IEEE Transactions on Signal Processing*, 53(10):3857–3868, October 2005.

[DWB06] M. A. Davenport, M. B. Wakin, and R. G. Baraniuk. Detection and estimation with compressive measurements. *Dept. of ECE, Rice University, Tech. Rep*, 2006.

[DY10] H. Dahrouj and W. Yu. Coordinated beamforming for the multicell multi-antenna wireless system. *IEEE Transactions on Wireless Communications*, 9(5):1748–1759, 2010.

[EAH12] O. El Ayach and R. W. Heath. Interference alignment with analog channel state feedback. *IEEE Transactions on Wireless Communications*, 11(2):626–636, February 2012.

[EALH12] O. El Ayach, A. Lozano, and R. W. Heath. On the overhead of interference alignment: Training, feedback, and cooperation. *IEEE Transactions on Wireless Communications*, 11(11):4192–4203, November 2012.

[EK12] Y. Eldar and G. Kutyniok. *Compressed sensing: theory and applications*. Cambridge University Press, 2012.

[Eri70] T. Ericson. A Gaussian channel with slow fading (Corresp.). *IEEE Transactions on Information Theory*, 16(3):353–355, 1970.

[FDM+12] G. Fodor, E. Dahlman, G. Mildh, S. Parkvall, N. Reider, G. Miklos, and Z. Turanyi. Design aspects of network assisted device-to-device communications. *IEEE Communications Magazine*, 50(3):170–177, 2012.

[FG98] G. J. Foschini and M. J. Gans. On limits of wireless communications in a fading environment when using multiple antennas. *Wireless personal communications*, 6(3):311–335, 1998.

[FKV06] G. Foschini, K. Karakayali, and R. Valenzuela. Coordinating multiple antenna cellular networks to achieve enormous spectral efficiency. *Communications, IEE Proceedings-*, 153(4):548–555, August 2006.

[Fos96] G. J. Foschini. Layered space-time architecture for wireless communication in a fading environment when using multi-element antennas. *Bell Labs Technical Journal*, 1(2):41–59, Autumn 1996.

[FR13] S. Foucart and H. Rauhut. *A Mathematical Introduction to Compressive Sensing*. Applied and Numerical Harmonic Analysis. Springer New York, New York, NY, 2013.

[GCJ08] K. Gomadam, V. R. Cadambe, and S. A. Jafar. Approaching the capacity of wireless networks through distributed interference alignment. In *IEEE GLOBECOM 2008 - 2008 IEEE Global Telecommunications Conference*, pages 1–6, December 2008.

[GG92] A. Gersho and R. M. Gray. *Vector Quantization and Signal Compression*. Kluwer, Boston, 1992.

[GG11] M. Guillaud and D. Gesbert. Interference alignment in partially connected interfering multiple-access and broadcast channels. In *Global Telecommunications Conference (GLOBECOM 2011), 2011 IEEE*, pages 1–5. IEEE, 2011.

[GHH+10] D. Gesbert, S. Hanly, H. Huang, S. Shamai Shitz, O. Simeone, and W. Yu. Multi-cell MIMO cooperative networks: A new look at interference. *IEEE Journal on Selected Areas in Communications*, 28(9):1380–1408, December 2010.

[GJ10] T. Gou and S. A. Jafar. Degrees of freedom of the K-user $M \times N$ MIMO interference channel. *IEEE Transactions on Information Theory*, 56(12):6040–6057, December 2010.

[GS13] M. Goldenbaum and S. Stańczak. Robust analog function computation via wireless multiple-access channels. *IEEE Transactions on Communincations*, 61(9):3863–3877, September 2013.

[HAH09] K. Huang, J. G. Andrews, and R. W. Heath. Performance of orthogonal beamforming for SDMA with limited feedback. *IEEE Transactions on Vehicular Technology*, 58(1):152–164, 2009.

[HHA07] K. Huang, R. W. Heath, and J. G. Andrews. Space division multiple access with a sum feedback rate constraint. *IEEE Transactions on Signal Processing*, 55(7):3879–3891, July 2007.

[HJ85] R. A. Horn and C. R. Johnson. *Matrix analysis*. Cambridge university press, 1985.

[HN06] J. Haupt and R. Nowak. Signal reconstruction from noisy random projections. *IEEE Transactions on Information Theory*, 52(9):4036–4048, Sept 2006.

[HPC10] H. Huh, H. C. Papadopoulos, and G. Caire. Multiuser MISO transmitter optimization for intercell interference mitigation. *IEEE Transactions on Signal Processing*, 58(8):4272–4285, 2010.

[HTC12] H. Huh, A. M. Tulino, and G. Caire. Network MIMO with linear zero-forcing beamforming: Large system analysis, impact of channel estimation, and reduced-complexity scheduling. *IEEE Transactions on Information Theory*, 58(5):2911–2934, 2012.

[IDM+11] R. Irmer, H. Droste, P. Marsch, M. Grieger, G. Fettweis, S. Brueck, H.-P. Mayer, L. Thiele, and V. Jungnickel. Coordinated multipoint: Concepts, performance, and field trial results. *IEEE Communications Magazine*, 49(2):102–111, 2011.

[Jaf05] S. A. Jafar. Degrees of freedom in distributed MIMO communications. In *IEEE Communication Theory Workshop*, Utah, 2005.

[JG05] S. A. Jafar and A. J. Goldsmith. Isotropic fading vector broadcast channels: The scalar upper bound and loss in degrees of freedom. *IEEE Transactions on Information Theory*, 51(3):848–857, 2005.

[Jin06] N. Jindal. MIMO broadcast channels with finite-rate feedback. *IEEE Transactions on Information Theory*, 52(11):5045–5060, November 2006.

[JRV+05] N. Jindal, W. Rhee, S. Vishwanath, S. A. Jafar, and A. Goldsmith. Sum power iterative water-filling for multi-antenna gaussian broadcast channels. *IEEE Transactions on Information Theory*, 51(4):1570–1580, April 2005.

[KdFG+07] M. Kountouris, R. de Francisco, D. Gesbert, D. T. M. Slock, and T. Sälzer. Efficient metrics for scheduling in MIMO broadcast channels with limited feedback. In *IEEE International Conference on Acoustics, Speech and Signal Processing*, volume 3, pages III–109–III–112, April 2007.

[KFV06] M. K. Karakayali, G. J. Foschini, and R. A. Valenzuela. Network coordination for spectrally efficient communications in cellular systems. *IEEE Wireless Communications*, 13(4):56–61, 2006.

[KKL05] J. S. Kim, H. Kim, and K. B. Lee. Limited feedback signaling for MIMO broadcast channels. *IEEE 6th Workshop on Signal Processing Advances in Wireless Communications*, pages 855–859, 2005.

[KKT12] P.-H. Kuo, H. Kung, and P.-A. Ting. Compressive sensing based channel feedback protocols for spatially-correlated massive antenna arrays. In *Wireless Communications and Networking Conference (WCNC), 2012 IEEE*, pages 492 –497, april 2012.

[KMLL12] J.-S. Kim, S.-H. Moon, S.-R. Lee, and I. Lee. A new channel quantization strategy for MIMO interference alignment with limited feedback. *IEEE Transactions on Wireless Communications*, 11(1):358–366, January 2012.

[Kri11] R. Krishnamachari. *A Geometric Framework for Analyzing the Performance of Multiple-Antenna Systems under Finite-Rate Feedback*. PhD thesis, University of Colorado, Boulder, 2011.

[KSEA03] K. Kiran Mukkavilli, A. Sabharwal, E. Erkip, and B. Aazhang. On beamforming with finite rate feedback in multiple–antenna systems. *IEEE Transactions on Information Theory*, 49(10):2562–2579, October 2003.

[KT79] M. S. Klamkin and G. A. Tsintsifas. *The Circumradius-Inradius Inequality for a Simplex*, volume 52. Mathematical Association of America, January 1979.

[KV10] R. T. Krishnamachari and M. K. Varanasi. Interference alignment under limited feedback for MIMO interference channels. In *2010 IEEE International Symposium on Information Theory (ISIT)*, pages 619–623, June 2010.

[LBG80] Y. Linde, A. Buzo, and R. Gray. An algorithm for vector quantizer design. *IEEE Transactions on Communications*, 28(1):84–95, January 1980.

[Led05] M. Ledoux. *The Concentration of Measure Phenomenon*, volume 89 of *Mathematical Surveys and Monographs*. American Mathematical Society, Providence, Rhode Island, February 2005.

[LHN+08] D. Love, R. W. Heath, V. N. Lau, D. Gesbert, B. Rao, and M. Andrews. An overview of limited feedback in wireless communication systems. *IEEE Journal on Selected Areas in Communications*, 26(8):1341–1365, October 2008.

[LLAH15] N. Lee, X. Lin, J. Andrews, and R. Heath. Power control for D2D underlaid cellular networks: Modeling, algorithms, and analysis. *Selected Areas in Communications, IEEE Journal on*, 33(1):1–13, Jan 2015.

[Llo57] S. P. Lloyd. Least squares qunatization in PCM. Unpublished Bell Laboratories Technical Note. Portions presented at the Institute of Mathematical Statistics Meeting Atlantic City New Jersey September 1957. Published in March 1982 Special Issue on Quantization of the IEEE Transaction on Information Theory, 1957, 1957.

[LSHC12] N. Lee, W. Shin, R. W. Heath, and B. Clerckx. Interference alignment with limited feedback for two-cell interfering MIMO-MAC. In *2012 International Symposium on Wireless Communication Systems (ISWCS)*, pages 566–570, August 2012.

[Lue68] D. G. Luenberger. *Optimization by vector space methods*. John Wiley & Sons, Inc., New York, NY, USA, 1968.

[LY13] T. Liu and C. Yang. On the feasibility of linear interference alignment for MIMO interference broadcast channels with constant coefficients. *Signal Processing, IEEE Transactions on*, 61(9):2178–2191, 2013.

[MF11] P. Marsch and G. P. Fettweis. *Coordinated Multi-Point in Mobile Communications: From theory to practice*. Cambridge University Press, 2011.

[MGMAK09] A. S. Motahari, S. O. Gharan, M.-A. Maddah-Ali, and A. K. Khandani. Real interference alignment: Exploiting the potential of single antenna systems. *arXiv preprint arXiv:0908.2282*, 2009.

[MK06] B. Mielczarek and W. Krzymien. Vector quantization of channel information in linear multi-user MIMO systems. In *Spread Spectrum Techniques and Applications, 2006 IEEE Ninth International Symposium on*, pages 302–306, Aug. 2006.

[NGJV12] B. Nazer, M. Gastpar, S. Jafar, and S. Vishwanath. Ergodic interference alignment. *IEEE Transactions on Information Theory*, 58(10):6355–6371, Oct 2012.

[NMAC14] V. Ntranos, M. A. Maddah-Ali, and G. Caire. Cellular interference alignment. *arXiv preprint arXiv:1402.3119*, 2014.

[PH11] S. W. Peters and R. W. Heath. Cooperative algorithms for MIMO interference channels. *IEEE Transactions on Vehicular Technology*, 60(1):206–218, January 2011.

[PK94] A. Paulraj and T. Kailath. Increasing capacity in wireless broadcast systems using distributed transmission/directional reception (dtdr), September 1994. US Patent 5,345,599.

[PL09] S.-H. Park and I. Lee. Analysis of degrees of freedom of interfering MISO broadcast channels. In *GLOBECOM 2009 - 2009 IEEE Global Telecommunications Conference*, pages 1–6. IEEE, November 2009.

[PL11] S.-H. Park and I. Lee. Degrees of freedom of multiple broadcast channels in the presence of inter-cell interference. *IEEE Transactions on Communications*, 59(5):1481–1487, 2011.

[PW98] H. V. Poor and G. W. Wornell. *Wireless communications: signal processing perspectives*. Prentice Hall PTR Upper Saddle River, New Jersey, 1998.

[QAN10] S. T. Qaseem and T. Y. Al-Naffouri. Compressive sensing for reducing feedback in MIMO broadcast channels. In *IEEE International Conference on Communications (ICC)*, pages 1–5, may 2010.

[RC09] S. Ramprashad and G. Caire. Cellular vs. network MIMO: A comparison including the channel state information overhead. In *IEEE 20th International Symposium on Personal, Indoor and Mobile Radio Communications*, pages 878–884, Sept 2009.

[RFLT98] F. Rashid-Farrokhi, K. Liu, and L. Tassiulas. Transmit beamforming and power control for cellular wireless systems. *IEEE Journal on Selected Areas in Communications*, 16(8):1437–1450, Oct 1998.

[RG12] M. Rezaee and M. Guillaud. Limited feedback for interference alignment in the K-user MIMO interference channel. *IEEE Information Theory Workshop*, pages 667–671, September 2012.

[RLL12] M. Razaviyayn, G. Lyubeznik, and Z. Luo. On the degrees of freedom achievable through interference alignment in a MIMO interference channel. *IEEE Transactions on Signal Processing*, 60(2):812–821, February 2012.

[RS57] C. Rogers and G. Shephard. *The difference body of a convex body*, volume 8-3. Springer, 1957.

[RSV08] H. Rauhut, K. Schnass, and P. Vandergheynst. Compressed sensing and redundant dictionaries. *Information Theory, IEEE Transactions on*, 54(5):2210–2219, May 2008.

[Rud80] W. Rudin. *Function theory in the unit ball of* $\mathbb{C}^n$. Classics in Mathematics. Springer Verlag, 1980.

[RZ97] C. A. Rogers and C. Zong. Covering convex bodies by translates of convex bodies. *Mathematika*, 44(01):215–218, June 1997.

[Sam06] R. Samsung. Downlink MIMO for EUTRA. *3GPP TSG RAN WG1 Meeting*, February 2006.

[SCR05] B. Song, R. Cruz, and B. Rao. Network duality and its application to multi-user MIMO wireless networks with SINR constraints. In *IEEE International Conference on Communications (ICC)*, volume 4, pages 2684–2689 Vol. 4, May 2005.

[SH05] M. Sharif and B. Hassibi. On the capacity of MIMO broadcast channels with partial side information. *IEEE Transactions on Information Theory*, 51(2):506–522, February 2005.

[SH09] W. Santipach and M. L. Honig. Capacity of a multiple-antenna fading channel with a quantized precoding matrix. *IEEE Transactions on Information Theory*, 55(3):1218–1234, March 2009.

[Sha48] C. E. Shannon. A mathematical theory of communication. *Bell System Technical Journal*, 27:379–423, 1948.

[Sha49] C. E. Shannon. Communication in the presence of noise. *Proceedings of the IRE*, 37(1):10–21, 1949.

[Sha95] I. R. Shafarevich. *Basic Algebraic Geometry I.* Springer-Verlag, second edition, 1995.

[SKB09] S. Stańczak, M. Kaliszan, and N. Bambos. Decentralized admission control for power-controlled wireless links. *arXiv preprint arXiv:0907.2896*, 2009.

[SLL+11] W. Shin, N. Lee, J.-B. Lim, C. Shin, and K. Jang. On the design of interference alignment scheme for two-cell MIMO interfering broadcast channels. *Wireless Communications, IEEE Transactions on*, 10(2):437–442, 2011.

[SLZ10] J. Sun, Y. Liu, and G. Zhu. On degrees of freedom of the cellular network. *Science China Information Sciences*, 53(5):1034–1043, April 2010.

[SSH04] Q. Spencer, A. Swindlehurst, and M. Haardt. Zero-forcing methods for downlink spatial multiplexing in multiuser MIMO channels. *IEEE Transactions on Signal Processing*, 52(2):461–471, February 2004.

[ST08] C. Suh and D. Tse. Interference alignment for cellular networks. In *2008 46th Annual Allerton Conference on Communication, Control, and Computing*, pages 1037–1044, September 2008.

[SY13] G. Sridharan and W. Yu. Degrees of freedom of MIMO cellular networks with two cells and two users per cell. In *IEEE International Symposium on Information Theory Proceedings (ISIT),*, pages 1774–1778. IEEE, 2013.

[Sye10] Syed A. Jafar. *Interference Alignment: A New Look at Signal Dimensions in a Communication Network*, volume 7. Foundations and TrendsÂ® in Communications and Information Theory, 2010.

[Tao12] T. Tao. *Topics in random matrix theory.* American Mathematical Society, 2012.

[TB09] I. Thukral and H. Bölcskei. Interference alignment with limited feedback. In *2009 IEEE International Symposium on Information Theory (ISIT)*, pages 1759–1763, July 2009.

[TBH08] M. Trivellato, F. Boccardi, and H. Huang. On transceiver design and channel quantization for downlink multiuser MIMO systems with limited feedback. *IEEE Journal on Selected Areas in Communications*, 26(8):1494–1504, October 2008.

[TBT07] M. Trivellato, F. Boccardi, and F. Tosato. User selection schemes for MIMO broadcast channels with limited feedback. *IEEE 65th Vehicular Technology Conference*, pages 2089–2093, April 2007.

[Tel99] E. Telatar. Capacity of multi-antenna gaussian channels. *European transactions on telecommunications*, 10(6):585–595, 1999.

[TG09] R. Tresch and M. Guillaud. Cellular interference alignment with imperfect channel knowledge. In *Communications Workshops, 2009. ICC Workshops 2009. IEEE International Conference on*, pages 1–5. IEEE, 2009.

[TSC98] V. Tarokh, N. Seshadri, and A. Calderbank. Space-time codes for high data rate wireless communication: performance criterion and code construction. *Information Theory, IEEE Transactions on*, 44(2):744–765, Mar 1998.

[Ver10] R. Vershynin. Introduction to the non-asymptotic analysis of random matrices. *arXiv preprint arXiv:1011.3027*, pages 210–268, 2010.

[VJG02] S. Vishwanath, N. Jindal, and A. Goldsmith. On the capacity of multiple input multiple output broadcast channels. In *IEEE International Conference on Communications (ICC)*, volume 3, pages 1444–1450. IEEE, 2002.

[VT02] P. Viswanath and D. Tse. Sum capacity of the multiple antenna gaussian broadcast channel. In *2002 IEEE International Symposium on Information Theory*, page 497. IEEE, 2002.

[Wil10] T. Wild. A rake-finger based efficient channel state information feedback compression scheme for the MIMO OFDM FDD downlink. In *2010 IEEE 71st Vehicular Technology Conference*, pages 1–5. IEEE, 2010.

[Wyn94] A. D. Wyner. Shannon-theoretic approach to a gaussian cellular multiple-access channel. *IEEE Transactions on Information Theory*, 40(6):1713–1727, 1994.

[Yat95] R. D. Yates. A framework for uplink power control in cellular radio systems. *Selected Areas in Communications, IEEE Journal on*, 13(7):1341–1347, 1995.

[YG06] T. Yoo and A. Goldsmith. On the optimality of multiantenna broadcast scheduling using zero-forcing beamforming. *IEEE Journal on Selected Areas in Communications*, 24(3):528–541, March 2006.

[YJG07] T. Yoo, N. Jindal, and A. Goldsmith. Multi-antenna downlink channels with limited feedback and user selection. *IEEE Journal on Selected Areas in Communications*, 25(7):1478–1491, September 2007.

[YJK10] C. M. Yetis, S. A. Jafar, and A. H. Kayran. On feasibility of interference alignment in MIMO interference networks. *IEEE Transactions on Signal Processing*, 58(9):4771–4782, September 2010.

[ZBH11] B. Zhuang, R. A. Berry, and M. L. Honig. Interference alignment in MIMO cellular. In *2011 IEEE International Conference on Acoustics, Speech and Signal Processing (ICASSP)*, pages 3356–3359, Prague, May 2011. IEEE.

[ZHG09] R. Zakhour, Z. K. M. Ho, and D. Gesbert. Distributed beamforming coordination in multicell MIMO channels. In *Vehicular Technology Conference, 2009. VTC Spring 2009.*, pages 1–5. IEEE, 2009.

[ZT03] L. Zheng and D. Tse. Diversity and multiplexing: a fundamental tradeoff in multiple-antenna channels. *Information Theory, IEEE Transactions on*, 49(5):1073–1096, May 2003.

[ZXC09] C. Zhang, W. Xu, and M. Chen. Multi-mode transmission for MIMO broadcast channels with PU2RC. In *2009 15th Asia-Pacific Conference on Communications*, pages 293–296. IEEE, October 2009.